

For Reference

NOT TO BE TAKEN FROM THIS ROOM

Ex LIBRIS
UNIVERSITATIS
ALBERTAENSIS





Digitized by the Internet Archive
in 2020 with funding from
University of Alberta Libraries

<https://archive.org/details/Reid1981>

T H E U N I V E R S I T Y O F A L B E R T A

RELEASE FORM

NAME OF AUTHOR Robert Stephen Reid

TITLE OF THESIS Nuclear Magnetic Resonance Studies of the

 Complexation Chemistry of Methylmercury(II)

 with Sulfhydryl Compounds in Aqueous Sol-

 utions and Human Erythrocytes

DEGREE FOR WHICH THESIS WAS PRESENTED Ph.D.

YEAR THIS DEGREE GRANTED 1981

Permission is hereby granted to THE UNIVERSITY OF ALBERTA LIBRARY to reproduce single copies of this thesis and to lend or sell such copies for private, scholarly or scientific research purposes only.

The author reserves other publication rights, and neither the thesis nor extensive extracts from it may be printed or otherwise reproduced without the author's written permission.

THE UNIVERSITY OF ALBERTA

NUCLEAR MAGNETIC RESONANCE STUDIES OF THE COMPLEXATION
CHEMISTRY OF METHYLMERCURY(II) WITH SULFHYDRYL COMPOUNDS
IN AQUEOUS SOLUTIONS AND HUMAN ERYTHROCYTES

by



ROBERT STEPHEN REID

A THESIS

SUBMITTED TO THE FACULTY OF GRADUATE STUDIES AND RESEARCH
IN PARTIAL FULFILMENT OF THE REQUIREMENTS FOR THE DEGREE
OF DOCTOR OF PHILOSOPHY
DEPARTMENT OF CHEMISTRY

EDMONTON, ALBERTA

FALL, 1981

THE UNIVERSITY OF ALBERTA
FACULTY OF GRADUATE STUDIES AND RESEARCH

The undersigned certify that they have read, and
recommend to the Faculty of Graduate Studies and Research,
for acceptance, a thesis entitled NUCLEAR MAGNETIC RESONANCE
.....
STUDIES OF THE COMPLEXATION CHEMISTRY OF METHYLMERCURY(II)
.....
WITH SULFHYDRYL COMPOUNDS IN AQUEOUS SOLUTIONS AND HUMAN
.....
ERYTHROCYTES
.....
submitted by ROBERT STEPHEN REID
.....
in partial fulfilment of the requirements for the degree of
Doctor of Philosophy.

To Susie

ABSTRACT

Part 1

The complexation behaviour of methylmercury(II) with several sulfhydryl ligands has been characterized using NMR spectroscopy. The monothiols thus studied were mercaptoacetic acid, mercaptoethanol, penicillamine, N-acetylpenicillamine, cysteine, homocysteine, glutathione, mercaptosuccinic acid and ergothioneine; dithiols studied were 2,3 dimercaptosuccinic acid, dithioerythritol and 2,3 dimercaptopropane-1-sulfonate. Formation constants of the various complexes are measured by allowing each ligand to compete with mercaptoacetic acid for methylmercury(II) and monitoring the degree of success of this competition. Substitution of the known value of the formation constant for the methylmercury(II)-mercaptoethanol complex then yields those for the other complexes. A variety of acid dissociation constant data is also obtained. This enables calculation of conditional formation constants as a function of pH, and also calculation of the formation constants of individual complex forms with different degrees of protonation. Formation constants are found to be well correlated with the acidity of the sulfhydryl group, although some effects due to other groups on the

ligands are apparent. Conditional formation constants at pH 7.4 are found to be only partly correlated with the relative order of merit of the same ligands used as antidotes for methylmercury(II) poisoning, suggesting that other factors may be important. Formation constants for dithiol molecules are slightly higher than predicted on the basis of the monothiol results, suggesting some chelation; however, the strength of the secondary interaction suggests that it is weak and ionic in nature.

The kinetics of displacement of one ligand (A) by another (B) at methylmercury(II) are investigated by analysis of the broadening of NMR lineshapes. Where ligands A and B are both mercaptoacetic acid, processes are relatively sluggish, due to the highly charged nature of the reactants; where A is mercaptoacetate and B penicillamine, cysteine or glutathione the rate constants show the trend expected for diffusion-controlled processes having a rate constant limit of about $10^{8.7} \text{ M}^{-1} \text{ s}^{-1}$. The slow kinetics for highly charged species are discussed as a possible reason for the good performance of antidote molecules such as 2,3 dimercaptosuccinic acid.

Part 2

Using high-field NMR instrumentation, and pulse

techniques such as the Spin-Echo Fourier Transform method, or the Transfer of Saturation by Cross-Relaxation method, measurements of the type shown in Part 1 are demonstrated in solutions containing macromolecules. The behaviour of the spectra of glutathione in hemolyzed human erythrocytes, as methylmercury(II) is added, is characterized in detail and shown to be consistent with that obtained in aqueous solution. Observation of these spectra as a function of added methylmercury(II) leads to an estimate for the hemoglobin-methylmercury(II) complex formation constant; a refined estimate is given, after development of a titration method for hemoglobin sulfhydryl content using NMR as an endpoint indicator. Binding to hemoglobin is about ten times weaker than to glutathione. The relative effectiveness of various sulfhydryl compounds at removing added methylmercury(II) from hemolyzed erythrocyte components was examined. The order of effectiveness correlated well with the formation constant studies of Part 1, but not with in vivo studies of drug effectiveness, suggesting that methylmercury(II)-erythrocyte binding, but not overall toxicity, is equilibrium-related. Highly-charged sulfhydryl compounds such as 2,3 dimercaptosuccinic acid again displayed sluggish kinetics, suggesting this as a factor in their high efficacy as antidotes. The

advantages of NMR for characterization of systems such as these are discussed; in particular, the non-invasive nature of the technique minimises disturbance of the highly labile equilibria involved.

ACKNOWLEDGEMENTS

My most sincere thanks go to Dr. D.L. Rabenstein for providing inspiration and guidance in the course of this research, and for his endless patience.

I am also grateful to all the members of the research group, past and present, both for stimulating discussions, advice and assistance in the chemical sense, and for the friendly atmosphere which minimised the trauma of writing this thesis. My thanks also go to other friends, my family and particularly my wife for their patience during this period.

Thanks are also due to Miss A. Wiseman, who ably (and speedily) transformed a tattered thesis manuscript into its present pristine form.

Financial support from the University of Alberta, from the Izaak Walton Killam Scholarship Fund and from the Alberta Heritage Foundation for Medical Research is gratefully acknowledged.

TABLE OF CONTENTS

<u>Chapter</u>	<u>Page</u>
List of Tables.....	xvii
List of Figures.....	xx

Part 1

The Binding of Methylmercury(II) by Sulfhydryl-Containing Molecules

I	Introduction.....	2
	A. General Complexation Chemistry of CH ₃ Hg(II).....	3
	B. The Chemistry of CH ₃ Hg(II)-Thiol Complexes.....	14
	C. The Use of NMR in Studies of CH ₃ Hg(II) Chemistry.....	24
II	Experimental.....	36
	A. Chemicals.....	36
	B. Preparation and Standardisation of Methylmercury(II) Hydroxide Solutions.....	37
	1. Preparation.....	37
	2. Standardisation.....	38
	C. Preparation and Standardisation of Thiol Solutions.....	41
	1. Preparation.....	41
	2. Standardisation.....	42

<u>Chapter</u>		<u>Page</u>
	D. Instrumentation.....	47
	1. pH measurements.....	47
	2. ^1H Nuclear Magnetic Resonance measurements.....	49
	3. Apparatus for potentiometric titrations.....	51
	E. Preparation of Solutions for pK Measurements.....	55
	1. NMR method.....	57
	2. Computer fit to pK during K_f study.....	59
	3. Potentiometric method.....	59
	F. Preparation of Solutions for Dis- placement Constant Measurements.....	60
	G. Determination of Displacement Constants by NMR.....	62
	H. Determination of Acid Dissociation Constants.....	66
	I. Measurement of Kinetic Parameters from NMR Linebroadening.....	68
III	The Binding of Methylmercury(II) by Mono- thiols.....	72
	A. Mercaptoacetic Acid Studies.....	78
	1. Selection of MAA as competing thiol...	78
	2. Determination of pK's for free MAA....	78
	3. Determination of pK's for methyl- mercury(II) complexed MAA.....	82

<u>Chapter</u>	<u>Page</u>
4. Competition studies between mercapto-ethanol and mercaptoacetic acid.....	85
a) Derivation of model.....	85
b) Notes on Completeness of Model...	88
c) Results.....	90
B. Determination of Formation Constants with Other Thiol Ligands.....	93
1. N-acetylpenicillamine.....	93
2. Penicillamine.....	95
3. Cysteine.....	100
4. Homocysteine.....	100
5. Mercaptosuccinic acid.....	101
6. Glutathione.....	103
7. Ergothioneine.....	107
8. Calculation of derived values.....	112
C. Discussion.....	115
1. General.....	115
2. The effect of acid-base chemistry at other sites of methylmercury(II) binding.....	119
3. The magnitude of methylmercury(II)-sulfhydryl complex formation constants.....	127
4. Methylmercury(II)-sulfhydryl binding data in the literature.....	130
5. Conditional Formation Constants: biological implications.....	134

<u>Chapter</u>		<u>Page</u>
IV	The Binding of Methylmercury(II) by Dithiol Molecules.....	140
	A. Introduction.....	140
	B. Results.....	144
	1. Acid dissociation constants for dithioerythritol.....	144
	2. Acid dissociation constants for 2,3 dimercaptosuccinic acid.....	148
	3. Acid dissociation constant for methylmercury(II)-bound DMSA.....	150
	4. Acid dissociation constant for methylmercury(II)-bound DTE.....	159
	5. Formation constants of $\text{CH}_3\text{Hg(II)}$ complexes of dithiols.....	160
	C. Discussion.....	166
	1. General.....	166
	2. Chelation in the 2,3 dimercapto-succinic acid- $\text{CH}_3\text{Hg(II)}$ complex.....	173
	3. Conditional formation constants in dithiol systems.....	178
V	The Kinetics of Methylmercury(II)-Sulfhydryl Ligand Exchange Processes.....	182
	A. Introduction.....	182
	B. Results.....	184
	1. MAA/MAA exchange kinetics.....	184
	2. Behaviour at very low pH.....	194
	3. Kinetics of displacement by other ligands.....	200

<u>Chapter</u>	<u>Page</u>
C. Discussion.....	212
1. MAA/MAA exchange kinetics.....	212
2. Exchange involving other ligands.....	219
Bibliography.....	225
Appendix I: Ionic Strength and Activity Con- siderations.....	236

Part 2

The Binding of Methylmercury(II) by Macromolecular Thiols and by Erythrocytes

VI	Introduction.....	243
	A. Methylmercury(II) in Biological Systems..	244
	B. Methylmercury(II) Antidotes.....	251
	C. Observation of Small-Molecule NMR Sig- nals in Biological Systems.....	256
	1. Pulsed Fourier Transform NMR: the single-pulse experiment.....	256
	2. The spin-echo Fourier transform (SEFT) experiment.....	260
	3. The transfer of saturation by cross- relaxation (TSCR) experiment.....	264
	D. Approach to the Present Study.....	266

<u>Chapter</u>		<u>Page</u>
VII	Experimental.....	269
	A. Preparation of Erythrocytes for NMR Studies.....	269
	B. Preparation and Assay of Hemoglobin Solutions.....	271
	C. Miscellaneous Experimental Details.....	274
	1. Lipoamide beads.....	274
	2. The use of deuterium oxide.....	276
	D. NMR Measurements.....	279
	1. Instrumentation and acquisition parameters.....	279
	2. NMR pulse techniques.....	279
VIII	The Binding of Methylmercury(II) to Human Erythrocytes and to Hemoglobin.....	281
	A. NMR Study of the $\text{CH}_3\text{Hg(II)}$ /GSH System in Aqueous Solution and in Erythrocytes.	282
	B. Measurement of $\log K_{\text{fC}}$ for the Hemo- globin- $\text{CH}_3\text{Hg(II)}$ Complex.....	299
	1. NMR titration of hemoglobin sulf- hydrys with $\text{CH}_3\text{Hg(II)}$	299
	2. The glutathione/hemoglobin comp- etition study.....	310
	C. Discussion.....	313
IX	The Effectiveness of Sulfhydryl Compounds as Releasing Agents for $\text{CH}_3\text{Hg(II)}$ in Human Erythrocytes.....	316

<u>Chapter</u>	<u>Page</u>
A. Introduction.....	316
B. Results.....	317
C. Discussion.....	324
Bibliography.....	331

LIST OF TABLES

<u>Table</u>	<u>Description</u>	<u>Page</u>
1	Rate constants for thiol exchange processes.	20
2	Selected values of $^2J_{1H-199Hg}$ for $CH_3Hg(II)$ complexes.	28
3	Structures and nomenclature of thiols studied	33
4	Typical results for standardisation of MAA stock solution by iodoacetamide addition and titration of the liberated proton.	46
5	Formation constants for $CH_3Hg(II)$ complexes.	76
6	Selected pK values for free and methylmercury(II) complexed mercaptoacetic acid.	83
7	Selected pK values for mercaptoethanol.	92
8	Literature pK_2 values for ergothioneine.	110
9	Derived methylmercury(II) formation and proton displacement formation constants.	116
10	Displacement constants and methylmercury(II) complex formation constants.	118
11	Acid dissociation constants for $CH_3Hg(II)$ -complexed thiols.	122
12	Acid dissociation constants for the thiol ligands.	124
13	Comparison of association constant values for cysteine and glutathione.	133
14	Conditional formation constants for the methylmercury(II)-thiol complexes at pH 7.4.	138
15	Values of acid dissociation and $CH_3Hg(II)$ complex formation constants for DMSA and DTE.	167

<u>Table</u>	<u>Description</u>	<u>Page</u>
16	Conditional formation constants for the $\text{CH}_3\text{Hg(II)}$ -thiol complexes at pH 7.4.	181
17	Reactions for the displacement or dissociation of MAA from the $\text{CH}_3\text{Hg(II)}$ complex.	187
18	Data for MAA/MAA exchange kinetics at methylmercury(II), pH 8.0 to 5.5.	193
19	Data for MAA/MAA exchange kinetics at methylmercury(II), pH 5.0 to 2.5.	196
20	Data for the kinetics of disappearance of the $\text{MAA-CH}_3\text{Hg(II)}$ complex, pH 1.0 to 0.0.	198
21	Data for the kinetics of disappearance of the $\text{MAA-CH}_3\text{Hg(II)}$ complex, in presence of other thiols, pH 1.2 to 0.3.	201
22	Data for kinetics of displacement of MAA from its $\text{CH}_3\text{Hg(II)}$ complex by penicillamine.	205
23	Data for kinetics of displacement of MAA from its $\text{CH}_3\text{Hg(II)}$ complex by cysteine.	207
24	Data for kinetics of displacement of MAA from its $\text{CH}_3\text{Hg(II)}$ complex by glutathione.	209
25	Rate constants for MAA/MAA exchange reactions at $\text{CH}_3\text{Hg(II)}$.	217
26	Rate constants for sulfhydryl ligand exchange at $\text{CH}_3\text{Hg(II)}$.	220
27	Equations for correction of acid dissociation constants.	241
28	Symptoms of $\text{CH}_3\text{Hg(II)}$ poisoning.	252
29	Complexing agents tested for $\text{CH}_3\text{Hg(II)}$ poisoning.	254
30	Assignments of resonances in ^1H NMR spectra of erythrocytes.	285

<u>Table</u>	<u>Description</u>	<u>Page</u>
31	Determination of hemoglobin sulfhydryl concentration by titration with $\text{CH}_3\text{Hg}(\text{II})$, using ergothioneine as indicator.	307
32	Results of erythrocyte-bound $\text{CH}_3\text{Hg}(\text{II})$ release studies.	323
33	Chemical shifts and intensities of $\text{CH}_3\text{Hg}(\text{II})$ methyl resonances observed in antidote studies.	327

LIST OF FIGURES

<u>Figure</u>	<u>Description</u>	<u>Page</u>
1	Structures of $\text{CH}_3\text{Hg(II)}$ complexes of chelating pyridyl ligands.	10
2	Ligand displacement rate constants at $\text{CH}_3\text{Hg(II)}$ as a function of $\log (K_{f,y}/K_{f,x})$.	13
3	Potentiometric titration of methylmercury(II) with chloride ion.	40
4	Schematic of TMA peaks; peak resolution as a function of linewidth $W_{1/2}$.	52
5	Predicted lineshapes at differing rates of exchange.	69
6	Mercaptoacetic acid species and equilibria in a solution containing $\text{CH}_3\text{Hg(II)}$.	73
7	Chemical shift versus pH data for a) free and b) $\text{CH}_3\text{Hg(II)}$ -complexed MAA.	81
8	Chemical shift versus pH data for a) free MAA, b) $\text{CH}_3\text{Hg(II)}$ -complexed MAA, c) as b) + 1 m.e. mercaptoethanol, d) as b) + 1 m.e. N-acetylpenicillamine.	91
9	Ionisation and $\text{CH}_3\text{Hg(II)}$ binding scheme for penicillamine.	97
10	Chemical shift versus pH data for a) free MAA, b) $\text{CH}_3\text{Hg(II)}$ -complexed MAA, c) as b) + 1 m.e. penicillamine, d) as b) + 1 m.e. cysteine.	99
11	Chemical shift versus pH data for a) free MAA, b) $\text{CH}_3\text{Hg(II)}$ -complexed MAA, c) as b) + 1 m.e. homocysteine, d) as b) + 1 m.e. mercaptosuccinic acid.	102
12	Microscopic and macroscopic ionisation schemes of free glutathione.	104

<u>Figure</u>	<u>Description</u>	<u>Page</u>
13	Chemical shift versus pH data for a) free MAA, b) CH ₃ Hg(II)-complexed MAA, c) as b) + 1 m.e. glutathione.	106
14	Ionisation, tautomerisation and binding scheme for ergothioneine.	108
15	Chemical shift versus pH data for a) free MAA, b) CH ₃ Hg(II)-complexed MAA, c) MAA:CH ₃ Hg(II):ergothioneine 1:1:2.32.	113
16	Derived binding constants for a thiol amino-acid.	114
17	Structures and formation constants for sulfhydryl ligands protonated and deprotonated at the amino group.	120
18	log K _f versus pK for a) MAA, b) ME, c),d) PSH, e) NAPSH, f),g) CSH, h),i) GSH and j) MSA.	128
19	Definition of Simpson's "association" constant K _A for glutathione.	132
20	log conditional formation constant versus pH for a) MSA, b) ME, c) NAPSH, d) PSH, e) MAA, f) CSH and g) GSH.	136
21	Structures of 2,3 dimercaptosuccinic acid and dithioerythritol.	143
22	Acid dissociation schemes for dithioerythritol.	145
23	Acid dissociation schemes for 2,3 dimercaptosuccinic acid.	149
24	Ionisation/binding scheme for DMSA.	153
25	Chemical shift versus pH data for a) free MAA, b) CH ₃ Hg(II)-complexed MAA, c) as b) +1 m.e. DMSA, d) as b) + 1 m.e. BALSO ₃ H, e) MAA:CH ₃ Hg(II):DTE 2:1:1 (single determination).	162

<u>Figure</u>	<u>Description</u>	<u>Page</u>
26	Full microdissociation/binding scheme for a symmetrical dithiol.	170
27	Fractional amounts of various DMSA species in a solution containing 1:1 DMSA:CH ₃ Hg(II).	174
28	Plot of log k_f versus pK for CH ₃ Hg(II) complexes of a) ME, b) MAA, c) MSA, d) DTE, and e) DMSA.	175
29	log conditional formation constants as a function of pH for the CH ₃ Hg(II) complexes of 1) DMSA, 2) DTE, 3) BALSO ₃ H, and 4) MAA.	179
30	Linewidths of the MAA methylene resonance as a function of pH for solutions containing A) MAA (0.21 M) and CH ₃ Hg(II) (0.13 M) and B) MAA (0.17 M) and CH ₃ Hg(II) (0.09 M).	186
31	log fractions of various MAA species as a function of pH.	189
32	Plot of $1/\tau_c/\alpha_{b2}[\text{SCH}_2\text{CO}_2^-]$ versus a_{H^+} for the MAA/MAA kinetic data of Table 18.	192
33	Plot of $1/\tau_c/\alpha_{b2}[\text{SCH}_2\text{CO}_2^-](a_{H^+})^2$ versus a_{H^+} for the MAA/MAA kinetic data of Table 19.	195
34	Plot of $1/\tau_c$ versus a_{H^+} for the kinetics of disappearance of the MAA-CH ₃ Hg(II) complex, pH 1.0 to 0.	197
35	$W_{1/2}$ for the MAA methylene resonance as a function of pH for solutions containing PSH:MAA:CH ₃ Hg(II), x:1:1.	202
36	$W_{1/2}$ for the MAA methylene resonance as a function of pH for solutions containing CSH:MAA:CH ₃ Hg(II), x:1:1.	203
37	$W_{1/2}$ for the MAA methylene resonance as a function of pH for solutions containing GSH:MAA:CH ₃ Hg(II), x:1:1.	204

<u>Figure</u>	<u>Description</u>	<u>Page</u>
38	$\log k_{C,DP}$ versus pH for data of Table 22.	213
39	$\log k_{C,DC}$ versus pH for data of Table 23.	214
40	$\log k_{C,DG}$ versus pH for data of Table 24.	215
41	Displacement rate constants as functions of $\log (K_{fB}/K_{fA})$ for the systems of Table 26.	223
42	Methylmercury(II) distribution in the body.	246
43	Schematic of the erythrocyte.	248
44	Schematic of the structure of hemoglobin.	249
45	Rotating-frame magnetisation diagram and resultant receiver signal for the single pulse Fourier transform NMR experiment.	258
46	400 MHz 1H NMR spectra of erythrocytes A) single pulse experiment, B) SEFT experiment.	261
47	Rotating-frame magnetisation diagram and resultant receiver signal for the spin-echo Fourier transform NMR experiment.	262
48	Spectra of hemolyzed erythrocytes a) single pulse, b) with presaturating pulse applied on HDO resonance, c) with presaturating pulse applied at 8.0 ppm vs. DSS.	265
49	The use of dithioerythritol and of CPG-lipoamide beads as antioxidants.	275
50	SEFT NMR spectrum of intact human erythrocytes at 400 MHz ($\tau_2 = .060$ s).	283
51	SEFT NMR spectra of intact human erythrocytes at 400 MHz. a) alone, b) with 0.5 mM $CH_3Hg(II)$, c) with 1.0 mM $CH_3Hg(II)$.	286
52	Single-pulse (A-C) and SEFT (A'-C') NMR spectra. A,A':GSH alone, B,B' $CH_3Hg(II)$:GSH = 0.581:1, C,C' $CH_3Hg(II)$:GSH = 1.09:1.	288

<u>Figure</u>	<u>Description</u>	<u>Page</u>
53	g5 resonance chemical shift versus CH ₃ Hg(II):GSH ratio (aqueous solution).	293
54	TSCR NMR spectra of hemolyzed erythrocytes on addition of increasing amounts of CH ₃ Hg(II).	294
55	Fraction of GSH complexed by CH ₃ Hg(II) as a function of total CH ₃ Hg(II) added in an erythrocyte sample.	296
56	Chemical shift of resonance e2 as a function of added CH ₃ Hg(II) (0.2) for 50 µl of 0.01 M ergothioneine, pH* = 7.	305
57	Chemical shift of resonance e2 as a function of µl CH ₃ Hg(II) (15.6 mM) added, for a sample of hemoglobin (2 mM) and ergothioneine (2.5 mM).	308
58	Glutathione g5 resonance chemical shift as a function of added CH ₃ Hg(II) (15.6 mM) for a sample containing hemoglobin (4.0 ₂ mM sulfhydryl) and glutathione (4.0 ₂ mM).	312
59	Intensity ratios for glutathione (gl), ergothioneine and creatine resonances in SEFT NMR spectra of hemolyzed erythrocytes as a function of CH ₃ Hg(II) (5.4 mM) added. A) gl/ergo, B) gl/cre, C) ergo/cre.	318
60	Portion of the SEFT NMR spectrum of hemolyzed erythrocytes. A) alone, B) + 2.1 mM CH ₃ Hg(II), C) + 4.3 mM CH ₃ Hg(II), D),E),F) as C) + 0, 1.3 mM and 2.0 mM BALSO ₃ H respectively.	319
61	TSCR spectra of the glutathione g5 resonance for the samples of Figure 60.	321
62	SEFT NMR spectra for hemolyzed erythrocytes with CH ₃ Hg(II) (4.3 mM) and indicated thiols (4 mM sulfhydryl).	322

<u>Figure</u>	<u>Description</u>	<u>Page</u>
63	CH ₃ Hg(II) methyl proton resonances for antidote studies involving A) PSH, B) BALSO ₃ H, C) DMSA, D) MAA and E) MSA.	325
64	Intensity ratios gl/ergo and gl/cre for the antidote studies, plotted versus log K _{fc} of the complexes.	326
64	Glutathione g5 resonance chemical shift for the antidote studies, plotted versus log K _{fc} of the complexes.	329

Part 1

The Binding of Methylmercury(II) by
Sulfhydryl-Containing Molecules

CHAPTER I

Introduction

Methylmercury(II), $\text{CH}_3\text{Hg(II)}$, is a chemical species of interest for two main reasons. It is large and easily polarisable; it is considered the classic example of a soft acid in terms of Pearson's classification (1), making the details of its co-ordination chemistry the subject of considerable investigation (2). Secondly, it is the most toxic form of mercury, having been demonstrated to be the source of poisoning in epidemics in Minimata and Nigata in Japan (3), and elsewhere (4).

These two aspects of $\text{CH}_3\text{Hg(II)}$ are intimately bound together. Jones and Vaughn, and, more recently, Nieboer and Richardson have shown that variations in toxicity between metals, and between different forms of the same metal, are correlatable with softness as defined in terms of the theory of Hard and Soft Acids and Bases (5,6). The latter proposed that the blanket term "heavy metals" should be replaced by a more chemically significant classification. They also point out that the well-documented ability of Hg(II) to undergo methylation by methylcobalamin to a stable derivative (7-10), in contrast to the behaviour of class A metals, is also a function of its class B behaviour. (While

demethylation mechanisms exist, these are not facile (8,11, 12). Early reports of facile alkyl exchange in the bromide and iodide complexes, based on the broadening of ^{199}Hg spin-spin coupled satellites in their ^1H N.M.R. spectra (13), was later shown to be due to quadrupolar interactions (14)).

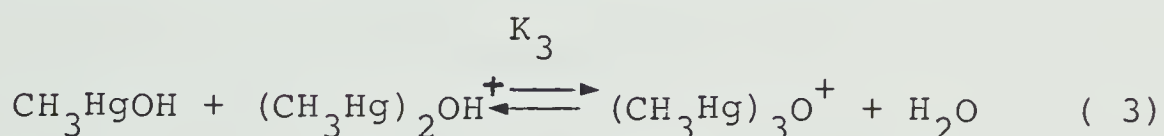
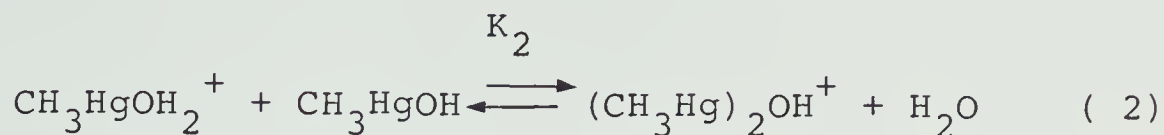
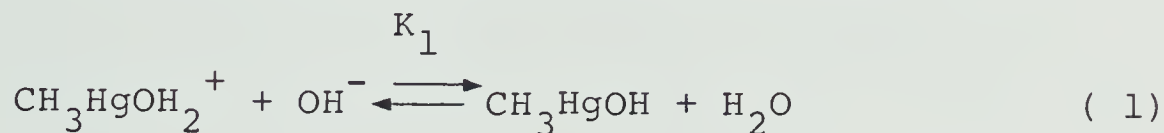
The complexation chemistry of $\text{CH}_3\text{Hg}(\text{II})$ with sulfhydryl (RSH) compounds is a subject of relevance to both these areas. As discussed below, much evidence exists to show that the distribution of $\text{CH}_3\text{Hg}(\text{II})$ in biological systems is heavily dominated by those interactions. The sulfur atom being a soft species, the interaction is also theoretically interesting. Thus, a study of the binding of $\text{CH}_3\text{Hg}(\text{II})$ by the sulfhydryl group should provide insight into both the chemistry and toxicology of $\text{CH}_3\text{Hg}(\text{II})$. Part 1 of this thesis reports the results of a detailed quantitative investigation, using nuclear magnetic resonance, of the binding behaviour of $\text{CH}_3\text{Hg}(\text{II})$ to the sulfhydryl group(s) of small molecules.

A. General Complexation Chemistry of $\text{CH}_3\text{Hg}(\text{II})$

This has been extensively investigated, and recently reviewed (2).

The solution chemistry of $\text{CH}_3\text{Hg}(\text{II})$, or in other terms

its complexation behaviour with OH^- and H_2O , is now well defined. It can be described by the three-stage model

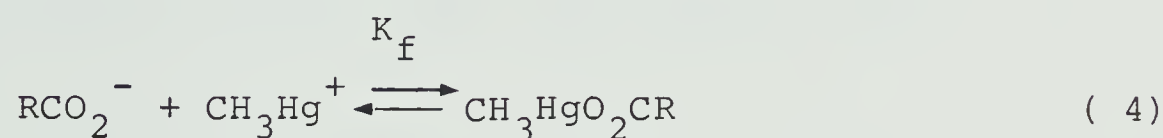


Values of $K_1 = 2.34 \times 10^9$ and $K_2 = 2.34 \times 10^2$ were determined by Schwarzenbach and Schellenberg, neglecting the K_3 process (15). Some controversy arose regarding the existence and stability of the trimeric species in solution (16-20). However, it was proven by Rabenstein et al., using Raman spectroscopy, that it did exist, albeit at low concentration (21). An approximate value for K_3 of 0.7 ± 0.3 was obtained; thus, at 0.1 M methylmercury(II) the maximum trimer concentration is never above ~ 1 mM.

Schwarzenbach and Schellenberg (15) also measured formation constants for the $\text{CH}_3\text{Hg(II)}$ halide complexes potentiometrically, obtaining values of $\log K_f = 1.50$, 5.25, 6.62 and 8.60 for the fluoride, chloride, bromide and iodide complex respectively. The figures are in good qualitative agreement with earlier approximate determinations by Waugh et al. (22) and by Simpson (23). This is

opposite in trend to the proton affinities of these ions, indicating that soft behaviour is indeed dominant.

Formation constants for the $\text{CH}_3\text{Hg(II)}$ complexes of several carboxylic acids have been determined (23-26). The values of $\log K_f$, defined in the expression

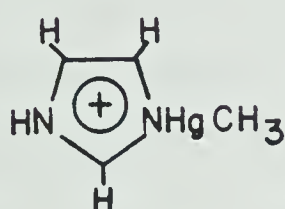


were in the range 1-3. Libich and Rabenstein found a strong correlation between pK and $\log K_f$ for such ligands (24); the relationship was $\text{pK} = 1.73 \log K_f - 1.05$. This correlation is expected, since oxygen atoms exhibit no "soft" behaviour. Similar trends were found for $\text{CH}_3\text{Hg(II)}$ -amine complexes (27); $\log K_f$ values were in the range 5-8.

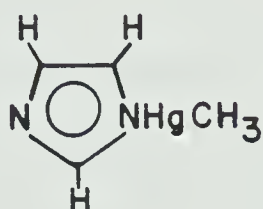
Numerous studies have elucidated binding of $\text{CH}_3\text{Hg(II)}$ to nucleotides and nucleosides, particularly following the report by Mulvihill that $\text{CH}_3\text{Hg(II)}$ is mutagenic (28) and observations of the denaturation of DNA by $\text{CH}_3\text{Hg(II)}$, possibly involving hydrogen-bond disruption by $\text{CH}_3\text{Hg(II)}$ binding (29). An early study by Simpson (30) showed that binding to the naturally occurring nucleosides was through N(1) (purines) or N(3) (pyrimidines). A series of later studies by Mancy, Tobias and coworkers on nucleosides, nucleotides and native DNA using differential Raman

spectroscopy and other techniques (17,31,32) gave the same conclusion, as did several recent crystal structure determinations (33-36); binding is preferential to the most basic site.

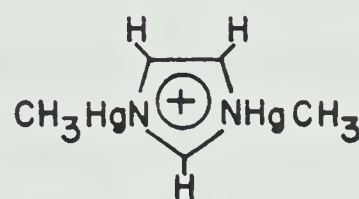
Rabenstein et al. characterised the $\text{CH}_3\text{Hg(II)}$ -imidazole system using N.M.R. The complex forms



MHIm^+



MIm



M_2Im^+

were detected in solution and their formation constants determined (37). Interestingly, $\log K$ for the process $\text{M}^+ + \text{MIm} \rightleftharpoons \text{M}_2\text{Im}^+$ was 8.26, whereas $\log K$ for the process $\text{M}^+ + \text{HIm} \rightleftharpoons \text{MHIm}^+$ was only 6.93. Thus, in the pH range where both MIm and MHIm^+ exist, a displacement reaction to give M_2Im^+ and HIm (free imidazole) is observed. In other terms, binding of methylmercury(II) to the first nitrogen "activates" the second towards attack. This effect has also been noted in studies with adenosine, cytidine and inosine (30).

The binding of $\text{CH}_3\text{Hg(II)}$ by the thioether group of

methionine was investigated by consideration of the ^1H N.M.R. spectra as a function of pH (38). $\log K_f$ for the complex was only 1.94; this binding is significant only below pH 3, where the carboxylate group of methionine is becoming protonated. At higher pH values, the $\text{CH}_3\text{Hg(II)}$ shifts again, to the amino group. The x-ray determined structure of solid methionato - methylmercury(II) bears out these conclusions (39).

While mercury in its divalent state can adopt either two coordinate (linear) or four coordinate (tetrahedral) geometry in its complexes (40), the mercury in methylmercury(II) complexes is in general linear two coordinate; this has been attributed to electron donation by the methyl group lessening the positive charge at the mercury atoms (41). Nevertheless, higher coordination numbers are observed, and are of some interest in view of the potentially multidentate character of many biological ligands. Schwarzenbach and Schellenberg (15) ascribed the increase of solubility of CH_3HgI in KI solution to the formation of $\text{CH}_3\text{HgI}_2^-$, obtaining a formation constant of about 2. More recent work with alkylmercury(II) halides has tended to be confusing. Goggin et al. have recently reviewed the field (42), and rationalised the differing results in terms of the widely differing solvents used (42,43).

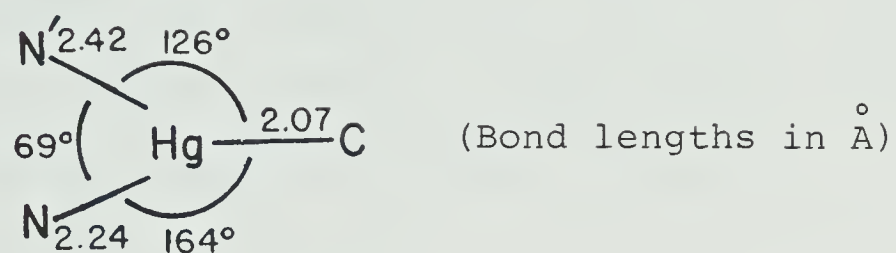
Some such ions (eg. $\text{CH}_3\text{HgCl}_2^-$) would form in poorly donating solvents but not in water or methanol, whereas some (notably $\text{CH}_3\text{Hg}(\text{CN})_2^-$) did not appear to form at all (41). Simpson had previously shown that K_f determinations for CH_3HgCN are invariant under large excesses of cyanide ion (23); the crystal structure of CH_3HgCN shows an exactly linear skeleton (44). Relf et al. (45) studied the higher complex $\text{CH}_3\text{Hg}(\text{SCN})_3^{2-}$; they concluded that both of the "extra" SCN groups were coordinated through weak interactions. Petrosyan and Reutov ascribed these to donation of ligand electron pairs into the vacant 6p orbitals of mercury (46).

Many of the crystal structures discussed elsewhere show small deviations from linearity in the C-Hg-X skeleton, associated with a weak (long-range) but plausible intra- and/or intermolecular interaction with another group. A typical example is the structure of L-cysteinatomethylmercury(II) determined by Taylor et al. (47), where the C-Hg-S angle is 178° and a weak secondary interaction to a carboxylate oxygen atom is identified. However, as Rabenstein has pointed out (2), it is probable that a strongly donating solvent such as water could disrupt these secondary interactions. For unambiguous evidence of chelation, detailed stability constant data is

most helpful. For instance, the glycine complex (N-bonded) has $\log K_f = 7.88$; that of β -alanine, with one more intervening carbon atom between amino and carboxylate groups, has $\log K_f = 7.56$. On the basis of the pK's of the amino groups, however, the opposite trend is expected; thus, it seems likely that chelation is occurring in the glycine case (27).

Chelation has been most unequivocally demonstrated for the 2-2'-bipyridine complex. Anderegg (48) obtained a value for the $\text{CH}_3\text{Hg(II)}$ complex formation constant of 7.2×10^5 , whereas the value for pyridine is 6.3×10^4 . A series of papers by Canty and coworkers (49-52) has examined this question in detail. The crystal structure of the complex showed a planar C-Hg-N-N' framework, with unsymmetrical geometry (see Figure 1). Spectral evidence indicated that such geometry persisted in methanolic solution. It was concluded that hybridisation at the mercury atom was essentially sp, and that the secondary interaction with N' was via overlap of the nitrogen lone pair with a vacant 6p orbital, in agreement with Petrosyan and Reutov (46). Recently, a crystal structure was published (52) of the $\text{CH}_3\text{Hg(II)}$ complex of 4,4',4''-triethyl-2,2':-6',2''-terpyridyl, in which the mercury atom is four coordinate (see Figure 1). The ligand is apparently bidentate

(a) 2,2' bipyridyls



(b) 4,4',4''-triethyl-2,2':6',2''-terpyridyl nitrate

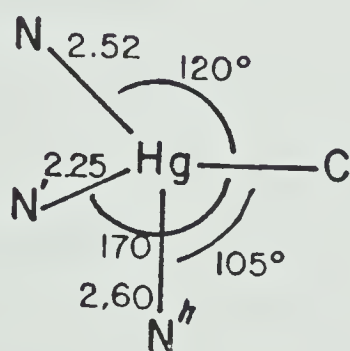


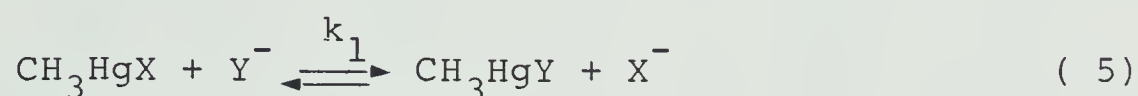
Figure 1. The structures of $\text{CH}_3\text{Hg(II)}$ complexes of chelating pyridyl ligands.

in methanol (52). In these structures, the Hg-C bond length is almost invariant, whereas the Hg-N primary interaction tends to be longer ($\sim 2.25 \text{ \AA}$) (53,54). This indicates that it is the strength of the primary Hg-N interaction which is compromised to accommodate the extra coordinating N atoms. The secondary Hg-N bond(s) are very long indeed. Kinetic studies on ligand exchange in these systems shows that they give no significant retardation relative to unidentate systems (55).

Another secondary interaction which occurs is that between the methylmercury(II) moiety and a suitably placed aromatic ring on the ligand. The effect was first postulated by Rabenstein et al. (27) on the basis of the enhanced stability of the phenylalanine complex, and the unusual proton chemical shift of the methyl group (assigned to ring current effects). The idea was confirmed for phenylalanine and L-tyrosine using ^{13}C NMR, by Brown et al. (56); a similar effect was noted by Bach and Weibel for the benzylmercaptan complex (57). Crystal structure determinations for the L-tyrosine and 2-amino-4-phenylbutanoic acid complexes showed that the interaction was edge-on, between the mercury atom and two ring carbons (58). Lampe and Moore carried out a systematic study by ^1H NMR of a variety of such complexes (59). Conformational analysis

of the data for the L-tyrosine complex gives a structure similar to that observed in the crystal.

The kinetics of $\text{CH}_3\text{Hg(II)}$ ligand exchange are apparently related to this weak tendency to expand its coordination number. A series of papers by Geier and coworkers has shown, using temperature-jump relaxation methods, that the reaction



proceeds by an associative mechanism for $\text{X} = \text{OH}^-$, pyridine ligands, or thiones and $\text{Y} =$ a variety of ligands (60-62). This is based on the observation that where $K_{\text{CH}_3\text{HgX}} > K_{\text{CH}_3\text{HgY}}$, $k_1 < k_1'$, and k_1 increases with $K_{\text{CH}_3\text{HgY}}$. Measurements by ^1H NMR made by Simpson on halide systems support this conclusion (63). Recently, it was demonstrated that hydroxide ion is anomalous; reactions involving it were generally slower than predicted. It may be that OH^- actually reacts as H_7O_4^- and hence the "dehydration energy" of the ion contributes to a higher activation energy (62). Some results are shown in Figure 2. The solid lines show the rate constants expected for an associative mechanism; those dashed are recalculated for the OH^- case with an empirical factor included to allow for the above effect.

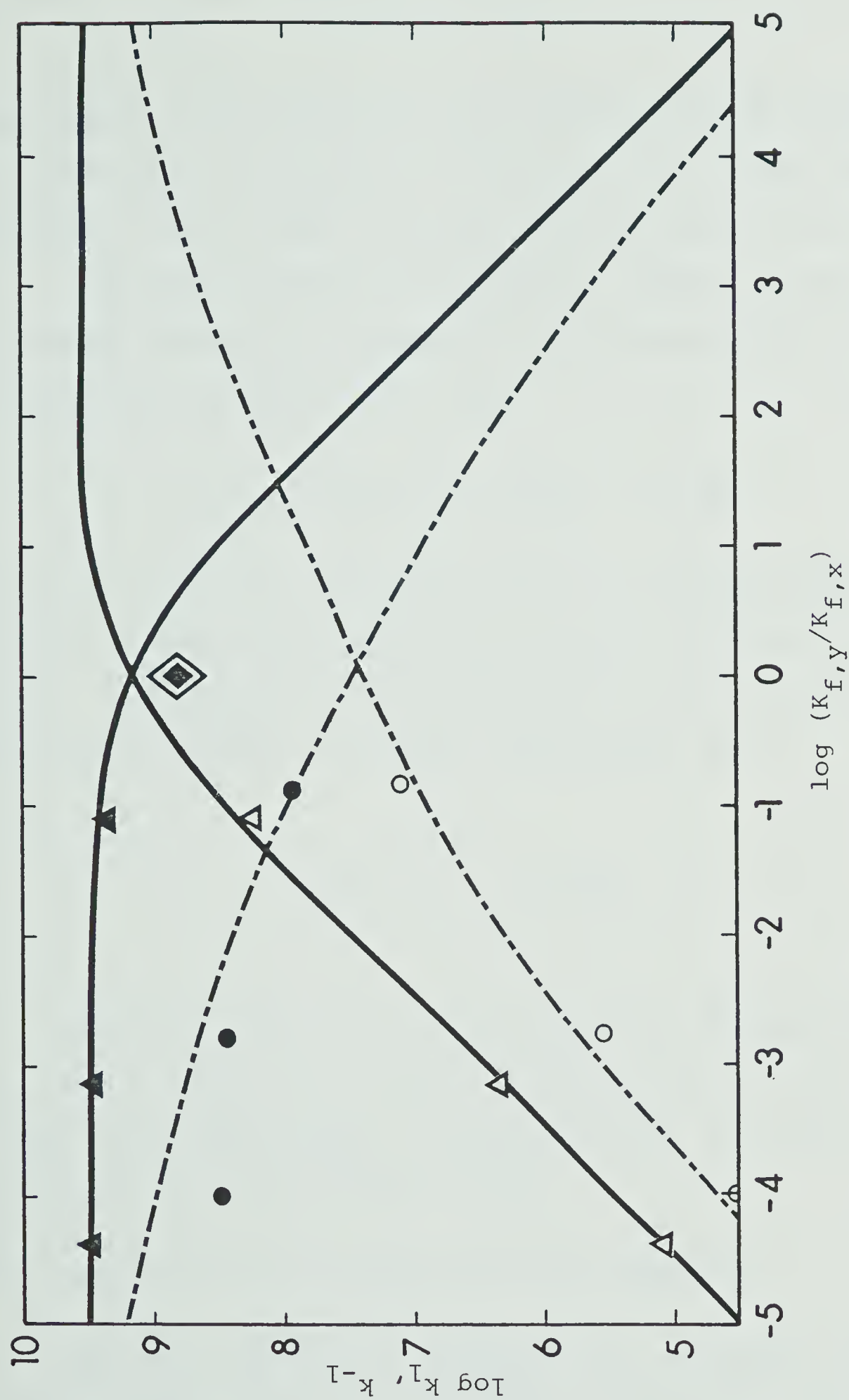


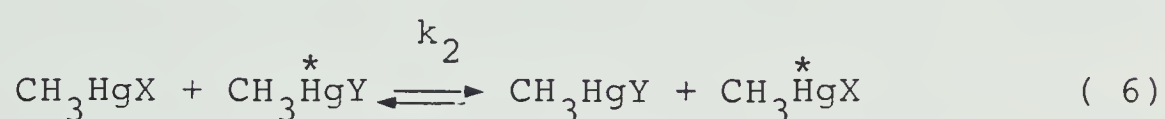
Figure 2. $\log k_1$ (solid symbols) and $\log k_{-1}$ (open symbols) versus $\log (K_{f,y}/K_{f,x})$.

▲ $y = \text{l-methylquinaldine-4-thione}$, $x = \text{Cl}^-$, Br^- , I^- (62). ● $y = \text{OH}^-$,

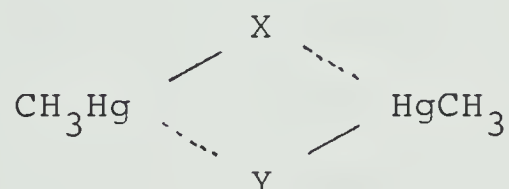
$x = \text{Cl}^-$, Br^- , I^- (62). ◆ $x, y = \text{GS}^-$ (64).

Also shown is the datum for the exchange of glutathione (γ -glutamylcysteinylglycine, GSH) between its free and $\text{CH}_3\text{Hg(II)}$ bound forms, discussed in more detail below (64).

A further exchange route exists. Simpson noted that rates of exchange, as measured by peak coalescence techniques, for systems of the type



were too fast to be accounted for by an anionic mechanism, given the small equilibrium free ligand concentrations (63). He proposed a "direct exchange", for which Murrell and Brown suggested a bridged intermediate (65):



Bach and Weibel have demonstrated the probable existence of this in mercaptide exchange processes, using spectroscopic and thermodynamic evidence (57,66). This work is described in greater detail below.

B. The Chemistry of $\text{CH}_3\text{Hg(II)}$ -Thiol Complexes

The high affinity of $\text{CH}_3\text{Hg(II)}$ for sulfhydryl groups has been recognised for some time. Hughes (67) proposed its

use as a protein sulfhydryl-determining reagent in 1950, and estimated $\log K_f$ for the complex with mercaptalbumin at about 22.

In 1961, Simpson measured "association constants" for the cysteine and glutathione complexes using liquid extraction into toluene (23). He did not account for any variations due to state of protonation at the amino group, quoting only values for "RS" complexation of $\log K_a = 15.7$ and 15.9 respectively; nevertheless, these large numbers support the conclusion that sulfhydryl group binding would dominate the behaviour of $\text{CH}_3\text{Hg(II)}$ where thiols were present. Schwarzenbach and Schellenberg (15) measured $\log K_f$ for the mercaptoethanol complex as 16.12 . These remain the only reliable values for K_f in the literature. Hojo et al. measured formation constants for $\text{CH}_3\text{Hg(II)}$ complexes with a variety of sulfhydryl ligands, including penicillamine, cysteine, glutathione, 2,3 dimercaptopropanol and N-acetylcysteine (68). Their results indicated a general increase in $\log K_f$ with pK of the sulfhydryl group, as demonstrated for other ligand types. Unfortunately, in terms of all other data available (see above and below) their values are ludicrously low ($7 < \log K_f < 9$); insufficient experimental details are available to correct here what is doubtless a systematic error

in calculation.

Bach and Weibel have estimated formation constants from the magnitude of the mercury-proton coupling constant (see below) (57). While such a correlation is observed for various other ligand types, it has not been demonstrated for sulfhydryl ligands. The values obtained were in the range $15 < \log K_f < 16.5$; the uncertainty in these, based on the correlation coefficient of their calibration line, is conservatively ± 0.5 .

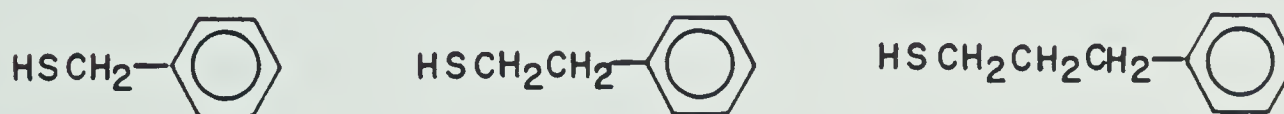
Various NMR studies support the qualitative conclusion that $\text{CH}_3\text{Hg(II)}$ binding to sulfhydryl groups is preferential. Rabenstein conducted an investigation into the microscopic acid dissociation constants of free and $\text{CH}_3\text{Hg(II)}$ -complexed glutathione (69). He concluded that sulfhydryl binding was the preferred mode, and suggested the possibility of binding of a second $\text{CH}_3\text{Hg(II)}$ to the complexed sulfhydryl group. (Schwarzenbach and Schellenberg had previously measured $\log K_f$ for the higher sulfide complexes $(\text{CH}_3\text{Hg})_2\text{S}$ and $(\text{CH}_3\text{Hg})_3\text{S}^+$ at 16.3 and ~ 7 respectively, indicating the possibility of residual basicity at a coordinated sulfur atom (15).) A qualitative study of the N-acetylcysteine complex by Simpson, Hopkins and Hague yielded similar conclusions (70). A year later, Rabenstein and Fairhurst (64) reported the results of a more comprehensive study

involving cysteine, penicillamine and glutathione. Over the pH range 1 to 13 the first $\text{CH}_3\text{Hg(II)}$ moiety was sulfhydryl bound. The coordination site of the second was pH dependent in the glutathione complex. Below pH 4, it was the already complexed sulfhydryl group; from pH 4 to 8 it shifted to the amino group, and above pH 10 it dissociated due to hydroxide complex formation. At very low pH, results for the 1:1 GSH complex suggested protonation at the $\text{CH}_3\text{Hg(II)}$ complexed sulfur atom, underlining the similarity already pointed out by Schwarzenbach and Schellenberg between $\text{CH}_3\text{Hg(II)}$ and H^+ binding. Such protonation has been observed for other metal-complexed sulfhydryls (71).

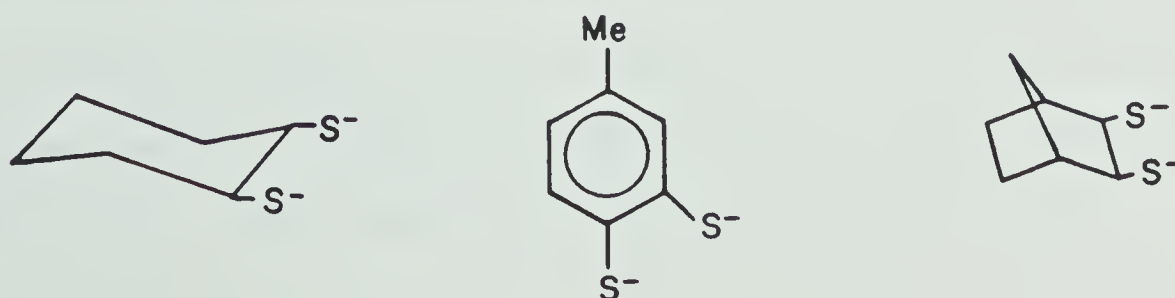
Preferential sulfhydryl binding is borne out by a number of X-ray crystallographic structure determinations by Carty and coworkers; in the cysteine (47), and penicillamine (72) 1:1 complexes binding was to the sulfhydryl site, while in the 2:1 $\text{CH}_3\text{Hg(II)}$:penicillamine complex the second $\text{CH}_3\text{Hg(II)}$ was bound to the amino group (73).

Some work has addressed the problem of chelation in methylmercury(II)-sulfhydryl systems. An early systematic determination of the NMR parameters of a variety of $\text{CH}_3\text{Hg(II)}$ complexes, including a series of thiophenols, was performed by Sytsma and Kline (74). On the basis of the observed

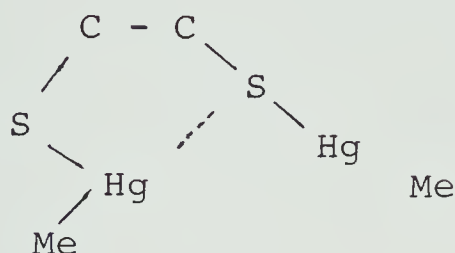
coupling constant, they concluded that no significant chelation was occurring; however (see below) this evidence is not conclusive. Using chemical shifts in deuteriochloroform, Lampe and Moore concluded that chelation through the ring-carbon/mercury atom mode discussed above, was occurring for the complexes of benzylmercaptan and (more strongly) 2phenylethylmercaptan:



but not for 3phenylpropylmercaptan (59). This is in accord with the normal ring-closing tendencies of 5, 6 and 7-membered rings (75). The effect was small, however, by comparison with that in amino complexes (see above); the charge in chemical shift engendered by the secondary interactions is smaller than in the amino case. In a more recent paper (76), Moore and coworkers investigated the possibility of more conventional chelation, using the sterically hindered dithiols



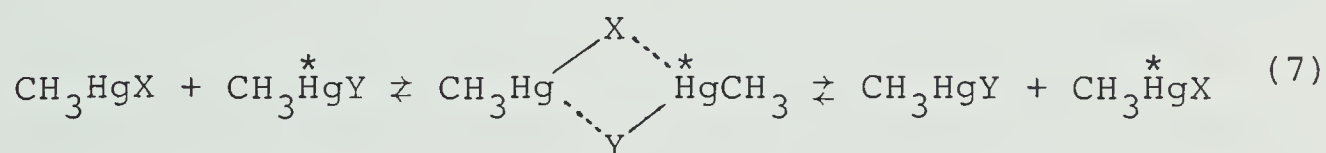
The crystal structures of the $\text{CH}_3\text{Hg(II)}$ complexes of these had the general structure



The magnitude of the ^{199}Hg - ^1H coupling constant (in non-donating solvents) supports this conclusion (see below). However, the comments of Goggin et al. (42) and of Rabenstein (2) regarding the influence of solvent type on such interactions should be borne in mind.

Kinetic studies of $\text{CH}_3\text{Hg(II)}$ thiol complexes are sparse. A list of relevant rate constants together with others for comparison is given in Table 1.

The work by Bach and Weibel (57) on the direct exchange mechanism



has already been mentioned. In their NMR study, they showed that as ligands X became more polarisable and hence better at bridging between mercury atoms (77), the rate of exchange between CH_3HgCN and CH_3HgX rose, supporting the above hypothesis. (By contrast, had an ionic mechanism

Table 1. Rate Constants for thiol exchange processes.

ligand X	ligand Y	$\log k_1^a$	$\log k_{-1}^a$	$\log k_2^b$	Source
$\text{GS}^{-\text{h}}$	$\text{GS}^{-\text{h}}$	8.8	8.8	--	c
H_2O	GSH^{h}	9.7	-2.6	--	c
CN^-	$^-\text{SCH}_3$	--	--	1.58^{f}	d
CN^-	$^-\text{SC}_6\text{H}_5$	--	--	1.60^{f}	d
CN^-	$^-\text{SC}(\text{CH}_3)_3$	--	--	1.99^{f}	d
CN^-	$^-\text{SCH}_2\text{CO}_2^-$	--	--	~ 3.1	e
CH_3S^-	$^-\text{SCHCH}_3\text{C}_6\text{H}_5$	--	--	7.5^{g}	d

a) As defined in Eqn. (5).

b) As defined in Eqn. (6).

c) Reference 64.

d) Reference 57.

e) Reference 63.

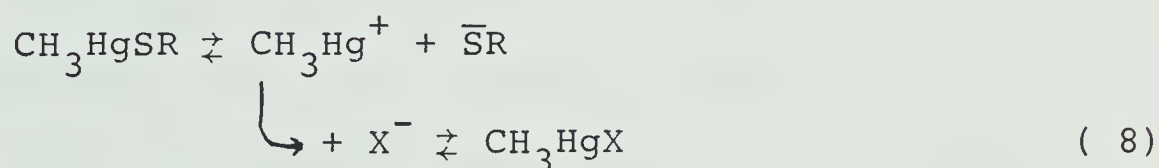
f) In dimethylformamide.

g) Exchange of $(\text{CH}_3)_3\text{CHg}(\text{II})$ complexes in $\text{HCF}_2\text{Cl}/\text{HCFC1}_2$.

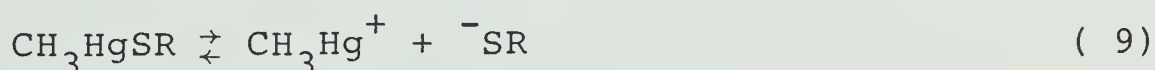
h) Deprotonated glutathione, GS^- ; protonated glutathione, GSH .

been operative, rates would be expected to *fall* with softer X ligands.) In further support, for $\text{CH}_3\text{HgX} / \text{CH}_3\text{HgSR}'$ systems, separate resonances for the $\text{CH}_3\text{Hg(II)}$ methyl groups could not be observed under any conditions, nor could any long-range coupling between ligand protons and those of $\text{CH}_3\text{Hg(II)}$. Determination of the rate constants of the cyanide exchange reactions as a function of temperature showed that the entropy of activation was consistently negative, as would be expected for a highly ordered bridged transition state.

The possibility of exchange via simple dissociation

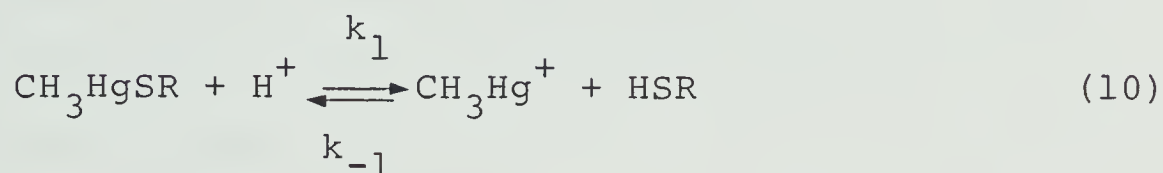


has been examined; in fact, Simpson et al. claimed that it was operative for the N-acetylcysteine/chloride ligand exchange system (70). However, as Rabenstein and Fairhurst pointed out (64), the equilibrium dissociation constant for a typical complex

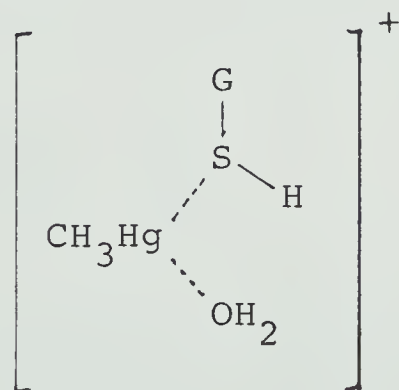


was already known to be $\sim 10^{-16} \text{ mol dm}^{-3}$ (23). Since the association rate constant must be $\sim 10^{10} \text{ mol}^{-2} \text{ dm}^6 \text{ s}^{-1}$ or less (this representing the diffusion-controlled limit) (78)

the dissociation rate constant must necessarily be 10^{-6} $\text{mol}^{-1} \text{dm}^3 \text{s}^{-1}$ or less. This invalidates the conclusions of Simpson et al. for simple dissociation. However, Rabenstein and Fairhurst demonstrated the existence of the low pH proton-facilitated dissociation process

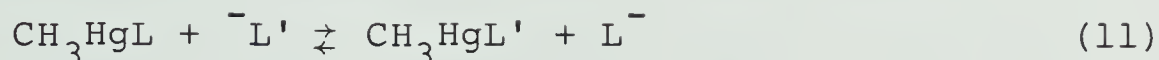


from the pH dependence of the rate of exchange of methylmercury(II) between different glutathione ligands, using ^{13}C NMR. The above argument does not apply here, because $\text{CH}_3\text{HgS}^+(\text{H})\text{R}$ has a much lower formation constant than CH_3HgSR . This dissociation reaction was fairly slow ($k_1 = 600 \pm 200 \text{ mol}^{-1} \text{dm}^3 \text{s}^{-1}$) and the association reaction effectively diffusion controlled ($\log k_{-1} = 9.7$). This is consistent with an associative mechanism involving a transition state such as



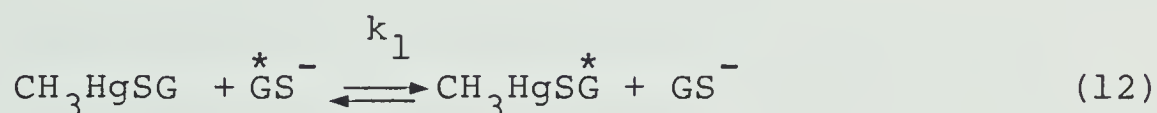
The associative nature of the anionic ligand displace-

ment mechanism:



was discussed above. Since (as detailed in Part 2 of this thesis) free thiol molecules under physiological conditions are invariably in vast excess over $\text{CH}_3\text{Hg(II)}$ -bound ones, this is undoubtedly the most significant exchange process in biological systems.

The process



where GS^- is the sulfhydryl-deprotonated form(s) of glutathione, was investigated by Rabenstein and Fairhurst (64). They estimated lifetimes for the complexed species from comparisons of experimental ^{13}C NMR lineshapes and those calculated from modified Bloch equations. Chapter V discusses the approach in more detail. These lifetimes were then fitted to the kinetic model

$$1/\tau_c = - \frac{d[C]}{dt} \cdot \frac{1}{[C]} \quad (13)$$

where τ_c is the mean complex lifetime and $[C]$ the complex concentration. They obtained a value for the rate constant of $\log k_1 = 8.8$. This is of the order of the value (9.1)

predicted by Erni and Geier for an associative-mechanism ligand displacement reaction involving two ligands of identical affinity (62), but somewhat lower. This was ascribed to steric effects.

C. The Use of NMR in Studies of $\text{CH}_3\text{Hg(II)}$ Chemistry

Methylmercury(II) is unusually suitable for NMR studies, in that all constituent atoms are to some extent NMR active; in addition to ^1H and ^{13}C , 16.9% of Hg is present as ^{199}Hg , another spin 1/2 nucleus.

^{13}C NMR parameters were determined by Brown et al. (56) for a variety of $\text{CH}_3\text{Hg(II)}$ halogen, pseudohalogen and amino acid complexes. In line with theory, which relates the paramagnetic contribution to the shift to the reciprocal of ΔE (essentially the $\sigma^* \leftarrow \sigma$ excitation energy), a decrease in bond energy led to a shift to lower field. Anomalous low shifts of the N-coordinated phenylalanine and tyrosine complexes were ascribed to ring-current effects, confirming Rabenstein's conclusion, based on ^1H NMR shifts, of ring-methylmercury(II) interaction (27). Solvent effects were minimal. The one-bond ^{13}C - ^{199}Hg coupling constants $^1J_{^{13}\text{C}-^{199}\text{Hg}}$, or simply 1J , were found to decrease with increasing bond strength (as do the ^{199}Hg - ^1H two-bond couplings; see below). This was attributed to a decrease

in electron density in the Hg 6s orbital at the nucleus, and possibly also to a decrease in the s-character of the (hybrid) orbital used in bonding. A marked increase in 1J was observed in nucleophilic solvents; this was said to be due either to rehybridisation or to a departure from strict molecular linearity due to weak coordination of solvent molecules. A study by Wilson et al. on a range of aryl- and alkylmercury(II) compounds reached similar conclusions (79). ^{13}C NMR has also been used to examine the state of complexation of methylmercury(II) with ligands such as GSH, where the highly coupled nature of the ligand 1H NMR spectrum makes quantitative measurement difficult (64).

A few workers have investigated $CH_3Hg(II)$ using ^{199}Hg NMR. Sens et al. (80) and Borzo and Maciel (81) measured ^{199}Hg chemical shifts δ_{Hg} for methylmercury(II) halides in a wide variety of solvents. The behaviour of δ_{Hg} and the rationalisation thereof broadly parallel those of δ_C given above, except that solvent effects are more marked; more polar solvents give shifts to lower frequency. Despite the vast chemical shift range (>2600 ppm) and hence high sensitivity to bonding patterns, studies applying ^{199}Hg NMR are sparse; Borzo and Maciel wrote:

"...the main strength of structure elucidations via chemical shift studies has lain in *empirical relationships* on well-substantiated patterns of experimental data. Such data are to a large extent lacking for many metal nuclides of interest."

Sudmeier et al. (82) have recently employed ^{199}Hg NMR to reevaluate the parameters of the aqueous solution chemistry of $\text{CH}_3\text{Hg}(\text{II})$ (see above); agreement with previous values was reasonable. A downfield shift of over 400 ppm was observed on complexation by one mole equivalent of glutathione. Goggin et al. (42) used $^1\text{H}-\{^{199}\text{Hg}\}$ INDOR to obtain ^{199}Hg chemical shifts of $\text{CH}_3\text{Hg}(\text{II})$ halides in solutions using a variety of solvents. In some solvents, addition of tetrabutylammonium chloride gave a large positive shift (100-200 ppm); this is expected for binding of an additional halide ion to the $\text{CH}_3\text{Hg}(\text{II})$ species, since this will increase the paramagnetic contribution to δ . The chemical shifts in different solvents were not consistent simply with electron density effect due to solvent coordination, as suggested previously (83). It appears that it is solvent-*halide* interactions rather than solvent-mercury interactions which determine the degree of formation of higher halide complex anions, since some relatively well-coordinated solvents (e.g. pyridine) did not impede the formation of higher complexes. Using variations in δ_{Hg} and $^2J_{^1\text{H}-^{199}\text{Hg}}$ (2J) as a function of added chloride, these authors were also able to obtain values for the formation constant of the higher complex in dichloromethane; this was higher than the corresponding value obtained from a similar

study in ethanol by Lucchini and Wells (84).

The most widely investigated NMR parameter of $\text{CH}_3\text{Hg(II)}$ complexes is the mercury-proton coupling constant, measured as the separation between the ^{199}Hg satellite peaks in the $\text{CH}_3\text{Hg(II)}$ methyl proton ^1H NMR spectrum. A selection of the many values in the literature is given in Table 2.

In 1963, Hatton, Schneider and Siebrand (13) showed that the magnitude of 2J depended upon the electronegativity of X in CH_3HgX ; they obtained values between 104 Hz ($(\text{CH}_3)_2\text{Hg}$) and 233 Hz ($\text{CH}_3\text{HgClO}_4$). This is expected, assuming that the magnitude of 2J is dominated by the Fermi contact interaction, which involves the s-electron density at the nuclei. As X grows more electronegative, the s-character of the hybrid orbital on Hg bonding to C will increase and the effective nuclear charge on Hg grow, giving a contraction of the 6s orbital. The above assumption was questioned by MacFarlane (85); however, more recent theoretical calculations by Heinneke support its validity (86).

In another study, Federov et al. (87) related trends in 2J to electronegativity. They also noted that an empirical equation for 2J could be set up. For a compound CH_3HgXR :

$$^2J = ^2J_0 + ^2J_X + ^2J_R \quad (14)$$

Table 2. Selected values of $^2J_{1\text{H}-199\text{Hg}}$ for $\text{CH}_3\text{Hg(II)}$ complexes^a.

Ligand	$^2J_{1\text{H}-199\text{Hg}}/\text{Hz}$
OH^-	203.0
Cl^-	215.2
Br^-	212.0
I^-	200.0
Acetate	233.3
Ethylamine	211.0
Glycine	216.0
Pyridine	229.6
2,2'-bipyridine	238.8
Cysteine	174.0
Mercaptoacetic acid	172.0
Glutathione	170.0
S^{2-}	146
Se^{2-}	143

a) From reference 2.

2J_0 is an "innate" contribution, 2J_X a contribution due to X (independent of the nature of R) and 2J_R one due to R (independent of the nature of X). The approach is similar to that used by Hammel and Taft to predict acidities; in fact, 2J_R was related with some success to the Taft parameter σ^* for the substituent R.

Many trends correlating 2J with pK of the ligand, $\log K_f$ of the complex or electronegativity have since been reported, for a large variety of ligands. 2J for carboxylic acid complexes (in COCl_3 , pyridine and in aqueous solution) correlates negatively with the pK of the acid group (24, 74, 88, 89). Similar correlations were observed for amine (27), pyridine, bipyridine and 1,10 phenanthroline complexes (51) and for those of phenols and thiophenols (74). It has been shown (90) that such a trend persists approximately over several orders of magnitude; thus, it is possible to deduce coordination sites of $\text{CH}_3\text{Hg(II)}$ directly from the magnitude of 2J .

2J is also solvent-dependent. In the carboxylic acid studies, Libich and Rabenstein noted that 2J values were ~ 22 Hz higher in aqueous solution than in chloroform. A recent systematic study by Goggin et al. (42) showed a continuous range of 2J values for CH_3HgCl between 202.1 Hz (COCl_3) and 223.6 Hz (D_2O) as the electron-donating ability

of the solvent increased.

The effect of expanded coordination numbers on 2J is interesting. Sytsma and Kline (74) predicted a decrease in 2J if chelation occurred for thiophenol complexes, on the grounds of increased electron density at the Hg atom. (In fact, no effect was observed.) Relf et al. showed that on adding SCN^- to CH_3HgSCN to form higher complexes, a small *increase* in 2J was obtained (45). It thus appears that no rehybridisation at Hg occurs on bonding additional SCN^- , and that the secondary interactions are substantially ionic in character. The small increase was ascribed to changes in the effective nuclear charge of the Hg atom. Similarly, the 2J data obtained for bipyridyl $CH_3Hg(II)$ complexes are systematically higher than for unidentate pyridine complexes, except for that of 3,3' dimethyl-2,2'-bipyridyl, which is too closely sterically hindered to permit chelation and whose 2J lies in the range of the pyridine complexes (51). Recently, Alcock et al. have demonstrated a similar increase in 2J for dithiol compounds; by analogy with crystal structures, it is suggested that the increase observed in 2J on chelation may be due to the slight bending of the primary interaction (76).

The above has described the theoretical interpretation of NMR parameters. An entirely distinct approach, used

widely in $\text{CH}_3\text{Hg(II)}$ studies, is the *analytical* use of NMR as an empirically based probe to monitor the exact contents of a solution. In 1957, Gruenwald et al. (91) demonstrated that a carbon-bonded proton close to an acidic site was responsive to the state of protonation at that site; thus empirical determination of chemical shifts in these two states, and of a mixture of the two at known pH, can yield the dissociation constant of the acid site. By monitoring the chemical shift of a proton remote from one acid site but close to another, the ionisation of the latter alone can be investigated, permitting the possibility of accurate measurement of microconstants. The approach is exemplified by the study of GSH and CH_3HgSG performed by Rabenstein (69). Determination of formation constants of ionised ligands with other species (such as $\text{CH}_3\text{Hg(II)}$) by competition with proton for acid sites, has been performed for amines, carboxylic acids and thioether compounds by Rabenstein and coworkers (2).

In Part 1 of this thesis, the binding of $\text{CH}_3\text{Hg(II)}$ by a variety of thiol molecules is studied by ^1H NMR spectroscopy. A competition method in which two different thiols compete for the $\text{CH}_3\text{Hg(II)}$, is developed for the measurement of formation constants for these complexes. With this method, formation constants have been determined

for a range of biologically and pharmaceutically important thiols, whose structures and nomenclature are presented in Table 3. In most cases the acid-base behaviour of both the free and complexed ligand is also fully characterised, permitting calculation of "microformation constants" for all forms, and prediction of apparent affinity for $\text{CH}_3\text{Hg(II)}$ at any pH value.

In Chapter IV, this method is applied to two dithiol molecules (2,3 dimercaptosuccinic acid and dithioerythritol) whose structures are also given in Table 3. Results are compared with those for the monothiols of Chapter III and discussed in the light of prevailing theories (see above) regarding the possibility of chelation in such systems.

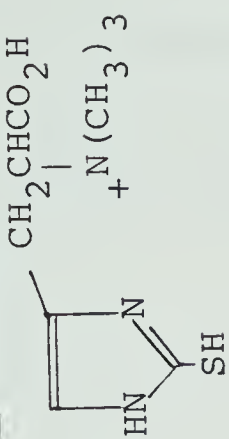
Chapter V is devoted to a study of the exchange kinetics of some of the ligands, measured using the linebroadening observed for the exchanging mercaptoacetate resonance. This is related to the complex lifetime using modified Bloch equations; the lifetimes in turn are related to a detailed kinetic scheme, and estimates of rate constants for exchange reactions involving individual acid-base species are obtained.

Thus, a wealth of data is obtained regarding the detailed solution chemistry of these complexes in these Chapters. Part 2 of this thesis, where a further extension

Table 3. Structure and nomenclature of thiols studied.

<u>Name</u>	<u>Abbreviation/Alternate Name(s)</u>	<u>Structure</u>
Mercaptoacetic acid	MAA, thioglycolic acid	$\text{HSCH}_2\text{CO}_2\text{H}$
Mercaptoethanol	ME	$\text{HSCH}_2\text{CH}_2\text{OH}$
Cysteine	CSH, β -mercaptoalanine	$\text{HO}_2\text{CCHNH}_2$ CH_2SH
Homocysteine	HCSH	$\text{HO}_2\text{CCHNH}_2$ $\text{CH}_2\text{CH}_2\text{SH}$
Penicillamine	PSH, β -mercaptovaline, 2,3 dimethylcysteine	$\text{HO}_2\text{CCHNH}_2$ $\text{CH}_3-\text{C}-\text{CH}_3$ SH
N-acetylpenicillamine	NPSH	$\text{HO}_2\text{CCHNHCCCH}_3$ $\text{CH}_3-\text{C}-\text{CH}_3$ SH
Mercaptosuccinic acid	MSA	$\text{HO}_2\text{CCH}_2\text{CHCO}_2\text{H}$ SH
Glutathione	GSH, γ -glutamylcysteinylglycine	$\text{HO}_2\text{CCHCH}_2\text{CH}_2\text{CNHCH(NH}_2\text{)CH}_2\text{CO}_2\text{H}$ NH ₂

Table 3 (continued)

<u>Name</u>	<u>Abbreviation/Alternate Name(s)</u>	<u>Structure</u>
Ergothioneine	Ergo	
Dithioerythritol	DTE	$\text{HSCH}_2\text{CH}(\text{SH})\text{CH}(\text{OH})\text{CH}_2\text{SH}$
2,3-Dimercaptosuccinic acid	DMSA	$\text{HO}_2\text{CCH}(\text{SH})\text{CH}(\text{SH})\text{CO}_2\text{H}$
2,3-Dimercaptopropane-1-sulfonic acid	BAL ^a SO ₃ H	$\text{HSCH}_2\text{CH}(\text{SH})\text{CH}_2\text{SO}_3\text{H}$

^aAbbreviation assigned by analogy with trivial name British Anti-Lewisite (BAL) for 2,3-dimercaptopropanol.

is made to studies involving hemoglobin and whole erythrocytes, provides an example of how quantitative data of this type can be of use in trying to understand more complex systems.

CHAPTER II

Experimental

A. Chemicals

Mercaptoethanol, mercaptoacetic acid (Eastman Kodak Co.), cysteine, penicillamine, 2 mercaptosuccinic acid (Aldrich Chemical Co.), glutathione, N-acetylpenicillamine, ergothioneine, 2,3 dithioerythritol, *meso* 2,3 dimercaptosuccinic acid (Sigma Chemical Co.) and homocysteine (Nutritional Biochemicals Corp.) were used as received. The preparation and determination of purity of the solutions of these thiols is described below.

Methylmercury(II) iodide was purchased from Terochem Laboratories Ltd. and Alfa Division, Ventron Corp., and converted to methylmercury(II) hydroxide by reaction with silver oxide. Details of the preparation and standardisation of solutions are given below.

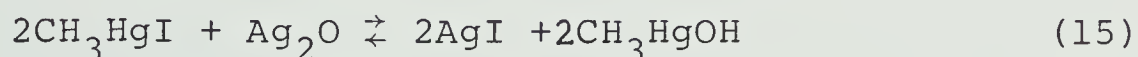
Iodoacetamide (Aldrich Chemical Co., Sigma Chemical Co.) was used as purchased.

All other chemicals were reagent grade and were used without further purification. Reagent water used for making solutions was doubly distilled and deionised by passage through a Barnstead D8902 Ultrapure mixed-bed ion exchange resin.

B. Preparation and Standardisation of Methylmercury(II) Hydroxide Solutions

1. Preparation.

Methylmercury(II) hydroxide was prepared from the iodide as follows. To silver oxide (2.32 g, 0.020 mole equivalents Ag) was added methylmercury(II) iodide (7.4 g, 0.022 mole equivalents Hg) and water (50 ml). The reaction is



The exact formulation of the hydroxide salt depends upon pH and concentration. Both methylmercury(II) iodide and silver iodide are insoluble in water. Silver oxide is sparingly soluble (solubility at 20°C = 1.3 mg per 100 ml (92)) so a slight excess of methylmercury(II) iodide was used to ensure no silver contamination of the product solution.

After stirring for ten hours, the solution was vacuum filtered twice, first through paper and then through a 0.2 μm pore size disposable millipore filter unit (Nalge Sybron Corp.), and diluted to 100 mls.

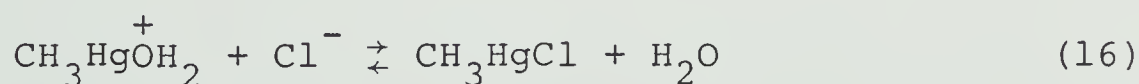
Previous studies using methylmercury(II) have found significant acetate contamination of methylmercury(II)

solutions (24). An ion-exchange method was developed to remove this. Since in the present study sulfhydryl groups are always present in stoichiometric amount or in excess, this additional step is unnecessary.

Yield (as determined by standardisation, see below) appeared virtually quantitative with respect to equivalents of silver ion added. In view of the toxicity of methylmercury(II), the concentrated stock solutions were opened only in the fumehood, and handled with gloves.

2. Standardisation.

Stock solutions were standardised using the titration with chloride ion developed by Fairhurst and Rabenstein (64). The reaction is



for which the formation constant is defined

$$K_f = \frac{[\text{CH}_3\text{HgCl}]}{[\text{CH}_3\text{HgOH}_2^+][\text{Cl}^-]} \quad (17)$$

The endpoint was detected potentiometrically using a silver/silver chloride indicating electrode and a saturated calomel reference electrode. To minimise the competition of hydroxide with titrant for $\text{CH}_3\text{Hg(II)}$ the titration was

performed in acidic solution, where the major fraction of methylmercury(II) exists as the hydrated cation. To increase the sharpness of the break at the endpoint, the titration was performed in a mixed water-ethanol system.

The procedure used involved pipetting 1 ml of the stock solution into a 100 ml beaker, and adding 5 mls of 1 *M* nitric acid, to reduce the pH to a low value. 40 mls of 95% ethanol were then added and the solution titrated with sodium chloride solution added from a Mettler DV10 autotitrator. The sodium chloride was dried for two days at 120°C and a sample carefully weighed, dissolved and diluted to volume. It was judged that within the precision of the methylmercury(II) titration itself, further prior standardisation of the chloride solution was superfluous.

The endpoint, taken as the point of maximum slope of the titration curve, was found from a graphical plot, such as in Figure 3. If any uncertainty existed, a differential plot was drawn to resolve the situation. The potential change on going from 1% before to 1% after the endpoint was typically 40 mV or greater. Replicates were taken until a relative precision of about 0.5% was obtained; normally, this entailed triplicate runs.

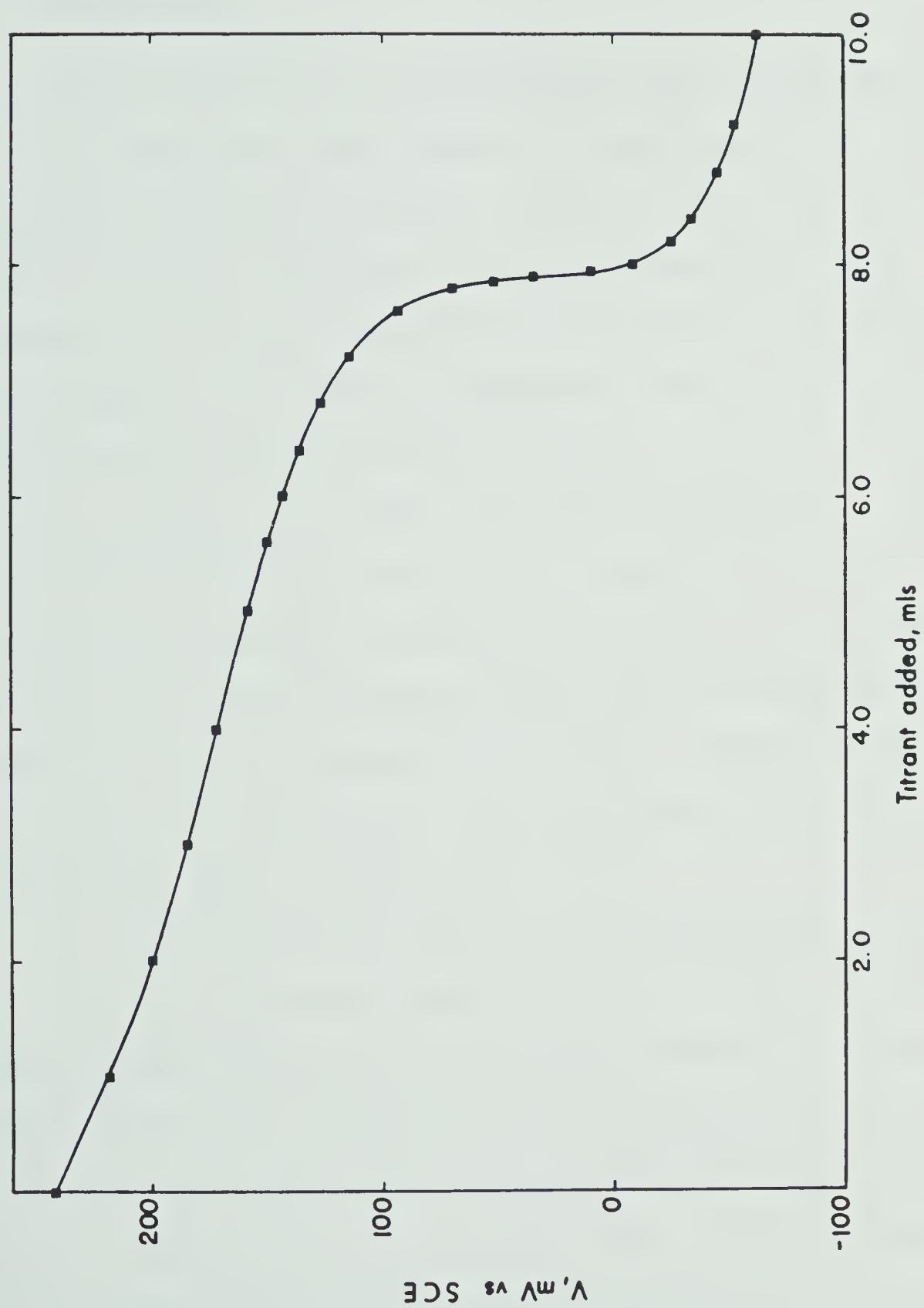


Figure 3. Potentiometric titration of methylmercury(II) with chloride ion.

C. Preparation and Standardisation of Thiol Solutions

1. Preparation.

Various studies (93,94) indicate that the stability of thiol solutions with respect to oxidation varies with the amount of oxygen present, trace levels of metal ions (which catalyze oxidation), pH and temperature. The preparation of thiol solutions was designed to minimise these factors. To freshly deionised water (10-50 ml) was added disodium EDTA solution (10^{-3} M, 0.2-1.0 ml) and the solution purged with argon for about ten minutes. The appropriate flask (10-50 ml) was flushed with argon before transferring the thiol (solid or liquid) to the flask. The solution was diluted to volume and the flask stoppered after filling the airspace with argon. The pH was checked before the final dilution; where necessary, this was adjusted to below 7 with nitric acid.

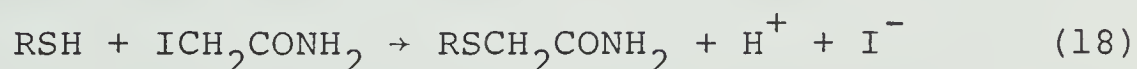
All the thiols but one were readily soluble at the 0.3 M level; this was a typical stock solution concentration. N-acetylpenicillamine displayed poor solubility in water; dissolution of the first portion of the solid lowers the pH to such an extent that the remainder will be in the neutral (presumably less soluble) form. Stepwise addition of the solid, with upwards pH adjustment to about 6

using sodium hydroxide, solved this problem.

The volumetric flask was then immediately transferred to the refrigerator (4°C) and never thereafter allowed to warm up, portions being withdrawn as required and the flask immediately returned to the refrigerator. Under these conditions, thiol solutions were fairly stable. Homocysteine, the least stable, showed only slight oxidation after two days; at the other extreme, mercaptoacetic acid solutions displayed no significant loss of thiol content over a period of four months.

2. Standardisation.

This was accomplished using a titration method based on that of Benesch and Benesch (95). A sulfhydryl group will react with iodoacetamide according to the reaction



The proton liberated during the reaction can be titrated with a strong base. However, in order for the reaction to be both quantitative and precise, several criteria must be fulfilled. If the protons liberated and titrated are to equal the sulfhydryl groups present, the initial and final pH must be identical, and low enough to ensure quantitative sulfhydryl protonation. However, the

pH selected should also be in a region of the acid-base titration curve of the sample where buffering does not occur, otherwise poor precision in the endpoint will result. Reaction must occur in a reasonable time; this necessitates raising the pH to approximately 9 after addition of the iodoacetamide.

The procedure is given here for mercaptoacetic acid. Since the pK of its carboxyl group is 3.50 and of the sulfhydryl 10.08, both quantitativity and good precision should be obtainable at pH 7.

A solution of sodium hydroxide ($\sim 0.07\text{ M}$) was prepared under carbonate-free conditions (96) and standardised against carefully weighed portions of potassium hydrogen phthalate (AnalaR, dried for 2 hours at 120°C) using phenolphthalein as indicator. Standard deviation among replicates was typically 1-2 ppt. A solution of nitric acid ($\sim 0.04\text{ M}$) was prepared and standardised against the sodium hydroxide solution using phenolphthalein as indicator. Standard deviation among replicates was 1-2 ppt.

Two standard solutions were prepared for colour-matching endpoints. The first contained pH 7 buffer (70 mls), phenolphthalein (0.1%, 6 drops) and bromothymol blue (0.1%, 4 drops), the second pH 7 buffer (120 mls), 6 drops phenolphthalein and 8 drops bromothymol blue. This

mixture of indicators is yellow at low pH, through green at pH 7 to blue, then to purple above pH 9.

To water (30 ml) in a 250 ml conical flask was added phenolphthalein (6 drops) and bromothymol blue (4 drops). The solution was purged with argon then 1 ml of sample pipetted in. The solution was brought to pH 7 (colour-match with first standard) and set aside under argon. The initial buret volumes (acid and base) were recorded.

Iodoacetamide (0.2 g) was dissolved in water (5 ml) and added to the flask. Base was immediately added from the buret to raise the pH and thus speed the alkylation reaction. Initially, as the reaction proceeded, the liberated protons lowered the pH (solution turned blue); more base was added to reestablish the purple colouration. Eventually, when the reaction was essentially complete, the purple persisted. The solution was set aside under argon for 2 minutes. Bromothymol blue (4 drops) was added, and acid from the buret added to lower the pH back to 7 (colour-matched with second standard). Final buret readings were recorded.

The amount of sulfhydryl present can be calculated from

$$\begin{aligned} \text{mmoles sulfhydryl present} &= \text{mmoles base} \\ &- \text{mmoles acid} \end{aligned} \quad (19)$$

The quantitativity of the reaction was established by Benesch and Benesch (95) and confirmed by Saetre (97) and Backs (98). Table 4 shows a typical set of results. Titrations were repeated until a precision of 5 ppt or better was achieved (usually 2 to 4 replicates). This procedure gave satisfactory results for mercaptoacetic acid, N-acetylpenicillamine, mercaptosuccinic acid and ergothioneine. For molecules with a sulfhydryl pK of below 10, a similar procedure employing a starting and final pH of 5.0 and a methyl red/phenolphthalein indicator system was employed. In principle this could be used for all the thiols, but the color changes involved are less clear and the possibility of carboxylate buffereing greater, so it was employed only when necessary.

Extension of the mid-titration "incubation" period at high pH had no apparent effect upon results obtained, except for some preliminary experiments with the vicinal dithiol sodium 2,3-dimercapto-1-propanesulfonate (BALSO_3Na). The titre in this case increased by about 2% when 5 minutes incubation was used. Since the sulfhydryl pK's (macro) for BALSO_3Na are about 9 and 11, it is probable that the small fraction of the second thiolate anion present at pH 9 accounts for the slow reaction. This is in agreement with the conclusions of Carlson et al., who studied

the kinetics of the thiol-iodoacetamide reaction in some detail (99). It may also be that attachment of one bulky $-\text{CH}_2\text{CONH}_2$ group to the molecule limits the accessibility of the second. No increase in titre for incubations beyond 10 minutes was observed. A similar effect was noted for 2,3 dimercaptosuccinic acid ($\text{pK}'\text{s} = 9.4$ and 11.0 respectively), also a vicinal dithiol; in this case a 5 minute incubation was sufficient. The 1,4-dithiol dithioerythritol predictably displayed no such effect and the normal 2 minute incubation was employed.

In all cases a titration blank was performed in the absence of any thiol. While the purity of the iodoacetamide used is not critical to the reaction itself, since it is added in excess, any acidimetric behaviour would lead to errors. The blank titre was small (~ 0.02 mls base or less) but varied from batch to batch, with the age of a batch, and with the time allowed in aqueous solution (it slowly decomposes). Blank values were subtracted from actual thiol standardisation titres, keeping incubation times similar for blanks and samples.

D. Instrumentation

1. pH measurements.

These were made at $25^\circ\text{C} \pm 1^\circ\text{C}$ with an Orion 701 digital

pH meter, equipped with either a standard glass electrode and a fibre tip junction saturated calomel reference electrode, or a micro-combination electrode. Fisher Certified Buffers of pH 4.00, 7.00 and 10.00 (nominal values) were used for routine three-point meter calibration. The exact pH of each of these buffers was established, and periodically checked, by comparison with freshly prepared N.B.S. pH standard solutions (100). Potassium hydrogen phthalate (0.05 *M*, pH(s) = 4.008 at 25°C), potassium dihydrogen phosphate/disodium phosphate (0.025 *M* in each, pH(s) = 6.865) and sodium carbonate/sodium bicarbonate (0.025 *M* in each, pH(s) = 10.012) were employed for this purpose. The uncertainty in the values of these solutions was about ± 0.005 pH units, and thus in any individual pH determination ± 0.01 pH units.

Some difficulties were experienced with measurements in solutions containing the dithiol molecules. After a few minutes' immersion, the pH reading would start to drift, typically over 0.3 pH units in 5 minutes. Such behaviour has been previously reported (although not explained) (101). The problem lies with the reference electrode; on switching to a double junction reference the problem disappeared. The reference electrode was immersed in 0.3 *M* potassium nitrate contained in a tube

with a porous ceramic plug at the lower end, which was immersed in the solution (standard or sample) of interest.

2. ^1H nuclear magnetic resonance measurements.

^1H NMR spectra were obtained at 60 MHz on a Varian Associates A60-D spectrometer equipped with a variable temperature controller. All spectra were run at 25°C, the temperature scale being calibrated by insertion of a narrow thermometer into the probe tube space.

Spectra were normally recorded at sweep rates of 0.1 Hz s^{-1} , with a pen response time constant of 0.25 s. Where lines became broad and low in intensity, the gain was increased and the pen time constant increased to 0.5, 1.0 or even 2.5 s to remove excess pen jitter. In these cases, the scan time was increased proportionally to avoid biasing of peak position. Reported data are the median of several scans taken in both directions.

Chemical shifts are reported relative to the methyl resonance of sodium 2,2-dimethyl-2-silapentane-5-sulfonate (DSS), but were measured relative to the central resonance of the tetramethylammonium (TMA) triplet, the tert-butyl resonance of *t*-butanol (TBA) or the single resonance of 1,4-dioxane. The chemical shifts of these are 3.17_5 , 1.24_3 and 3.74_8 ppm downfield respectively from DSS. A

particular reference was selected for an experiment to give a small (<50 Hz) shift separation between analytical resonance and reference, thus allowing the use of a narrow sweep width.

Calibration of spectrometer frequency sweep widths was checked periodically using a sample of TMA in water. The frequency offset was adjusted to centralise the TMA triplet on the chart paper, and the signal modulated with a low audio frequency signal (Hewlett-Packard Model 200 AB audio signal generator). The apparent sideband separation as recorded, and the actual frequency applied (as shown by a Heath Digital Frequency Meter) were then compared.

A similar method was used to establish accurately the TMA-dioxane chemical shift separation. A sample containing both was used. The audiofrequency was adjusted until the sideband from the dioxane resonance was exactly superimposed on the central TMA resonance; the separation of the peaks then equalled the audiofrequency applied.

For the accurate measurement of linewidths (width at half peak height) in the kinetic studies, it was also necessary to establish the "instrumental linewidth", the observed width for a nonexchanging signal. Comparison of many spectra run on the A60 D spectrometer shows the minimum value obtainable to be 0.37 ± 0.02 Hz, in agree-

ment with Fairhurst's estimate for the same machine (102). However, short-term variations are possible, due to magnetic instability. If for some reason shimming is non-optimal, part of the linebroadening observed could be incorrectly assigned to chemical exchange processes, unless variations in homogeneity are monitored. This was accomplished using the TMA triplet signal. The three peaks are ~ 0.5 Hz apart, thus (as shown schematically in Figure 4) the degree of resolution between these peaks provides a sensitive and convenient indication of field homogeneity. Observed linewidths were therefore corrected downwards by the amount by which the TMA linewidth(s) exceeded 0.37 Hz.

The high field spectrometers used in Part 2 will be described in Chapter VII.

3. Apparatus for potentiometric titrations.

Potentiometric pK determinations were performed using a minicomputer-controlled titrant addition and data collection system designed and built by J. Nolan (103). The author is grateful to Mr. Nolan for making this apparatus available.

The titration was performed in a 100 ml beaker, maintained at 25°C with a thermostatically controlled water circulating jacket. Titrant is added through a

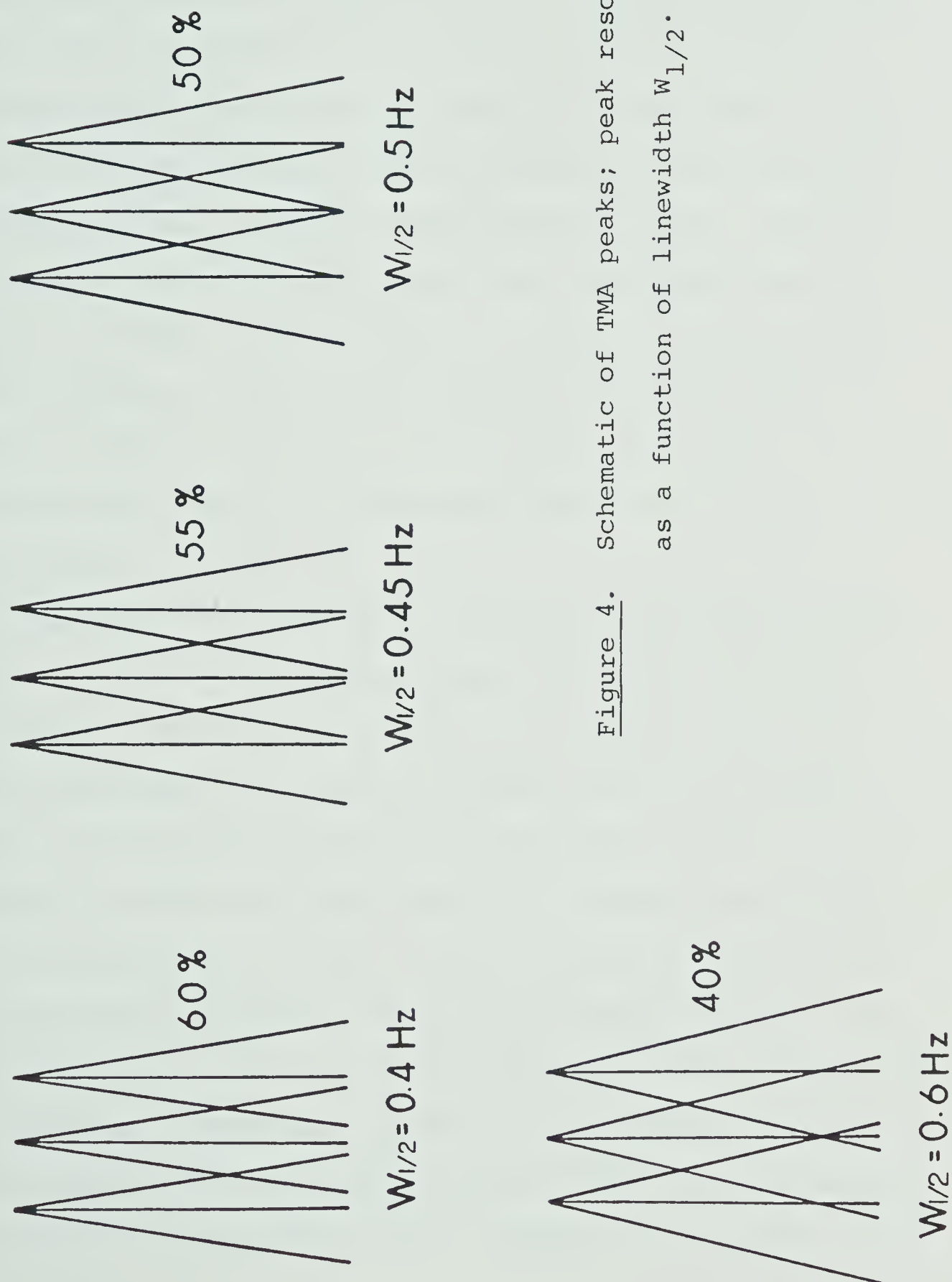


Figure 4. Schematic of TMA peaks; peak resolution as a function of linewidth $w_{1/2}$.

finely extruded glass tip placed under the surface of the sample (diffusion of titrant from the tip was found to be insignificant). Addition of titrant from the reservoir is controlled using an electromagnetic pinch valve. The weight of titrant delivered is monitored by placing the reservoir on an electronic top-loading balance. The pH is measured using the electrode setup described above. Values of weight and pH, as well as being displayed, are routed through a multiplexer/interface into the mini-computer (Digital Equipment Corp. model PDP 11-03). A further line from the computer controls the delivery pinch valve.

Operation is as follows. Firstly, a parameter input routine is run. This asks the user for value of final pH desired, pH increment between data points, size of initial delivery of titrant, minimum size of delivery, number of digitised values of pH and weight to be averaged for each recorded datum, and maximum permissible standard deviation in each. These parameters are stored in a specified parameter file on the magnetic floppy disc.

Next, the pH setup is standardised in the usual manner, the reservoir filled and placed on the balance, and the sample added to the titration vessel. The delivery system is carefully checked for kinks, bubbles, etc. in the

tubing and then the tip is immersed in the sample. The titration program is started in the computer. This asks for parameter file and data file names.

Hereafter, operation is automatic. The computer monitors the digitised values of pH and weight until the standard deviation in each (measured over the specified number of readings), is less than the specified minimum, typically .002 and .001 respectively. It then records these values on the printer and places them in the data file. The pinch valve is opened for a time corresponding to the initial delivery specified. When pH and weight readings have again settled down, they are recorded and the next addition is made. The size of the second and subsequent additions required to give the right pH increment between points is predicted by the computer. The slope ($\text{pH increment} \div \text{weight increment}$) between present and last point is compared with that between last and next-to-last. Assuming that the trend observed will continue to the next point, the slope to that point and hence its position can be predicted. The computer then opens the pinch valve for the required time. In regions of moderate slope, this approach works very well; in regions of high slope, the predicted slope tends to oscillate about the true value. This results in successive titrant additions

being alternately too large then too small, leading to clustering of data points in pairs. The problem is alleviated by specifying a slightly larger minimum addition, which also has the advantage of not generating an unreasonable amount of data (based on minute additions) in intermediate endpoint regions.

Sample solutions are described below. Details of the algebraic models used to interpret the results are given in subsequent sections.

E. Preparation of Solutions for pK Measurements

Where a trustworthy value for the acid dissociation constant of an ionisable group existed in the literature, this was usually adopted. A value was considered "trustworthy" if experimental conditions (especially ionic strength, temperature and constant type) were given, the uncertainty in the figure was stated and some attention was paid to the purity of the compound. Unfortunately, as is seen below, many literature values fail some or all of these criteria. Backs made compilations of reliable sulfhydryl-containing amino-acid pK's (104) and these were extensively used.

If no reliable value could be found, necessary pK's were measured. As in the formation constant studies, ionic

strength was maintained at or close to 0.3 throughout. See Appendix I for a discussion of ionic strength considerations. Three methods were employed for the measurement of pK's:

1. Preparation of a series of samples of the acid at known pH values, and measurement of the observed chemical shift of some resonance in fast exchange between two or more acid-base forms. This method was used for all pK's, except as noted below.
2. Computer-fitting of binding study data using the pK as an additional unknown parameter. This was found to be satisfactory provided simultaneous determination of too many parameters was not attempted. All pK's for methylmercury(II) bound species were determined thus, except for the carboxylate pK of methylmercury(II)-N-acetylpenicillamine (method 1) and the sulfhydryl pK of the monomethylmercury(II)-complexed dithiols (method 3).
3. Potentiometric titration, i.e. determination of the pH as a function of the degree of neutralisation, as calculated from the fraction of equivalents of acid or base added. This was used for all dithiol pK measurements.

The preparation of solutions for each of these will be

discussed in turn below. Details of the actual experiments, results and interpretations are given subsequently.

1. NMR method.

Solutions were made to be typically 0.05 - 0.10 M in the compound of interest, and also contained TMA nitrate (150-250 mg) or 1,4-dioxane (50 μ l) as a chemical shift reference. 10 to 30 mls (depending on the number of samples to be withdrawn) of solution were equilibrated at 25 °C under argon and the pH adjusted with a measured amount of potassium hydroxide to the highest value desired. Potassium hydroxide was used as base to remove sodium error in pH readings at the alkaline end of the pH scale. Concentrated potassium nitrate solution was added to adjust the ionic strength to 0.3. To maintain ionic strength at 0.3 thereafter, two approaches were used:

1. In the case of the pK 's of mercaptoacetic acid, which are essential to this work, ionic strength was initially adjusted to exactly 0.3 and the first sample withdrawn. The pH was adjusted for the next sample with nitric acid. The volume required was entered into a program in a Texas Instruments TI-58 calculator, previously entered with all concentrations, initial volume, size of withdrawal and approximate pK 's. The

program calculated existing ionic strength and returned as output the quantity of either KNO_3 solution or water required to restore ionic strength to 0.3. Final recording of the pH was done after this adjustment, although usually it had no effect on the reading.

2. For monobasic acids, the initial solution was made up to an ionic strength of 0.3. The titrating acid was also made 0.3 M in KNO_3 . Since the nitrate counter ion added exactly equals the hydroxyl ion or deprotonation site removed from solution, the ionic strength will always be 0.3.

After each pH was attained, a sample (0.3-0.5 ml) was withdrawn using an Eppendorf automatic pipettor, and put into the NMR tube, which was flushed out with argon before being capped. Sample tubes were stored in the refrigerator while waiting to be run.

The number of samples taken, and the pH spacing between them, varied with the individual experiments. Where a pK was known already to, say, 0.1, six tubes at 0.05 pH unit spacing would suffice; where both pK's for a dibasic acid were unknown, 25 or 30 samples from pH 2-11 might be taken.

Most pK's determined thus were for free sulfhydryl species. Those for the methylmercury(II) complexes were

generally determined by method 2 below. The exceptions are the carboxylate pK' for the methylmercury(II) complexes of N-acetylpenicillamine and MAA, which were determined by a method similar to the above.

2. Computer fit to pK during K_f study.

See below, under "Preparation of solutions for K_d measurements".

3. Potentiometric method.

Stock solutions, between $2 \times 10^{-3} M$ and $5 \times 10^{-2} M$ depending upon the solubility of the substance, were prepared as described above, and the sulfhydryl group(s) standardised. For the actual titration, an aliquot was taken so that the eventual concentration would be 1-5 mM. A quantity of stock methylmercury(II) hydroxide solution corresponding to the desired stoichiometry was then added from a 2.5 ml Gilmont micrometer-driven syringe. Ionic strength was adjusted and the solution diluted to final volume with argon-saturated water.

Titration, accomplished using the minicomputer-controlled system described above, were performed in both directions. Free dithiol molecules were at least sparingly soluble even at low pH, and a simple titration with con-

centrated ($\sim 0.5\ M$) base was employed. The monomethylmercury(II)-complexed forms of both dithiols (2,3 dimercaptosuccinic acid and 2,3-dithioerythritol) were very insoluble in their neutral, fully protonated forms. In these cases, stock solutions were made up with a known excess of standard base and a back-titration performed with concentrated acid, terminating at the onset of precipitation.

F. Preparation of Solutions for Displacement Constant Measurements

As explained below in detail (Section G) the $\text{CH}_3\text{Hg(II)}$ binding strengths of the different thiols were measured by competing each in turn with MAA for the $\text{CH}_3\text{Hg(II)}$ present. The main requirement in preparing the solutions was therefore that the relative amounts of MAA, $\text{CH}_3\text{Hg(II)}$ and competing thiol be exactly known. Usually the mole ratio was 1:1:1.

For the earlier part of the study, stoichiometry as predicted by the independent standardisations of thiol and methylmercury(II) solutions, was checked using the following procedure. Sufficient MAA to make the final solution 0.05 to 0.10 M in MAA was added from a 5 ml buret to a 30 ml beaker containing 150-250 mg TMA nitrate. An amount of methylmercury(II) hydroxide corresponding to 99% of

the MAA was added, and the solution adjusted to pH 12 and diluted slightly.

A sample of 0.3 ml was withdrawn, the NMR spectrum run and the MAA methylene resonance chemical shift determined. As shown below, this shift is -12.3 Hz for free MAA and +20.5 Hz, relative to TMA at 60 MHz, for the methylmercury(II) complex. Thus, provided fast exchange applies, δ_{obs} , the observed chemical shift, can be related to the mole ratio:

$$\text{Mole ratio (Methylmercury(II):MAA)} = \frac{\delta_{\text{obs}} + 12.3}{20.5 + 12.3} \quad (20)$$

In the region close to a ratio of 1.00, δ_{obs} provides a sensitive indication of the ratio $\delta_{\text{obs}} = 20.5$ gives a ratio of 1.00, 20.4/0.997, 20.3/0.994 and so on.

On the basis of the chemical shift observed, the mole ratio was adjusted to exactly 1:1 by addition of the calculated necessary amount of methylmercury(II), allowing for the sample already withdrawn. The calculated necessary amount of the competing thiol (based on its standardisation and that of MAA) was then added to give a 1:1:1 mixture.

This procedure was carried out for several of the

thiol molecules studied; however, it was found that stoichiometries given by the measurements did not differ significantly from those predicted. In later studies the various solution components were simply mixed together, the final composition being as above.

Samples were withdrawn for NMR analysis as before, titrating down in pH with nitric acid. Typically ten to twenty-five samples were taken, depending upon the parameters to be determined.

In the absence of the information the experiment is designed to find it is impossible accurately to predict the ionic strength behaviour of such a solution. It was found that by starting at high pH with an ionic strength of 0.4 and titrating with nitric acid 0.3 *M* in KNO₃, ionic strength (as calculated later) remained between 0.4 and 0.25. This was judged acceptable, since in this range activity coefficients are almost constant. See Appendix I.

G. Determination of Displacement Constants by NMR

Displacement constants, K_d , describing the process



are defined as follows:

$$K_d = \frac{[\text{CH}_3\text{HgSR}'] [\text{RS}^-]}{[\text{CH}_3\text{HgSR}] [\text{R}'\text{S}^-]} \quad (22)$$

These were calculated from the chemical shift behaviour of the MAA methylene resonance, as a function of pH and the amounts of the various solution components.

K_d can be calculated if the various concentration terms at equilibrium are known. In the present work the MAA was always exchanging, at a rate fast on the NMR timescale, between its various forms. Thus only a single resonance was observed. Its position at any pH is the weighted average of that for free and for bound MAA at that pH, the weightings being the fractions of total MAA free and bound respectively. Provided, then, that the complete pH profile of the chemical shift is known for these two extreme situations, the fraction of MAA free and bound can be determined. Substitution of these fractions into the mass-balance equations yields a solution for K_d . The final expression also contains various pH-dependent terms, which allow for the fact that only a (pH-dependent) fraction of total free, or bound, MAA is present in the particular state of protonation involved in the K_d expression given above. Algebraic derivations of these expressions will be given in Chapters III and IV.

In practise, a set of MAA chemical shifts and corresponding pH values were given to the general non-linear least-squares fitting routine KINET (105). The program takes the entire set of independent (x) variables and calculates predicted dependent (y) variable values, using any supplied constants, the current estimates of unknown parameters, and a user-supplied subroutine. These calculated y-values are then compared with the experimental ones, and the squared deviations employed in a matrix inversion method to yield new, better unknown estimates. In this way, the sum of squares of deviations is minimised, while the set of parameter estimates converges towards the optimal. In the present application, the independent variable would be pH, the constants for calculation previously determined pK values and chemical shifts of individual MAA species, the unknown(s) K_d and possibly some pK' values, and the dependent variable chemical shift.

A warning against using non-linear least-squares techniques to attempt to extract more information from data than is really there has appeared in the chemical literature (106). It is quite possible to fit data to an unjustified number of parameters. A convincing fit can be obtained but at least some of the estimates returned will be meaningless. Some care was devoted to avoiding this in

the present study. KINET supplies three indications as to the plausibility of a fit:

1. The final size of the sum of squares of deviations.

If a fit involving more parameters is attempted and the final deviation square sum is not significantly lower than for the previous, less sophisticated, fit, then the use of the extra parameter(s) is probably not justified.

2. The estimated standard deviation for the final value of each parameter. If this is large, it indicates that the data has at best only a peripheral dependence on the value of that parameter; asking KINET to estimate it simply raises the chances of biasing in the value of another parameter. The safest course is to determine the problem parameter independently in another experiment, and re-enter as a constant.

3. The correlation coefficient, an expression of the degree to which the estimates of two or more parameters can vary independently. A high value means that errors in estimates of these "coupled" parameters will tend to compensate for each other, making both (or all three, etc.) unreliable. In this case, independent determination of one or more of the coupled parameters is again the safest course. Alternatively, an assumption can be

made about the relative magnitude of the coupled parameters and a single parameter fit carried out; in that case, of course, the results are as good as the assumption made.

H. Determination of Acid Dissociation Constants

The acid dissociation constant, defined for the acid-base pair HA and A^- as

$$K = \frac{a_{H^+}[A^-]}{[HA]} \quad \text{or} \quad pK = -\log_{10}(K) \quad (23)$$

is used extensively throughout this work, since the pH dependent fractions of various acid-base forms of ligand molecules appear in displacement constant expressions. Methods for pK determination generally involve the simultaneous measurement of a_{H^+} , from the pH, and either the absolute values of $[A^-]$ and $[HA]$ or their ratio. In the present study, two methods were used: potentiometric titration and an NMR method.

In the potentiometric titration, a standardised solution of HA is titrated with standardised base, or a solution of A^- with acid. The concentrations of HA and A^- are then easily calculated from the fraction neutralised. The theoretical and experimental aspects of the approach

are discussed in some detail in the monograph by Albert and Serjeant (107).

In the NMR method, the chemical shifts for the same resonance in the HA and A^- forms of the molecule are determined. Provided fast exchange occurs between these forms, the chemical shift observed at any pH will be the mean of these two extremes, weighted according to their relative amounts. Thus, from this shift, the ratio $[A^-]/[HA]$ can again be obtained.

The precision in the measurement by the NMR method depends on that of the chemical shift measurement; this is often intrinsically less than in the potentiometric method. However, the potentiometric approach often requires prior standardisation of both sample and titrant and any errors in these will contribute to the final result. In practise the measurements yielded by the two methods were found to be comparable in precision.

Both methods yielded a set of data points, either titrant added or chemical shift as a function of pH. These were then fitted using KINET, as described above, to yield the best estimate for the pK. Methods for multiple pK's (separate or overlapping) are similar; particular cases will be described in Chapters III and IV below.

I. Measurement of Kinetic Parameters from NMR Linebroadening

Determinations of rates of reaction, and hence in some cases of rate constants, were made using a method based on broadening of the MAA NMR signals due to its exchange between free and bound forms. Figure 5 accompanies Becker's excellent discussion of lineshapes (108). This figure shows that for a proton on a molecule which is exchanging between two forms having distinct chemical shifts, assuming each form to have the same population, any of the illustrated spectra may result, depending upon conditions.

The critical parameter is the ratio of the rate of interchange (R in Fig. 5) to the resonant frequency difference between the two magnetic environments, in Hz. (Note that therefore this ratio is field dependent; at higher fields the separation *in ppm* will be the same but the separation *in Hz* larger.) In a) the rate is slow, and separate peaks are observed for the two species. In b) the rate is slightly faster and the peaks, although still distinct, begin to broaden. As the rate of interconversion increases further, in c) and d) the central valley between the peaks disappears and a single broad peak appears at the *mean* position. In practise, peaks in c) and d) will often be so broad as to be undetectable. As the rate again increases, in e), this single peak sharpens up; in the fast

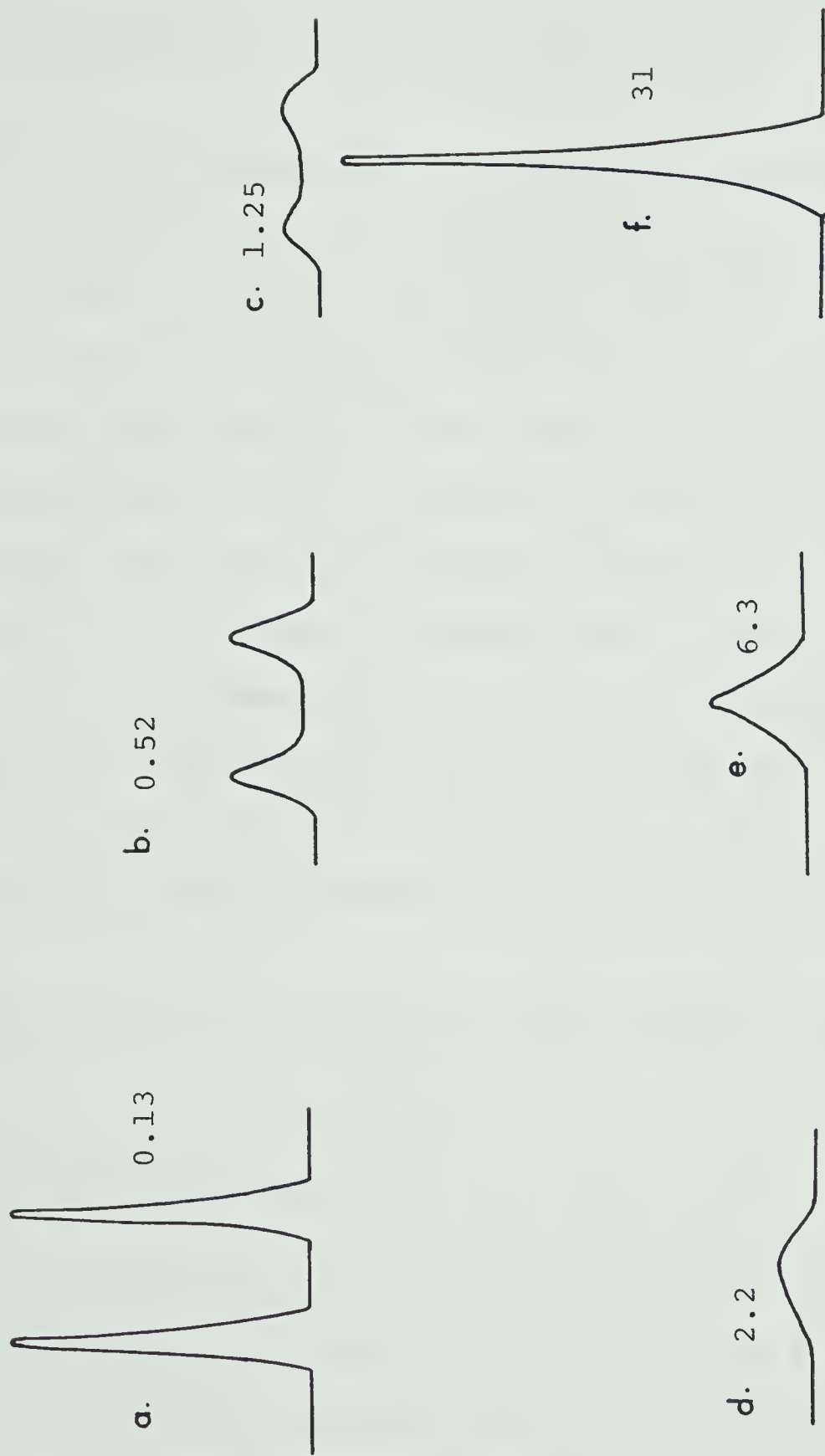


Figure 5. Predicted lineshapes at differing rates of exchange (108). Numbers shown are the ratio of the rate of interchange between the two sites to the separation (in Hz) of their resonances.

exchange limit, f), both its position and linewidth are the weighted mean of those for the separate peaks observed in a).

The present study used data collected in region e). Region d) yields lines too broad to be precisely measured, and f) lines too narrow, but in e) a fairly precise estimate of linebroadening can be made. Linebroadening is defined as that portion of the linewidth not due to instrumental factors or to intrinsic (relaxation-based) linewidth. The derivation of the equation relating linebroadening to the rate of exchange has been given in detail elsewhere (108); basically, it involves solution (109,110) of the Bloch equations for the time-dependence of magnetisation (111), suitably modified to account for interchange of the nuclei between two chemical environments (112).

The final equation for two-site exchange is of the form:

$$M_{ij} = \text{function}(\Delta w_c, \Delta w_f, T_{2c}, T_{2f}, \tau_c, \tau_f, P_c, P_f) \quad (24)$$

where M_{ij} is the magnetisation, Δw a Larmor precession frequency, T_2 a spin-spin relaxation time, τ the lifetime of a species and P its fractional population, and where the subscripts c and f refer to complexed and free species

respectively. The explicit form of (24) is complicated and will not be given.

In the present work, the complex lifetime τ_c was estimated by varying it until the optimal match between experimental (measured) lineshape and that predicted by equation (24) was attained. (A FORTRAN program written by Dr. D.L. Rabenstein, and modified for interactive operation, was employed for this calculation.)

Experiments involved mixing methylmercury(II) and MAA together in a 1:1 ratio as before, then adding a known amount of another thiol (cysteine, glutathione, penicillamine or MAA itself). Samples were withdrawn for NMR analysis as described above at carefully measured pH values. Both the chemical shift and the linewidth of the MAA methylene resonance were determined. P_f (and hence P_c) can be calculated from the chemical shift observed, knowing the chemical shifts for both free and bound MAA at that pH. Thus, the lifetime of the complex can be determined, as described above.

On the basis of the added concentrations of the three components, the pH, and some knowledge of pK 's and K_f 's, it is possible to calculate the concentrations of all species in solution. Thus various kinetic hypotheses can be tested against the observed rate versus pH profile. Details of this work are reported in Chapter IV.

CHAPTER III

The Binding of Methylmercury(II) by Monothiols

The purpose of this study was to characterise in as much detail as possible the distribution of methylmercury(II) among small sulfhydryl-containing ligands of biological or pharmaceutical significance. The problem can be conveniently divided into two parts: elucidation of the acid-base behaviour of the ligands, both free and in their methylmercury(II) complexes, and characterisation of the actual binding behaviour itself.

The first of these areas reduces to measurement of the acid dissociation constants (pK 's) of the various ionisable groups, for which standard techniques exist, as described in Chapter II.

The second reduces to measurement of formation constants (K_f 's) for methylmercury(II)-thiol complexes. It should be noted that in most cases studied, the complex can exist in more than one form, the various forms differing in the state of protonation at any other ionisable group. For instance, Figure 6, which shows the acid-base and complexation equilibria for mercaptoacetic acid (MAA) in a solution containing $CH_3Hg(II)$, indicates that two

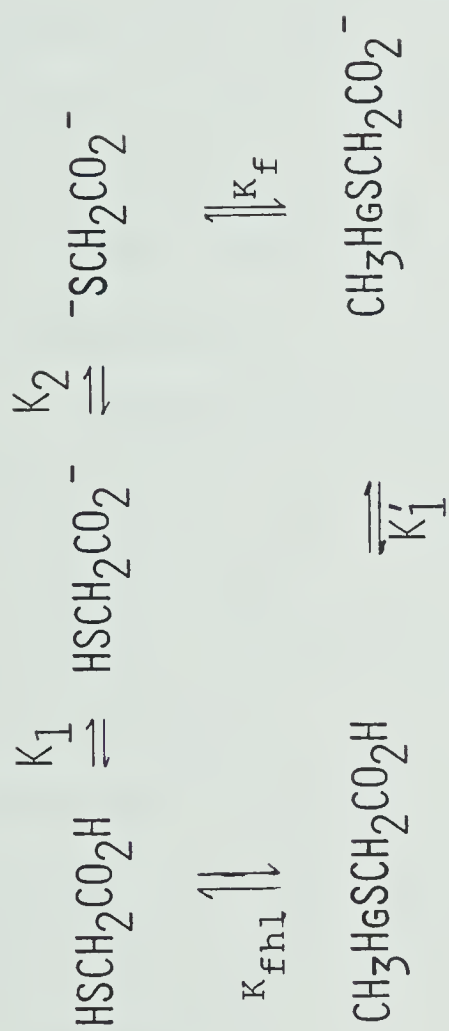


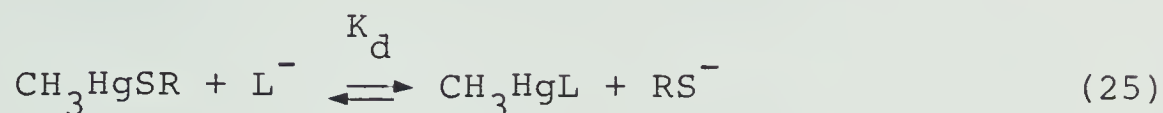
Figure 6. Mercaptoacetic acid species and equilibria in a solution containing methylmercury(II).

complexes form, $\text{CH}_3\text{HgSCH}_2\text{CO}_2^-$ and $\text{CH}_3\text{HgSCH}_2\text{CO}_2\text{H}$. Nevertheless, as shown below in Section 4b, measurement of any one formation constant suffices to describe the behaviour of a given system at any pH, provided all pK's are also known. Other K_f 's (defined in terms of different acid-base species) can then be calculated, as the product of the original K_f and a ratio of K's.

As discussed in the introduction (Chapter I) there exists in the literature only a single precise, unambiguous measurement of a K_f for a methylmercury(II)-thiol complex. Schwarzenbach and Schellenberg were able to measure $\log K_f = 16.12$ for the mercaptoethanol complex (15). However, much of the success of their potentiometric method was due to the simplicity of mercaptoethanol's acid-base chemistry. At all reasonable pH values, only the sulfhydryl ionisation is significant. The ligands of the present study have generally more complex ionisation behaviour, so poorly defined potentiometric titration curves would result. It therefore seemed likely that monitoring speciation by NMR would yield more precise results. A wide variety of studies (2) have demonstrated that small equilibrium constants can be measured with good precision by this method.

In order to measure *large* formation constants, it is

desirable to employ a *competing* ligand, L^- , and measure instead the position of the *displacement* equilibrium:



for which is defined the displacement constant, K_d :

$$K_d = K_{f_2} / K_{f_1} \quad (26)$$

where K_{f_1} is the formation constant of CH_3HgSR and K_{f_2} that of CH_3HgL .

It was then necessary to find a competing ligand for $CH_3Hg(II)$ sufficiently strong in its binding to reduce K_d to a reasonable value (ideally 0.1 to 10).

Table 5 shows formation constants for a wide variety of methylmercury(II) complexes. It can be seen that no ligand, except possibly CN^- , is sufficiently strong to give a small K_d . (In fact, it turns out that most sulfhydryl K_f 's are higher than mercaptoethanol's, so CN^- is not suitable (113).) On the other hand, S^{2-} is too strong. For this reason, it was decided here to employ another thiol molecule as the competing ligand. This approach has three advantages:

1. In the presence of excess thiol, free methylmercury(II) concentration is indeed minute, as assumed in the neglecting of possible acetate contamination described

Table 5. Formation constants for $\text{CH}_3\text{Hg(II)}$ complexes.

<u>Ligand</u>	<u>$\log K_f^b$</u>
F^-	1.50
Cl^-	5.25
Br^-	6.62
I^-	8.60
NH_3 (N) ^a	7.60
$\text{NH}_2\text{CH}_2\text{CH}_2\text{NH}_2$ (N)	8.25
CN^- (C)	14.1
$\text{HOCH}_2\text{CH}_2\text{S}^-$ (S)	16.12
S^{2-}	21.2

a) Letters in parentheses indicate coordinating atom.

b) From reference 15.

in Chapter II. (In fact, K_d terms, as the ratio of two formation constants, contain no explicit mention of free methylmercury(II) at all.)

2. Since different sulfhydryl groups are likely to have similar formation constants, K_d is likely to be small in all cases (i.e. between 0.1 and 10).
3. It is intuitively satisfying to measure the *comparative* binding strengths of different thiols, since it is these parameters, not actual binding strength to any one ligand, which will help determine the distribution of methylmercury(II) in biological systems. In addition, since the absolute value of $\log K_f$ for the mercaptoethanol complex is known, $\log K_f$ for the other thiols can be calculated. (This, of course, presupposes that the MAA/mercaptoethanol competition study is performed.)

Section A below describes the selection of mercaptoacetic acid (MAA) as the competing ligand for these studies, measurement of its acid dissociation constants and the competition study with mercaptoethanol. Section B reports studies with other ligands. Section C summarises the data obtained, and gives some discussion and conclusions.

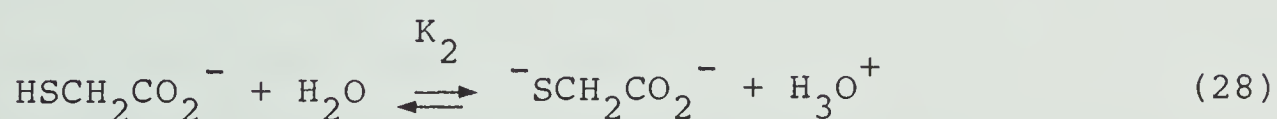
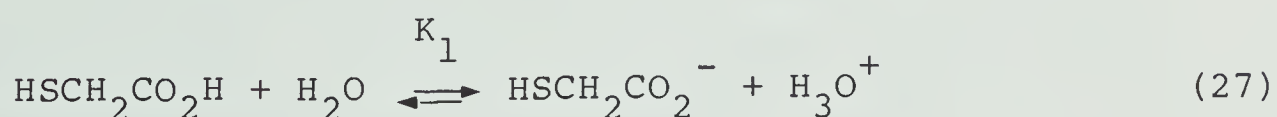
A. Mercaptoacetic Acid Studies

1. Selection of MAA as competing thiol.

Mercaptoacetic acid (MAA), $\text{HSCH}_2\text{CO}_2\text{H}$ was chosen as competing thiol for three reasons. Firstly, it is known (and was confirmed) to be relatively resistant to oxidation by air exposure (114). Secondly, it has relatively simple acid-base behaviour, two $\text{pK}'\text{s}$ in the free form and only one in the complexed form (see, however, below). Further, its NMR spectrum consists of only a single line whose position is strongly dependent on both state of protonation and degree of complexation. The chemical shift of this resonance formed the basis of all measurements discussed in Chapters III, IV and V.

2. Determination of $\text{pK}'\text{s}$ for free MAA.

Consider the ionisations of MAA:



for which the (mixed) ionisation constants are defined:

$$K_1 = \frac{[\text{HSCH}_2\text{CO}_2^-] a_{\text{H}^+}}{[\text{HSCH}_2\text{CO}_2\text{H}]} \quad (29)$$

$$K_2 = \frac{[\text{SCH}_2\text{CO}_2^-] a_{\text{H}^+}}{[\text{HSCH}_2\text{CO}_2^-]} \quad (30)$$

It is easily shown that the fractions, α , of the total MAA in each of the three forms are given by

$$\alpha_{\text{HSCH}_2\text{CO}_2\text{H}} = \alpha_1 = (a_{\text{H}^+})^2 / D \quad (31)$$

$$\alpha_{\text{HSCH}_2\text{CO}_2^-} = \alpha_2 = a_{\text{H}^+} \cdot K_1 / D \quad (32)$$

$$\alpha_{\text{SCH}_2\text{CO}_2^-} = \alpha_3 = K_1 \cdot K_2 / D \quad (33)$$

where

$$D = (a_{\text{H}^+})^2 + a_{\text{H}^+} \cdot K_1 + K_1 \cdot K_2 \quad (34)$$

Each of the three forms will display a distinct chemical shift. Provided fast exchange applies, the observed shift will be the weighted average:

$$\delta_{\text{obs}} = \delta_1 \alpha_1 + \delta_2 \alpha_2 + \delta_3 \alpha_3 \quad (35)$$

where δ_{obs} is the observed shift and δ_1 , δ_2 , δ_3 those for

the individual species.

Thus, by varying pH and observing δ_{obs} , it was possible to determine K_1 , K_2 and the three chemical shifts. Figure 7a shows the chemical shift data. Crude estimates can be obtained by inspection, the chemical shifts from the plateaux, the pK's from the inflection points of the curve. The non-linear least-squares computer routine KINET was used to provide more precise estimates based on a fit to the entire curve. This was accomplished as follows: firstly, the values of δ_1 , δ_2 and δ_3 were supplied to the KINET routine as constants. For every datum point, the program then calculated the values of α_1 , α_2 and α_3 according to equations (31)-(34) above, using initial estimates of K_1 and K_2 . The value of the observed chemical shift *expected* was then calculated according to equation (35) and the deviation from the actual measured value obtained. KINET summed the square of all such deviations, and performed a numerical routine to *alter* the K_1 and K_2 estimates so as to lessen the deviation square sum. This process was repeated until K_1 and K_2 both settled down to within the specified amount (in this case, 0.1%). More details on the operation of KINET were given in Chapter II. δ_3 , δ_2 and δ_1 were found to be 2.96_8 ppm, 3.18_4 ppm and 3.39_0 ppm respectively.

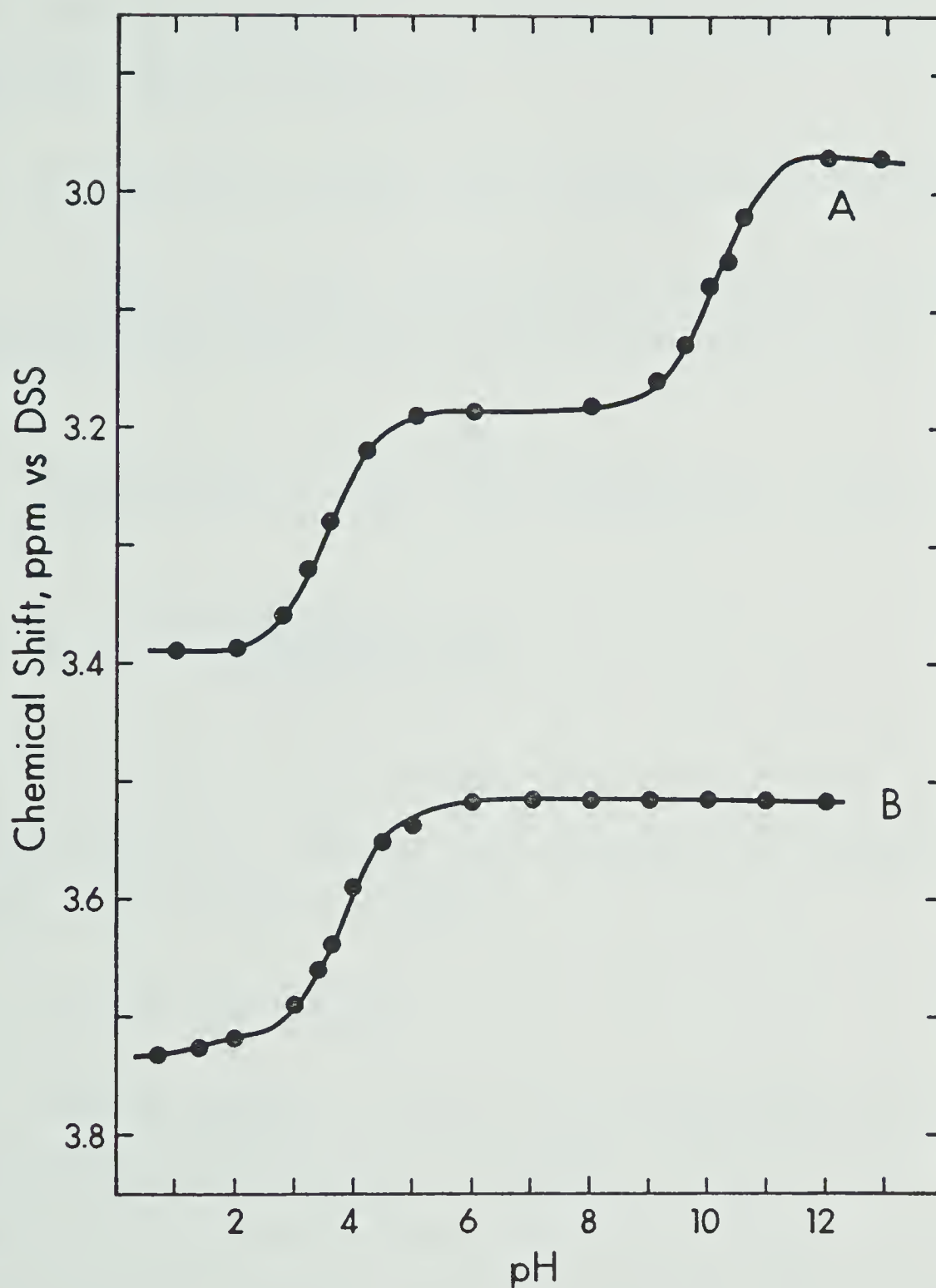
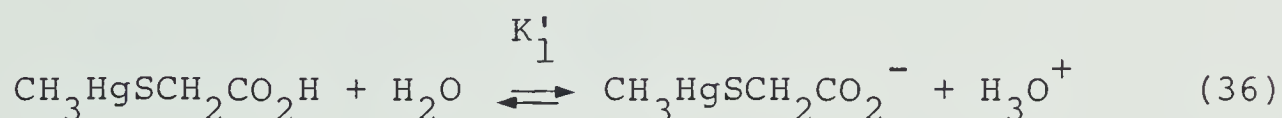


Figure 7. Chemical shift vs. pH data for A) free and B) methylmercury(II)-complexed mercaptoacetic acid. Points (here and elsewhere) are experimental and lines calculated from derived values of chemical shifts and equilibrium constants.

pK values are tabulated in Table 6 with literature values for comparison; given the considerable scatter in these, agreement seems reasonable.

3. Determination of pK's for methylmercury(II) complexed MAA.

It was initially assumed that methylmercury(II) complexed MAA would have only one ionisation step:



$$K'_1 = \frac{[\text{CH}_3\text{HgSCH}_2\text{CO}_2^-] a_{\text{H}^+}}{[\text{CH}_3\text{HgSCH}_2\text{CO}_2\text{H}]} \quad (37)$$

The prime in this context will always refer to a methylmercury(II) complex acid dissociation parameter. By analogy with Section 2 above:

$$\delta_{\text{obs}} = \delta_1' \alpha_1' + \delta_2' \alpha_2' \quad (38)$$

Thus as before, a plot of δ_{obs} versus pH will yield the three parameters δ_1' , δ_2' and pK'_1 . This is shown in Figure 7b. δ_1' was determined to be 3.715 ppm, δ_2' 3.517 ppm, and pK'_1 3.80. However, the non-plateau behaviour seen at low pH suggested that a further protonation could be occurring:

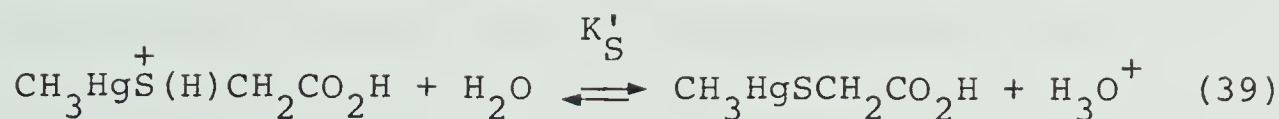
Table 6. Selected pK values for free and methylmercury(II) complexed mercaptoacetic acid.

pK_1^a	pK_2	pK_1'	Type ^c	Conditions	pK_1^b	pK_2^b	$pK_1'^b$	Reference
3.50 ±0.01	10.08 ±0.02	3.80 0.01	M	$\mu = 0.3$	3.50	10.08	3.80	This work
3.55	10.22	--	T	--	3.40	10.07	--	115
3.68	--	--	T	--	3.53	--	--	116
3.42	10.20	--	T	--	3.27	10.05	--	117
3.68	10.55	--	T	--	3.53	10.40	--	118

a) All values at 25°C.

b) Corrected to an ionic strength of 0.3.

c) T = thermodynamic, M = mixed.



$$K'_S = \frac{[\text{CH}_3\text{HgSCH}_2\text{CO}_2\text{H}] a_{\text{H}^+}}{[\text{CH}_3\text{HgS}^+(\text{H})\text{CH}_2\text{CO}_2\text{H}]} \quad (40)$$

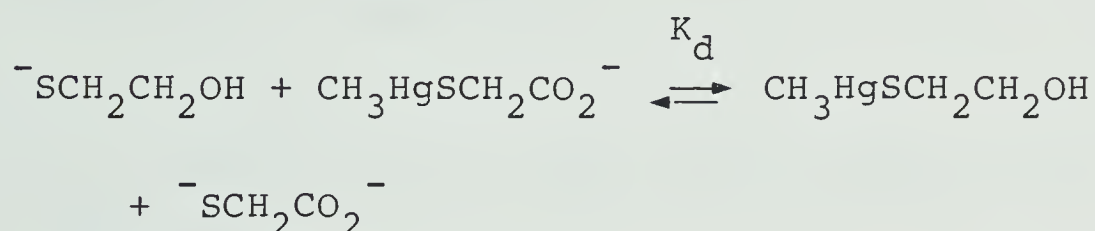
Since the sulfur atom in the postulated low pH form has three identifiable ligands rather than two, this process was termed "superprotonation". The experiment was repeated in greater detail between pH 0.5 and 2.0 in an attempt to determine $\text{p}K'_S$ and δ'_S (the chemical shift of the superprotonated species); however, the data obtained were inconclusive, due probably to the inability to maintain ionic strengths at reasonable levels. It was found that a slow shift to higher values occurred as the pH was lowered. A similar effect was observed by Fairhurst and Rabenstein for the glutathione-methylmercury(II) complex (64). At the lowest pH levels normally used in these studies (about 2) calculation shows that the maximum error incurred in predicted chemical shift by ignoring this effect would be ~ 0.002 ppm, comparable to the uncertainty in measuring chemical shifts. The inclusion or exclusion of this reaction appeared to have no effect on the calculated results from later experiments, therefore it was excluded.

4. Competition studies between mercaptoethanol and mercaptoacetic acid.

a. Derivation of Model

This model will be derived for the competition between mercaptoethanol and MAA for methylmercury(II) and then generalised for other competitions.

The displacement reaction can be written



where

$$K_d = \frac{[\text{SCH}_2\text{CO}_2^-][\text{CH}_3\text{HgSCH}_2\text{CH}_2\text{OH}]}{[\text{SCH}_2\text{CH}_2\text{OH}][\text{CH}_3\text{HgSCH}_2\text{CO}_2^-]} = \frac{K_{f,ME}}{K_{f,MAA}} \quad (41)$$

K_f 's being defined in the usual manner. Note that K_d does not depend on $[\text{CH}_3\text{Hg}^+]$; thus, the changes in speciation of $\text{CH}_3\text{Hg(II)}$, free in solution, are of no concern here.

Now if P_f is defined as the total MAA which is uncomplexed:

$$P_f = \frac{1}{C_{MAA}} \{ [\text{SCH}_2\text{CO}_2^-] + [\text{HSCH}_2\text{CO}_2^-] + [\text{HSCH}_2\text{CO}_2\text{H}] \} \quad (42)$$

where C_{MAA} is the total MAA concentration (free and com-

plexed). From the acid-base behaviour of MAA, it can be shown that

$$\alpha_{\text{SCH}_2\text{CO}_2^-} = \frac{K_1 \cdot K_2}{(a_{\text{H}^+})^2 + a_{\text{H}^+} \cdot K_1 + K_1 \cdot K_2} = \alpha_1 \quad (43)$$

where α_1 is the fraction of *free* MAA in the $\text{SCH}_2\text{CO}_2^-$ form. Thus

$$[\text{SCH}_2\text{CO}_2^-] = C_{\text{MAA}} \cdot P_f \cdot \alpha_1 \quad (44)$$

Similarly, considering the bound forms of MAA, it can be shown that

$$[\text{CH}_3\text{HgSCH}_2\text{CO}_2^-] = C_{\text{MAA}} \cdot (1 - P_f) \alpha_2 \quad (45)$$

where

$$\alpha_2 = \frac{K'_1}{(a_{\text{H}^+} + K'_1)} \quad (46)$$

Mercaptoethanol species are now considered. It is assumed that all methylmercury(II) is bound either to one thiol or the other (an extremely good approximation). Thus, provided $C_{\text{MAA}} = C_{\text{ME}}$, the concentration of *bound* mercaptoethanol must equal that of *free* MAA, i.e.:

$$[\text{CH}_3\text{HgSCH}_2\text{CH}_2\text{OH}] = C_{\text{ME}} \cdot P_f = C_{\text{MAA}} \cdot P_f \quad (47)$$

At reasonable pH values this will be the only likely form of bound ME. For the sake of generality, another α term, similar to the above, will be introduced at this point:

$$[\text{CH}_3\text{HgSCH}_2\text{CH}_2\text{OH}] = P_f \cdot C_{\text{MAA}} \cdot \alpha_3 \quad (48)$$

α_3 is unity here, but will vary in form for other thiols. By a similar argument, it can be shown that

$$(1-P_f)C_{\text{MAA}} = [\text{SCH}_2\text{CH}_2\text{OH}] + [\text{HSCH}_2\text{CH}_2\text{OH}] \quad (49)$$

giving eventually

$$[\text{SCH}_2\text{CH}_2\text{OH}] = (1-P_f) \cdot C_{\text{MAA}} \cdot \alpha_4 \quad (50)$$

where

$$\alpha_4 = \frac{K_{1,\text{ME}}}{(a_{\text{H}^+} + K_{1,\text{ME}})} \quad (51)$$

Substitution of equations (44), (45), (48) and (49) into (41) yields

$$\begin{aligned} K_d &= \frac{P_f \cdot C_{\text{MAA}} \cdot \alpha_1 \cdot P_f \cdot C_{\text{MAA}} \cdot \alpha_3}{(1-P_f)C_{\text{MAA}} \cdot \alpha_2 \cdot (1-P_f) \cdot C_{\text{MAA}} \cdot \alpha_4} \\ &= \frac{P_f^2}{(1-P_f)^2} \cdot \frac{\alpha_1 \alpha_3}{\alpha_2 \alpha_4} \end{aligned} \quad (52)$$

P_f is measured from the observed chemical shift, as described previously:

$$\delta_{\text{obs}} = \delta_f \cdot P_f + \delta_b \cdot (1 - P_f) \quad (53)$$

Thus

$$P_f = \frac{(\delta_{\text{obs}} - \delta_b)}{(\delta_f - \delta_b)} \quad (54)$$

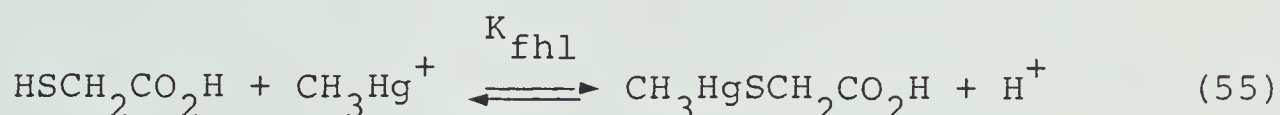
Since δ_f and δ_b can be calculated at any pH given the information in sections 2 and 3 above and the acid dissociation constants necessary for the calculation of the α 's have been determined, K_d is entirely described in terms of known quantities. In practice, more than one measurement is made, to improve precision.

Provided 1:1:1 mole ratios are used, equation (52) will apply equally well to competition of MAA with other thiols, provided the forms of α_3 and α_4 are modified suitably to account for the acid-base equilibria involved.

b. Notes on Completeness of Model

The above derivation relates the behaviour of the competition system to a single displacement constant. This may seem at first surprising, since there are (at least) two distinct complexes and hence, logically, two displacement reactions.

The apparent paradox is resolved with the help of Figure 6, which shows all MAA species (except super-protonated) and interrelating equilibria. K_{fhl} , the proton displacement/formation constant for the reaction



is the "missing" constant. However, thermodynamic principles dictate that the position of equilibrium in any reaction is independent of the reaction route taken. Here, there is a circular system of equilibrium constants; hence it follows that

$$K_{fhl} = \frac{K_f K_1 K_2}{K'_1} \quad (56)$$

which illustrates that K_{fhl} contains no new data not already contained in the other constants. In other terms: the model represented by equation (52), while not explicitly including K_{fhl} , does allow for the concentrations of all the species involved in that constant. K_{fhl} can easily be calculated. It is quite possible to reformulate the model entirely in terms of K_f and K_{fhl} ; in this case, K'_1 is redundant but can be calculated.

c. Results

15 samples containing a 1:1:1 mole ratio of MAA, mercaptoethanol and $\text{CH}_3\text{Hg(II)}$ were prepared between pH 12 and 2, as described in the experimental section (Chapter II). Figure 8c shows the plot obtained for the MAA methylene resonance as a function of pH. The plots for free and bound MAA are reproduced for comparison. Qualitatively, mercaptoethanol can be seen to compete relatively poorly with MAA for methylmercury(II), since the curve lies closer to that for bound MAA than for free, indicating that relatively little of the MAA has been displaced. The chemical shift vs. pH data was submitted to KINET and fitted to the relevant model, as described above.

Table 7 shows selected literature values for pK_1 of mercaptoethanol. The value of 9.62 obtained by Backs (119) was used since it was determined under the conditions most closely approximating those used in this study. Nonlinear least-squares fitting of the data with KINET yielded a satisfactory fit with $K_d = 0.16 \pm 0.01$. Allowing the value of $K_{1,\text{ME}}$ to vary as a second parameter did not significantly improve the fit, indicating that the value of $\text{pK}_{1,\text{ME}}$ used was reasonable.

Assuming the value of $\log K_{f,\text{ME}}$ measured by Schwarzenbach and Schellenberg, 16.12, it is possible to calculate

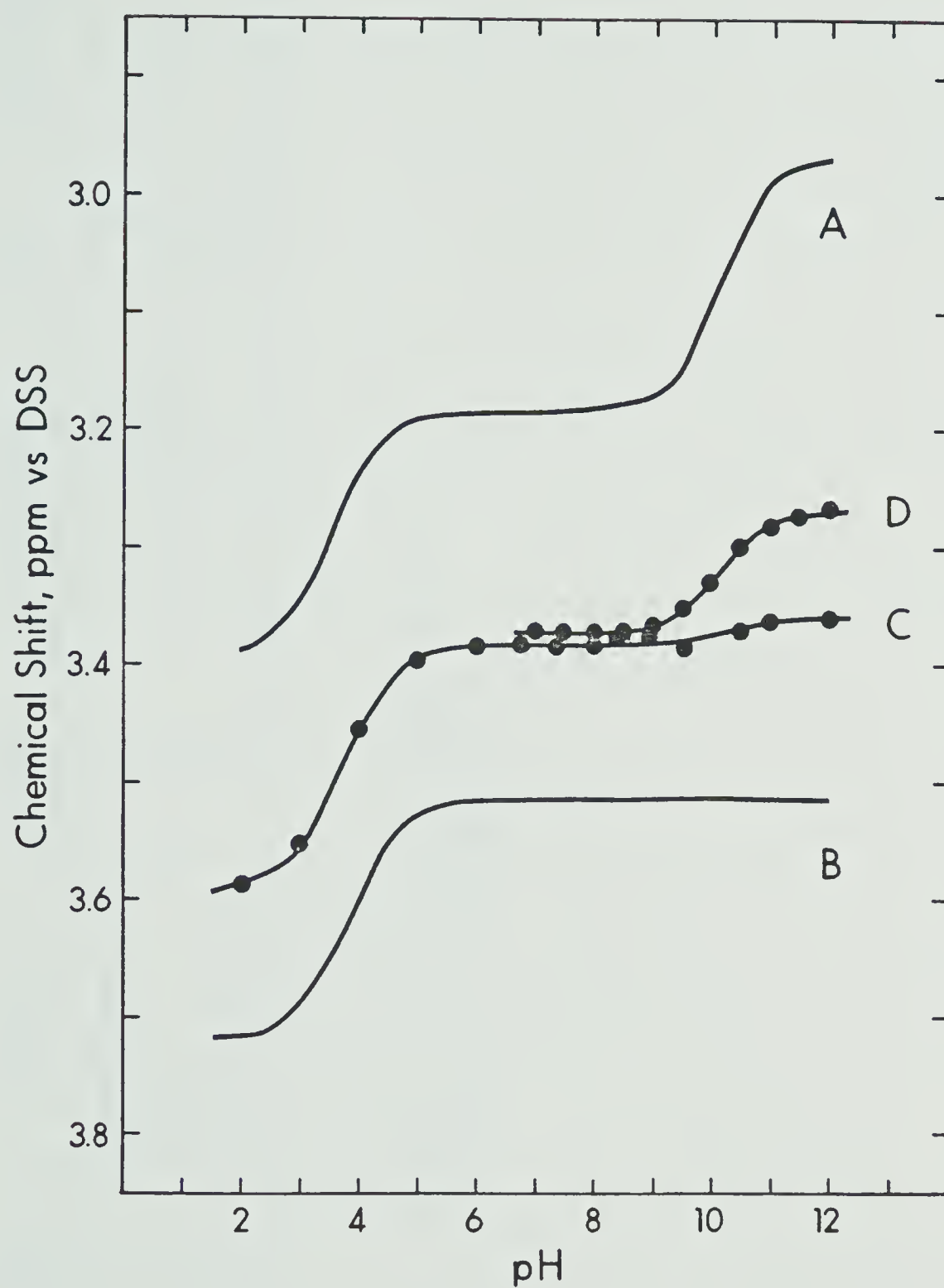


Figure 8. MAA methylene chemical shift vs. pH for a) free MAA, b) $\text{CH}_3\text{Hg(II)}$ -complexed MAA, c) as b) + 1 m.e. mercaptoethanol, d) as b) + 1 m.e. N-acetylpenicillamine.

Table 7. Selected pK values for mercaptoethanol.

pK	Method	Type ^c	Conditions ^a	pK ^b	Reference
9.57	Potentiometric	M	$\mu = 0.3$ NaClO ₄	9.57	119
9.62	N.M.R.	M	$\mu = 0.3$ NaClO ₄	9.62	119
9.52	Potentiometric	C	$\mu = 0.1$ KNO ₃	9.60	15

a) All values at 25°C.

b) Corrected to an ionic strength of 0.3.

c) M = mixed, C = concentration.

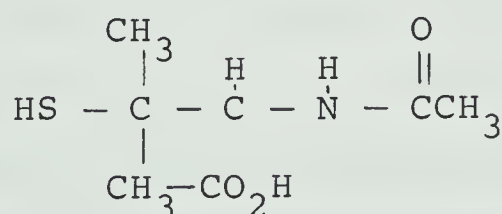
$\log K_{f,MAA}$ from this value for K_d ; a value of 16.92 is obtained, supporting the qualitative conclusion about the binding strengths of ME and MAA drawn above. The precision in this value, based on that in the K_d measurement, is ± 0.03 ; to this should be added any inaccuracy in the value taken for $\log K_{f,ME}$.

These values, and those of conditional and other derived formation constants, will be discussed below in conjunction with results for the other thiols.

B. Determination of Formation Constants with Other Thiol Ligands

1. N-acetylpenicillamine.

N-acetylpenicillamine (NPSH) has the structure



The amide nitrogen is non basic; the molecule has only two ionisable groups, the sulfhydryl and the carboxylic acid, and its acid-base scheme is therefore identical to that for MAA, differing only in the values of pK_1 and pK_2 . The values determined by Doornbos (120) for these, when corrected to an ionic strength of 0.3, are 3.33 and 10.19

respectively.

A 1:1:1 methylmercury(II):MAA:NPSH solution was prepared as described previously and 24 samples withdrawn. A plot of the results is shown in Figure 8d. As the pH was lowered towards 7 the MAA resonance became very broad; apparently chemical exchange of MAA between its free and bound forms is slow in this region. Below pH 7, no signal was observed; thus, it was impossible to obtain a value for pK'_1 for NPSH. However, since at pH 7 the carboxylate group is essentially quantitatively deprotonated in the free (and, as seen below, in the bound) form, the data available can be fitted using the mercaptoethanol model, to yield a value for K_d . KINET gave a satisfactory fit to such a model with $K_d = 0.70 \pm 0.02$, corresponding to $\log K_f = 16.76$ for the $\text{CH}_3\text{Hg(II)-NPSH}$ complex.

In order to check the validity of this assumption and complete the characterization of the solution chemistry of the N-acetylpenicillamine-methylmercury(II) complex, a further experiment was performed to evaluate pK'_1 . A 1:1 solution of $\text{CH}_3\text{Hg(II):NPSH}$ was prepared as before. The α -carbon methine proton should give the largest shift upon carboxylate protonation; unfortunately, this lies very close to the water peak and was difficult to observe. pK'_1 was evaluated using the small but definite change upon

protonation in the separation of the two β -methyl group resonances. (These methyl groups are nonequivalent, despite presumably rapid rotation around the main chain C-C bond, because the carboxylate-bearing carbon is a centre of asymmetry. Detailed conformational analysis shows that, barring coincidence, the *perceived* chemical shifts (which are an average of those in the various conformers, weighted by their populations) will be different for the two methyls (121).

11 samples between pH 4 and pH 2 were taken. KINET was employed to fit the equation:

$$\delta_{\text{obs}} = \delta_1' \cdot \alpha_1' + \delta_2' \cdot \alpha_2' \quad (57)$$

where δ_{obs} , δ_1' and δ_2' are peak separations. A satisfactory fit was achieved with $\delta_1' = 1.54 \pm 0.05$ Hz, $\delta_2' = 3.28 \pm 0.06$ Hz and $\text{pK}_1' = 3.10 \pm 0.07$. The precision in the measurement is not particularly good, due to the relatively small change observed, but does show that the assumption made above, that at pH 7 carboxylic acid protonated species could be neglected for the purposes of evaluation K_d , was justified.

2. Penicillamine.

The full acid-base dissociation scheme for penicillamine

is shown in Figure 9. Since the pH range in which the sulfhydryl and amino groups deprotonate is approximately the same, a full description of ionisation in this range necessitates the use of microconstants. Backs (119) calculated the following values, based on the measurements of Wilson and Martin (122) corrected to 25°C and an ionic strength of 0.3:

$$\begin{aligned} \text{pk}_1 &= 1.94, \text{pk}_{12} = 8.03, \text{pk}_{13} = 8.61, \text{pk}_{123} = 10.29, \\ \text{pk}_{132} &= 9.70 \end{aligned}$$

Note that the lower-case k here implies micro-equilibrium constants.

Where the exact relative amounts of the intermediate species (I and II in Fig. 9) are irrelevant, as in, for instance, calculation of the fraction of fully deprotonated penicillamine, a simpler model can be used:



K_2 and K_3 are macroscopic ionisation constants, describing only the extent of protonation of the whole molecule, without specifying the site where this is occurring. K_2 and K_3 are intuitively seen to be related to k_{12} , k_{13} , k_{123} and k_{132} . It has been shown (123) that

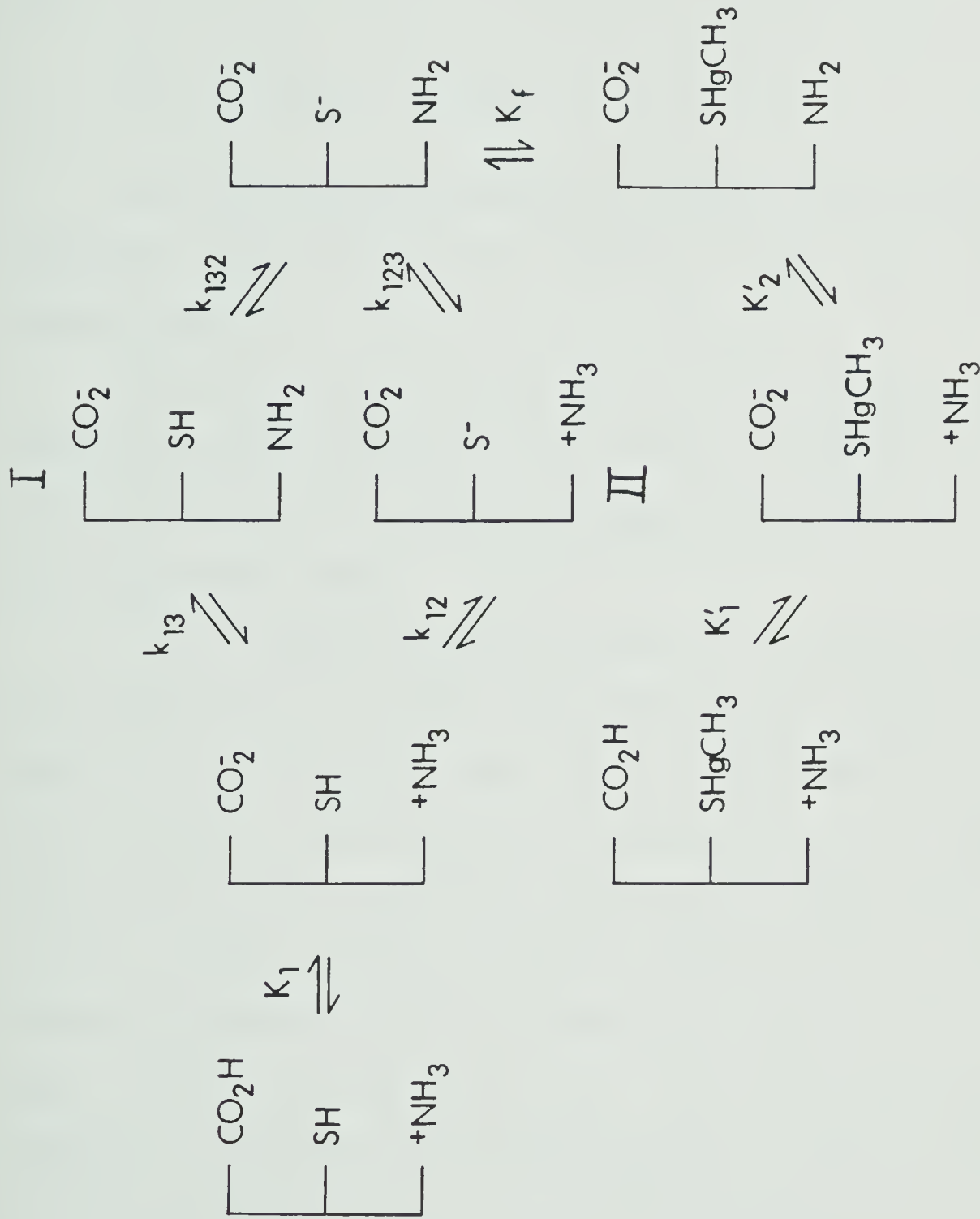


Figure 9. Ionisation and $\text{CH}_3\text{Hg(II)}$ binding scheme for penicillamine.

$$K_2 = k_{12} + k_{13} \quad (59)$$

and

$$1/K_3 = 1/k_{123} + 1/k_{132} \quad (60)$$

The values calculated for K_2 and K_3 , using the micro-constants given on page 96, were $pK_2 = 7.93$, $pK_3 = 10.39$ respectively.

The acid dissociation scheme for methylmercury(II)-complexed penicillamine is also shown in Figure 9. Again, the possibility of superprotonation was discounted in the pH range under study.

A 1:1:1 methylmercury(II):MAA:penicillamine solution was prepared as previously described and 23 samples withdrawn as the pH was varied. The chemical shift of the MAA resonance is plotted as a function of pH in Figure 10c. The chemical shift data was submitted to KINET and fitted to the relevant model as before. The fit shown in Figure 10c was achieved with the values $pK'_1 = 2.33 \pm 0.05$, $pK'_2 = 8.14 \pm 0.01$ and $K_d = 1.06 \pm 0.02$. The value obtained for $\log K_f$ for the PSH complex is 16.94, comparable to that for MAA. However, as discussed below, the differing acid-base chemistries of the two molecules dictate that at more moderate pH values their effective affinities for methylmercury(II) will differ.

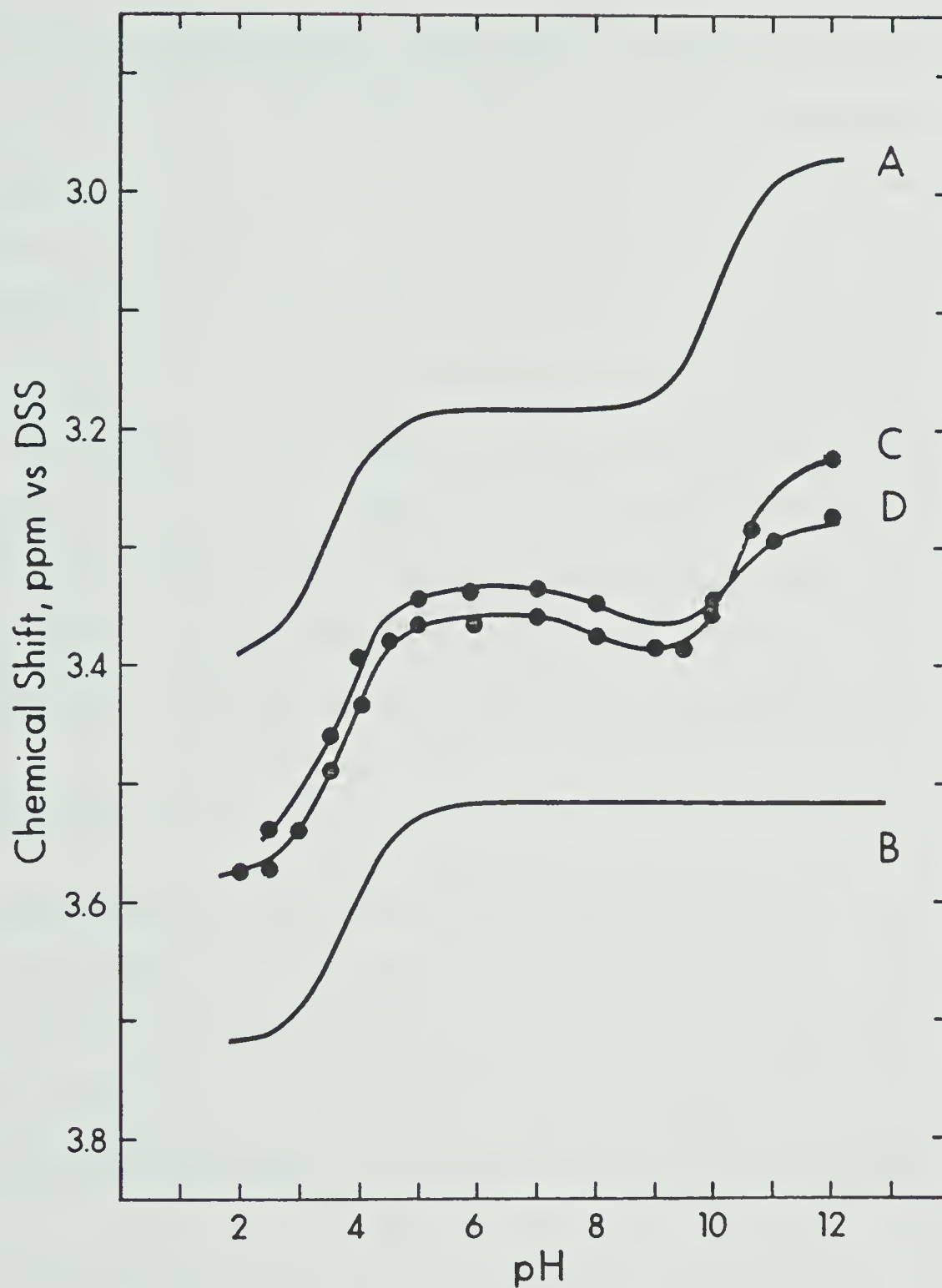


Figure 10. MAA methylene chemical shift vs. pH for a) free MAA, b) $\text{CH}_3\text{Hg(II)}$ -complexed MAA, c) as b) + 1 m.e. penicillamine, d) as b) + 1 m.e. cysteine.

3. Cysteine.

Cysteine ($\text{HSCH}_2\text{CH}(\text{NH}_2)\text{CO}_2\text{H}$) has one carboxylic acid, one amino and one sulfhydryl group, and can therefore be described by the same ionisation scheme as penicillamine. The macro pK values of 1.93, 8.22 and 10.25 corrected from the measurements of Ritsma et al. (124) and Coates et al. (125) by Backs to an ionic strength of 0.3 (119) were used here. 22 samples were taken as described above. Chemical shift data is shown in Figure 10d. The data obtained was submitted to KINET with the above constants, and a successful fit obtained with $K_d = 0.57 \pm 0.01$, $\text{pK}'_1 = 2.44 \pm 0.08$ and $\text{pK}'_2 = 8.80 \pm 0.02$. $\log K_f$ is calculated as 16.67.

4. Homocysteine.

Homocysteine ($\text{HSCH}_2\text{CH}_2\text{CH}(\text{NH}_2)\text{CO}_2\text{H}$) exhibits the same acid-base behaviour as cysteine and penicillamine, therefore the same schemes apply (see Fig. 9). The values obtained by Wallenfels et al. (126) for pK_2 and pK_3 gave 8.66 and 10.55 respectively when corrected to an ionic strength of 0.3.

A literature value for pK_1 could not be found. This was therefore measured in a separate experiment. A small triplet downfield from TMA in the NMR spectrum, due to the single methine proton on the α carbon atom, was found to

shift downfield about 0.4 ppm on protonation. Ten samples of homocysteine were taken between pH 3.00 and 1.20. The data was fitted in the usual manner to the equation

$$\delta_{\text{obs}} = \delta_1 \cdot \alpha_1 + \delta_2 \cdot \alpha_2 \quad (61)$$

A satisfactory fit was achieved with $\delta_1 = 4.260$ ppm, $\delta_2 = 3.87_7$ ppm and $\text{pK}_1 = 2.27$. Precision in the latter value was estimated at ± 0.02 by the program; however, in view of the low pH involved an uncertainty of ± 0.05 was assigned.

For the competition run to determine K_d , 22 samples were taken. Results are shown in Figure 11c. KINET yielded a satisfactory fit with $K_d = 0.34 \pm 0.01$, $\text{pK}'_1 = 2.26 \pm 0.06$, $\text{pK}'_2 = 9.12 \pm 0.02$. $\log K_f$ was calculated to be 16.45.

5. Mercaptosuccinic acid.

Mercaptosuccinic acid ($\text{HO}_2\text{CCH}(\text{SH})\text{CH}_2\text{CO}_2\text{H}$) has three ionisable groups, two carboxylic acid and one sulfhydryl. Values for the macroscopic ionisation constants in the literature show considerable variation; those determined by Porter and Perrin (127) appeared the most reliable. Corrected to an ionic strength of 0.3, these are $\text{pK}_1 = 3.13$, $\text{pK}_2 = 4.63$ and $\text{pK}_3 = 10.46$.

19 samples were taken between pH 12.0 and pH 2.5. The

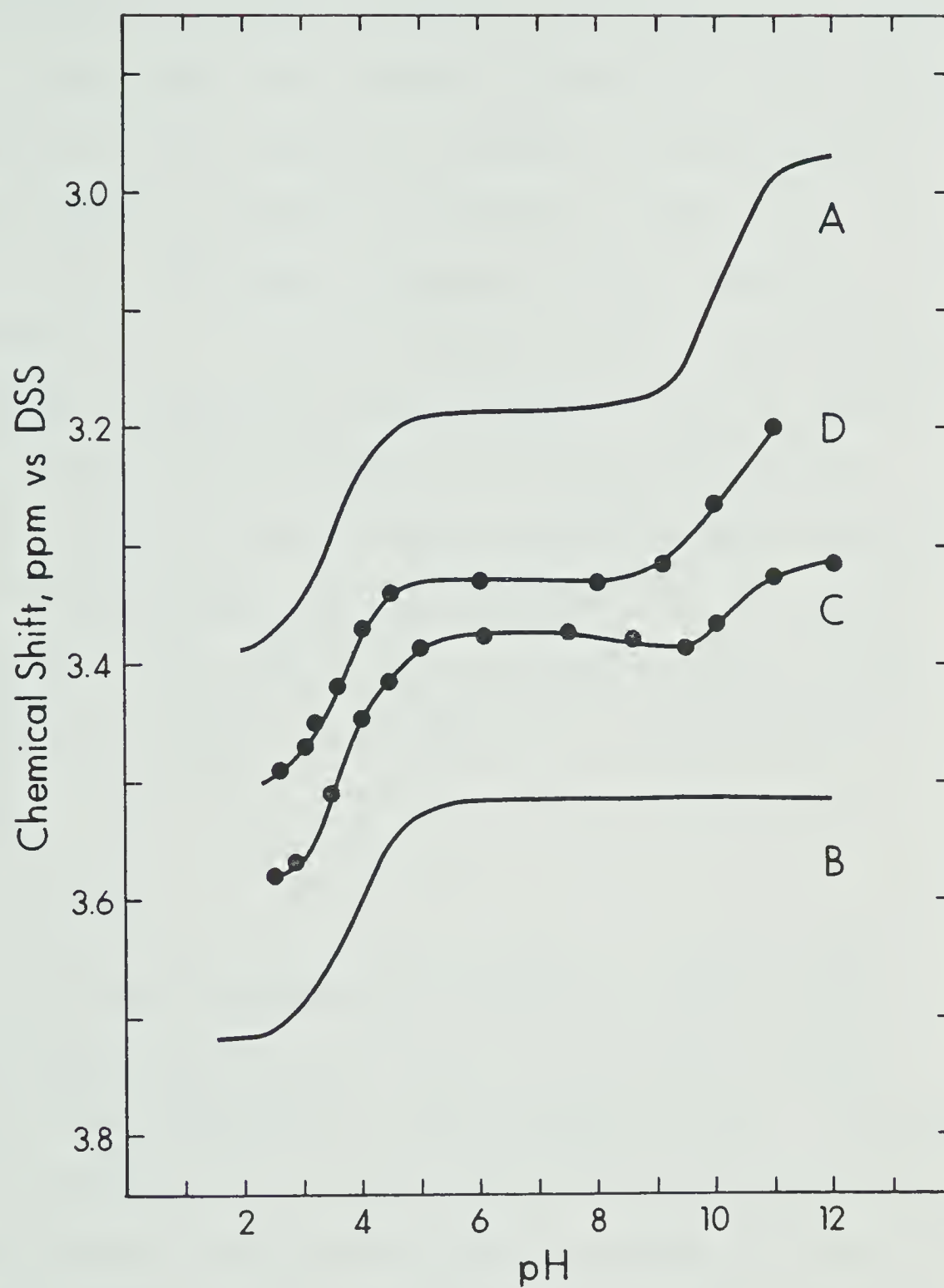


Figure 11. MAA methylene chemical shift vs pH for a) free MAA, b) $\text{CH}_3\text{Hg(II)}$ -complexed MAA, c) as b) + 1 m.e. homocysteine, d) as b) + 1 m.e. mercaptosuccinic acid.

chemical shift of the MAA resonance at pH 12.0 gave partial overlap of this peak with the TMA reference so the chemical shift could not be accurately measured. This part was therefore omitted. Results are shown in Figure 11d. A KINET run using the above pK values did not yield a satisfactory fit. A rerun allowing pK_3 to vary as a fourth unknown gave a very much more successful fit; the sum of residual squares was reduced by an order of magnitude. The estimates of the other three parameters were essentially unchanged. The value of pK_3 returned was 10.26 ± 0.02 . pK'_1 was 3.53 ± 0.03 , pK'_2 4.85 ± 0.02 and K_d 2.50 ± 0.06 , giving $\log K_f = 17.31$, the highest value measured for a monothiol.

6. Glutathione.

The sulfhydryl-containing tripeptide glutathione (γ -glutamylcysteinylglycine) has four ionisable groups (one amino, one sulfhydryl, two carboxylic acid). In order to describe fully the acid-base behaviour it is necessary to specify eight microdissociation constants, as shown in Figure 12a. However, for the purposes of the competition study the simplified scheme involving four macro constants shown in Figure 12b, is adequate. The values determined for these by Rabenstein (69), when corrected to an ionic

Figure 12a. Microscopic ionisation scheme of free Glutathione.

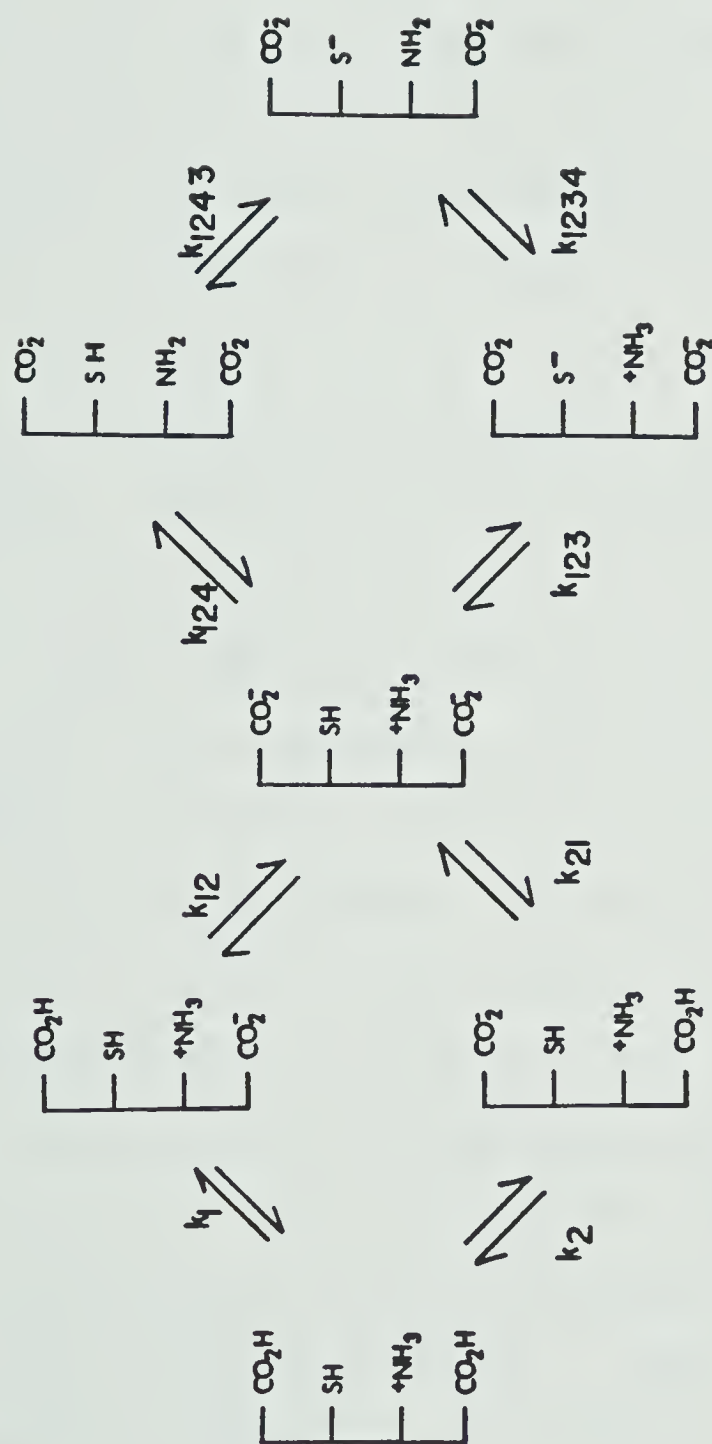
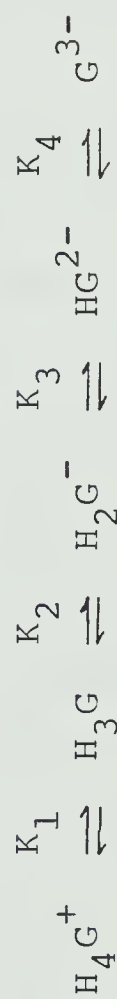


Figure 12b. Macroscopic ionization scheme of free Glutathione.



strength of 0.3, are 2.15, 3.49, 8.76 and 9.56 respectively.

20 samples were taken between pH 12 and pH 2.5.

Results are shown in Figure 13. KINET gave a satisfactory fit with $K_d = 0.12 \pm 0.002$, $pK'_2 = 3.63 \pm 0.04$ and $pK'_3 = 9.25 \pm 0.02$. No valid estimate was returned for pK'_1 ; the uncertainty exceeded the estimate itself.

Rabenstein previously determined values for pK'_1 , pK'_2 and pK'_3 (69). Corrected to an ionic strength of 0.3, these are 2.23 ± 0.07 , 3.52 ± 0.12 and 9.20 ± 0.02 . These values do not differ significantly from those determined in the present study. However, in view of the importance of this particular result, upon which much of Part 2 of this thesis is based, several additional KINET runs were performed in order to assess the sensitivity of the K_d value returned to the pK' values inputted. As the only valid estimate of pK'_1 , 2.23 was used throughout. Input of either, or both, of Rabenstein's values for pK'_2 and pK'_3 as constant(s) gave slight differences in quality of fit, but the values of any pK' values entered as unknowns remained in the range defined by the two sets of values above. In none of these fits did K_d vary to any significant extent; a value of 0.12 ± 0.01 is reported overall. Thus, $\log K_f$ (for fully protonated glutathione) is 16.00.

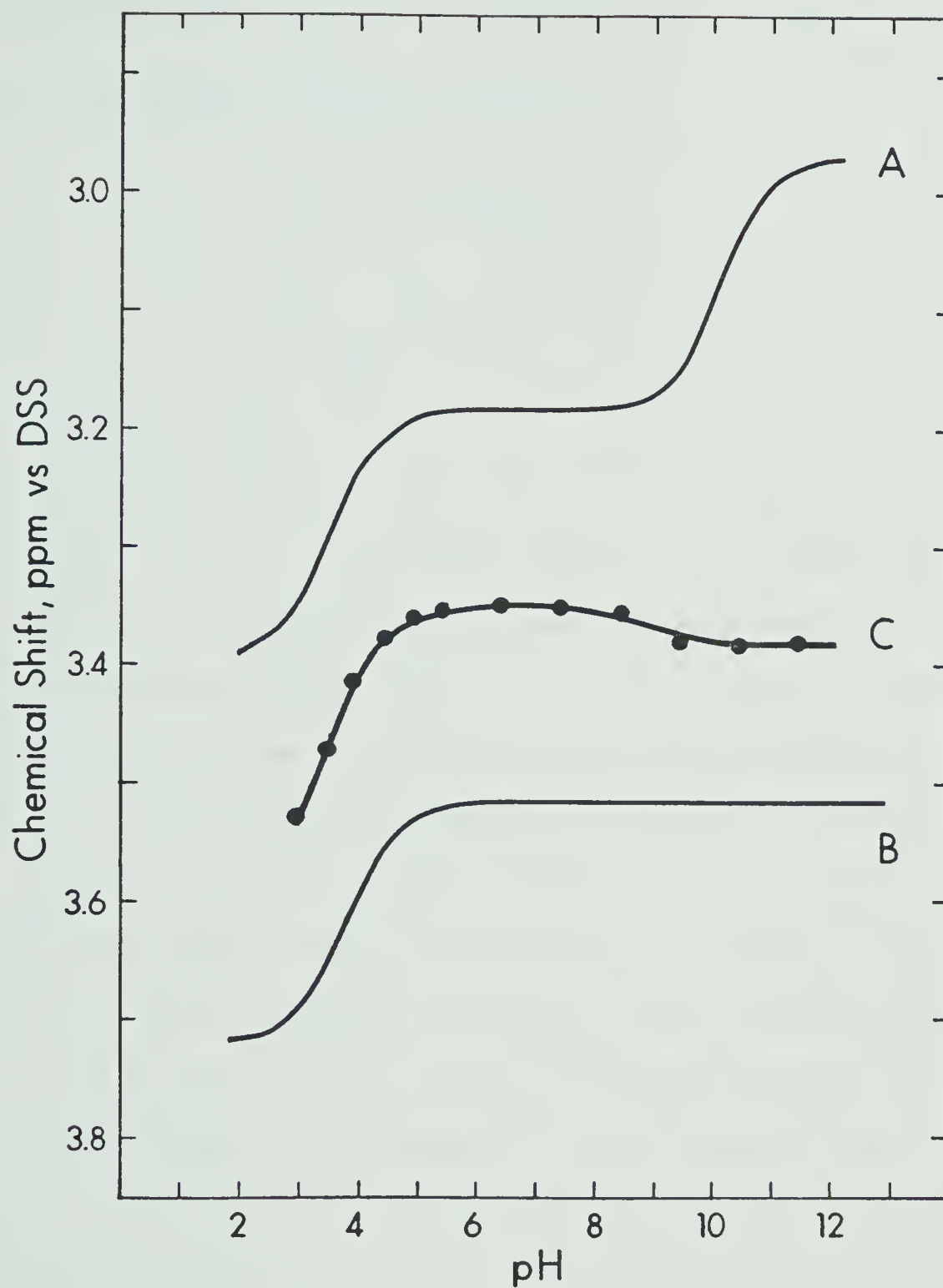
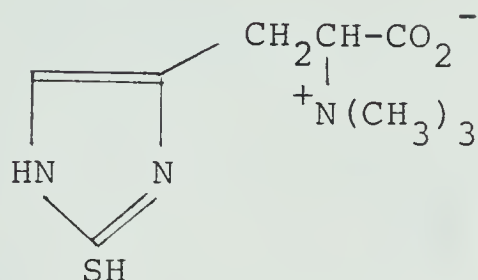


Figure 13. MAA methylene chemical shift vs pH for a) free MAA, b) $\text{CH}_3\text{Hg(II)}$ -complexed MAA, c) as b) + 1 m.e. glutathione.

7. Ergothioneine.

The structure of ergothioneine is



in its sulfhydryl form. Due, however, to thiol/thione tautomerism at the sulfur atom, many of the properties of this molecule are atypical. It was anticipated that K_d would be relatively low since only the fraction of ergothioneine present in the SH form would bind $\text{CH}_3\text{Hg(II)}$ strongly. (Calculations based on the results of Erni and Geier (62) give $\log K_f \approx 8.1$ for the complex of 1-methylpyridine-2-thione, another N-heterocyclic thione compound.) Support for this viewpoint comes also from observations of Hg(II) in red blood cells, where binding to other thiols (e.g. glutathione) is preferential over ergothioneine binding, as judged by the order in which resonances shift as increasing amounts of Hg(II) are titrated in (120).

The generally accepted ionisation/tautomerisation scheme for ergothioneine is shown in Figure 14. Note that due to tautomerisation, pK_2 is not strictly a dissociation constant per se, but also includes the thiol/thione equilibrium constant embedded in it.

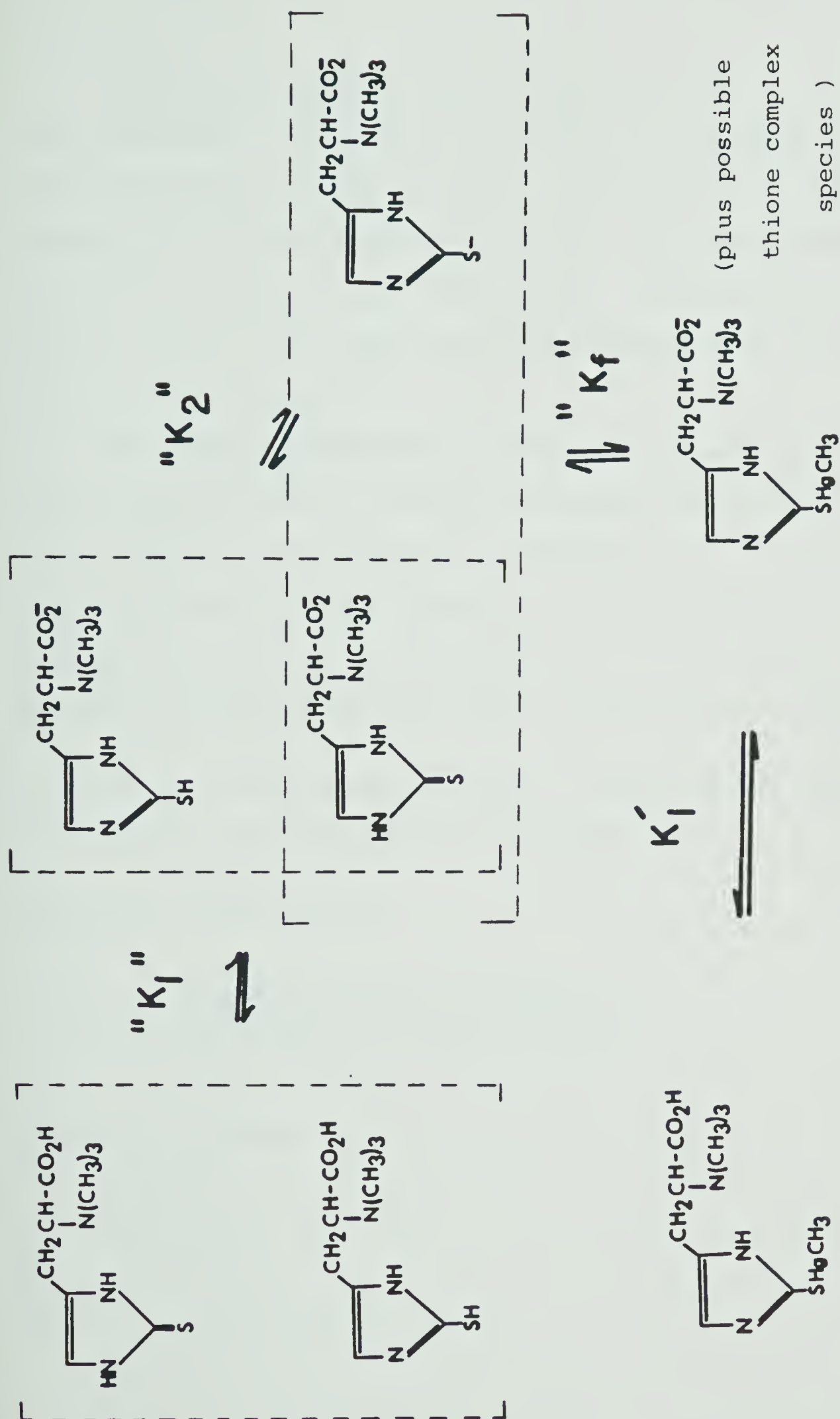


Figure 14. Ionisation, tautomerisation and binding scheme for ergothioneine.

Literature values for pK_2 , listed in Table 8, show poor agreement. The value of Sakurai and Takeshima (129) was selected as the most reliable; corrected to an ionic strength of 0.3, this is 10.40 ± 0.04 . pK_1 was estimated at ~ 1.3 by Stanovink and Tisler (130). Since only pH values above 5 were involved in the present study this protonation was ignored.

Preliminary experiments showed that competition by one mole-equivalent of ergothioneine was indeed minimal. For this reason, the study was repeated at a mole ratio of 1:2.32 in favour of ergothioneine. Interpreting the results obviously requires adjustment to the algebraic model previously developed; this is given below in summary.

Let C = concentration of MAA = concentration of $\text{CH}_3\text{Hg}(\text{II})$

Let xC = concentration of ergothioneine

As before, K_d is defined

$$K_d = \frac{[\text{CH}_3\text{HgS(Ergo)CO}_2^-][^- \text{SCH}_2\text{CO}_2^-]}{[\text{CH}_3\text{HgSCH}_2\text{CO}_2^-][^- \text{S(Ergo)CO}_2^-]} \quad (62)$$

and also as before

$$[^- \text{SCH}_2\text{CO}_2^-] = P_f \cdot C \cdot \alpha_1 \quad (63)$$

Also

Table 8. Literature pK_2 values for ergothioneine.

pK_2	Type ^a	Conditions	Method	pK_2^b	Reference
10.75	?	$\mu = ?$, 21°C	Spectrophotometric	--	130
10.5	?	$\mu = ?$, 22°C	Potentiometric	--	131
10.39	?	$\mu = ?$, 25°C	Potentiometric	--	132
10.44	M	$\mu = 0.1$, 25°C	Potentiometric	10.40	129

a) M = mixed.

b) Corrected to an ionic strength of 0.3.

$$[\text{CH}_3\text{HgSCH}_2\text{CO}_2^-] = (1-P_f) \cdot C \cdot \alpha_2 \quad (64)$$

Now considering the bound ergothioneine, since any $\text{CH}_3\text{Hg(II)}$ not bound to MAA will be bound to ergothioneine:

$$P_f \cdot C = [\text{CH}_3\text{HgS(Ergo)CO}_2^-] + [\text{CH}_3\text{HgS(Ergo)CO}_2\text{H}] \quad (65)$$

which gives as before

$$[\text{CH}_3\text{HgS(Ergo)CO}_2^-] = P_f \cdot C \cdot \alpha_3 \quad (66)$$

where

$$\alpha_3 = K'_{1,\text{ergo}} / (a_{\text{H}^+} + K'_{1,\text{ergo}}) \quad (67)$$

Free ergothioneine can then be calculated by difference:

$$\begin{aligned} (x-P_f)C &= [\text{HS(Ergo)CO}_2\text{H}] + [\text{HS(Ergo)CO}_2^-] + \\ &[\text{S(Ergo)CO}_2^-] \end{aligned} \quad (68)$$

giving eventually

$$[\text{S(Ergo)CO}_2^-] = (x-P_f) \cdot C \cdot \alpha_4 \quad (69)$$

α_4 is of exactly the same form as α_1 .

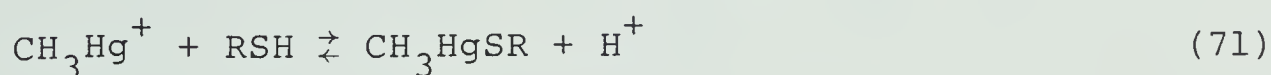
Substitution into the expression for K_d gives

$$K_d = \frac{P_f^2}{(1-P_f)(x-P_f)} \cdot \frac{\alpha_1 \alpha_3}{\alpha_2 \alpha_4} \quad (70)$$

Ten samples were withdrawn between pH 10 and pH 5. The chemical shift data is shown in Figure 15. The final fit by KINET was fairly satisfactory, given the relatively poor precision in the data; even with the higher amount of ergothioneine, the observed curve lay very close to that for bound MAA. The value of K_d returned was $\sim 6 \times 10^{-4}$ ($\pm 2 \times 10^{-4}$), yielding $\log K_f = 13.7 \pm 0.2$. This is considerably less than for the other thiols; K_f is about 10^{-2} that for glutathione and 10^{-3} that for MAA. Detailed discussion will be given below.

8. Calculation of derived values.

Once the methylmercury(II)-sulfhydryl interaction for a given molecule has been characterized as above, derived constants can be conveniently calculated. The approach is illustrated by the penicillamine results. Figure 16 gives the full scheme; reactions involving desired constants are shown dashed. K_{fh} constants are proton displacement formation constants describing processes of the type



K'_f terms are derived binding constants of the normal kind.

After some algebra, it can be shown that

$$K'_{f1} = \frac{K_f k_{123}}{K'_2} \quad (72)$$

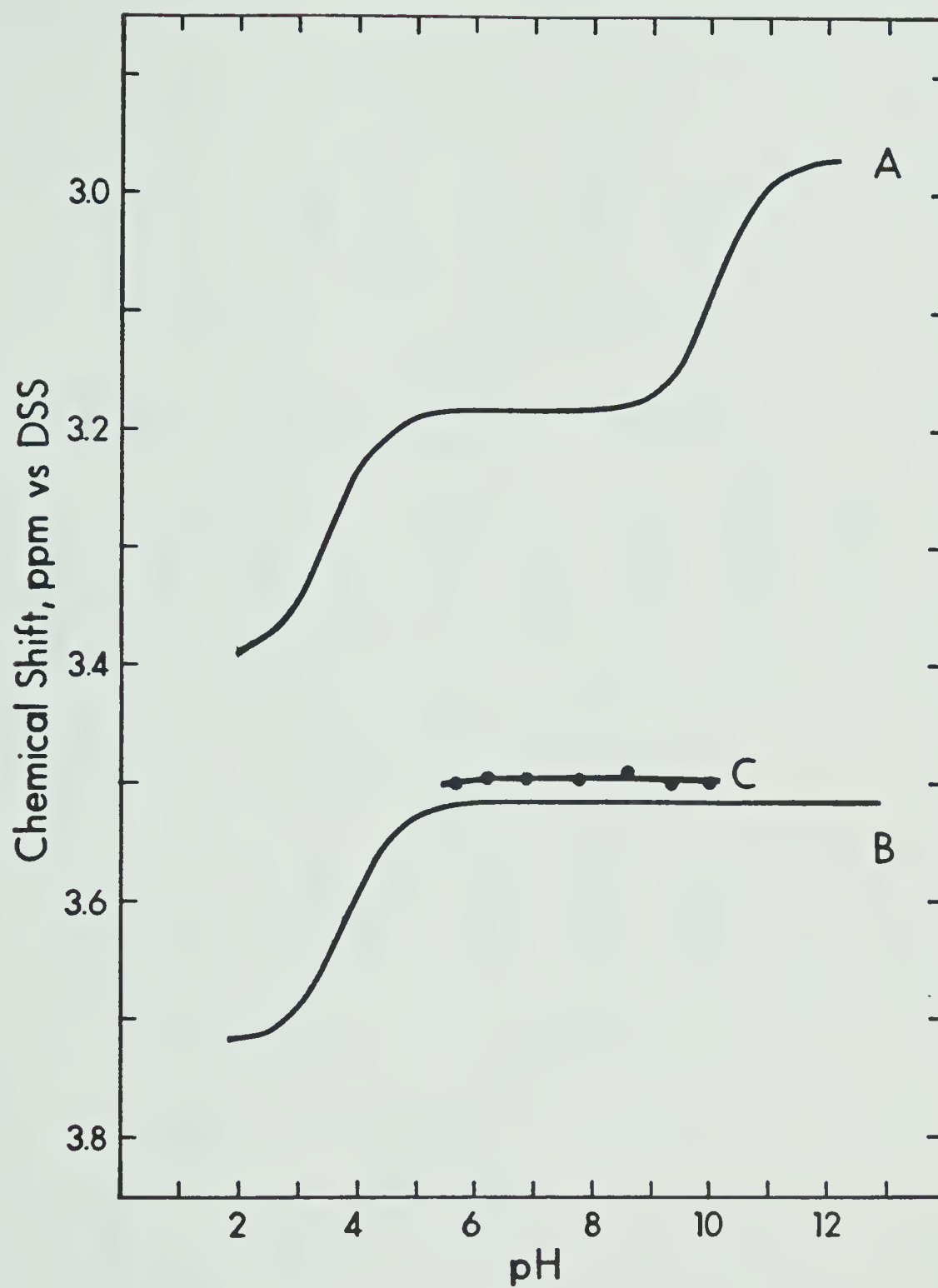


Figure 15. MAA methylene resonance as a function of pH for
 a) free MAA, b) methylmercury(II)-bound MAA,
 c) MAA:methylmercury(II):ergothioneine, 1:1:2.32.

$$K_{fh3} = K_f \cdot k_{132} \quad (73)$$

$$K_{fh2} = \frac{K_f K_2 K_3}{K'_2} \quad (74)$$

and

$$K_{fh1} = \frac{K_f K_1 K_2 K_3}{K'_1 K'_2} \quad (75)$$

The total number of K_{fh} terms equals the number of possible methylmercury(II)-complexed species (neglecting possible superprotonation) and the total number of K_f 's and K'_f 's the number of free species deprotonated at the sulfhydryl group; this is a general result.

Desired constants for all the thiols studied are given in Table 9. Since (see section 4b above) these derived values contain no information not implicit in their constituent constants, discussion will be confined to the latter.

C. Discussion

1. General.

In this section the data determined above will be summarised, some rationalisation of observed trends made, and comparisons drawn with the literature. Lastly, the

Table 9. Derived methylmercury(II) formation and proton displacement formation constants.

Ligand	$\log K_f^a$	$\log K_{fh}^a$
Mercaptoacetic acid	none	7.14, 6.84
Mercaptoethanol	none	none
Penicillamine	14.79 ^b	7.15, 6.76, 7.24 ^b
N-Acetylpenicillamine	none	6.34, 6.57
Cysteine	15.38 ^b	7.51, 7.00, 6.93 ^b
Homocysteine	? ^c	6.35, 6.36 ^b , ? ^c
Glutathione	15.85 ^b	7.10, 7.02 (macro) ^d , 6.88, 6.92 ^b
Meraptosuccinic acid	none	7.67, 7.27 (macro) ^d , 7.05

a) As defined in text. K_{fh} values in order (see Figure 16).

b) Using values of necessary microdissociation constants as taken in text.

c) Microdissociation constant(s) not available.

d) i.e. These values are composites for the molecule protonated at *either* site.

implications of the results in the light of clinical methylmercury(II) antidote studies will be discussed.

As described in Chapter I, previous studies have indicated preferential sulfhydryl binding of methylmercury(II) over virtually the entire pH range (64); no evidence emerged in the present studies to challenge that conclusion. The strength of binding observed and the approximate magnitude of the ^{199}Hg - ^1H spin-spin coupling constants in the methyl resonance of $\text{CH}_3\text{Hg(II)}$ support it.

$\log K_f$ values are tabulated in Table 10. The values refer to the complexation of $\text{CH}_3\text{Hg(II)}$ by the fully deprotonated (i.e. high pH) forms of the various ligands. The very low value for ergothioneine is interesting. While it is anomalously weak methylmercury(II)-sulfhydryl binding, by the standards of the other ligands, it is still too strong plausibly to be assigned to any other mode of binding. For instance $\log K_f$ for amine nitrogen binding of methylmercury(II) is typically ~ 7.5 (27) and for carboxylate groups $\log K_f = 3.5$ or less (24). The low value relative to those for thiol ligands is ascribed to the preponderance of the thione tautomer in the aqueous speciation of ergothioneine.

Table 10. Displacement constants and methylmercury(II) complex formation constants.

Thiol	K_d	$\log K_f$
Mercaptoacetic acid	1.00 ^a	16.92
Mercaptoethanol	0.16	16.12 ^b
Penicillamine	1.06	16.94
Cysteine	0.57	16.67
N-acetylpenicillamine	0.70	16.76
Glutathione	0.12	16.00
Homocysteine	0.34	16.45
Mercaptosuccinic acid	2.50	17.31
Ergothioneine	$\sim 6 \times 10^{-4}$	~ 13.7

a) By definition.

b) Determined by Schwarzenbach and Schellenberg (15).

2. The effect of acid-base chemistry at other sites on methylmercury(II) binding.

Figure 17 gives the structures and methylmercury(II) complex formation constants of cysteine, penicillamine and glutathione, both protonated and deprotonated at the amino group. In all three cases K_f falls as the amino group is protonated, showing the effect of the additional positive charge on the electron density available at the sulfhydryl sulfur atom. In the case of glutathione, where the amino group is relatively distant, the effect is small (0.15 log units drop in log K_f); for penicillamine and cysteine it is much larger (2.15, 1.29 log units respectively). An alternative formulation of the same behaviour is also possible: the change in amino group pK upon complexation. The changes involved are necessarily the same in magnitude, due to the cyclic nature of the reaction schemes, and the trends can be rationalised using a reversal of the argument presented above.

It should be emphasised that no such approach can be applied to the carboxylate acid-base behaviour observed in these studies. Since only proton displacement formation constants for methylmercury(II) binding are available at low pH, the effect on the carboxylate pK is that of a combination of a proton dissociation *and* of methylmercury(II)

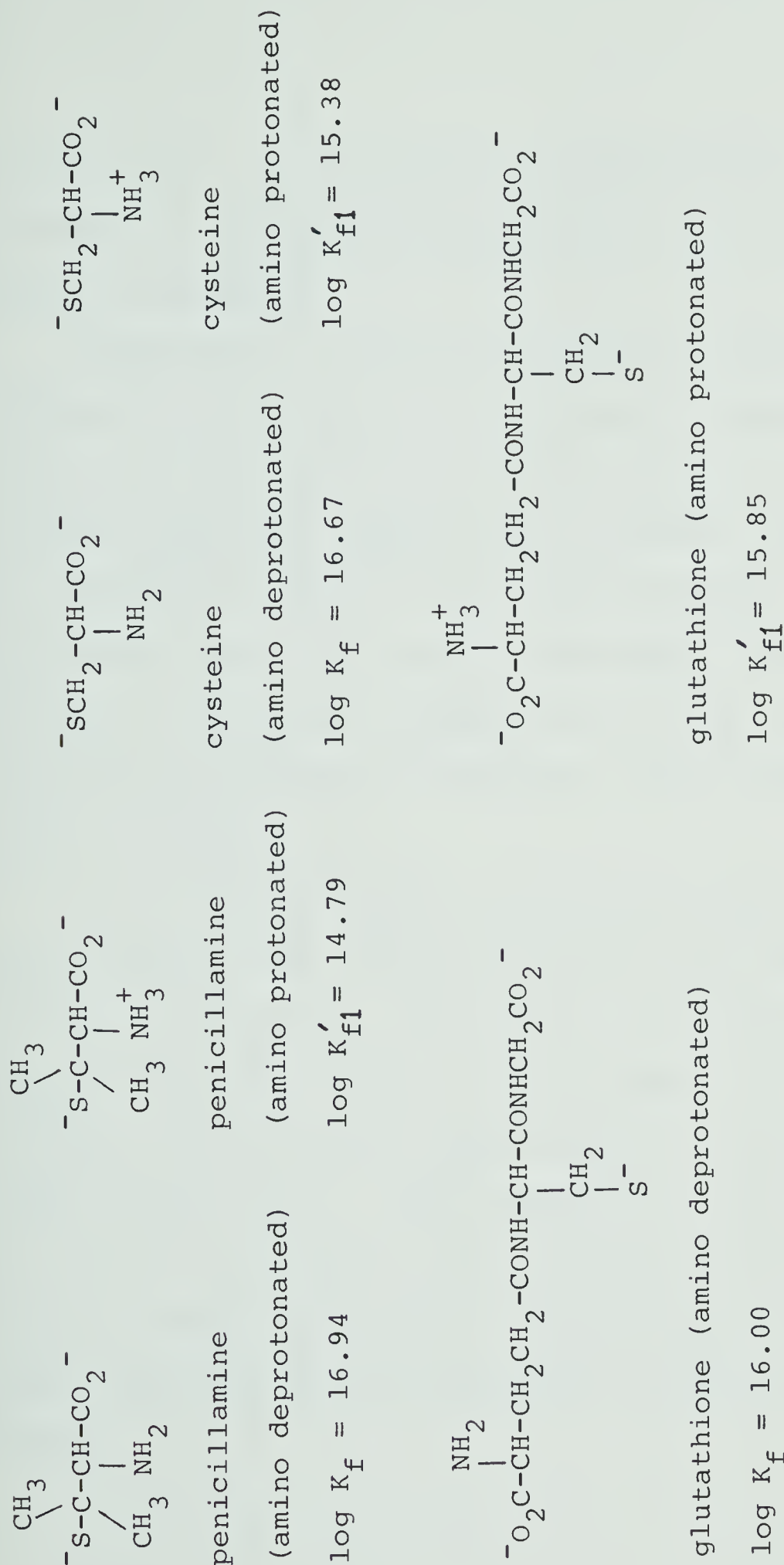


Figure 17. Structures and log methylmercury(II) formation constants for sulfhydryl ligands protonated and deprotonated at an amino group.

complexation. It is unknown how these two factors add or subtract. Certainly the probability of a clear trend cannot be assumed.

Comparison of the acid dissociation constants for the carboxylic acid groups of the $\text{CH}_3\text{Hg(II)}$ -complexed ligands (Table 11) with those for the same groups in the free ligands (Table 12) indeed shows no trend. Complexation of the sulfhydryl groups of MAA, penicillamine, cysteine and mercaptosuccinic acid causes a decrease in acidity at the carboxylic acid group, complexation to the sulfhydryl in N-acetylpenicillamine an increase, and in homocysteine almost no change.

It is also of interest to note that the acid dissociation constants for the amino groups of the complexed forms of both penicillamine and cysteine lie closer to k_{13} than k_{123} in the microscheme for free ligand. Such is also the case for the analogous trimethyllead(IV) complexes of these ligands (119). This suggests that when complexed to the sulfhydryl group both methylmercury(II) and trimethyllead(IV) mimic a similarly bonded hydrogen ion in terms of their effect on the acid strength of neighbouring ammonium groups.

Table 11. Acid dissociation constants for $\text{CH}_3\text{Hg}(\text{II})$ -complexed
thiols^a.

Complex	Acid Group(s)	Acid Dissociation Constant	pK'
$\text{CH}_3\text{HgSCH}_2\text{CO}_2\text{H}$	CO_2H	K'_1	3.80 ± 0.01
$\text{CH}_3\text{CONHCHCO}_2\text{H}$ $\text{C}(\text{CH}_3)_2\text{SHgCH}_3$	CO_2H	K'_1	3.10 ± 0.07
$\text{H}_3\text{N}^+\text{CHCO}_2\text{H}$ $\text{C}(\text{CH}_3)_2\text{SHgCH}_3$	CO_2H	K'_1	2.33 ± 0.05
	NH_3^+	K'_2	8.14 ± 0.01
$\text{H}_3\text{N}^+\text{CHCO}_2\text{H}$ $\text{CH}_2\text{SHgCH}_3$	CO_2H	K'_1	2.44 ± 0.08
	NH_3^+	K'_2	8.80 ± 0.02
$\text{H}_3\text{N}^+\text{CHCO}_2\text{H}$ $\text{CH}_2\text{CH}_2\text{SHgCH}_3$	CO_2H	K'_1	2.26 ± 0.06
	NH_3^+	K'_2	9.12 ± 0.02

(cont'd.)

Table 11. (continued)

Complex	Acid Group(s)	Acid Dissociation Constant	pK'
$\text{HO}_2\text{CCHCH}_2\text{CO}_2\text{H}$ SHgCH_3	$\text{CO}_2\text{H} + \text{CO}_2\text{H}$ $\text{CO}_2\text{H} + \text{CO}_2\text{H}$	K_1^{b} K_2^{b}	3.53 ± 0.03 4.85 ± 0.02
$\text{HNOCCCH}_2\text{CH}_2\text{CH}(\text{CO}_2\text{H})\text{NH}_3^+$ $\text{CH} - \text{CONHCH}_2\text{CO}_2\text{H}$ $\text{CH}_2\text{SHgCH}_3$	$\text{CO}_2\text{H} + \text{CO}_2\text{H}$ $\text{CO}_2\text{H} + \text{CO}_2\text{H}$ NH_3^+	K_1^{b} K_2^{b} K_3'	2.23^{c} 3.63 ± 0.04 9.25 ± 0.02

a) At 25°C and 0.3 M ionic strength.

b) Macroscopic values.

c) From reference 69.

Table 12. Acid dissociation constants for the thiol ligands^{a,b,c}.

Ligand	Acid Group	Acid Dissociation Constant	pK	Reference
Mercaptoacetic acid	CO ₂ H	K ₁	3.50±0.01	d
	SH	K ₂	10.08±0.02	d
Mercaptoethanol	SH	K ₁	9.62	119
N-acetylpenicillamine	CO ₂ H	K ₁	3.33	120
	SH	K ₂	10.19	120
Penicillamine	CO ₂ H	K ₁	1.94	119
	NH ₃ ⁺ + SH	K ₂ ^e	7.93	119
	NH ₃ ⁺ + SH	K ₃ ^e	10.39	119
	SH	k ₁₂ ^f	8.05	119
	NH ₃ ⁺	k ₁₃ ^f	8.61	119
	NH ₃ ⁺	k ₁₂₃ ^f	10.29	119
	SH	k ₁₃₂ ^f	9.74	119

(cont'd.)

Table 12. (continued)

Ligand	Acid Group	Acid Dissociation Constant	pK	Reference
Homocysteine	CO ₂ H	K ₁	2.27±0.02	d
	NH ₃ ⁺ + SH	K ₂ ^e	8.66	126
	NH ₃ ⁺ + SH	K ₃ ^e	10.55	126
Mercaptosuccinic acid	CO ₂ H + CO ₂ H	K ₁ ^g	3.13	127
	CO ₂ H + CO ₂ H	K ₂ ^g	4.63	127
	SH	K ₃	10.26	d
Ergothioneine	SH	K ₂	10.40	129
Glutathioneine	CO ₂ H + CO ₂ H	K ₁ ^g	2.15	69
	CO ₂ H + CO ₂ H	K ₂ ^g	3.49	69
	NH ₃ ⁺ + SH	K ₃ ^e	8.76	69
	NH ₃ ⁺ + SH	K ₄ ^e	9.56	69
	SH	k ₁₂₃ ^h	8.97	69

(cont'd.)

Table 12. (continued)

Ligand	Acid Group	Acid Dissociation Constant	pK	Reference
Glutathione (cont'd.)	NH_3^+	k_{124}^h	9.17	69
	NH_3^+	k_{1234}^h	9.35	69
	SH	k_{1243}^h	9.08	69

- a) 25°C and 0.3 *M* ionic strength.
- b) Literature values corrected to an ionic strength of 0.3 *M* using the Davies equation. See Appendix I.
- c) Mixed constants: a_{H^+} and concentration of acid and its conjugate base.
- d) This work.
- e) Composite macroscopic ionisation constants due to simultaneous dissociation of NH_3^+ and SH groups over the same pH region. See text p. 96.
- f) Macroscopic constants as defined in Figure 9.
- g) Composite macroscopic ionisation constants, due to simultaneous ionisation of two carboxylic acid groups over the same pH region.
- h) Macroscopic constants as defined in Figure 12.

3. The magnitude of methylmercury(II)-sulfhydryl complex formation constants.

In each of the complexes studied above, it is evident from the strength of binding that the $\text{CH}_3\text{Hg(II)}$ is bonded to the deprotonated sulfhydryl group. Nevertheless, the formation constants listed in Table 10 are seen to cover a reasonably large range of values. If the log formation constants are plotted as a function of the acid dissociation constants of the corresponding sulfhydryl groups, as shown in Figure 18, approximately linear behaviour is apparent. Thus, it appears that the Brønsted basicity of a sulfhydryl group when deprotonated is a major factor in determining the affinity of that group for methylmercury(II). A linear least-squares fit to these data yields the regression equation

$$\log K_f = 1.00 \text{ pK} + 6.86 \quad (76)$$

However, the scatter in this plot is quite marked; the calculated correlation coefficient is 0.93. Libich and Rabenstein demonstrated a much stronger correlation between pK and $\log K_f$ for carboxylic acid complexes of methylmercury(II) (24).

A detailed discussion of the origin of such linear free energy relationships as equation (76) lies outside the scope

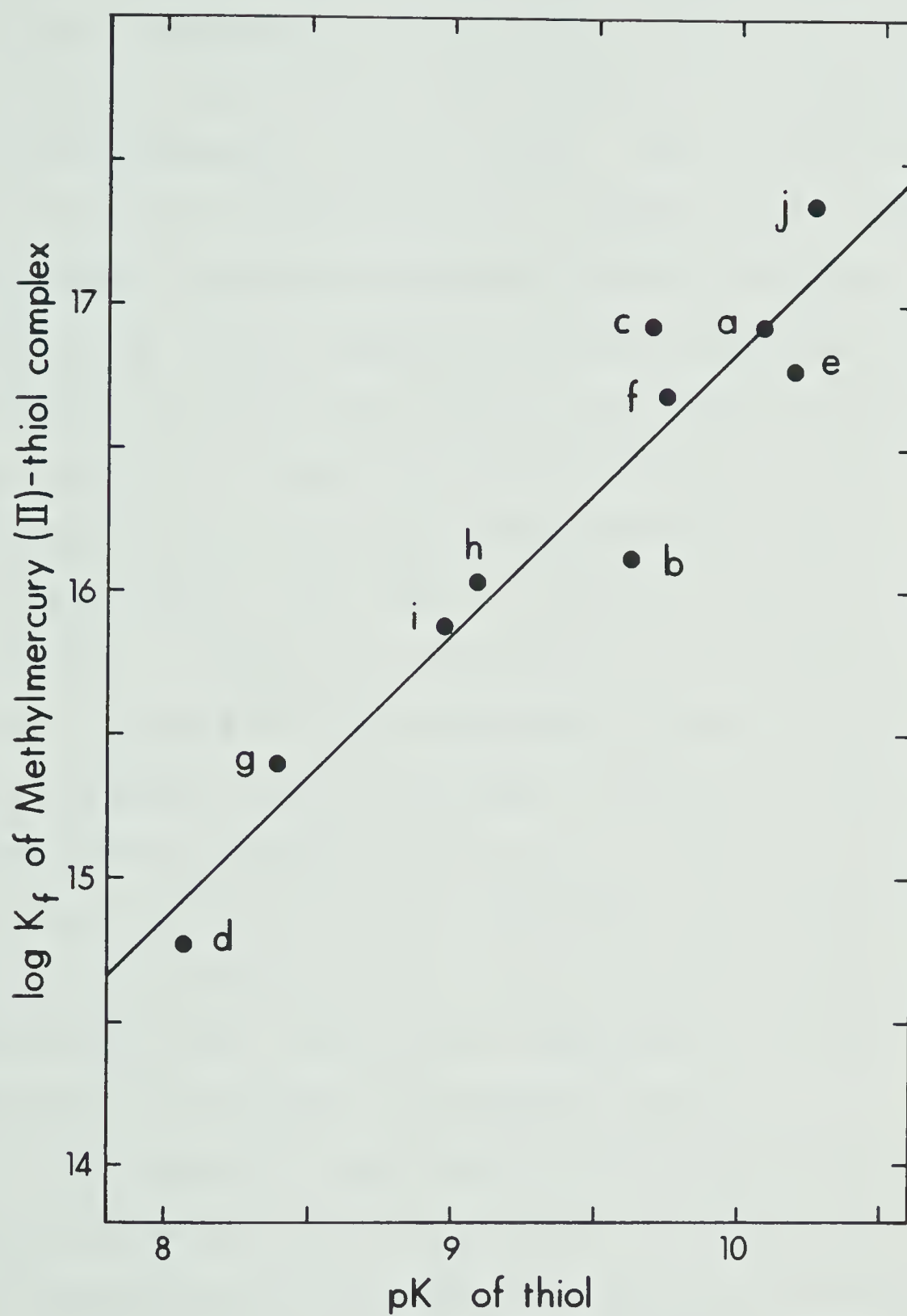


Figure 18. $\log K_f$ versus pK for a) MAA, b) ME, c), d) PSH, e) NPSH, f), g) CSH, h), i) GSH and j) MSA.

of this thesis; however, some preliminary conclusions can be drawn. Examination of the plot of Figure 18 suggests that the scatter may be due to the influence of carboxylate groups situated elsewhere on the ligands. This is borne out by previous x-ray crystallographic studies, which showed that a significant degree of interaction with carboxylate oxygen could occur in the sulfhydryl-bonded methylmercury(II) complexes of thiol amino-acids such as penicillamine (72). The majority of molecules studied have one proximal carboxylate group, except for mercaptoethanol (none) and mercaptosuccinic acid (two). All have a fully accessible sulfhydryl, except for penicillamine and N-acetylpenicillamine. These have flanking methyl groups on the sulfur-bearing carbon atom; these might therefore be expected to give rise to anomalous results due to steric and inductive effects. Removal of these compounds from consideration in Figure 18, leaving points a, f, g, h and i, gives a very much better line (correlation coefficient = 0.997). The scatter is now within experimental error.

The datum for ergothioneine in Figure 18 lies well below and to the right of the line. As noted above, both the apparent pK and the apparent $\log K_f$ for ergothioneine are composites of the true value and the tautomerisation equilibrium constant. Thus, assuming these *intrinsic*

values follow the correlation line, it is possible to estimate them, and the tautomerisation constant, K_t (defined as the thiol/thione ratio at equilibrium). The values obtained are: $pK_i \sim 8.6$, $\log K_{fi} \sim 15.6$ and $K_t \sim 10^{-2}$, where the subscript i refers to an intrinsic value. This also assumes that binding to the thione form is not important; as discussed above, this appears reasonable. As far as could be ascertained, this is the first time the value of K_t has been estimated.

4. Methylmercury(II)-sulfhydryl binding data in the literature.

These were discussed in Chapter I. Here the agreement between the present work and values previously determined will be evaluated.

No comment can be made about the measurement of $\log K_f = 16.12$ for the mercaptoethanol complex by Schwarzenbach and Schellenberg (15), since this value was assumed to be correct for the purposes of this study. (Should it subsequently prove to be erroneous, a simple systematic correction to all K_f values can be made; the *relative* binding strengths would of course be unchanged.)

It is worthwhile comparing values determined in this study for the cysteine and glutathione complexes with

those reported by Simpson (23). These are two of the very few values in the literature for complexation of $\text{CH}_3\text{Hg}(\text{II})$ by a biological thiol, and have therefore been widely used in discussions of the chemistry of $\text{CH}_3\text{Hg}(\text{II})$ in biological systems. Simpson's constants are actually a composite of binding, sulfhydryl acid-base and amino acid-base behaviour. This is illustrated in Figure 19. The term K_A is Simpson's "association constant". It is easily shown that

$$K_A = K_f \cdot \frac{K_4}{K'_3} \quad (77)$$

It was also necessary to correct the early pK values used in Simpson's paper to the ones accepted and used above. Agreement with the present study is then found to be excellent (see Table 13).

Such agreement is not, however, obtained with the results of Hojo et al. (68), who reported $\log K_f = 6.72$ and 7.19 for the $\text{CH}_3\text{Hg}(\text{II})$ complexes of penicillamine and cysteine respectively. As explained in the Introduction, these results appear invalid. That for cysteine is also in total disagreement with the approximate figure of $\log K_f \sim 15$ determined by Fairhurst (113) using a large excess of competing cyanide ion, whereas the present figure

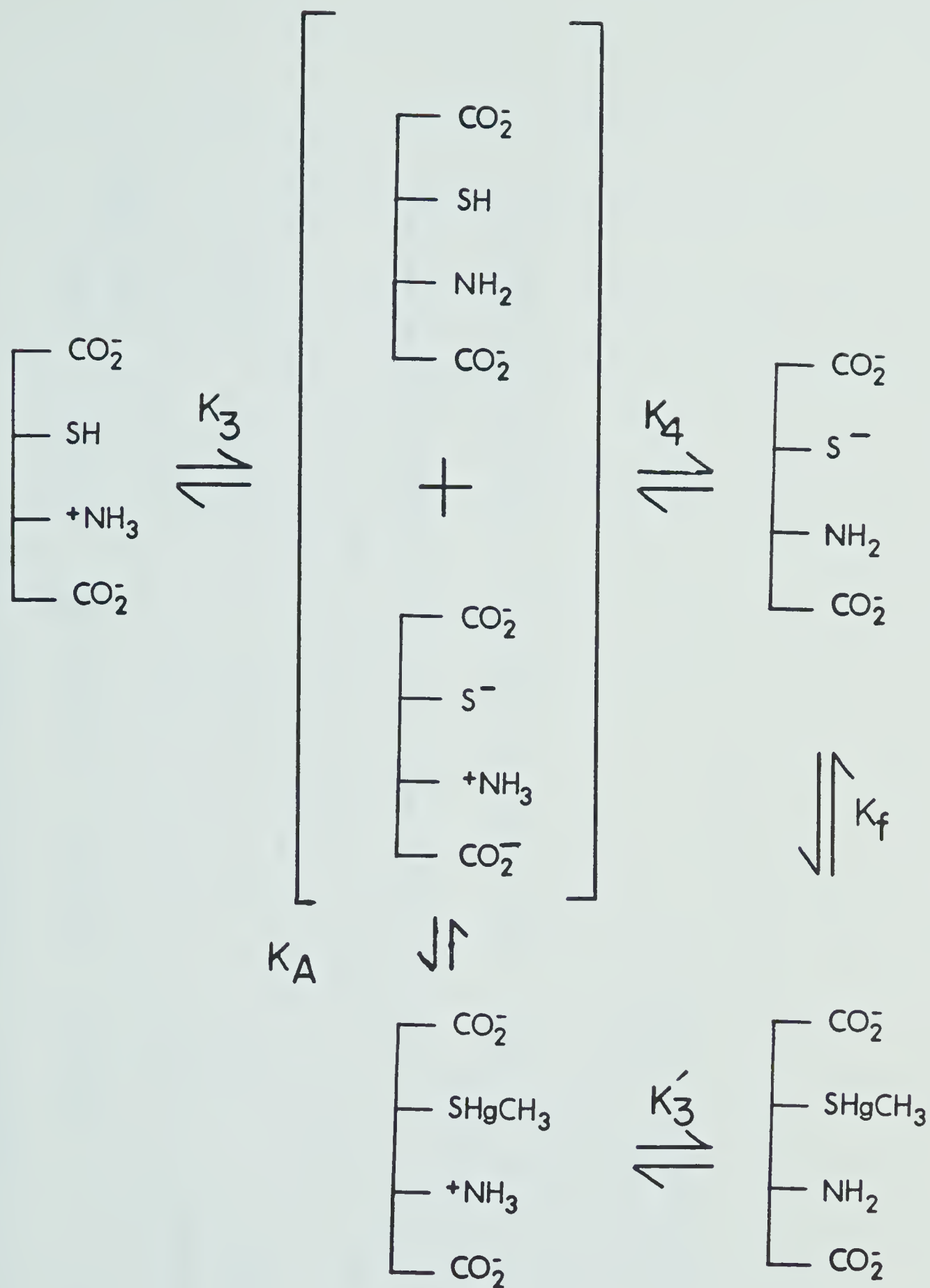


Figure 19. Definition of Simpson's "association" constant K_A for glutathione.

Table 13. Comparison of association constant values.

Thiol	$\log K_A^a$	pK used	correct pK^b	$\log K_A^c$	$\log K_A$ (this work)
Glutathione	15.9	9.0	8.8	15.7^d	15.6_9^e
Cysteine	15.7	8.6	8.2	15.3^d	15.2_2^e

a) Log association constant, as determined by Simpson (23).

b) See text. In view of large uncertainties no attempt made to correct ionic strength.

c) Corrected for pK's. The method used gave $K_A = \text{const}/K$; thus $\log K_A$ falls with pK.

d) Uncertainty $\sim \pm 0.1$.

e) Uncertainty $\sim \pm 0.07$.

is somewhat closer.

5. Conditional formation constants: biological implications.

The formation constants listed in Table 10 are seen to decrease in the order mercaptosuccinic acid > penicillamine > mercaptoacetic acid > N-acetylpenicillamine > cysteine > homocysteine > mercaptoethanol > glutathione. However, because of competing reactions, this order is rather misleading as a measure of *effective* stability of the complexes. At lower pH, hydrogen ions compete with $\text{CH}_3\text{Hg(II)}$ for the deprotonated sulfhydryl group, whilst at high pH hydroxide ions compete with the sulfhydryl group for $\text{CH}_3\text{Hg(II)}$. Because the pK values of the different thiols have discrete values, pH dependence of effective binding strength is also distinct for each complex. The effects, noted above, of acid-base behaviour at other sites, such as amino or carboxylic acid groups, further complicates the issue.

The overall effect of these various competition reactions on the binding strength can be most easily visualised using conditional formation constants, K_{fc} . These are pH-dependent "constants" which do not allow for the acid-base behaviour of the molecule involved, considering only its total free and bound concentrations. For example, in the case of mercaptoethanol:

$$K_f = \frac{[\text{CH}_3\text{HgSR}]}{[\text{CH}_3\text{Hg}^+][^-\text{SR}]} \quad (78)$$

whereas

$$K_{fc} = \frac{[\text{CH}_3\text{HgSR}]}{[\text{CH}_3\text{Hg}^+]([\text{HSR}] + [^-\text{SR}])} = K_f \cdot \frac{K_1}{(a_{\text{H}^+} + K_1)} \quad (79)$$

A conditional displacement constant, K_{dc} , is defined as the ratio of two such terms. It can be shown that K_{dc} for any thiol over MAA can be estimated directly from the MAA chemical shift observed in the competition studies:

$$K_{dc} = \frac{P_f^2}{(1-P_f)^2} = \left(\frac{\delta_b - \delta_o}{\delta_o - \delta_f} \right)^2 \quad (80)$$

This provides a convenient quick way of estimating K_{fc} at any pH directly from the experimental data, given a value for K_{fc} of the mercaptoacetic acid complex at that pH.

$\log K_{fc}$ is plotted versus pH in Figure 20. In all cases, K_{fc} is orders of magnitude smaller than K_f , due to competing reactions. The conditional formation constants are pH dependent, reaching a maximum in each case near pH 7 and decreasing at higher and lower pH values due to competing reactions. The exact pH dependence is strongly linked to the acid-base chemistry of the sulfhydryl group;

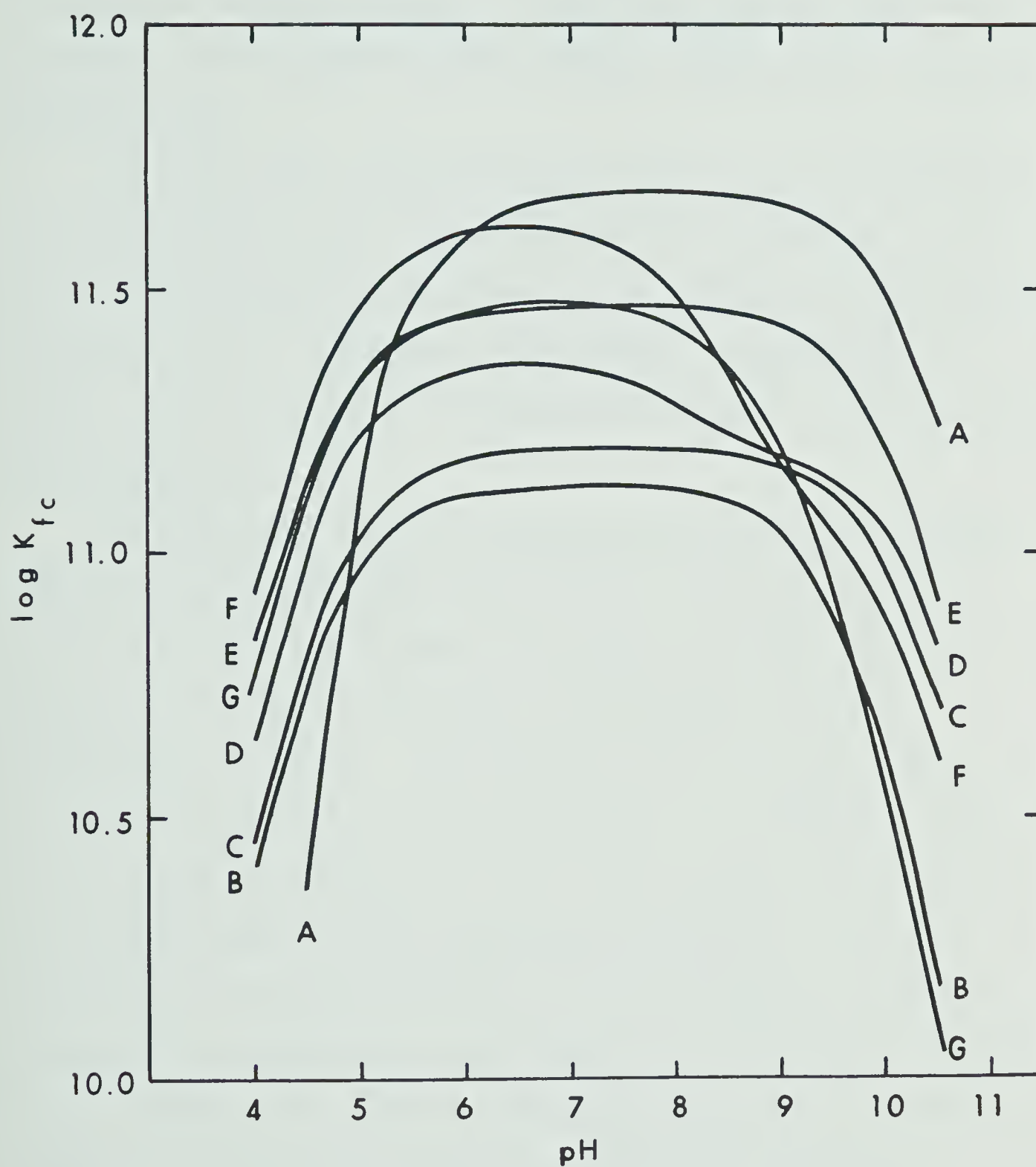


Figure 20. \log conditional formation constants versus pH for
 a) MSA, b) ME, c) NAPSH, d) PSH, e) MAA, f) CSH
 and g) GSH.

thus the relative order of affinity undergoes major changes as the pH varies. At pH 10 K_{fc} for the mercapto-succinic acid complex is the largest, while at pH 4 it is the smallest.

Of particular interest with respect to the chemistry of methylmercury(II) toxicology are the values of K_{fc} at pH 7.4 (see Table 14). The order of affinity is mercapto-succinic acid > cysteine > glutathione > mercaptoacetic acid > penicillamine > N-acetylpenicillamine > homocysteine > mercaptoethanol.

As discussed in the introduction to Part 2, mercapto-succinic acid, N-acetylpenicillamine and penicillamine have been found to increase the rate of elimination of $\text{CH}_3\text{Hg(II)}$ in animal studies, in declining order of efficiency (133,134). This order is not exactly that predicted by the K_{fc} values in Table 14. Further, given that K_{fc} for glutathione at pH 7.4 is larger than those for penicillamine and N-acetylpenicillamine, and that glutathione is quite abundant in most mammalian erythrocytes, it is surprising that these are efficient antidotes. These observations lead to the conclusion that factors in addition to relative binding strengths are important. These could include the ease with which the thiol ligand can penetrate cellular membranes and convert the non-

Table 14. Conditional formation constants for the
methylmercury(II)-thiol complexes at pH 7.4.

<u>Ligand</u>	<u>log $K_{f,conditional}$</u>
Mercaptoethanol	11.13
Mercaptoacetic Acid	11.47
N-acetylpenicillamine	11.20
Penicillamine	11.33
Cysteine	11.57
Homocysteine	11.15
Mercaptosuccinic Acid	11.68
Glutathione	11.46

diffusible intracellular methylmercury(II) into freely diffusible complexes (133).

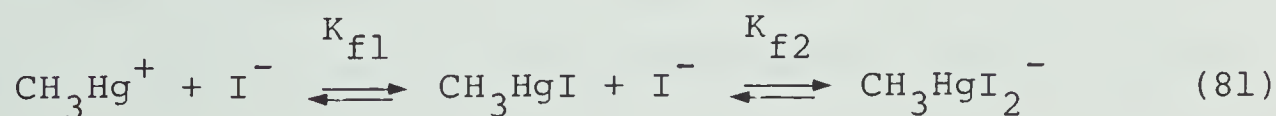
CHAPTER IV

The Binding of Methylmercury(II) by Dithiol Molecules

A. Introduction

Dithiol molecules have traditionally been favoured antidotes for inorganic metal poisoning, such as with Hg(II), due to their undoubted chelating ability and hence high binding strengths (135). Some, notably 2,3 dimercapto-succinic acid, have also been used successfully for the treatment of methylmercury(II) poisoning (134).

Such success is of theoretical interest in the light of the many studies (see Chapter I) which show the tendency of the mercury in $\text{CH}_3\text{Hg(II)}$ to expand its coordination number from two to three or more. Studies by crystallography, NMR and other techniques demonstrate unequivocally that this does occur, but tend to suggest that rather than true chelation, the bonding scheme generally involves a strong primary interaction with strong covalent character, and a secondary ionic-type interaction which is much weaker. For instance, Schwarzenbach and Schellenberg estimated the stepwise iodide complex formation constants in the scheme



to be 4×10^8 and 2 respectively (15). Conclusions drawn from studies of potentially chelating nitrogen-donor ligands are similar (136).

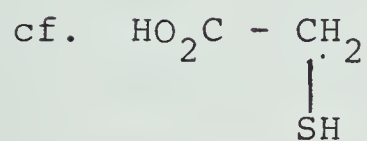
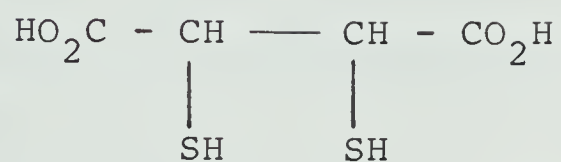
Moore et al. have examined the possibility of chelation in $\text{CH}_3\text{Hg(II)}$ systems as a means of raising the affinity of antidotes for the toxic species. Using crystallography, they were able to demonstrate some degree of apparent chelation in sterically rigid vicinal dithiol- $\text{CH}_3\text{Hg(II)}$ complexes; however, no actual stability constant data were determined (76). While comparative studies on pyridine and 2,2' bipyridine show an approximate tenfold increase in K_f due to chelation (48), such an increase cannot be assumed in the dithiol case, due to the very different electronic nature of the sulfur-mercury interaction.

The studies reported in Chapter III showed that competition with MAA for $\text{CH}_3\text{Hg(II)}$ gave a precise measurement of the $\text{CH}_3\text{Hg(II)}$ complex formation constant for a monothiol. If the corresponding constants for dithiols were found to be significantly larger, this would provide convincing evidence for chelation occurring in solution for the first time. A study similar to that in Chapter III was therefore initiated here for two dithiol molecules: 2,3 dimercaptosuccinic acid (DMSA) and dithioerythritol (DTE). These molecules were selected for three reasons:

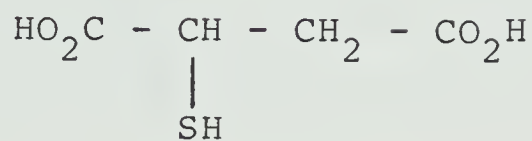
1. Both have bilaterally symmetric structures. This simplifies the algebraic description of methylmercury(II) binding and acid-base behaviour considerably since all microconstants are either half or twice the corresponding macro-values.
2. Both molecules are "dimers" in a sense of molecules whose behaviour has already been fully characterized. See Figure 21. DTE corresponds to two mercaptoethanol moieties, DMSA to two mercaptoacetic acid units.
(Actually, given the effect of proximal carboxylates on sulfhydryl properties demonstrated in Chapter III, a better comparison for DMSA is probably mercaptosuccinic acid, also characterized there.)
3. The two molecules provide a contrast concerning sulfhydryl group placement. DMSA has these on adjacent carbon atoms, DTE four carbons apart. Thus, contrasts in the degree of chelation or pseudochelation observed, if any, are to be anticipated. Qualitatively, a trend with "ring-size" has already been noted for "chelation" via an aromatic-ring/Hg atom secondary interaction (59).
4. In addition, DMSA is of interest because of its therapeutic use (134).

In this Chapter, the investigation of the detailed

2,3 dimercaptosuccinic acid

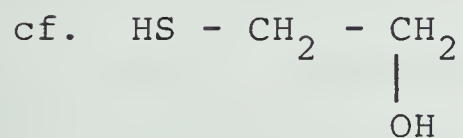
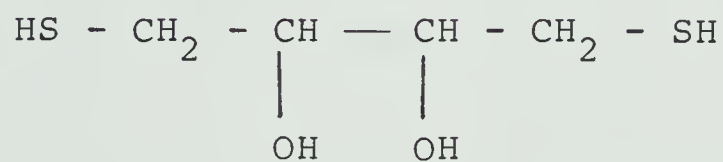


Mercaptoacetic acid



Mercaptosuccinic acid

Dithioerythritol



Mercaptoethanol

Figure 21. Structures of 2,3 dimercaptosuccinic acid and dithioerythritol.

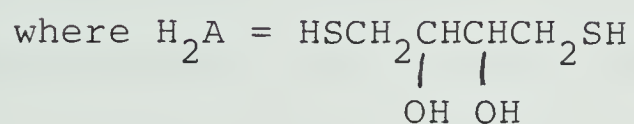
$\text{CH}_3\text{Hg(II)}$ binding and acid-base behaviour of these two dithols is reported. Competition study data from an experiment involving 2,3 dimercaptopropane-1-sulfonate (RAlSO_3H) are also presented, from which the conditional formation constant for this complex is evaluated as a function of pH. Section B describes the results obtained, and Section C discusses these, in the light of the observations above.

B. Results

1. Acid dissociation constants for dithioerythritol.

DTE displays the acid-base behaviour shown in Figure 22. The macroionisation scheme of the molecule as a whole is given in Figure 22a; the microionisation scheme, relating to the acidity of any one site, in Figure 22b. Since by definition $K_1 = k_{1a} + k_{1b}$ and $k_{1a} = k_{1b}$, $k_1 = K_1/2$. Similarly, $k_2 = 2K_2$. In non-mathematical terms, K_1 is twice k_1 since the fully protonated molecule as a whole has twice the chance of either individual sulfhydryl of losing a proton; conversely K_2 is half k_2 since the fully deprotonated molecule is twice as likely as either site to gain a proton. Thus, simple measurement of K_1 and K_2 suffices to characterize the acid-base behaviour.

(a) Macroionisation scheme.



(b) Microionisation scheme.

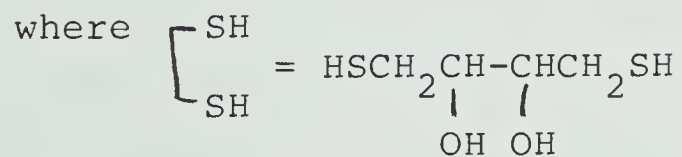
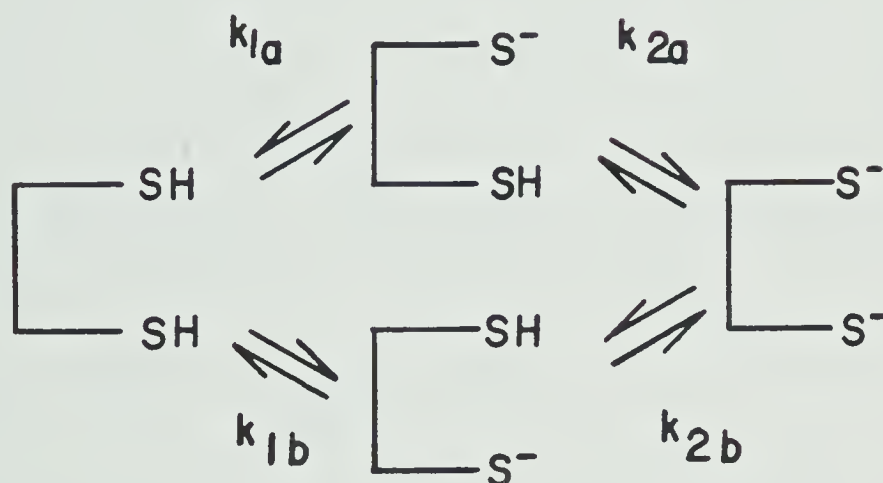


Figure 22. Acid dissociation schemes for Dithioerythritol.

It was hoped to characterize K_1 and K_2 by ^1H NMR, in the same manner as for MAA (Chapter III); however, this proved impossible. Firstly, DTE has a very highly coupled second order NMR spectrum. At reasonable concentrations, signal-to-noise ratio on the A60D spectrometer was very poor. A spectrum was collected at 200 MHz of a 0.1 M solution at pH 7. This had the general appearance of an ABX spectrum but displayed additional splittings; the molecular structure predicts an AA'BB'XX' spin system. No attempt was made at spectral analysis.

Even in the absence of detailed chemical shift and coupling constant data, it is possible to use the observed position of an individual peak as a function of pH to determine pK values. The equation is similar to that given above (Chapter II, equation (35)):

$$\delta_{\text{obs}}^* = \delta_1^* \cdot \alpha_1 + \delta_2^* \cdot \alpha_2 + \delta_3^* \cdot \alpha_3$$

where δ^* values are *apparent* chemical shifts, a resultant of the true chemical shift and one or more coupling constants. However, in such studies, the values of δ_1^* , δ_2^* and δ_3^* are generally determined by inspection from measurements on samples containing a vast preponderance of one form. In the present case, K_1 and K_2 lie very close together; thus, there is no region where the singly protonated form pre-

dominates and δ_2^* cannot be easily evaluated. In principle, given an entire δ_{obs}^* versus pH curve, it would be possible to fit by KINET to a three-parameter model in K_1 , K_2 and δ_2^* ; in practise, this was unsuccessful, due probably to strong algebraic coupling of the parameters.

To evaluate these pK's, a potentiometric method was employed instead. 50 ml of ~5 mM DTE were titrated with concentrated KOH from ambient pH (about 6.7) to pH 11.0, using the automated system described in Chapter II. Triplicate runs were performed. These were fitted to the standard potentiometric model, including correction for hydroxyl ion at high pH (107), using KINET. The sulfhydryl groups are only weakly acidic, and no discernible break was generated. The titre (weight of base to complete neutralisation) was calculated from the sulfhydryl concentration (as determined by prior iodoacetamide standardisation) and the titrant concentration (in mol g⁻¹). The replicates returned for pK₁ were 9.22, 9.19 and 9.21, giving a median of 9.21 ± 0.02; those for pK₂ were 9.97, 9.99 and 10.06, giving a median of 9.99 ± 0.05. The quality of fit was acceptable. In view of the closeness of the successive pK's the correlation coefficient was necessarily fairly high (~0.6), but error estimates in pK values returned by KINET were also acceptable.

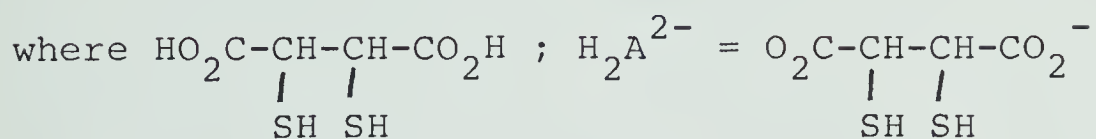
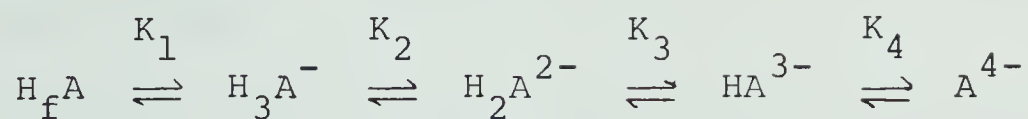
2. Acid dissociation constants for 2,3 dimercaptosuccinic acid.

DMSA displays the ionisation behaviour shown in Figure 23. The comments on microconstants given above with reference to DTE also apply here; they apply in addition to the two carboxylic acid groups.

Some problems were experienced with solubility; DMSA was not soluble in water at the 50 mM level normally used for stock solutions. 1 L of 2 mM stock solution was prepared, standardised in 100 ml aliquots, and used for potentiometric work undiluted. Triplicate titrations were performed. The intermediate endpoint observed gave the carboxylic acid titre, which can be compared with the (calculated) sulfhydryl titre. A ratio of .96 was obtained, comparable with a typical figure of 97% for the purity of the monothiols (Chapter III).

The carboxylate region was fitted by KINET to the standard model, yielding $pK_1 = 2.69, 2.75, 2.65$ (median, 2.69 ± 0.05) and $pK_2 = 3.44, 3.44, 3.43$ (median, 3.44 ± 0.01). The thiol regions gave $pK_3 = 9.40, 9.44, 9.42$ (median, 9.42 ± 0.02) and $pK_4 = 11.05, 11.12, 11.05$ (median, 11.05 ± 0.04).

a) Macroionization scheme:



b) Microionization scheme:

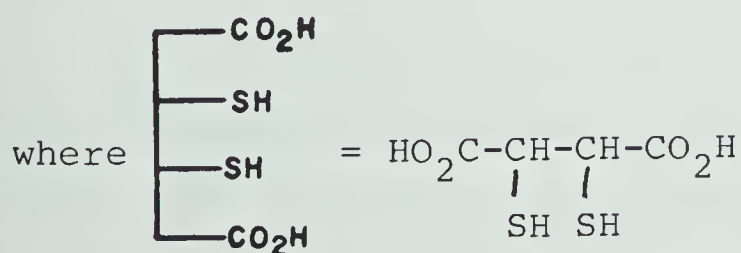
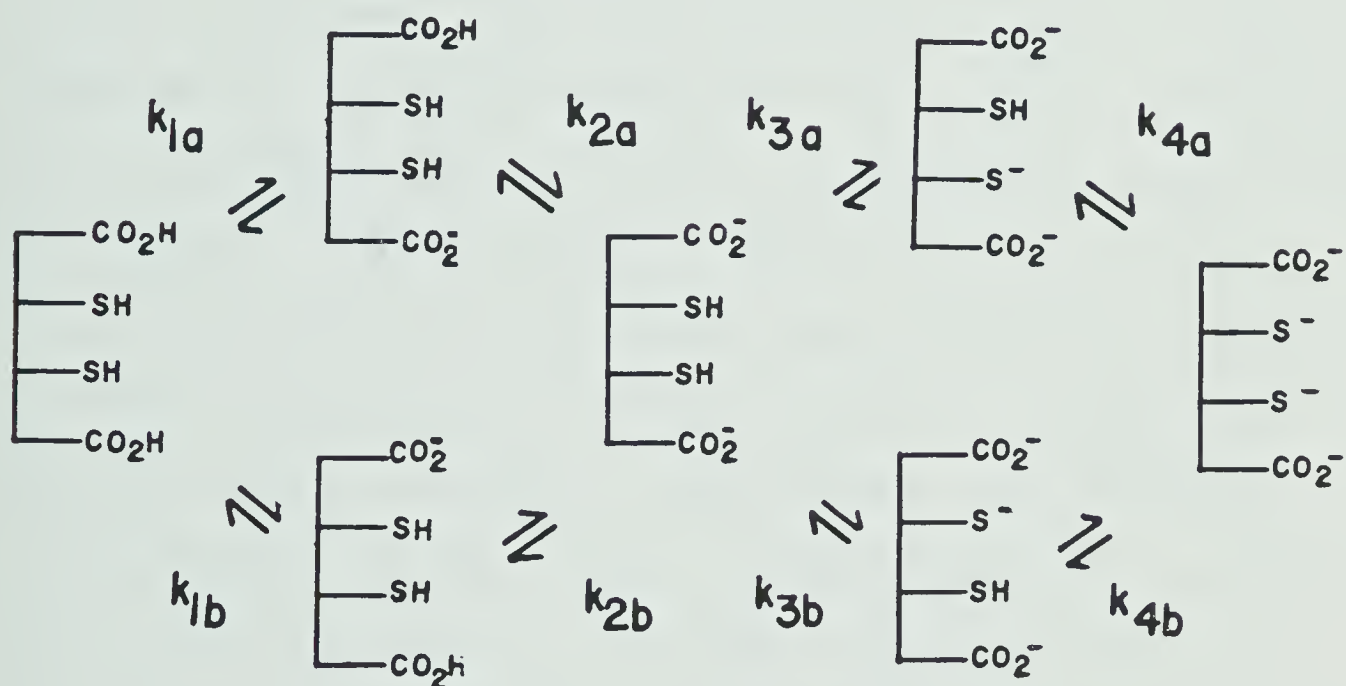


Figure 23. Acid dissociation schemes for 2,3 dimercaptosuccinic acid.

3. Acid dissociation constants for methylmercury(II) bound DMSA.

At first sight, addition of one mole equivalent of $\text{CH}_3\text{Hg(II)}$ to DTE or DMSA should yield a system having just one pK, that of the unbound sulfhydryl. In fact (see below) the situation is somewhat more complicated.

A small amount of 1:1 $\text{CH}_3\text{Hg(II)}:\text{DMSA}$ was prepared in H_2O ; a white precipitate was observed, insoluble even at the 1 mM level. This is not unexpected, since DMSA itself is fairly insoluble (see above) and the binding of $\text{CH}_3\text{Hg(II)}$ might be anticipated to exacerbate the problem. Preparation of another sample at pH 10 gave no precipitate, even at the 0.2 M level. The pH could be reduced to about 4, then slow precipitation was observed, suggesting that provided at least one carboxylate on the complex is ionised, the molecule will be soluble. Unfortunately, the kinetics of dissolution are very slow; a sample prepared at low pH would not dissolve in a reasonable time until a pH of about 10 was reached, thus precluding the possibility of titrating with base and simply ignoring any potentiometric data collected before the sample dissolved.

To circumvent these problems, the DMSA stock solution was reprepared in a known amount of previously standardised base. The sulfhydryl content was established as before.

An aliquot was then mixed with 1 mole equivalent $\text{CH}_3\text{Hg(II)}$, diluted to 50 ml (~ 5 mM) and again titrated potentiometrically. Duplicate runs were performed. In view of precipitation problems, no effort was made to evaluate pK'_1 and pK'_2 , the carboxylic acid dissociation constants for the 1:1 methylmercury(II) complexed DMSA molecule.

Evaluation of pK'_3 , for the sulfhydryl group in the 1:1 complex, is complicated by the possibility of formation of the 2:1 complex. The binding of $\text{CH}_3\text{Hg(II)}$ by imidazole, which reacts in a similar way, has been studied in detail (37). In the imidazole system, which contains two potential N-coordinating sites, it was found that binding of $\text{CH}_3\text{Hg(II)}$ at one site enhanced the affinity of the other for $\text{CH}_3\text{Hg(II)}$, to the point where it would remove $\text{CH}_3\text{Hg(II)}$ from another molecule (37). A similar effect is not necessarily involved in the present case; sulfhydryls are soft, not hard, ligands and they are probably not so intimately electronically linked as were the imidazole nitrogens. Nevertheless, such a possibility should be allowed for. It can be formalised as the reaction



where

$$K_{dp} = \frac{[\overline{M M}] [\overline{H -}]}{[\overline{- M}] [\overline{H M}]} \quad (83)$$

This will be loosely referred to as a "disproportionation" reaction. The resulting full acid-base/binding scheme is given in Figure 24. Only data above pH 7 is considered so the presence of the carboxylate groups can be ignored. The algebraic model derived from this scheme is given below.

"Disproportionation" reaction

Now

$$K_{dp} = \frac{[\overline{M M}] [\overline{H -}]}{[\overline{H M}] [\overline{- M}]} \quad (84)$$

but

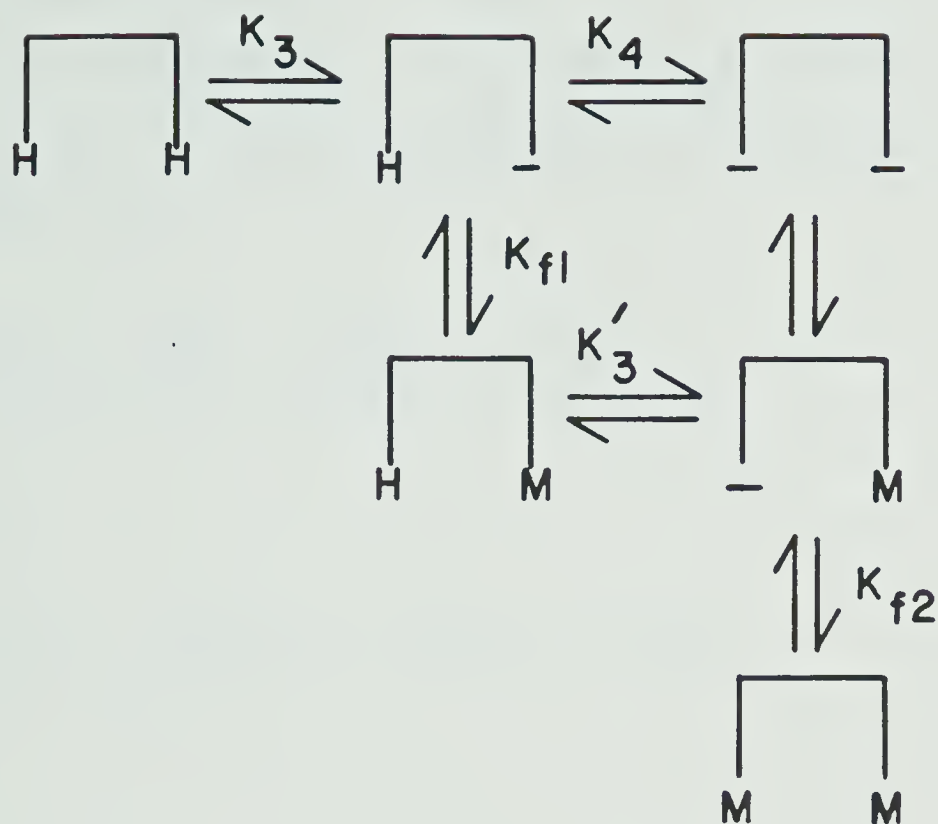
$$K_{f_2} = \frac{[\overline{M M}]}{[\overline{- M}] [M]} \quad (85)$$

and

$$K_{f_1} = \frac{[\overline{H M}]}{[\overline{H -}] [M]} \quad (86)$$

thus

$$K_{dp} = K_{f_2} / K_{f_1} \quad (87)$$




where  = $\begin{array}{c} ^-\text{O}_2\text{C}-\text{CH}-\text{CH}-\text{CO}_2^- \\ | \quad | \\ \text{SH} \quad \text{SH} \end{array}$ and M = methylmercury (II)

Figure 24. Ionization/binding scheme for DMSA.

Stoichiometric balance

Since 1 equivalent of $\text{CH}_3\text{Hg(II)}$ is present for every one of DMSA, for every equivalent of $\overline{\text{M M}}$ there is one of free DMSA, i.e.

$$\overline{\text{M M}} = \overline{\text{H -}} + \overline{\text{H H}} + \overline{\text{- -}} \quad (88)$$

But

$$\overline{\text{H -}} = \alpha_a \left(\overline{\text{H -}} + \overline{\text{H H}} + \overline{\text{- -}} \right) \quad (89)$$

where

$$\alpha_a = \frac{a_{\text{H}^+} \cdot K_3}{(a_{\text{H}^+})^2 + a_{\text{H}^+} \cdot K_3 + K_3 K_4} \quad (90)$$

Thus,

$$\overline{\text{H -}} = \alpha_a \overline{\text{M M}} \quad (91)$$

Also,

$$\overline{\text{H M}} = \overline{\text{- M}} \frac{a_{\text{H}^+}}{K_3'} \quad (92)$$

from the definition of K_3' . Substitution of these into equation (87) gives

$$K_{dp} = \frac{\alpha_a [\overline{M M}]^2 K'_3}{[\overline{- M}]^2 a_{H^+}} \quad (93)$$

which, when rearranged, gives

$$[\overline{M M}]^2 = \frac{K_{dp}}{\alpha_a} \cdot \frac{a_{H^+}}{K'_3} [\overline{- M}]^2 \quad (94)$$

Thus,

$$[\overline{M M}] = A [\overline{- M}] \quad (95)$$

where

$$A = \left(\frac{K_{dp}}{\alpha_a} \cdot \frac{a_{H^+}}{K'_3} \right)^{1/2} \quad (96)$$

Mass balance in DMSA

Now

$$C_{DMSA} = [\overline{H H}] + [\overline{H -}] + [\overline{- -}] + [\overline{H M}] + [\overline{- M}] + [\overline{M M}] \quad (97)$$

where C_{DMSA} is the total concentration of DMSA in solution.

Substitution from (88) gives:

$$C_{\text{DMSA}} = [\overline{\text{H M}}] + [\overline{- \text{M}}] + 2[\overline{\text{M M}}] \quad (98)$$

and from (92):

$$C_{\text{DMSA}} = [\overline{- \text{M}}] \left\{ 1 + \frac{a_{\text{H}^+}}{K_3'} \right\} + 2[\overline{\text{M M}}] \quad (99)$$

and from (95):

$$C_{\text{DMSA}} = [\overline{- \text{M}}] \left\{ 1 + \frac{a_{\text{H}^+}}{K_3'} + 2A \right\} \quad (100)$$

Thus

$$[\overline{- \text{M}}] = \frac{C_{\text{DMSA}}}{\left\{ 1 + \frac{a_{\text{H}^+}}{K_3'} + 2A \right\}} \quad (101)$$

Total charge balance

$$[\overline{\text{H -}}] + 2[\overline{- -}] + [\overline{- \text{M}}] + [\text{OH}^-] + [\text{Cl}^-] = C_{\text{Na}} + [\text{H}^+] \quad (102)$$

where C_{Na} is the Na^+ concentration added with excess base, adjusted for the fact that carboxylate groups are being ignored. This, of course, is known.

At the endpoint $[\text{Cl}^-] = C_{\text{Cl}}$ also known from prior standardisations. Before the endpoint $[\text{Cl}^-] = xC_{\text{Cl}}$ where x is the fraction of the titre delivered.

Thus,

$$[Cl^-] = xC_{Cl} = C_{Na} + [H^+] - [OH^-] - \{ \overline{[H^-]} + 2\overline{[- -]} + \overline{[- M]} \} \quad (103)$$

Now, as before

$$\overline{[H^-]} = \alpha_a \overline{[M M]} = \alpha_a A \overline{[- M]} \quad (104)$$

Similarly

$$\overline{[- -]} = \alpha_b \overline{[M M]} = \alpha_b A \overline{[- M]} \quad (105)$$

where

$$\alpha_b = \frac{K_3 K_4}{(a_{H^+})^2 + a_{H^+} K_3 + K_3 K_4} \quad (106)$$

Substitution gives

$$xC_{Cl} = C_{Na} + [H^+] - [OH^-] - \overline{[- M]} \{ 1 + A(\alpha_a + 2\alpha_b) \} \quad (107)$$

Final substitution

Substitute (101) into (107):

$$x = \frac{(C_{Na} + [H^+] - [OH^-])}{C_{Cl}} - \frac{C_{DMSA}}{C_{Cl}} \frac{1 + A(\alpha_a + 2\alpha_b)}{1 + \frac{a_{H^+}}{K_3'} + 2A} \quad (108)$$

where: C_{Na} = added Na^+ concentration

C_{Cl} = chloride concentration at endpoint

C_{DMSA} = total DMSA concentration

$$\alpha_a = \frac{a_{H^+}K_3}{(a_{H^+})^2 + a_{H^+}K_3 + K_3K_4} ; \alpha_b = \frac{K_3K_4}{(a_{H^+})^2 + a_{H^+}K_3 + K_3K_4}$$

and $A = \left(\frac{K_{dp}}{\alpha_a} \cdot \frac{a_{H^+}}{K_3'} \right)^{1/2}$ where in turn $K_{dp} = \frac{K_{f2}}{K_{f1}}$

Note that equation (108) contains the term $[OH^-]$.

Since the operational scale of pH is designed to correspond as far as possible to $-\log_{10} a_{H^+}$ (137), in order to evaluate $[OH^-]$ as opposed to a_{OH^-} a value for the activity coefficient, γ_{OH^-} , of OH^- ion in 0.3 M KNO_3 is required. No literature value could be found for this, so a value was estimated by two different methods. Firstly, a value was calculated from the Davies equation. Kieland (138) obtained satisfactory activity coefficients assuming for OH^- a fairly typical ion-size parameter, so this approach should be valid. The value obtained was $\gamma = 0.71$. Secondly, experimental mean activity coefficients at $\mu = 0.3$ for potassium nitrate and a variety of salts with similarly

sized ions (139) were averaged; the value obtained was 0.69. The value assumed in calculations was 0.70.

A two parameter fit involving K'_3 and K_{dp} was run with KINET; this gave a successful fit to the data, with a pK'_3 value of 9.86 ± 0.02 and $K_{dp} = 0.6 \pm 0.2$. Since the correlation coefficient was high, supplementary runs were performed to check the validity of these results, inputting K_{dp} as a constant and fitting only to pK'_3 . Various values of K_{dp} between 10 and .1 were used; the quality of fit started to degrade significantly when K_{dp} was outside the range 0.4-0.8. The value of pK'_3 was coupled to some extent, changing by about 0.1 over the range of K_{dp} values 0.2-10. In view of this, the values $pK'_3 = 9.86 \pm 0.06$ and $K_{dp} = 0.6 \pm 0.2$ are reported for discussion.

4. The acid-dissociation constant for $CH_3Hg(II)$ bound DTE.

Severe solubility problems were encountered in this case. Solutions of 1:1 $CH_3Hg(II)$:DTE could be prepared at high pH (>12) but started to precipitate slowly at lower pH values. It appeared that the neutral species



was insoluble, and that deprotonation at the other sulfhydryl was necessary for dissolution. For instance, it

was observed that the lower the concentration of complex prepared, the lower the pH attainable before the onset of precipitation. Again, kinetics were sluggish.

Triplicate potentiometric back-titrations were performed, terminating when visible precipitation was evident, typically at pH ~ 9 .

Attempts to fit the data to a two-parameter model in pK'_1 and K_{dp} , as for DMSA, were not successful, probably because data below pH 9 were not accessible due to precipitation of the sample. As will be shown below, however, the value of K_{dp} determined for DMSA yields values for K_{f1} and K_{f2} which display the same trend (relative to the pK 's for these sulfhydryls) as did the various monothiols characterized in Chapter III. If the assumption is made that this is the case also for DTE, then K_{dp} for the DTE system can be related to K'_1/K_1 (details are given in Section C). Since K_1 is known, the model thus reduces to a one-parameter fit. This yielded a satisfactory result: the quality of fit was as high as in the two-parameter case for DMSA, supporting the validity of the assumption. The value of pK'_1 returned was 9.55 ± 0.03 .

5. Formation constants of $CH_3Hg(II)$ complexes of dithiols.

In the DMSA case, since all other parameters (K_3 , K_4 ,

K'_3 , K_{dp}) were now determined, only K_{f1} remained as an unknown. Figure 25 shows the MAA methylene resonance chemical shift as a function of pH for a 1:1:1 mixture of methylmercury(II), MAA and DMSA. Also shown is a similar curve for competition with 2,3 dimercapto-propane-1-sulfonate ($BALSO_3H$). While this species is not symmetrical, and therefore a full formation constant study was not attempted, this curve enables evaluation of a conditional formation constant for this ligand as a function of pH (see below). The algebraic model in the DMSA case is similar to that given in Chapter III for monothiols, except that the possibilities of sulfhydryl deprotonation in the complex, and of a second complexation, complicate matters.

The full binding scheme for a symmetrical dithiol is illustrated in Figure 24. Again, the symbolism is used throughout the derivation.

Mass balance in MAA

Now

$$C_{MAA} = [\tilde{H}] + [\overset{\sim}{-}] + [\tilde{M}] \quad (109)$$

where C_{MAA} is the total MAA concentration in solution.

Now

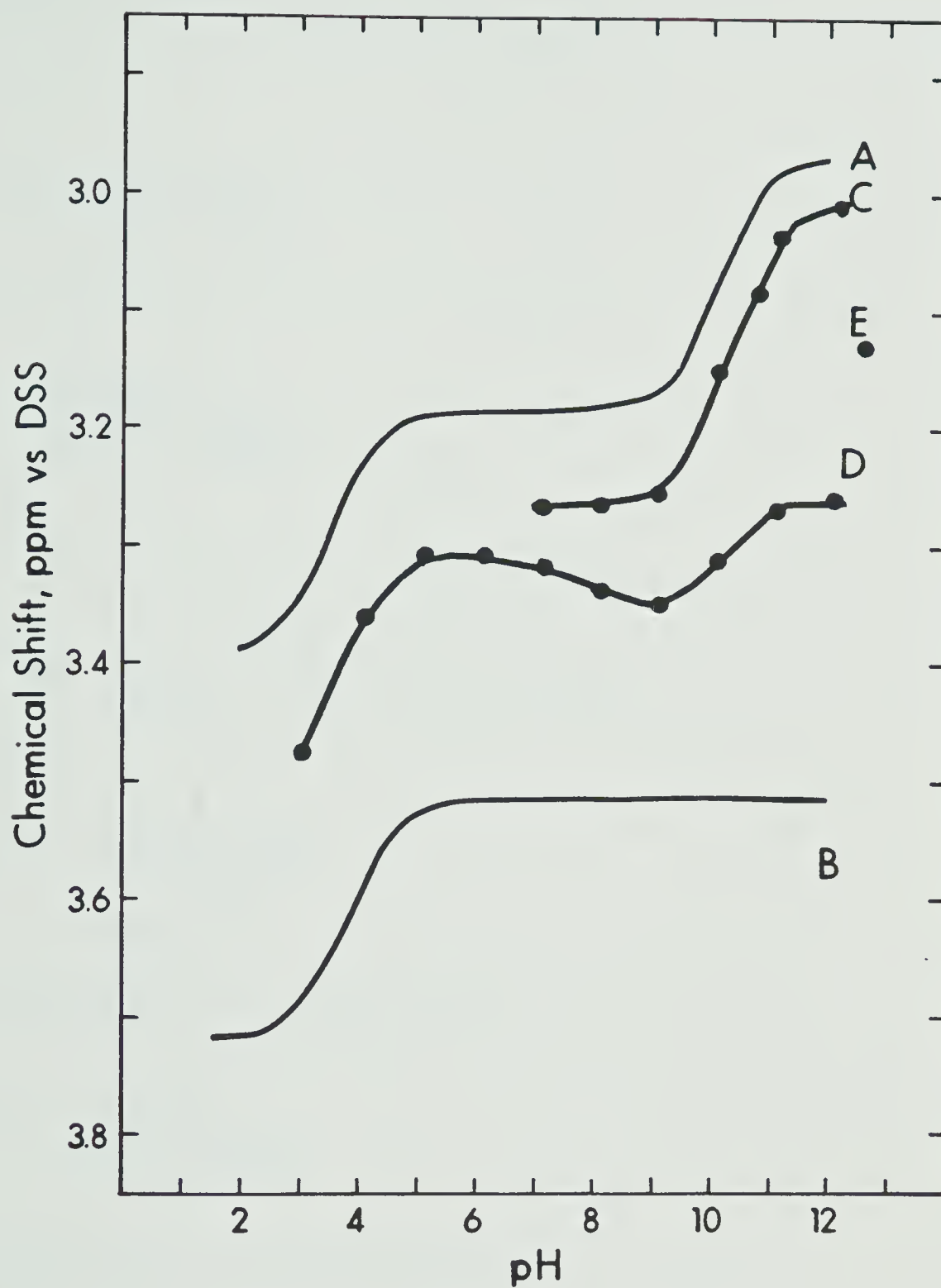


Figure 25. MAA chemical shift as a function of pH for
 a) free MAA, b) $\text{CH}_3\text{Hg(II):MAA}$ 1:1, c) as b) +
 1 m.e. DMSA, d) as b) + 1 m.e. BALSO_3H ,
 e) $\text{MAA:CH}_3\text{Hg(II):DTE}$ 2:1:1 (single determination).

$$[\overline{H}] + [\overline{-}] = P_f \cdot C_{MAA} \quad (110)$$

Thus

$$[\overline{-}] = \alpha_2 P_f \cdot C_{MAA} \quad (111)$$

where

$$\alpha_2 = \frac{K_{2MAA}}{a_{H^+} + K_{2MAA}} \quad (112)$$

Also

$$[\overline{M}] = K_{fMAA} [\overline{-}] [M] = (1-P_f) \cdot C_{MAA} \quad (113)$$

Thus

$$[M] = \frac{(1-P_f) \cdot C_{MAA}}{K_{fMAA} [\overline{-}]} \quad (114)$$

Substituting from (111) in (114):

$$[M] = \frac{(1-P_f)}{P_f \cdot \alpha_2 \cdot K_{fMAA}} \quad (115)$$

Mass balancing in methylmercury(II)

Now

$$C_M = [\overline{M}] + [\overline{H M}] + [\overline{- M}] + 2[\overline{M M}] \quad (116)$$

But $C_M = C_{MAA}$, $[M] = (1-P_f) \cdot C_{MAA}$ and $[M]$ is negligible.

Thus

$$P_f \cdot C_{MAA} = [H M] + [- M] + 2[M M] \quad (117)$$

Now make the following substitutions:

$$[H M] = K_{f1} [H -] [M]$$

$$[- M] = [H M] \frac{K'_3}{a_{H^+}} = \frac{K_{f1} K'_3}{a_{H^+}} [H -] [M]$$

$$[M M] = K_{f2} [- M] [M] = \frac{K_{f1} K_{f2} K'_3}{a_{H^+}} [H -] [M]^2$$

Thus:

$$[H -] = \frac{P_f \cdot C_{MAA}}{\{K_{f1} [M] + \frac{K_{f1} K'_3 [M]}{a_{H^+}} + \frac{2K_{f1} K_{f2} K'_3}{a_{H^+}} [M]^2\}} \quad (118)$$

Mass balance in DMSA

Now

$$C_{DMSA} = [H H] + [H -] + [- -] + [H M] + [- M] + [M M] \quad (119)$$

Now make the following substitutions:

$$[\overline{H H}] = [\overline{H -}] \frac{a_{H^+}}{K_3} ; [\overline{- -}] = [\overline{H -}] \frac{K_4}{a_{H^+}} ; [\overline{H M}] = K_{f1} [\overline{H -}] [M] ;$$

$$[\overline{- M}] = \frac{K_{f1} K'_3}{a_{H^+}} [\overline{H -}] [M] ; [\overline{M M}] = \frac{K_{f1} K_{f2} K'_3}{a_{H^+}} [\overline{H -}] [M]^2$$

Thus:

$$\frac{C_{DMSA}}{C_{MAA}} = P_f \cdot \frac{\{1 + \frac{a_{H^+}}{K_3} + \frac{K_4}{a_{H^+}} + K_{f1} [M] + K_{f1} \frac{K'_3}{a_{H^+}} [M] + K_{f1} K_{f2} \frac{K'_3}{a_{H^+}} [M]^2\}}{\{K_{f1} [M] + K_{f1} \frac{K'_3}{a_{H^+}} [M] + 2K_f K_{f2} \frac{K'_3}{a_{H^+}} [M]^2\}} \quad (120)$$

$$\text{where } [M] = \frac{(1-P_f)}{P_f \cdot \alpha_2 \cdot K_{fMAA}} \text{ where in turn } \alpha_2 = \frac{K_{2MAA}}{a_{H^+} + K_{2MAA}}$$

In the present case, $C_{DMSA}/C_{MAA} = 1$. Rearranging, and substituting $K_{f2} = K_{dp} K_{f1}$:

$$K_{f1} ([M] + \frac{K'_3}{a_{H^+}} [M]) + K_{f1}^2 (2K_{dp} \frac{K'_3}{a_{H^+}} [M]^2) = P_f (1 + \frac{a_{H^+}}{K_3} + \frac{K_4}{a_{H^+}}) + K_{f1} (P_f [M] + P_f [M] \frac{K'_3}{a_{H^+}}) + K_{f1}^2 (P_f K_{dp} \frac{K'_3}{a_{H^+}} [M]^2) \quad (121)$$

Thus

$$K_{fl}^2 \left\{ K_{dp} \frac{K'_3}{a_{H^+}} [M]^2 (2 - P_f) \right\} + K_{fl} \left\{ [M] \left(1 + \frac{K'_3}{a_{H^+}} \right) (1 - P_f) \right\} - P_f \left(1 + \frac{a_{H^+}}{K_3} + \frac{K_4}{a_{H^+}} \right) = 0 \quad (122)$$

Direct substitution of the chemical shift titration data into equation (122) yielded a value of $\log K_{fl} = 17.16 \pm 0.05$. Predictably, the value obtained was coupled to the value of K_{dp} used; in view of the uncertainty in K_{dp} , $\log K_{fl}$ is reported as 17.2 ± 0.2 .

In the case of the DTE complex, it was not possible to generate a competition study chemical shift titration curve, due to solubility problems. Several replicate measurements were performed on a 2:1:1 MAA:CH₃Hg(II):DTE sample at pH 12.24. The observed chemical shift (3.132 ppm) for the MAA methylene resonance was substituted into an equation similar to (122) above; the value of $\log K_{fl}$ returned was 16.6.

C. Discussion

1. General

Table 15 shows all values determined above. In drawing comparisons with monothiol, microconstants are more useful, since they relate to the properties of the

Table 15. Values of acid dissociation and $\text{CH}_3\text{Hg(II)}$ complex formation constants for DMSA and DTE.

Ligand	Macroconstant ^a	Definition ^b	Value ^c	Microconstant	Value ^d
DMSA	pK_1	1st carboxylate	2.69	pk_1	2.99
	pK_2	2nd carboxylate	3.44	pk_2	3.14
	pK_3	1st sulfhydryl	9.42	pk_3	9.72
	pK_4	2nd sulfhydryl	11.05	pk_4	10.75
	pK'_3	Complex sulfhydryl ^g	9.86	pk'_3	9.86
	$\log K_{f1}$	$\frac{\sqrt{[\text{H M}]}}{[\text{H}^-] [\text{M}]}$ ^h	17.2 ³	$\log k_{f1}$	17.2 ^e
	$\log K_{f2}$	$\frac{\sqrt{[\text{M M}]}}{[\text{M}^-] [\text{M}]}$	16.9 ^e	$\log k_{f2}$	17.2 ³

(continued)

Table 15. (continued)

Ligand	Macroconstant ^a	Definition ^b	Value ^c	Microconstant	Value ^d
DTE	pK ₁	1st sulfhydryl	9.21	pK ₁	9.51
	pK ₂	2nd sulfhydryl	9.99	pK ₂	9.69
	pK' ₁	Complex sulfhydryl ^g	9.55	pK' ₁	9.55
	log K _{f1}	$\frac{\sqrt{[H^+][M]}}{[H^+][M]}$ ^h	16.6 ^e	log K _{f1}	16.6 ^e
	log K _{f2}	$\frac{\sqrt{[M]}}{[M]}$	16.3 ^f	log K _{f2}	16.6 ^f
		$\frac{\sqrt{[M]}}{[M]}$			

- a) Parameter measured.
- b) In terms of group involved; see Figs. 22 and 23.
- c) Unless otherwise stated, ± 0.05.
- d) See text for calculation.
- e) ± 0.2 due to uncertainty in K_{dp} (see text)
- f) From a one-parameter fit.
- g) i.e. pK of the single remaining sulfhydryl group.
- h) See Fig. 24 for symbolism.

sulfhydryl group rather than to those of the molecule as a whole. The relationships of microconstants to their corresponding macro values can be confusing; to clarify the issue, the ionisation/binding scheme shown in Figure 26 presents the actually identical "microspecies" as if they were distinct chemical entities. The relationships can then be determined, as follows:

$$K_{f2} = \frac{[\overline{M \ M}]}{(\overline{- \ M} + \overline{M \ -}) [M]}$$

where $\overline{- \ M}$ now refers to an individual microspecies, $\text{CH}_3\text{Hg}(\text{II})$ complexed at the right-hand sulfhydryl. But

$$k_{f2} = \frac{[\overline{M \ M}]}{[\overline{- \ M}] [M]} \quad \text{or} \quad \frac{[\overline{M \ M}]}{[\overline{M \ -}] [M]}$$

$$\text{Thus, } K_{f2} = \frac{k_{f2}}{2}$$

It can be demonstrated similarly that

$$K_2 = \frac{k_2}{2} ; K_1 = 2k_1 ; K'_1 = k'_1 \text{ and } K_{f1} = k_{f1}$$

All discussion hereafter will be in terms of microconstants.

Trends in the free acid dissociation constants are as

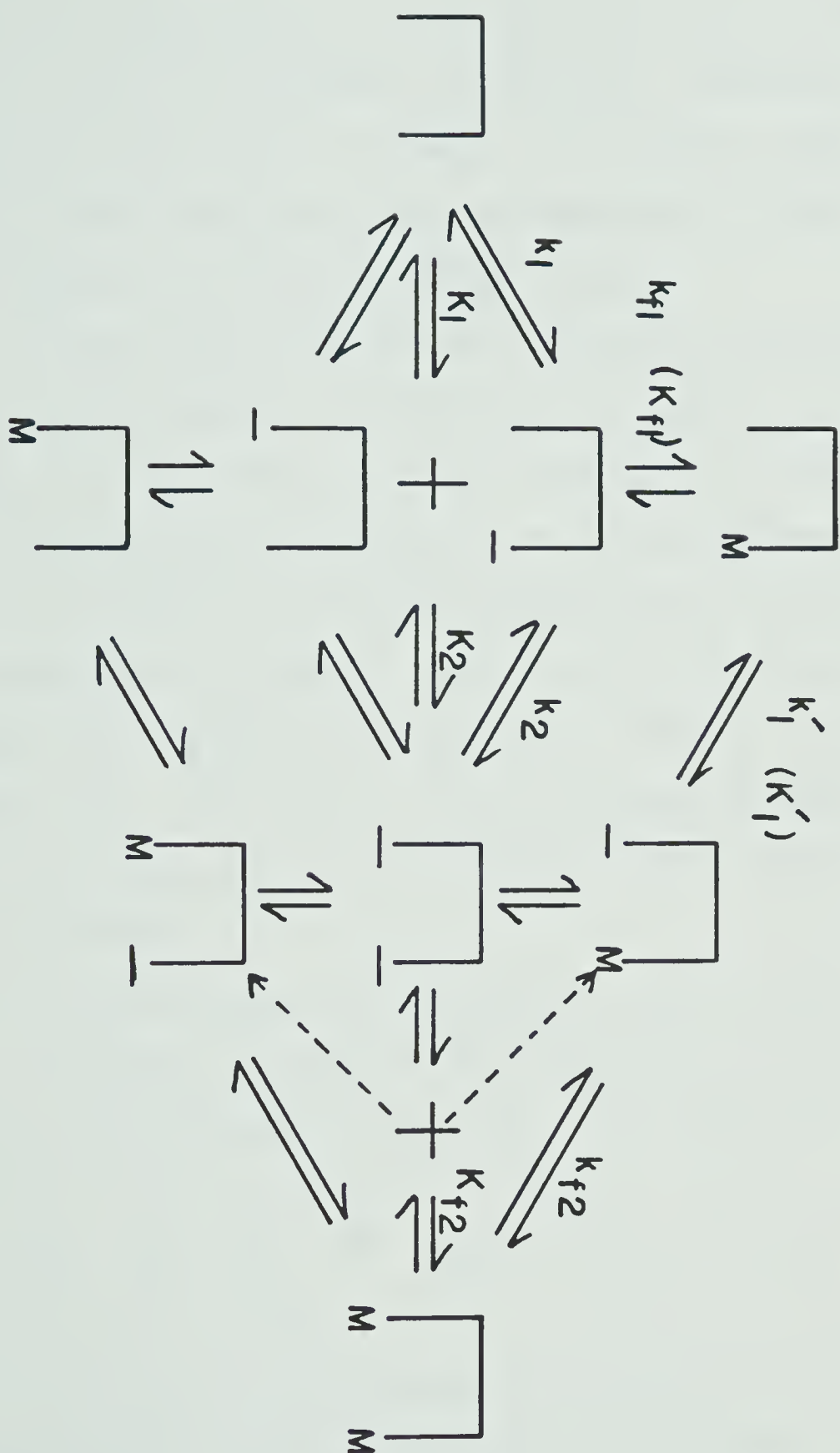


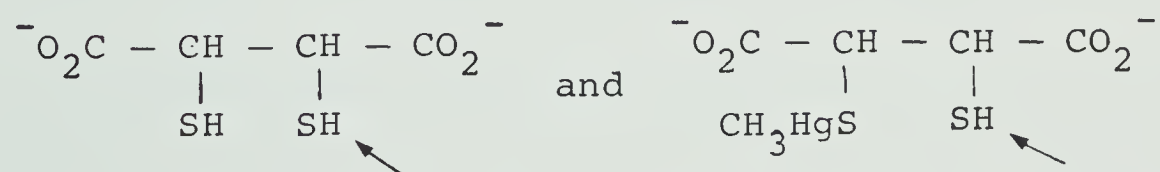
Figure 26. Full microdissociation/binding scheme for a symmetrical dithiol.

expected. In the case of DTE, the two thiols are fairly isolated; ionisation of the first has a pK (*microconstant*) of 9.51 and of the second a pK of 9.69, indicating little interaction between the groups. (A similar trend is observed for the carboxylate ionisations of DMSA, which also pertain to fairly isolated groups.)

On the other hand, the two sulfhydryl microdissociation constants for DMSA indicate some interaction. pK_3 is 9.72 and pK_4 10.75. Once the first sulfhydryl is deprotonated, deprotonation of the second is markedly inhibited.

The trends can also be characterized in terms of the macroconstants K_1 and K_2 . For totally non-interacting groups, $K_1 = 4K_2$ due to statistical effects (see page 144, Chapter IV). For DTE, $K_1 = 6K_2$, whereas for DMSA $K_1 = 43K_2$, indicating much more influence of one group on the other in DMSA.

In neither case was any marked effect noted on the pK of a sulfhydryl group when the proton on the *other* sulfhydryl was replaced by $CH_3Hg(II)$. The molecules



have pK values at the indicated sulfhydryl of 9.72 and 9.86 respectively. For the analogous DTE molecules, the values

for the $\text{CH}_3\text{Hg(II)}$ complexes of cysteine, penicillamine and glutathione were closer to values for the free ligands protonated at the sulfhydryl than deprotonated. The present results show that such a trend also applies to the $\text{pk}'\text{s}$ at a second proximal sulfhydryl group.

It was established in Chapter III that for compounds with the same number of proximal carboxylate groups, the value of $\log K_f$ rises approximately linearly with that of the pk of the sulfhydryl group involved. For DMSA, the $\text{pk}'\text{s}$ involved rise (9.72 and 9.86 respectively), predicting a slight but definite "activation" of the second sulfhydryl toward attack by $\text{CH}_3\text{Hg(II)}$ when the first is complexed already. In quantitative forms:

$$K_{dp} = \frac{K_{f2}}{K_{f1}} \quad (87)$$

but $K_{f1} = k_{f1}$ and $K_{f2} = \frac{k_{f2}}{2}$ thus

$$K_{dp} = \frac{k_{f2}}{2k_f} \quad \text{or} \quad \log K_{dp} = \log k_{f2} - \log k_{f1} - \log 2 \quad (123)$$

But $\log k_{f1} = \text{pk}_3 + c$ and

$$\log k_{f2} = \text{pk}'_3 + C \quad (124)$$

where C is a constant; thus

$$\log K_{dp} = pk'_3 - pk_3 - \log 2 \quad (125)$$

This gives a predicted value of 0.7 for K_{dp} , a slight but definite activation. The value determined by experiment (above) was 0.6 ± 0.2 ; it appears that the relationship between $\log k_f$ and pk also holds for dithiol molecules.

Figure 27 shows the manner in which DMSA distributes itself between its various species in the 1:1 $CH_3Hg(II)$:DMSA system. At pH 5 (the lowest pH value calculated since the complex carboxylate pk 's are unknown) the predominant species is \overline{HM} , although \overline{HH} and \overline{MM} also exist at a level of 0.25 each. Given the very similar properties of the binding sites (see above) this is as expected. When the pH is raised to about 8, \overline{HM} starts to deprotonate; its concentration decreases in favour of \overline{M} . \overline{HH} also decreases in favour of the intermediate $\overline{H-}$ form; as the pH is raised further this in turn decreases again in favour of the fully deprotonated high pH form $\overline{-}$. At high pH, the predominant species is \overline{M} , with about 15% each of \overline{MM} and $\overline{-}$.

2. Chelation in the 2,3 dimercaptosuccinic acid- $CH_3Hg(II)$ complex.

Figure 28 reproduces some of the values shown on the plot of $\log K_f$ as a function of pk in Figure 18 (Chapter

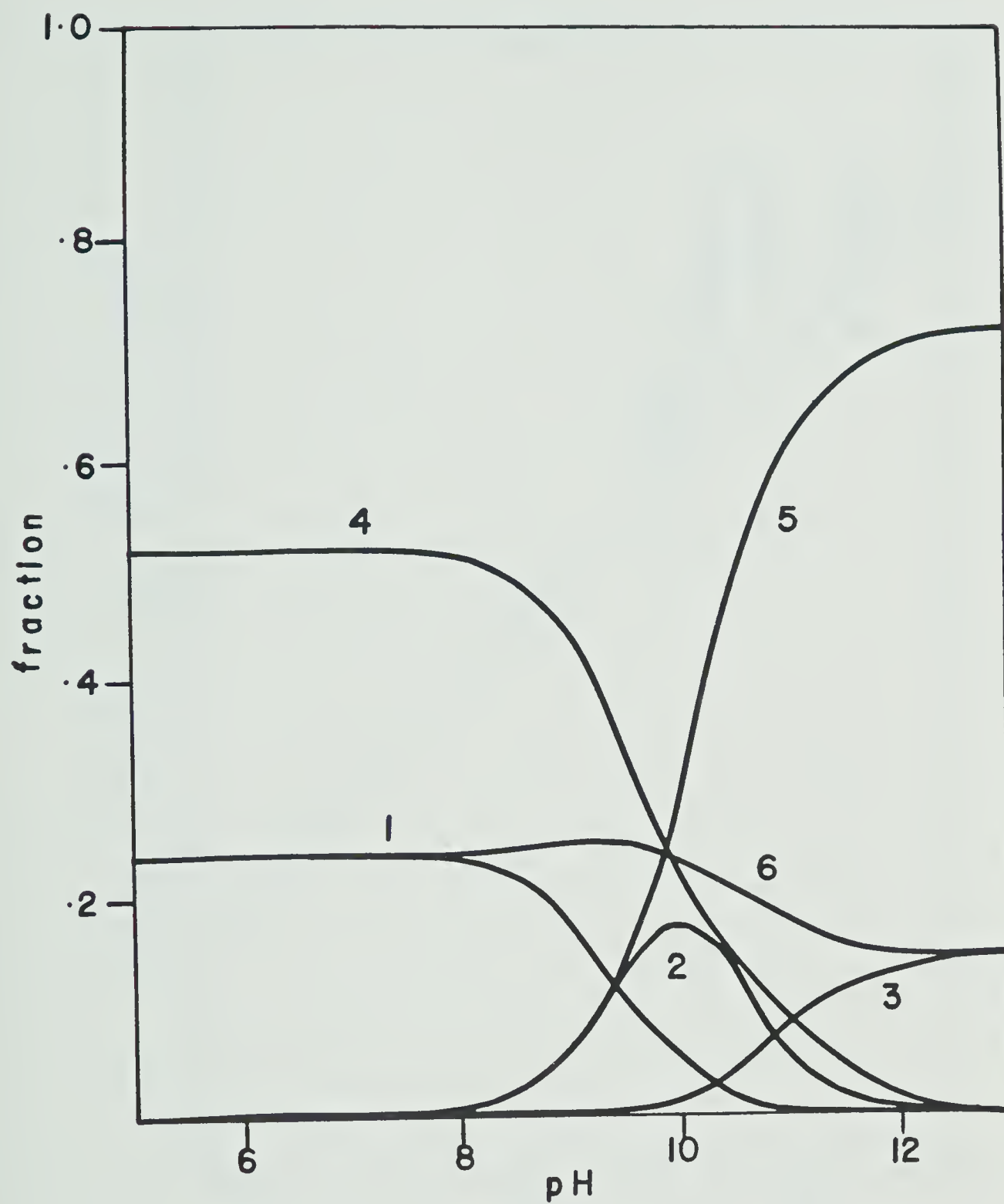


Figure 27. Fractional amounts of various DMSA species in a solution containing 1:1 DMSA:methylmercury(II).

1 $\overline{\text{H H}}$, 2 $\overline{\text{H}^-}$, 3 $\overline{-}$, 4 $\overline{\text{H M}}$, 5 $\overline{- \text{M}}$, 6 $\overline{\text{M M}}$

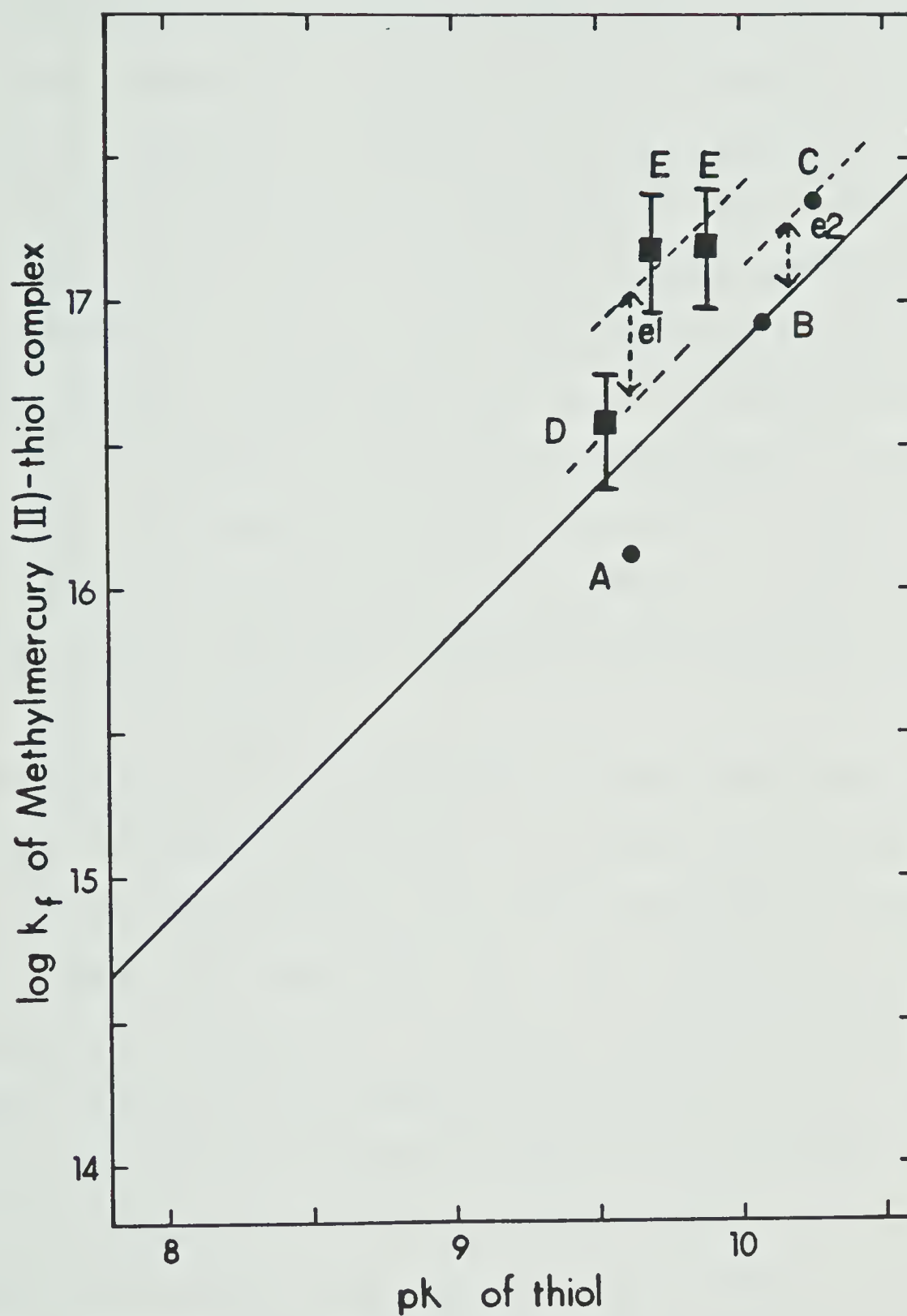


Figure 28. Plot of $\log k_f$ vs pK for methylmercury(II) complexes of a) mercaptoethanol, b) MAA, c) mercaptosuccinic acid, d) dithioerythritol and e) 2,3 di-mercaptosuccinic acid.

III), together with those determined above for the dithiols.

It was observed in Chapter III that compounds containing one proximal carboxylic acid group generally laid along a line of unity slope (shown solid); for instance, MAA. Those containing no carboxylic acid groups (such as mercaptoethanol) lay below this line, and those containing two such groups lay above the line, e.g. mercaptosuccinic acid. It may be that this is due to some degree of chelation, the carboxylate(s) acting as secondary coordinating sites. Crystal structures of, for instance, the $\text{CH}_3\text{Hg(II)}$ -cysteine complex show some degree of mercury-carboxylate O atom interaction (47).

It appears that for both DTE and DMSA some degree of chelation is present, involving the second sulfhydryl, since the values are higher than the corresponding monothiol values would have predicted. The values for DMSA (e) in Figure 28 lie about 0.3 log units higher than the value for MSA (c) would have indicated (displacement e1). This is not a particularly dramatic effect; for instance, the stability enhancement (e2) from MAA (b) to MSA (c), due to addition of a second carboxylate group, is about 0.25 log units. Obviously, therefore, the effects of sulfhydryl and carboxylate groups in a *chelating* role are not related to their relative binding strengths as "primary ligands",

since these are about 10^{17} and 10^3 respectively. It was noted in the Introduction (Chapter I) that studies with halide complexes suggest that the "extra" ligands in the higher complexes interact only weakly, in a largely ionic manner. It seems probable that the same is true here, since in a purely ionic situation the softness of the sulfur atom will not enhance its binding capabilities.

The conclusion that chelation is weak is also supported by the trend observed in the acidity of the "second" sulfhydryl. In the case of MAA, the free sulfhydryl has a pK of 10.08; the complexed molecule has a pK at the sulfur atom of between 0 and 1. Since no observable decrease in pK at the second sulfhydryl results when the first is complexed, it seems that the energy involved in the secondary interaction is negligible by the standards of the primary interaction.

The enhancement in K_f for DTE, relative to the value previously found (15) for mercaptoethanol, is unexpected (see parts a) and d) in Fig. 28). Various speculations are possible; however, it should principally be borne in mind that due to the assumption which was made of the value of K_{dp} this value is only an estimate.

3. Conditional formation constants in dithiol systems.

The *conditional* formation constants of the dithiol ligands are illustrated as a function of pH in Figure 29. These are defined as:

$$K_{fc} = \frac{[\text{bound dithiol sulfhydryls}]}{[\text{free dithiol sulfhydryls}][\text{free CH}_3\text{Hg(II)}]} \quad (126)$$

Note that the expression (126) involves *sulfhydryl*, rather than *molecule* concentrations; thus what is in effect being evaluated is the affinity of a "typical" sulfhydryl on the dithiol toward $\text{CH}_3\text{Hg(II)}$, which makes direct comparisons with the monothiol curves of Chapter III (Fig. 20) possible.

The curves in Figure 29 for DTE and DMSA are calculated from the measured values of the various equilibrium constants; that for BALSO_3H is calculated directly from the chemical shift-pH titration curve presented earlier. The corresponding curve for MAA, a fairly typical monothiol, is also shown for comparison.

The DMSA curve lies highest of all those studied. Data were not calculated below pH 5, since the complex carboxylate pK's are not known. $\log K_{fc}$ for a sulfhydryl on DTE is seen to be somewhat lower, fairly similar to MAA. The curve for BALSO_3H lies lowest of the dithiols studied, the non-symmetrical shape of the plot, in contrast

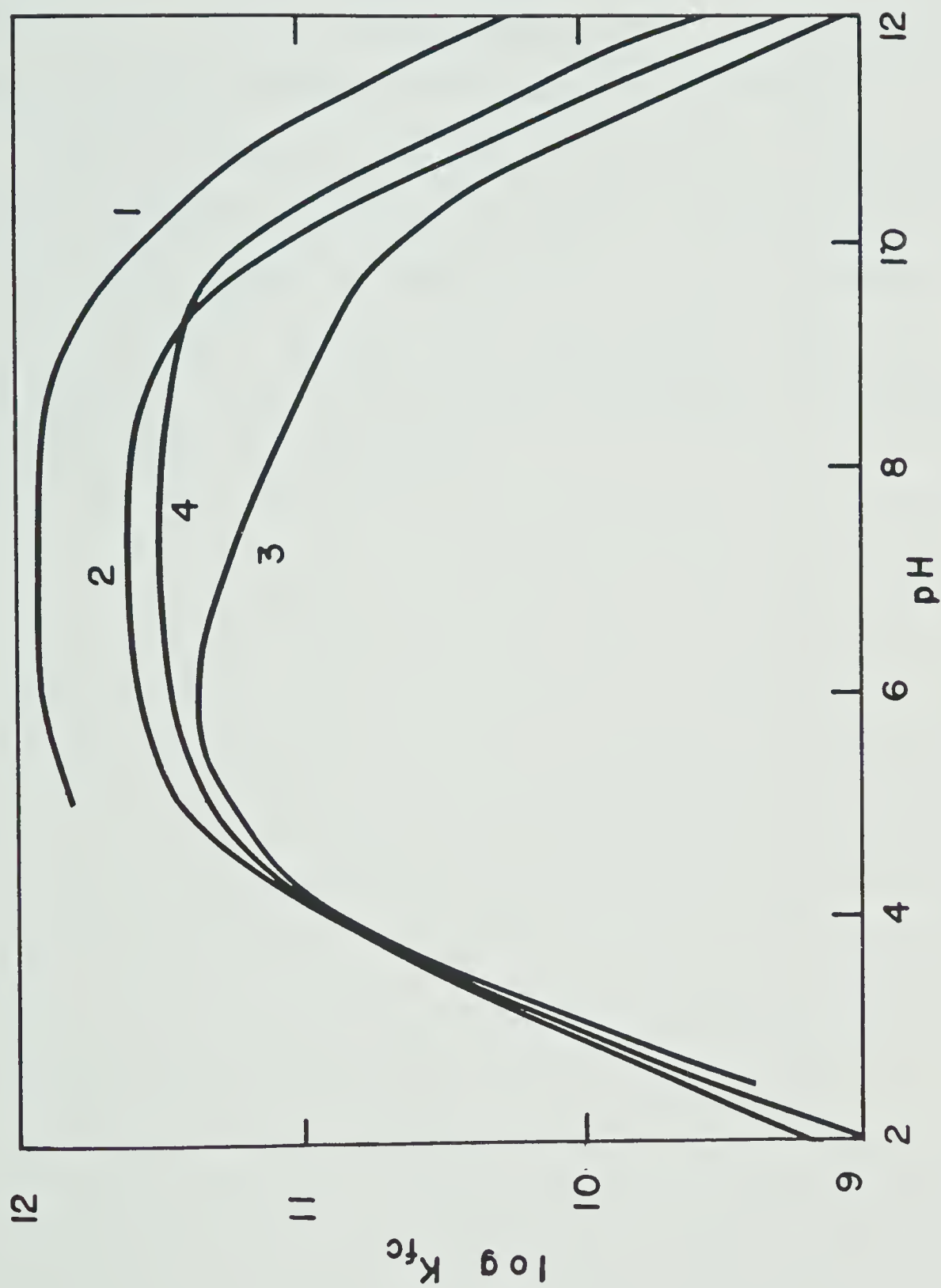


Figure 29. log conditional formation constant as a function of pH for the methylmercury(II) complexes of 1) 2,3 dimercaptosuccinic acid, 2) dithioerythritol, 3) BALSO_3H , 4) MAA.

to the others, should be noted. Although detailed data is not available, it appears that the lack of success of this ligand is due to the high pK of the second sulfhydryl (values of ~ 12 have been reported (140)), making proton competition successful even at elevated pH values.

Table 16 gives the values of K_{fc} at pH 7.4 for all ligands studied in Chapters III and IV; these figures will be discussed further in Chapter VIII, in the light of actual "antidote" studies with erythrocytes, where the effectiveness of the various thiol compounds at removing added $\text{CH}_3\text{Hg(II)}$ is evaluated.

Table 16. Conditional formation constants for the
 $\text{CH}_3\text{Hg(II)}$ -thiol complexes at pH 7.4.

Ligand	$\log K_{fc}$
Mercaptoethanol	11.13
Homocysteine	11.15
2,3 dimercapto-propane-1-sulfonate	11.20 ^a
N-acetylpenicillamine	11.20
Penicillamine	11.33
Glutathione	11.46
Mercaptoacetic acid	11.47
Cysteine	11.57
2,3 dithioerythritol	11.59 ^a
Mercaptosuccinic acid	11.68
2,3 dimercaptosuccinic acid	11.92 ^a

a) Conditional formation constant to a *single* *sulphydryl* on these molecules. See text.

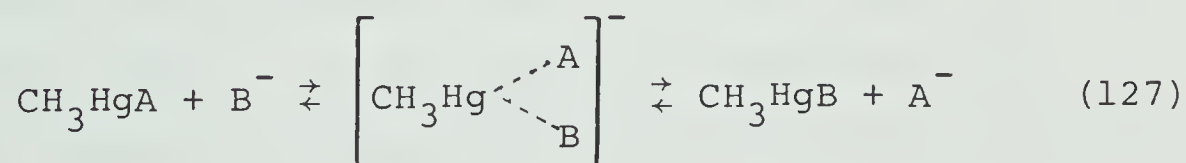
CHAPTER V

THE KINETICS OF METHYLMERCURY(II)-SULFHYDRYL LIGAND EXCHANGE PROCESSES

A. Introduction

The kinetics of $\text{CH}_3\text{Hg(II)}$ -sulfhydryl ligand exchange processes are of both chemical and biological relevance. As was shown in Chapters III and IV, $\text{CH}_3\text{Hg(II)}$ -thiol complexes are very stable thermodynamically, having log formation constants in the 15-17 range. Thus, the apparent lability of such systems, described in Chapter I (Section B) is of fundamental interest. Further, since biological systems usually exist under steady-state rather than equilibrium conditions, equilibrium measurements cannot fully describe in vivo behaviour; a knowledge of the relative *rates* of processes is also necessary.

Various routes by which exchange can occur were detailed in Chapter I (Section B). The dominant process appears to be a bimolecular anionic one proceeding by an associative mechanism (60)



This is in line with the slight but definite ten-

dency of the mercury in $\text{CH}_3\text{Hg(II)}$ to expand its coordination number. Fairhurst and Rabenstein obtained a log rate constant of 8.8 for such a process, where A and B are deprotonated glutathione (64).

Two subsidiary mechanisms have been identified. Dissociation of a thiol complex to give free $\text{CH}_3\text{Hg(II)}$ is demonstrably extremely slow, except at low pH where it is facilitated by proton attack (64). A direct exchange mechanism involving two $\text{CH}_3\text{Hg(II)}$ complex molecules has been identified (57,63); however, no kinetic data is available for sulfhydryl ligand systems. Even if such kinetics are extremely rapid, the vast excess of free ligand over bound ligand in vivo will discriminate in favour of the process detailed above in equation (127). Thus, despite comments to the contrary in the literature (57), the reference of the direct exchange route in vivo seems peripheral.

In this Chapter an investigation will be described, using NMR linebroadening measurements, of the ligand exchange kinetics at $\text{CH}_3\text{Hg(II)}$ of mercaptoacetic acid (MAA) with itself, penicillamine (PSH), cysteine (CSH) and glutathione (GSH). In the case of the MAA/MAA "homo-exchange" process, the kinetics associated with particular acid-base species are characterized. Results are dis-

cussed in terms of the approach of Geier and Erni, which relates predicted rate constants to the free energy difference between the two complexes involved (CH_3HgA and CH_3HgB in equation (127)) (62).

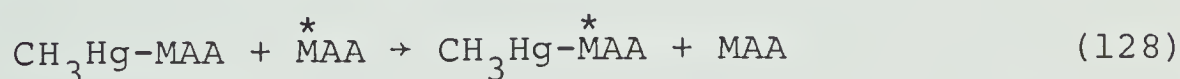
B. Results

In the course of formation constant studies (Chapter III) significant broadening of the MAA methylene proton resonance was often observed, especially as the pH was reduced. In some cases, notably the N-acetylpenicillamine experiments, the resonances flattened to invisibility.

This observation is fortuituous since, as discussed in Chapter II (Section I) it is expected only over a narrow range of exchange rates. Since the *equilibria* involved in displacement of MAA from $\text{CH}_3\text{Hg(II)}$ by PSH, CSH and GSH were known already, it was possible to use this broadening to estimate the lifetimes of the various species and hence to study the kinetics of their exchange reactions.

1. MAA/MAA exchange kinetics.

The reaction under study is



(The asterisk refers to a particular MAA molecule.) The

reaction is nontrivial since it limits the life of any one complex molecule (even though it creates another); linebroadening is a function of lifetime (see Chapter II, Section I). Further, in experiments involving other thiols both free and bound MAA are necessarily present and it is therefore necessary to subtract the contribution of the MAA/MAA process to the observed behaviour.

Figure 30 shows the linebroadening observed for $\text{CH}_3\text{Hg(II)}$ solutions containing an excess of MAA; approximate conditions are given. Detailed data are tabulated in the analysis given below. It is immediately obvious that such a curve is too complex to permit interpretation in terms of a simple model involving only RSH and RS^- , as was found to be possible for the analogous GSH process (64). This is not unexpected. In GSH the other ionisable sites are not proximal to the sulfhydryl, so their state of ionisation has little effect on the kinetics there, whereas in MAA the carboxylate lies very close and has a marked effect.

Consideration of all likely combinations of the various free and bound MAA species is then necessary. The reactions considered are given in Table 17. It will be apparent that reaction 2, where one of the three ionising sites (carboxylate on either free or bound MAA, or sulfhydryl of free) is protonated, can be formulated in several

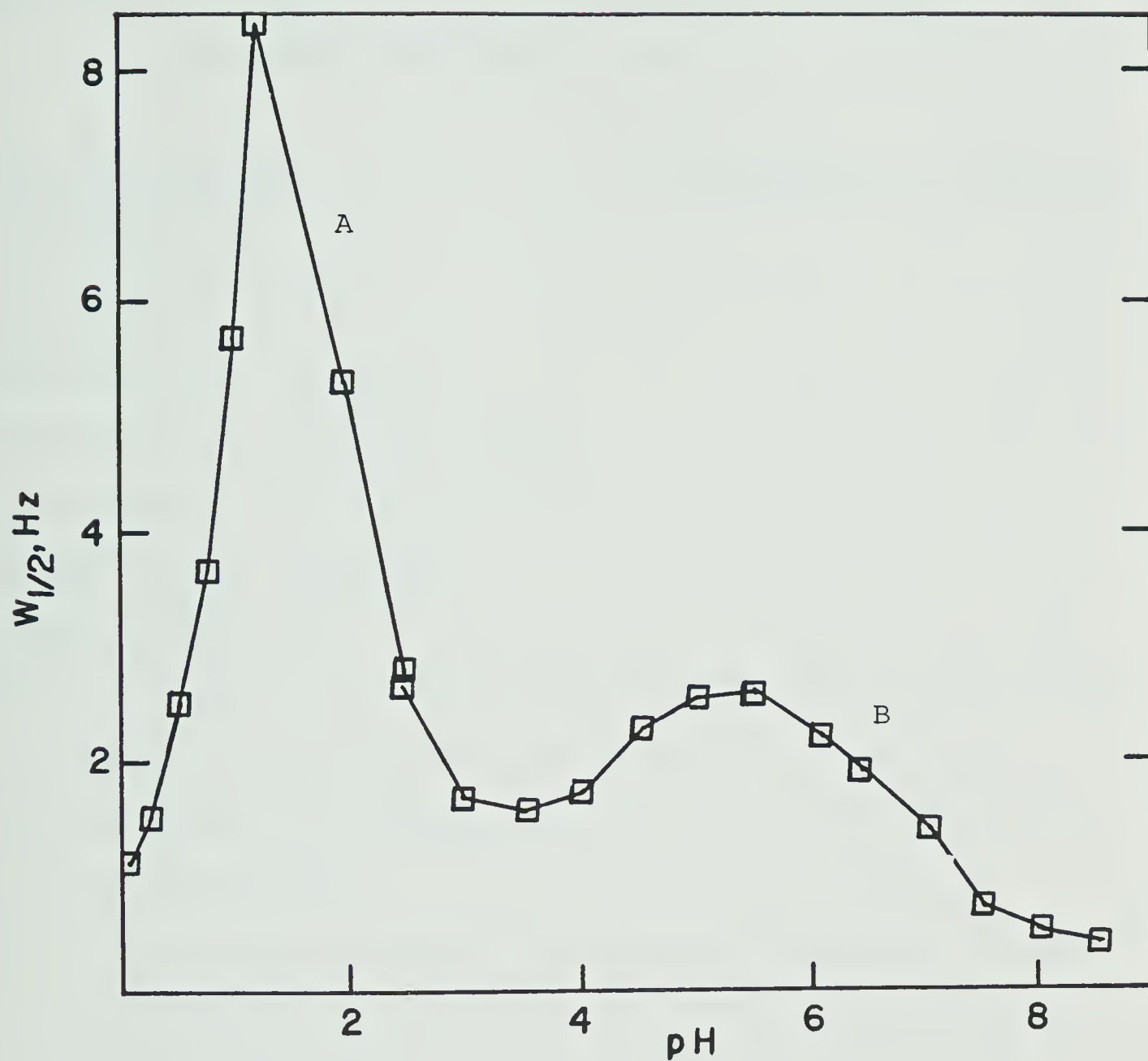


Figure 30. Linewidth of the MAA methylene resonance as a function of pH for solutions containing A) MAA (0.21 M) and $\text{CH}_3\text{Hg(II)}$ (0.13 M) and B) MAA (0.17 M) and $\text{CH}_3\text{Hg(II)}$ (0.09 M).

Table 17. Reactions for displacement or dissociation of MAA from the $\text{CH}_3\text{Hg}(\text{II})$ complex.

Reacting Species	Reaction Nomenclature	Rate Constant
$\text{CH}_3\text{HgSCH}_2\text{CO}_2^-$ ^{-a}	D	k_D
$\text{CH}_3\text{HgSCH}_2\text{CO}_2^-$, OH^- ^{-b}	0	k_0
$\text{CH}_3\text{HgSCH}_2\text{CO}_2^-$, $^- \text{SCH}_2\text{CO}_2^-$ ^{-c}	1	k_1
$\text{CH}_3\text{HgSCH}_2\text{CO}_2^-$, $^- \text{SCH}_2\text{CO}_2^-$, $\text{H}^{+c,d}$	2	k_2
$\text{CH}_3\text{HgSCH}_2\text{CO}_2^-$, $^- \text{SCH}_2\text{CO}_2^-$, $2\text{H}^{+c,d}$	3	k_3
$\text{CH}_3\text{HgSCH}_2\text{CO}_2\text{H}$, $\text{HSCH}_2\text{CO}_2\text{H}^c$	4	k_4
$\text{CH}_3\text{HgSCH}_2\text{CO}_2\text{H}$, H^{+e}	H	k_H

a) Dissociation of CH_3Hg^+ from ligand.

b) Displacement of ligand by OH^- .

c) Ligand exchange.

d) Tri- or tetra-molecular reaction not implied. Protons indicated are ligand-bound, but site(s) of protonation unknown. See text.

e) Proton-assisted dissociation.

ways, depending on where the proton is attached. However, since all such reactions give the same pH dependence, they must necessarily be considered together. k_2 may thus be a composite of several true rate constants. Possible contributions of individual reactions towards k_2 will be examined in the discussion (Section C below). The above also applies to reaction 3. The fraction of total sulfhydryl ligand, either free or bound in any one form can be calculated given the dissociation constants measured in Chapter III, as shown in Figure 31. This helps predict where a particular reaction will have maximal rate--for instance, processes 1 and 4 at high and low pH respectively.

It was shown previously (Chapter I, Section B) that process D was never significant. Fairhurst and Rabenstein concluded that process O was significant only at very elevated pH values, if at all (64).

Process H was significant for the GSH/GSH system only at very low pH (<1) (64). The observed decrease in broadening for the MAA/MAA system at low pH (see Fig. 30B) is discussed below (Section 2), where it is found to be due to a similar process.

The overall rate equation for the curve of Figure 30A is therefore:

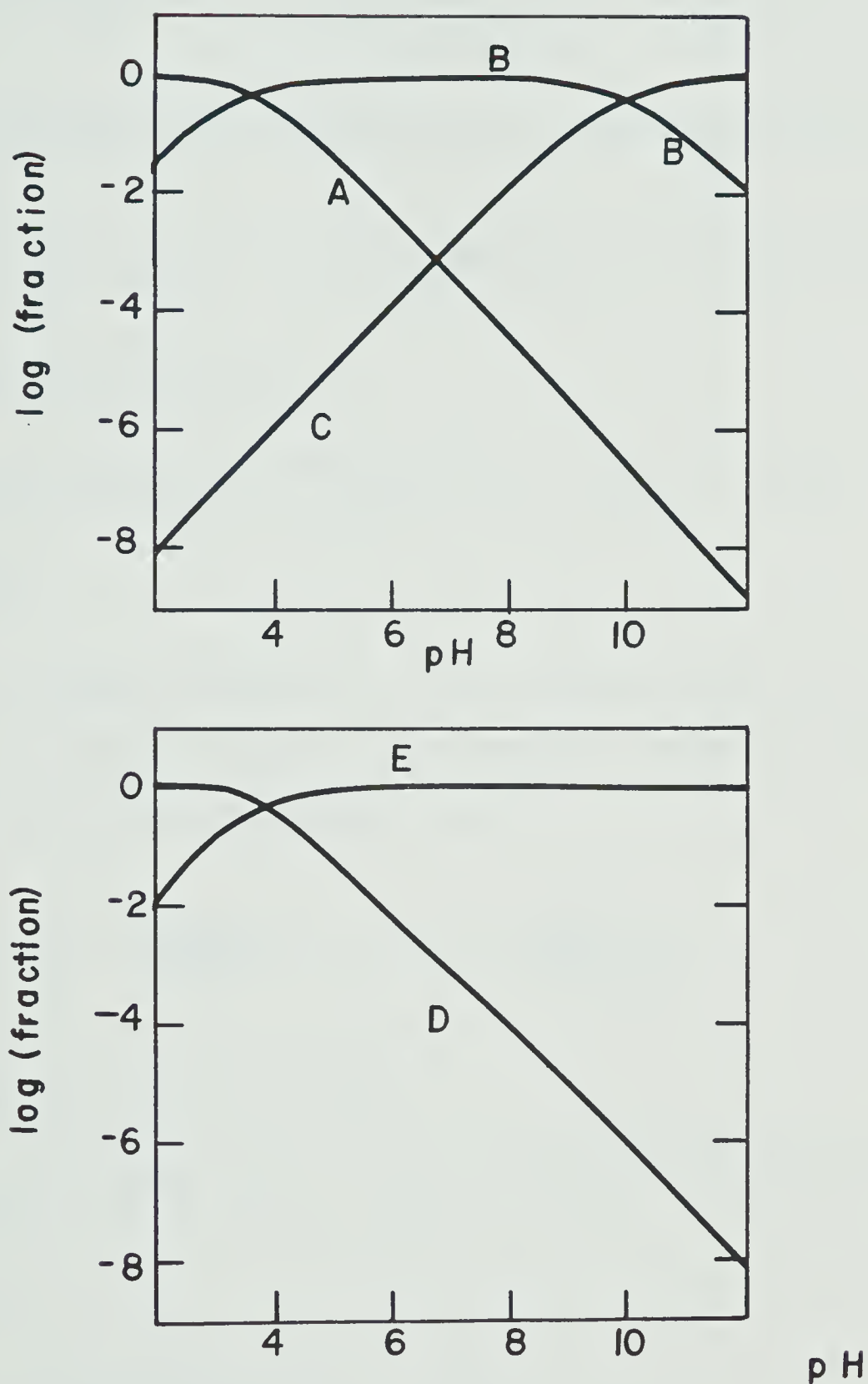


Figure 31. log fractions of various MAA species as a function of pH. a) $\text{HSCH}_2\text{CO}_2\text{H}$, b) $\text{HSCH}_2\text{CO}_2^-$, c) $^-\text{SCH}_2\text{CO}_2^-$, d) $\text{CH}_3\text{HgSCH}_2\text{CO}_2\text{H}$, e) $\text{CH}_3\text{HgSCH}_2\text{CO}_2^-$.

$$\begin{aligned} \text{Rate} = \frac{-d[\text{CH}_3\text{Hg-MAA}]}{dt} &= k_1 [\text{CH}_3\text{HgSCH}_2\text{CO}_2^-] [\text{SCH}_2\text{CO}_2^-] + \\ &k_2 [\text{CH}_3\text{HgSCH}_2\text{CO}_2^-] [\text{SCH}_2\text{CO}_2^-] a_{\text{H}^+} + k_3 [\text{CH}_3\text{HgSCH}_2\text{CO}_2^-] \\ &[\text{SCH}_2\text{CO}_2^-] (a_{\text{H}^+})^2 + k_4 [\text{CH}_3\text{HgSCH}_2\text{CO}_2^-] [\text{SCH}_2\text{CO}_2^-] a_{\text{H}^+}^3 \quad (129) \end{aligned}$$

Collecting terms gives

$$\begin{aligned} \text{Rate} &= [\text{CH}_3\text{HgSCH}_2\text{CO}_2^-] [\text{SCH}_2\text{CO}_2^-] \{k_1 + k_2 a_{\text{H}^+} + k_3 a_{\text{H}^+}^2 + \\ &k_4 a_{\text{H}^+}^3\} \quad (130) \end{aligned}$$

The average lifetime, τ_c , of a complex molecule is equal to the total complex concentration divided by the rate at which this disappears, i.e.

$$\tau_c = \frac{C_{\text{complex}}}{\text{Rate}} \quad \text{or} \quad 1/\tau_c = \frac{\text{Rate}}{C_{\text{complex}}} \quad (131)$$

Substitution into (130) yields

$$1/\tau_c = \alpha_{b2} [\text{SCH}_2\text{CO}_2^-] \{k_1 + k_2 a_{\text{H}^+} + k_3 (a_{\text{H}^+})^2 + k_4 (a_{\text{H}^+})^3\} \quad (132)$$

where

$$\alpha_{b2} = \frac{[\text{CH}_3\text{HgSCH}_2\text{CO}_2^-]}{C_{\text{complex}}} = \frac{K'_1}{a_{\text{H}^+} + K'_1} \quad (133)$$

In principle, a four-parameter fit of the kinetic model of equation (132) to the experimental values of τ_c resulting from the linebroadening observed, would directly yield k_1 - k_4 . Such a fit was not achieved, due to several factors: the variation of a_{H^+} over several orders of magnitude, the variability in quality of the lifetime data because of that in the linebroadenings observed, the lack of estimates for k_1 - k_4 and, as shown below, the fact that at a particular pH the lifetime is independent of the value(s) of one or more parameters. A more successful approach was to split both the data and the model into different regions and fit to two-parameter (linear) equations.

The data between pH 9 and 5.5 was compared to the model

$$1/\tau_c = \alpha_{b2} [^-SCH_2CO_2^-] \{k_1 + k_2 a_{H^+}\}$$

which corresponds to the first half of equation (132).

A plot of $1/\tau_c / \alpha_{b2} [^-SCH_2CO_2^-]$ versus a_{H^+} , shown in Figure 32, is reasonably linear (correlation coefficient = 0.999), with a slope (k_2) of 3.2×10^{13} and an intercept (k_1) of 4.2×10^6 . The data is given in Table 18.

The data between pH 5 and 2.5 was compared to the model

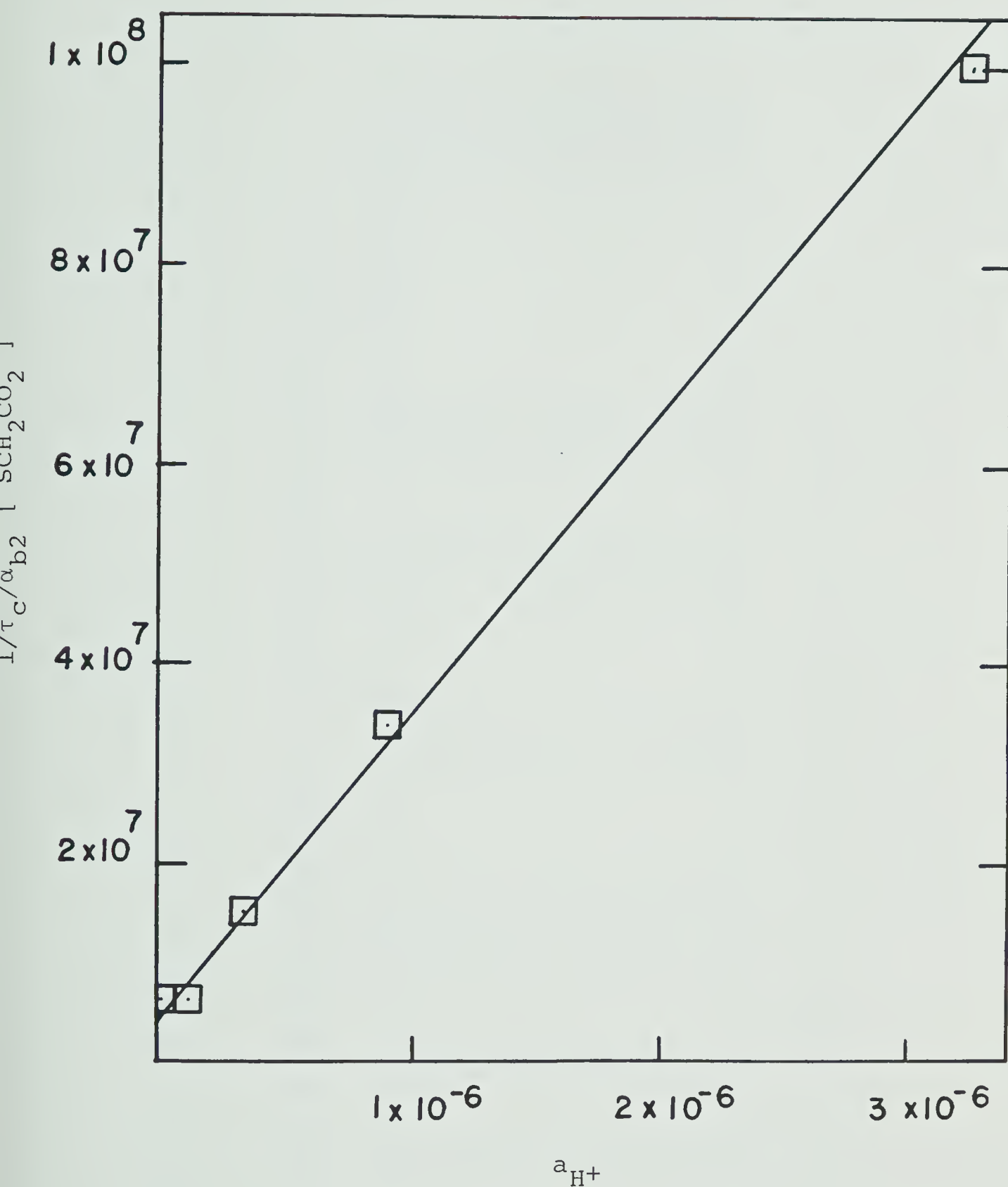


Figure 32. Plot of $1/\tau_c/\alpha_{b2} [\text{SCH}_2\text{CO}_2^-]$ versus a_{H^+} for the MAA/MAA exchange kinetics of Table 18.

Table 18. Data for MAA/MAA exchange kinetics at methylmercury(II), pH 8.0 to 5.5.

Sample	pH	α_{b2}^a	$[\text{SCH}_2\text{CO}_2^-]$ (M)	$W_{1/2}$ (Hz)	τ_c (s) ^b	$1/\tau_c / \alpha_{b2} \cdot [\text{SCH}_2\text{CO}_2^-]$	a_{H^+} (M)
1	9.01	1.000	1.038×10^{-2}	0.42	6×10^{-5}	1.6×10^6	9.77×10^{-10}
2	8.45	1.000	3.030×10^{-3}	0.43	8×10^{-5}	4.1×10^6	3.55×10^{-9}
3	7.99	1.000	1.078×10^{-3}	0.49	1.6×10^{-4}	5.8×10^6	1.02×10^{-8}
4	7.53	1.000	3.771×10^{-4}	0.72	4.8×10^{-4}	5.5×10^6	2.95×10^{-8}
5	7.03	1.000	1.196×10^{-4}	1.41	1.4×10^{-3}	6.0×10^6	9.33×10^{-8}
6	6.47	1.000	3.293×10^{-5}	1.88	2.0×10^{-3}	1.5×10^7	3.39×10^{-7}
7	6.04	0.994	1.227×10^{-5}	2.18	2.4×10^{-3}	3.4×10^7	9.12×10^{-7}
8	5.49	0.980	3.454×10^{-6}	2.54	2.9×10^{-3}	1.0×10^8	3.24×10^{-6}

a) As defined in equation (133).

b) Estimated from comparison of calculated and experimental linewidths.

$$1/\tau_c = \alpha_{b2} [\text{SCH}_2\text{CO}_2^-] (a_{\text{H}^+})^2 k_3 + k_4 a_{\text{H}^+}$$

corresponding to the second half of equation (132). A plot of $1/\tau_c / \alpha_{b2} [\text{SCH}_2\text{CO}_2^-] (a_{\text{H}^+})^2$ versus a_{H^+} is shown in Figure 33. (The τ_c values were corrected for the contribution of the high pH processes treated above using the fact that reciprocal lifetimes, like rates, are additive.) The plot displays curvature in the region $a_{\text{H}^+} = 10^{-5}$ - 10^{-4} , however, as Table 19 shows, corrected values in this region are heavily dependent upon the high pH contribution. Where this is negligible ($a_{\text{H}^+} = 10^{-3.5}$ - $10^{-2.5}$) the plot is linear with a slope (k_4 of 3.6×10^{20} and an intercept (k_3) of 1.0×10^{18} . A duplicate run gave values of 3.3×10^{20} and 1.4×10^{18} ; in view of the cumulative errors in such calculations this was judged acceptable agreement.

The results obtained for k_1 , k_2 , k_3 and k_4 are discussed in Section C below after removal of embedded pK's to yield the true rate constants.

2. Behaviour at very low pH.

Figure 34 shows $1/\tau_c$ as a function of a_{H^+} between pH 1 and 0 for the system of Figure 30B, the data is given in Table 20. It appears that the conclusions of Fairhurst and Rabenstein for the analogous GSH system, that at very low pH process H is dominant, are substantiated here also.

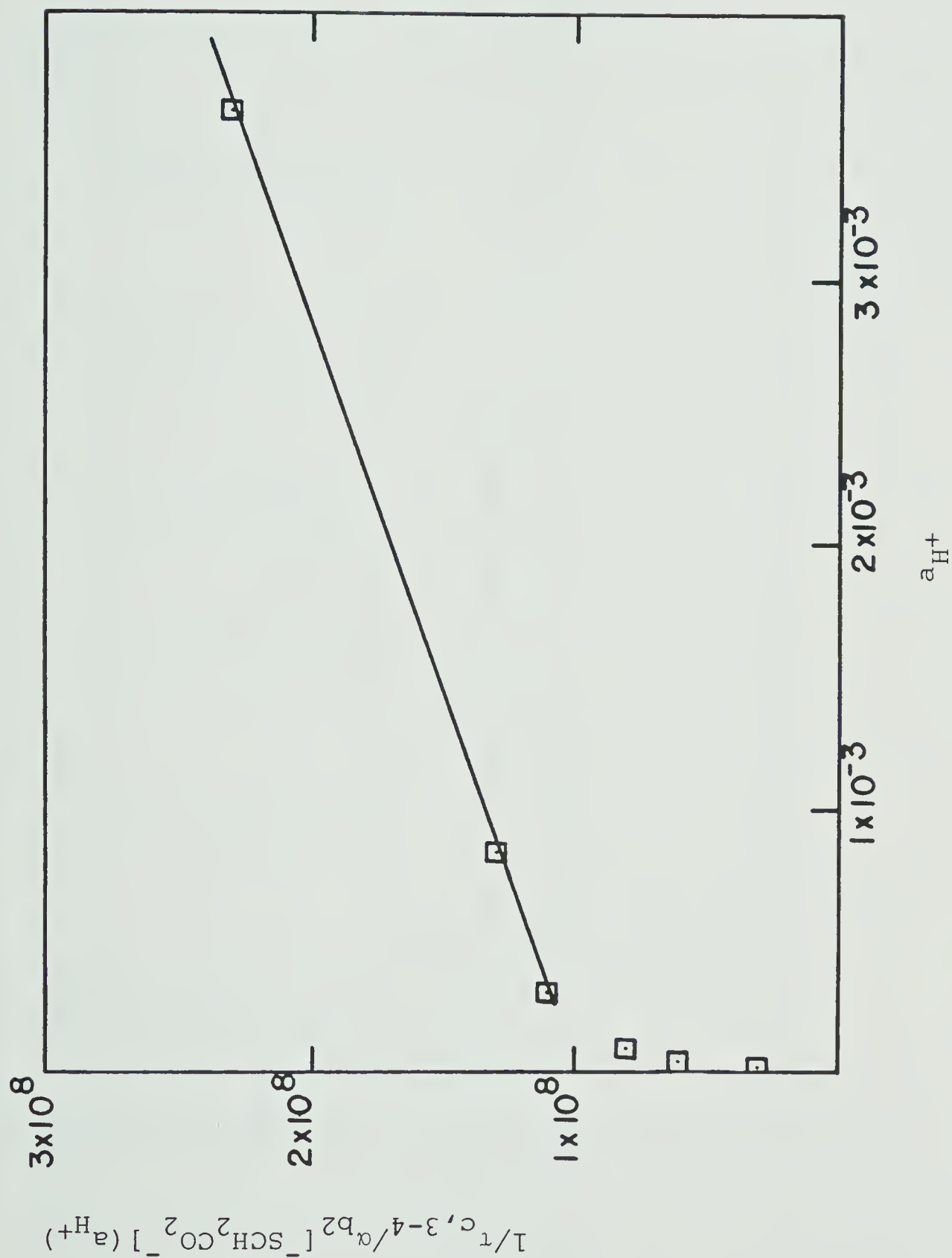


Figure 33. Plot of $1/\tau_{c, 3-4} / \alpha_{b2} [^{-}SCH_2CO_2^{-}] (a_{H^{+}})$ versus $a_{H^{+}}$ for the MAA/MAA exchange kinetics of Table 19.

Table 19. Data for MAA/MAA exchange kinetics at methylmercury(II), pH 5.0 to 2.5.

Sample	pH	α_{b2}^a	$[\text{SCH}_2\text{CO}_2^-] \text{ (M)}$	$w_{1/2}$ (Hz)	$\tau_c(s)^b$	$\tau_{c,1-2}(s)^c$	$\tau_{c3-4}(s)^d$	$1/\tau_{c,3-4}/\alpha_{b2} [\text{SCH}_2\text{CO}_2^-] (a_{H^+})^2$	a_{H^+}
9	5.01	.942	1.11×10^{-6}	2.5_2	2.8×10^{-3}	3.0×10^{-3}	3.9×10^{-2}	3×10^{17}	9.77×10^{-6}
10	4.53	.843	3.54×10^{-7}	2.2_4	2.3×10^{-3}	3.5×10^{-3}	6.6×10^{-3}	6×10^{17}	2.95×10^{-5}
11	4.03	.629	9.89×10^{-8}	1.7_3	1.6×10^{-3}	5.4×10^{-3}	2.3×10^{-3}	8×10^{17}	9.33×10^{-5}
12	3.52	.343	2.08×10^{-8}	1.5_1	1.3×10^{-3}	1.4×10^{-2}	1.4×10^{-3}	1.1×10^{18}	3.02×10^{-4}
13	3.09	.163	4.38×10^{-9}	1.6_3	1.6×10^{-3}	5.4×10^{-2}	1.6×10^{-3}	1.3×10^{18}	8.13×10^{-4}
14	2.44	.042	2.44×10^{-10}	2.8_2	3.2×10^{-3}	8.4×10^{-2}	3.2×10^{-3}	2.3×10^{18}	3.63×10^{-3}

a) As defined in equation (133).

b) Estimated from Comparison of calculated and experimental linewidthths.

c) For processes 1 and 2 (see Table 17). Calculated using equation (132) and the values $k_1' = 4.2 \times 10^6$, $k_2' = 3.2 \times 10^{13}$.

d) Value observed after correction for contribution of processes 1 and 2.

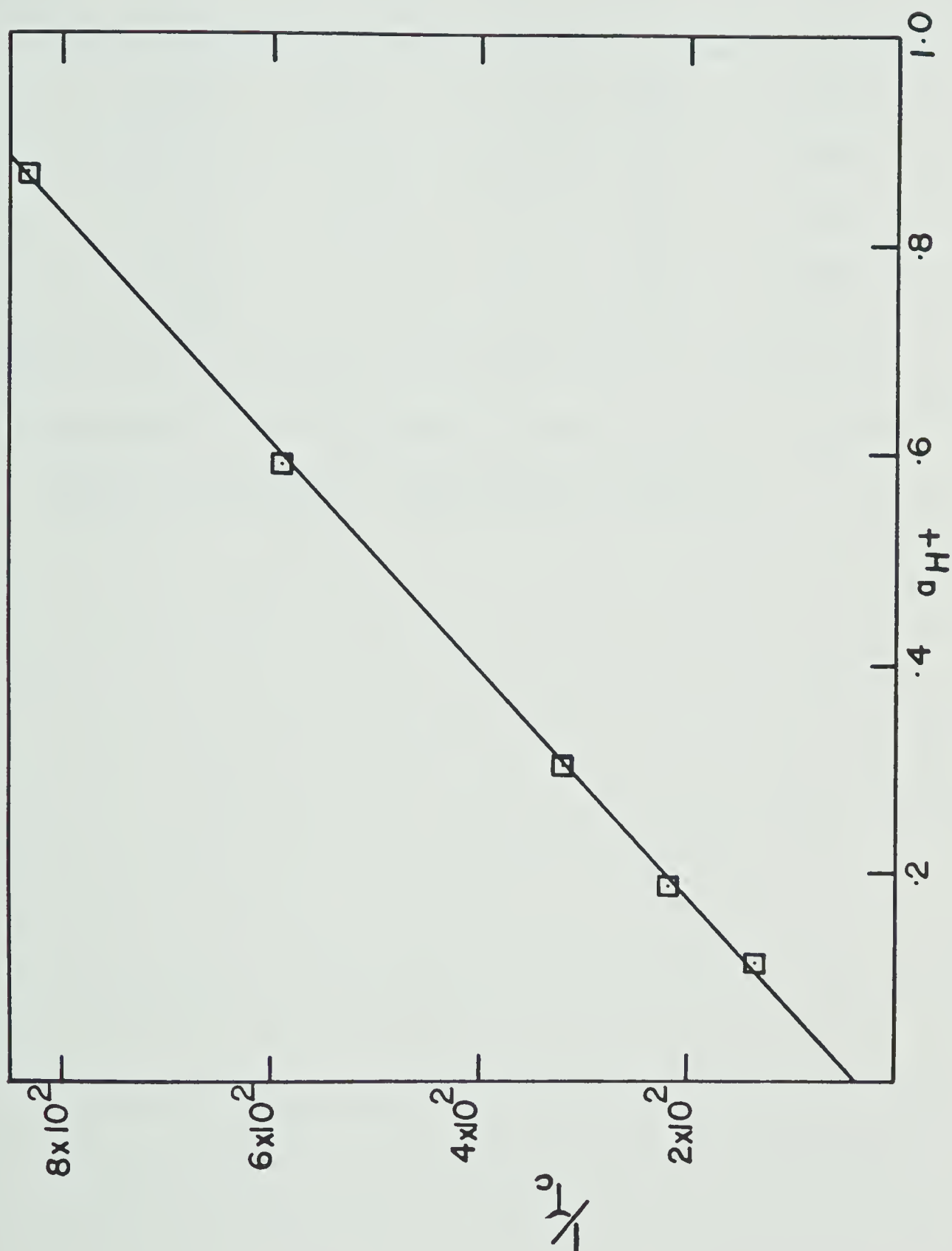


Figure 34. Plot of $1/\tau_c$ versus a_{H^+} for the kinetics of disappearance of the MAA-methylmercury(II) complex, pH 1.0 to pH 0.

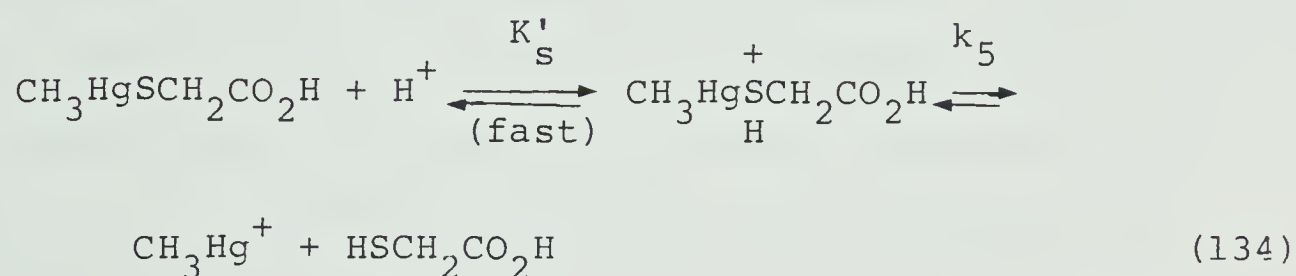
Table 20. Data for kinetics of disappearance of the
MAA-CH₃Hg(II) complex, pH 1.0 to 0.0.

Sample	pH	$W_{1/2}$ (Hz)	$1/\tau_c$ (Hz) ^a	a_{H^+} (M)
1	0.96	5.7	1.35×10^2	.110
2	0.73	3.6	2.27×10^2	.186
3	0.52	2.5	3.2×10^2	.302
4	0.23	1.5	5.9×10^2	.589
5	0.06	1.1	8.3×10^2	.871

a) Estimated from comparison of calculated and experimental linewidths. See text for details.

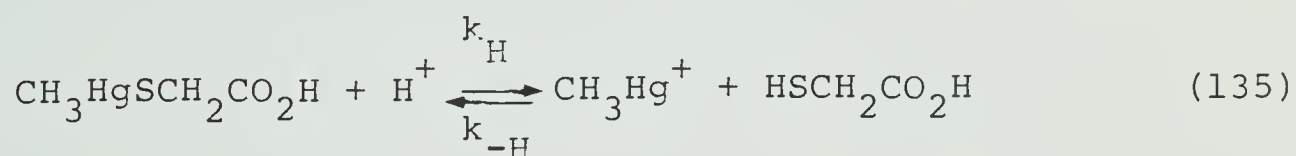
The line has a correlation coefficient of .9996 and a slope (k_H) of $9 \times 10^2 M^{-1}s^{-1}$. The non-zero intercept is due to a small contribution from reaction 4 (see Section 1).

It was established in Chapter III that in this pH region $CH_3HgSCH_2CO_2H$ exists as a stable entity, so presumably the actual process occurring is



where K'_S is as defined in Chapter III, and k_5 is the (unimolecular) rate constant for dissociation. This is the only plausible way of reconciling the proton activity dependence with the demonstrated existence of the "super-protonated" species as a stable entity.

It is instructive to consider the *reverse* rate constant for the process, k_H , defined in the scheme:



which can be evaluated since the equilibrium constant for this reaction (k_H/k_{-H}) can be calculated from the results of Chapter III (Tables 10, 11 and 12) to be $10^{-7.1}$. Thus

$\log k_{-H}$ is calculated to be 10.1 in reasonable agreement with a fairly typical value for a diffusion-controlled bimolecular reaction involving no charge repulsion (78).

Since reaction 4 involves no free thiol species, the apparent rate should be independent of the concentration and identity of free thiols present. Table 21 gives data obtained at low pH with other thiols present. Slopes of plots such as Figure 34 above are tabulated; within experimental error (estimated at 200-300) these are not significantly different from the figure obtained above for MAA alone.

3. Kinetics of displacement by other ligands.

Each of the three sulfhydryl ligands studied--penicillamine, cysteine and glutathione--was added to a 1:1 mixture of $\text{CH}_3\text{Hg(II)}$ and MAA. Three runs, with differing amounts of RSH (the competing thiol) added, were performed for each. The chemical shift and width of the MAA methylene resonance were then measured as a function of pH, as in Sections 1 and 2 above, and lifetimes τ_c calculated as before.

Qualitatively, the behaviour of the linewidth as a function of pH (Figures 35 through 37) was similar to that observed in the MAA/MAA exchange system. Tables 22

Table 21. Data for kinetics of disappearance of the MAA-CH₃Hg(II) complex, in presence of other thiols, pH 1.2 to 0.3.

Sample	pH	Competing thiol	Stoichiometry ^a	C _{MAA} (M) ^b	C _{RSH} (M) ^c	W _{1/2} (Hz)	1/ τ_c (Hz) ^d	a _{H+} (M)	Slope ^e
1	1.01	Penicillamine	0.54	2.90×10 ⁻²	1.85×10 ⁻²	3.2	1.2×10 ²	9.77×10 ⁻²	
2	0.71	Penicillamine	0.54	2.89×10 ⁻²	1.77×10 ⁻²	2.2	2.1×10 ²	1.95×10 ⁻¹	9 ×10 ²
3	0.46	Penicillamine	0.54	2.56×10 ⁻²	1.93×10 ⁻²	1.3	3.6×10 ²	3.47×10 ⁻¹	
4	1.12	Cysteine	0.47	3.96×10 ⁻²	1.62×10 ⁻²	2.7	1.5×10 ²	7.59×10 ⁻²	
5	0.72	Cysteine	0.47	3.29×10 ⁻²	1.77×10 ⁻²	1.1	4.6×10 ²	1.91×10 ⁻¹	1.2×10 ³
6	0.46	Cysteine	0.47	2.31×10 ⁻²	1.96×10 ⁻²	0.8	5.0×10 ²	3.47×10 ⁻¹	
7	1.17	Glutathione	0.50	2.64×10 ⁻²	1.43×10 ⁻²	3.0	1.3×10 ²	6.76×10 ⁻²	
8	0.71	Glutathione	0.50	2.57×10 ⁻²	1.36×10 ⁻²	2.1	2.1×10 ²	1.95×10 ⁻¹	6 ×10 ³
9	0.32	Glutathione	0.50	2.28×10 ⁻²	1.38×10 ⁻²	0.9	3.9×10 ²	4.79×10 ⁻¹	

a) Mole equivalents of competing thiol per m.e. of MAA and of CH₃Hg(II).

b) Total MAA concentration in all free forms.

c) Total competing thiol concentration in all free forms.

d) Estimated by comparison of calculated and experimental linewidths.

e) Calculated linear least-squares slope of plot 1/ τ_c versus a_{H+}.

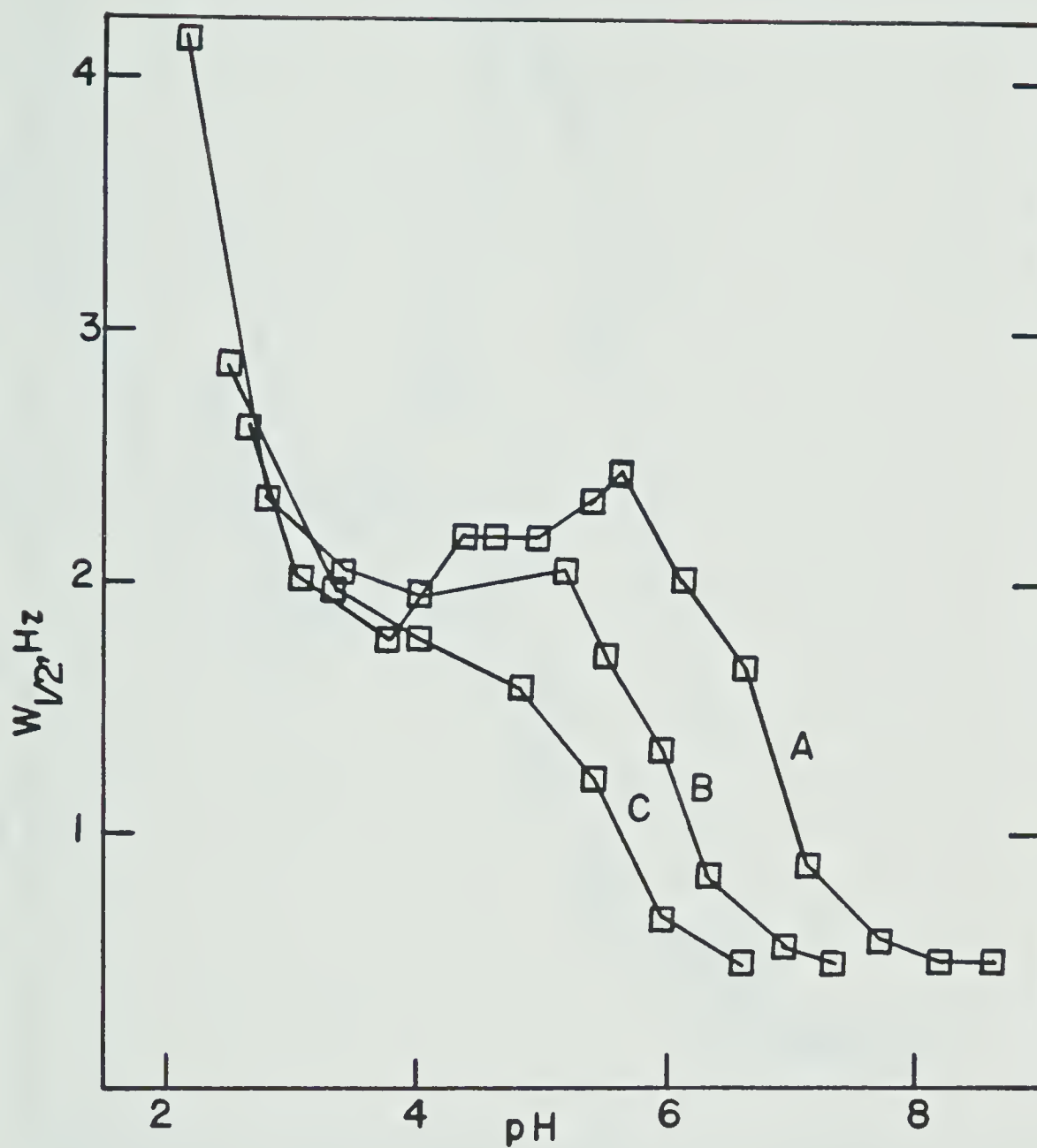


Figure 35. $W_{1/2}$ for MAA methylene resonance as a function of pH for solutions containing PSH:MAA:methylmercury(II) in an x:1:1 ratio. x = (A) .54, (B) 1.24, (C) 2.17.

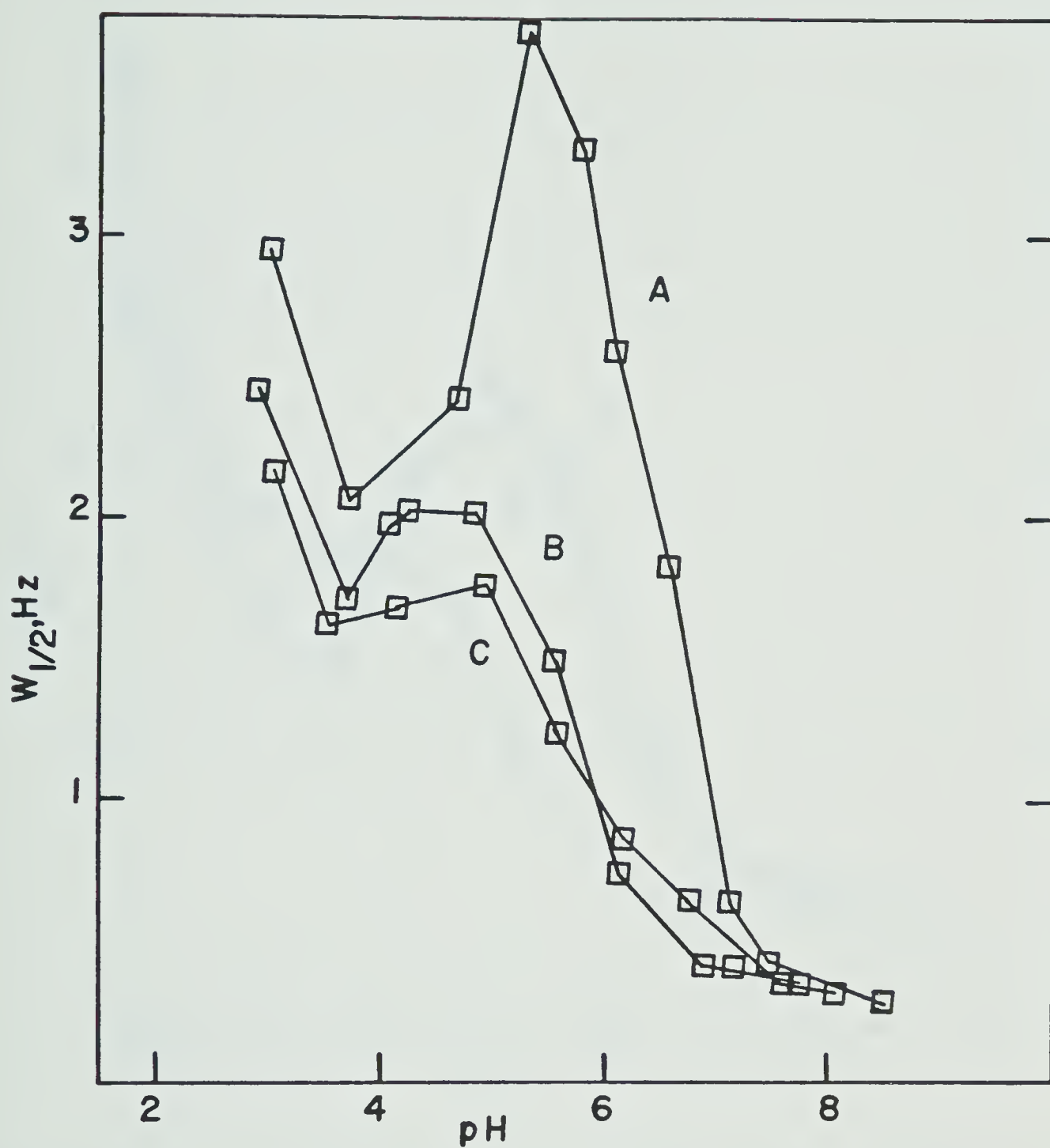


Figure 36. $W_{1/2}$ for MAA methylene resonance as a function of pH for solutions containing CSH:MAA:methylmercury(II) in an x:1:1 ratio. x = (A) .47, (B) .80, (C) .78.

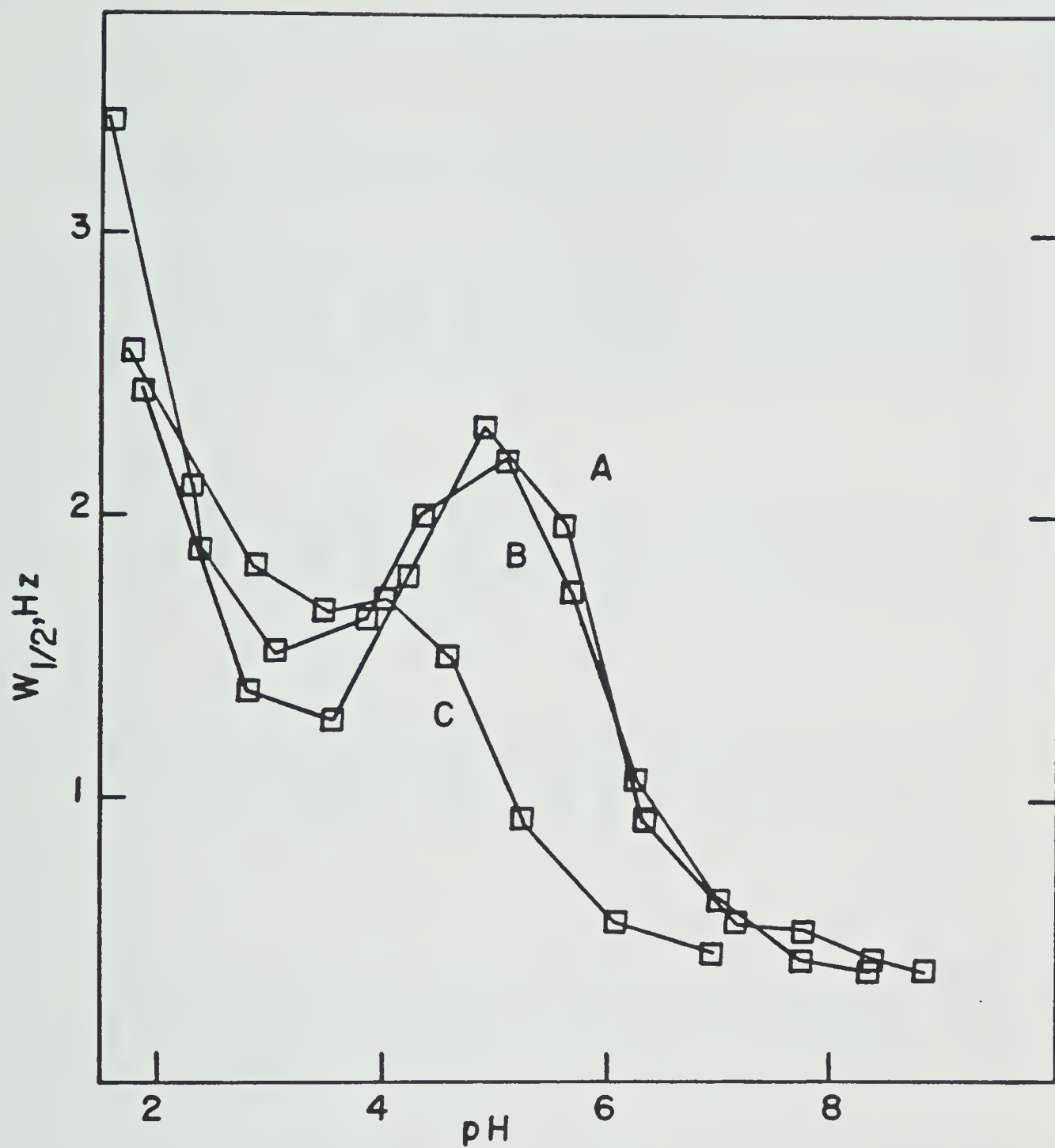


Figure 37. $W_{1/2}$ for MAA methylene resonance as a function of pH for solutions containing GSH:MAA:methylmercury(II) in an x:1:1 ratio. x = (A) .50, (B) .85, (C) 1.56.

Table 22. Data for kinetics of displacement of MAA from its $\text{CH}_3\text{Hg(II)}$ complex by penicillamine.

pH	P_f	$W_{1/2}$ (Hz)	τ_c (s) ^a	$[\text{SCH}_2\text{CO}_2^-]$ (M)	$1/\tau_{c,DM}$ (Hz) ^b	$1/\tau_{c,DP}$ (Hz) ^c	C_{PSH} (M) ^d	$\log k_{c,DP}$ ^e
7.30	.52	.49	1.8×10^{-4}	6.77×10^{-5}	3.93×10^2	5.2×10^3	5.73×10^{-2}	4.96
6.89	.53	.56	2.9×10^{-4}	2.69×10^{-5}	2.24×10^2	3.2×10^3	5.65×10^{-2}	4.75
6.28	.53	.86	7.2×10^{-4}	6.62×10^{-6}	1.40×10^2	1.2×10^3	5.64×10^{-2}	4.33
5.96	.53	1.3	1.5×10^{-3}	3.14×10^{-6}	1.26×10^2	5.4×10^2	5.66×10^{-2}	3.98
5.48	.52	1.7	2.0×10^{-3}	1.04×10^{-6}	1.23×10^2	3.8×10^2	5.63×10^{-2}	3.83
5.13	.54	2.0	2.4×10^{-3}	4.65×10^{-7}	1.32×10^2	2.8×10^2	5.58×10^{-2}	3.70
4.58	.56	2.2	2.5×10^{-3}	1.28×10^{-7}	1.69×10^2	2.3×10^2	5.42×10^{-2}	3.63
4.02	.60	2.0	1.9×10^{-3}	3.17×10^{-8}	2.47×10^2	2.8×10^2	5.05×10^{-2}	3.74
3.38	.63	2.0	1.9×10^{-3}	4.23×10^{-9}	2.48×10^2	2.8×10^2	4.82×10^{-2}	3.76
2.79	.59	2.3	2.7×10^{-3}	3.55×10^{-10}	1.33×10^2	2.4×10^2	5.43×10^{-2}	3.65
2.17	.51	4.1	5.7×10^{-3}	2.17×10^{-11}	7.8×10^1	9.8×10^1	5.66×10^{-2}	3.24
6.55	.66	.47	1.4×10^{-4}	1.16×10^{-5}	1.54×10^2	7.0×10^3	9.09×10^{-2}	4.89
5.93	.66	.68	4.2×10^{-4}	2.77×10^{-6}	1.19×10^2	2.3×10^3	9.10×10^{-2}	4.40
5.37	.66	1.2	1.1×10^{-3}	7.58×10^{-7}	1.17×10^2	7.9×10^2	9.09×10^{-2}	3.94
4.79	.68	1.6	1.6×10^{-3}	1.98×10^{-7}	1.41×10^2	4.8×10^2	8.89×10^{-2}	3.73
4.02	.72	1.8	2.0×10^{-3}	2.87×10^{-8}	2.23×10^2	2.8×10^2	8.71×10^{-2}	3.51
3.37	.76	2.0	3.3×10^{-3}	3.75×10^{-9}	2.27×10^2	7.6×10^1	8.42×10^{-2}	2.96
2.49	.67	2.9	7.1×10^{-3}	9.08×10^{-11}	9.6×10^1	4.5×10^1	8.88×10^{-2}	2.70

(cont'd.)

Table 22 (cont'd.)

- a) Observed mean lifetime of MAA complex as estimated by comparison of predicted and experimental lineshapes. See text for details.
- b) Contribution of processes involving displacement by MAA to the total mean reciprocal lifetime of MAA complex. Calculated from the results of Section B.1.
- c) Contribution of processes involving displacement by penicillamine to the total mean reciprocal lifetime of MAA complex. Calculated by difference between total reciprocal lifetime and b) above.
- d) Concentration of free PSH in all forms.
- e) log Conditional Rate Constant for displacement of MAA from its complex by PSH.

Table 23. Data for kinetics of displacement of MAA from its $\text{CH}_3\text{Hg(II)}$ complex by cysteine.

pH	P_f	$W_{1/2}$ (Hz)	τ_c (s) ^a	$[\text{SCH}_2\text{CO}_2^-]$ (M)	$1/\tau_{c,DM}$ (Hz) ^b	$1/\tau_{c,DC}$ (Hz) ^c	C_{CSH} (M) ^d	$\log k_{c,DC}$ ^e
7.78	.44	.45	1.4×10^{-4}	2.21×10^{-4}	1.05×10^3	6.1×10^3	3.75×10^{-2}	5.21
7.15	.48	.50	2.2×10^{-4}	5.70×10^{-5}	3.69×10^2	4.2×10^3	3.32×10^{-2}	5.10
6.74	.48	.74	6.2×10^{-4}	2.22×10^{-5}	2.23×10^2	1.4×10^3	3.32×10^{-2}	4.62
6.10	.49	.97	9.8×10^{-4}	5.20×10^{-6}	1.57×10^2	8.6×10^4	3.20×10^{-2}	5.53
5.48	.49	1.3	1.5×10^{-3}	1.24×10^{-6}	1.47×10^2	5.2×10^4	3.18×10^{-2}	5.21
4.81	.50	1.8	2.2×10^{-3}	2.62×10^{-7}	1.77×10^2	2.8×10^4	3.07×10^{-2}	3.96
4.04	.51	1.8	1.8×10^{-3}	3.69×10^{-8}	2.69×10^2	2.9×10^4	2.97×10^{-2}	3.99
3.37	.48	1.7	1.9×10^{-3}	4.02×10^{-9}	2.43×10^2	2.8×10^4	3.26×10^{-2}	3.93
2.86	.47	2.2	2.9×10^{-3}	5.27×10^{-10}	1.57×10^2	1.9×10^4	3.34×10^{-2}	3.76
8.37	.37	.40	$\sim 7 \times 10^{-5}$	7.27×10^{-4}	3.15×10^3	$\sim 1.1 \times 10^4$	4.15×10^{-2}	5.42
7.72	.42	.45	1.6×10^{-4}	1.89×10^{-4}	9.09×10^2	5.3×10^3	3.60×10^{-2}	5.17
6.90	.47	.50	2.3×10^{-4}	3.15×10^{-5}	2.59×10^2	4.1×10^3	3.18×10^{-2}	5.11
6.11	.48	.83	7.7×10^{-4}	5.23×10^{-6}	1.54×10^2	1.1×10^3	3.06×10^{-2}	4.56
5.44	.48	1.6	2.0×10^{-3}	1.10×10^{-6}	1.44×10^2	3.6×10^2	3.08×10^{-2}	5.07
4.72	.51	2.1	2.6×10^{-3}	2.13×10^{-7}	1.86×10^2	2.0×10^2	2.78×10^{-2}	3.86
4.09	.52	2.1	2.3×10^{-3}	4.13×10^{-8}	2.56×10^2	1.8×10^2	2.66×10^{-2}	3.83
3.53	.52	1.8	1.8×10^{-3}	7.61×10^{-9}	2.81×10^2	2.8×10^2	2.66×10^{-2}	4.02
2.72	.49	2.5	3.4×10^{-3}	3.02×10^{-10}	1.43×10^2	1.5×10^2	2.97×10^{-2}	3.70

(cont'd.)

Table 23. (cont'd.)

- a) As for Table 22.
- b) As for Table 22.
- c) Contribution of processes involving displacement by cysteine to the total mean reciprocal lifetime of MAA complex.
- d) Concentration of free CSH in all forms.
- e) log Conditional Rate Constant for displacement of MAA from its complex by CSH.

Table 24. Data for kinetics of displacement of MAA from its $\text{CH}_3\text{Hg(II)}$ complex by glutathione.

pH	P_f	$w_{1/2}$	(Hz)	τ_c (s) ^a	$[\text{SCH}_2\text{CO}_2^-]$ (M)	$1/\tau_{c,DM}$ (Hz) ^b	$1/\tau_{c,DG}$ (Hz) ^c	C_{GSH} (M) ^d	$\log k_{c,DG}$ ^e
8.35	.42	.41		$\sim 8 \times 10^{-5}$	6.82×10^{-4}	2.96×10^3	9.5×10^3	3.78×10^{-2}	5.40
7.77	.46	.42		$\sim 8 \times 10^{-5}$	2.00×10^{-4}	9.49×10^2	1.2×10^4	3.40×10^{-2}	5.50
7.00	.49	.65		4.6×10^{-4}	3.61×10^{-5}	2.67×10^2	1.9×10^3	3.16×10^{-2}	4.78
6.22	.41	1.2		1.3×10^{-3}	6.18×10^{-6}	1.47×10^2	6.2×10^2	3.01×10^{-2}	4.31
5.72	.48	1.7		2.2×10^{-3}	1.84×10^{-6}	1.25×10^2	3.3×10^2	3.23×10^{-2}	4.01
5.09	.47	2.2		3.0×10^{-3}	4.11×10^{-7}	1.29×10^2	2.0×10^2	3.34×10^{-2}	3.78
4.38	.48	2.0		2.5×10^{-3}	7.35×10^{-8}	1.80×10^2	2.2×10^2	3.29×10^{-2}	3.83
3.80	.51	1.6		1.7×10^{-3}	1.54×10^{-8}	2.43×10^2	3.5×10^2	2.99×10^{-2}	4.07
3.04	.49	1.5		1.7×10^{-3}	9.84×10^{-10}	1.65×10^2	4.2×10^2	3.10×10^{-2}	4.13
2.39	.44	1.9		2.8×10^{-3}	5.48×10^{-11}	8.4×10^1	2.7×10^2	3.47×10^{-2}	3.89
1.56	.43	3.4		5.6×10^{-3}	1.23×10^{-12}	5.8×10^1	1.2×10^2	3.36×10^{-2}	3.55
8.21	.49	.40		$\sim 4 \times 10^{-5}$	5.07×10^{-4}	2.23×10^3	2.3×10^4	6.29×10^{-2}	5.56
7.58	.62	.41		$\sim 6 \times 10^{-5}$	1.24×10^{-4}	6.25×10^2	1.6×10^4	6.12×10^{-2}	5.42
6.95	.63	.43		$\sim 8 \times 10^{-5}$	3.00×10^{-5}	2.34×10^2	1.2×10^4	6.01×10^{-2}	5.30
6.05	.64	.55		2.4×10^{-4}	3.81×10^{-6}	1.27×10^2	4.0×10^3	5.96×10^{-2}	4.83
5.23	.65	.92		7.3×10^{-4}	5.73×10^{-7}	1.26×10^2	1.2×10^3	5.92×10^{-2}	4.31
4.56	.69	1.5		1.4×10^{-3}	1.23×10^{-7}	1.73×10^2	5.4×10^2	5.62×10^{-2}	3.98

(cont'd.)

Table 24. (cont'd.)

pH	P _f	W _{1/2} (Hz)	τ_c (s) ^a	[⁻ SCH ₂ CO ₂ ⁻] (M)	1/ $\tau_{c,DM}$ (Hz) ^b	1/ $\tau_{c,DG}$ (Hz) ^c	C _{GSH} (M) ^d	log k _{c,DG} ^e
4.01	.77	1.7	1.7×10 ⁻³	3.20×10 ⁻⁸	2.57×10 ²	3.3×10 ²	5.12×10 ⁻²	3.81
3.44	.89	1.7	2.6×10 ⁻³	6.01×10 ⁻⁹	2.93×10 ²	9.2×10 ¹	4.36×10 ⁻²	3.32
2.92	.93	1.8	2.6×10 ⁻³	8.47×10 ⁻¹⁰	2.08×10 ²	1.8×10 ²	4.07×10 ⁻²	3.65
2.30	.76	2.1	2.5×10 ⁻³	4.68×10 ⁻¹¹	1.01×10 ²	3.0×10 ²	5.05×10 ⁻²	3.77
1.79	.66	2.6	3.0×10 ⁻³	3.94×10 ⁻¹²	6.8 ×10 ¹	2.6×10 ²	5.60×10 ⁻²	3.67

a) As for Table 22.

b) As for Table 22.

c) Contribution of processes involving displacement by glutathione to the total reciprocal mean lifetime.

d) Concentration of free GSH in all forms.

e) Conditional Rate Constant for displacement of MAA from its complex by GSH.

through 24 give the data for these runs. As discussed in Section 1, it is necessary to correct measured lifetimes for the contribution made by the MAA/MAA exchange process; these corrections are also shown. For runs performed at low RSH concentrations, these corrections dominated (and sometimes, due to errors in the values determined above, exceeded) the measured lifetime. These runs were therefore excluded from further consideration.

Attempts to fit lifetimes to detailed kinetic schemes, as was accomplished above for the MAA case failed, due presumably to the large cumulative errors accrued in calculation of lifetimes and correction of these for MAA/MAA exchange processes. However, it is still possible to gain some information from these experiments.

Qualitatively, exchange rates involving these other thiols are seen to decrease with decreasing pH, suggesting that the deprotonated sulfhydryl is the displacing species. At about pH 4-5, however, the rate levels off and may even increase slightly, suggesting (as for the MAA/MAA case) that carboxylate protonation, probably at the proximal carboxylate on the MAA-CH₃Hg(II) complex, may influence the rate significantly.

Since $1/\tau_c = \frac{\text{Rate}}{C_{\text{complex}}}$ (equation 131) if we define
 Rate = $k_{c,DR} \cdot C_{\text{complex}} \cdot C_{\text{RSH}}$ then

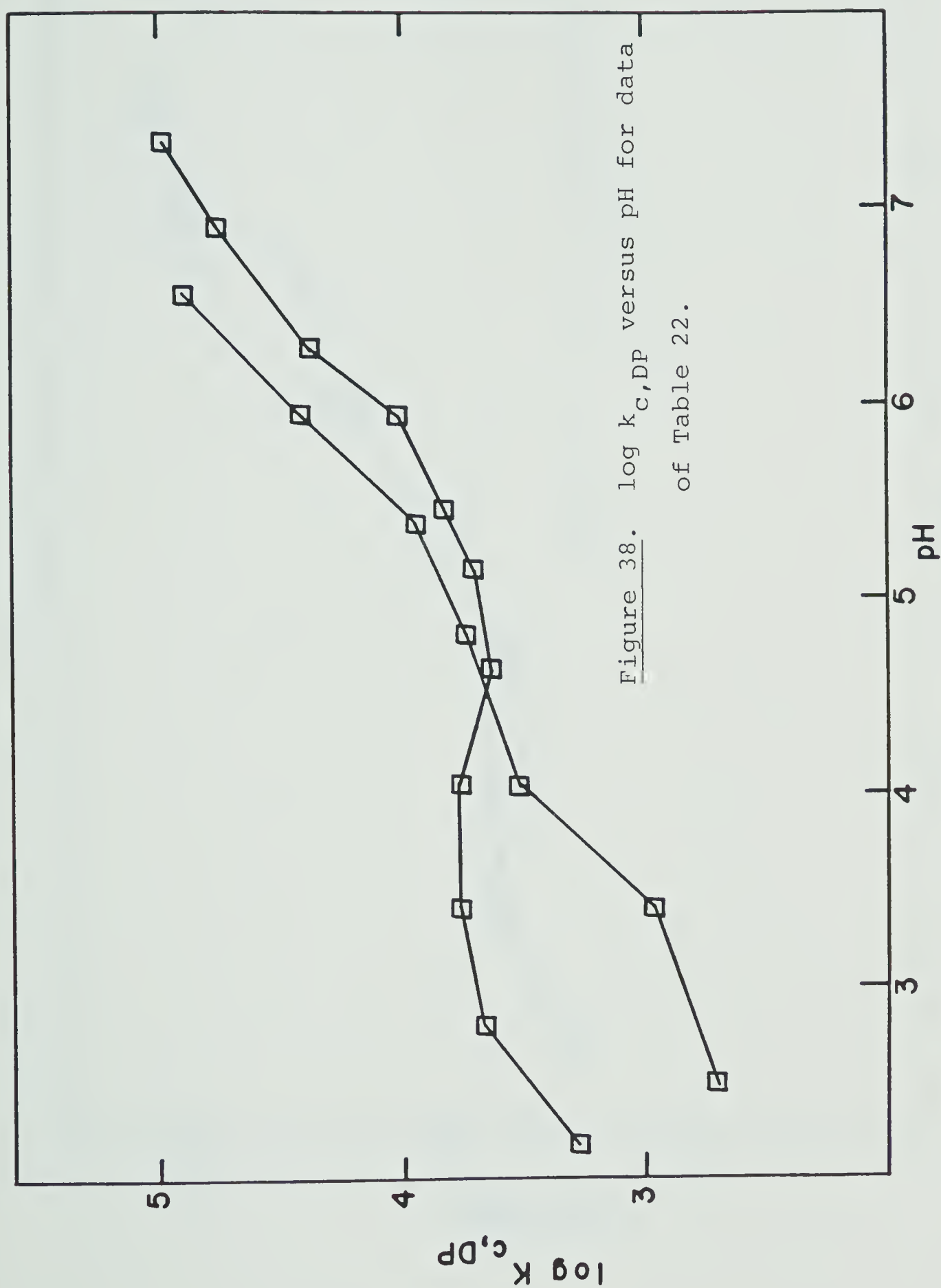
$$k_{C,DR} = \frac{1/\tau_C}{C_{RSH}} \quad (136)$$

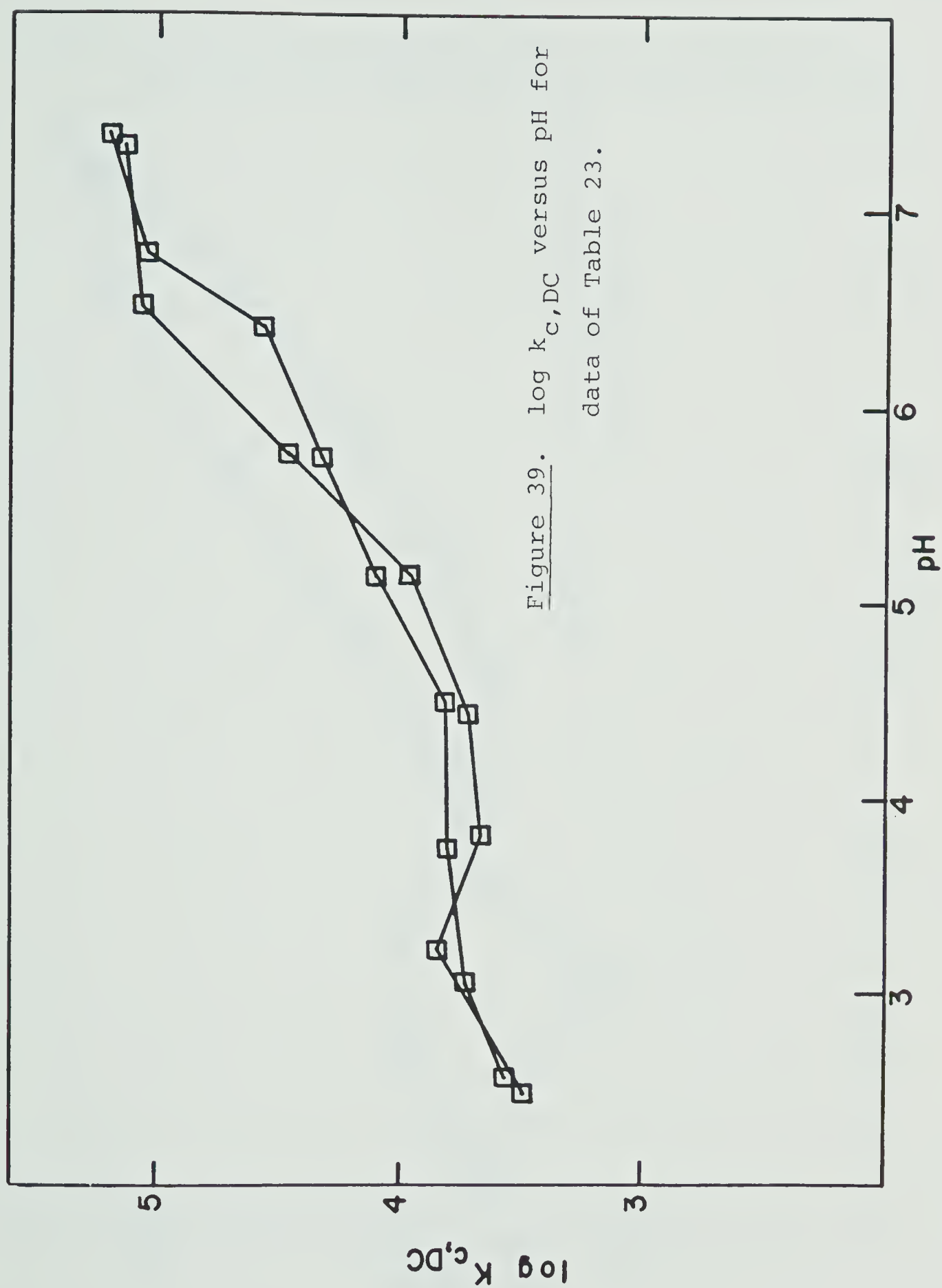
where $k_{C,DR}$ is a conditional rate constant for the displacement of MAA from its $\text{CH}_3\text{Hg(II)}$ complex by thiol RSH and C_{RSH} its free concentration. $k_{C,DR}$ is a pH-dependent function of individual rate constants, acid dissociation constants, and a_{H^+} . $k_{C,DR}$ was evaluated for all the data; values are shown in Tables 22 through 24. The values from different runs are poorly reproducible, due to the uncertainty in the correction for MAA/MAA processes. Plots of $\log k_{C,DR}$ versus pH are shown in Figures 38 through 40. Values at pH 6.0 will be used for discussion below; at higher pH values narrow lines make lifetime calculations imprecise, whereas below this carboxylate effects complicate the issue. Based on the runs performed at the highest RSH concentrations (where the influence of MAA/MAA process is minimal) values at pH 6.0 are $\log k_{C,DP} = 4.4$, $k_{C,DC} = 4.5$ and $\log k_{C,DG} = 4.8$ respectively. Uncertainty in these is estimated at ± 0.3 .

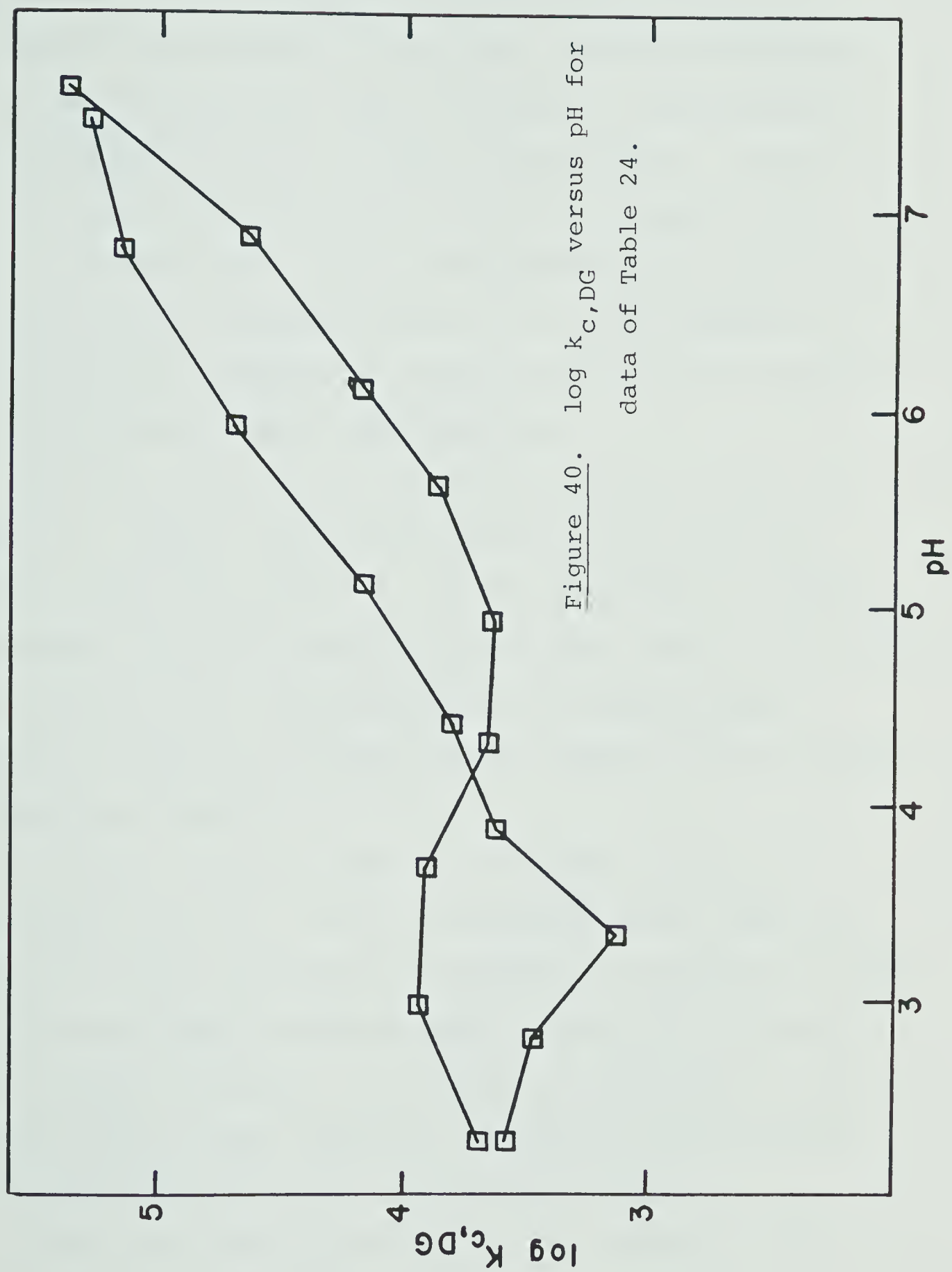
C. Discussion

1. MAA/MAA exchange kinetics.

The model for MAA/MAA exchange kinetics summarised







by equation (132) considered the situation in terms of effective rate constants (k_1 - k_4) for processes involving an aggregate protonation (sum of protons or carboxylates and sulfhydryl) of 0, 1, 2 and 3 respectively. In this Section some speculation will be offered regarding the sites of protonation. Given acid-dissociation constants for the various ionisable groups, it is then possible to calculate rate constants (k') for the reaction of specific acid-base forms of free and bound MAA.

Process 1 has only one possible reaction, shown in Table 25. $\log k'_1$ (the rate constant for this specific reaction) has the value 6.6. By the standards of typical bimolecular diffusion-controlled reactions ($\log k \sim 9.5$ (62)) this is very slow, probably because of strong charge repulsion between the singly charged complex and the doubly charged free ligand.

Process 4 also has only one reaction. $\log k'_4$ is calculated to be 3.2. This is very much slower than processes involving deprotonated sulfhydryl, presumably because the reaction requires proton loss at the sulfur during or after complex formation. If this is so, this will be the fastest such process; negative charges on either complex or ligand would retard the proton loss further.

Three reactions can be written for Process 2. The

Table 25. Rate constants for MAA/MAA exchange reactions at $\text{CH}_3\text{Hg}(\text{II})$.

Process Rate Constant	log (value) ^a	Possible Reaction(s)	Contribution to Process Rate Constant	log rate constant for reaction (maximum) ^b
k_1	6.6	$[\text{CH}_3\text{HgSCH}_2\text{CO}_2^-][\text{SCH}_2\text{CO}_2^-]$	k_1^c	6.6 ^d
k_2	13.5	a) $[\text{CH}_3\text{HgSCH}_2\text{CO}_2^-][\text{HSCH}_2\text{CO}_2^-]$	k_{2a}'/K_2	3.4
		b) $[\text{CH}_3\text{HgSCH}_2\text{CO}_2\text{H}][\text{SCH}_2\text{CO}_2^-]$	k_{2b}'/K_1'	9.7
		c) $[\text{CH}_3\text{HgSCH}_2\text{CO}_2\text{H}][\text{SCH}_2\text{CO}_2\text{H}]$	k_{2c}'/K_1^{*e}	? ^f
k_3	18.1	a) $[\text{CH}_3\text{HgSCH}_2\text{CO}_2^-][\text{HSCH}_2\text{CO}_2\text{H}]$	k_{3a}'/K_1K_2	4.5
		b) $[\text{CH}_3\text{HgSCH}_2\text{CO}_2\text{H}][\text{HSCH}_2\text{CO}_2^-]$	$k_{3b}'/K_1'/K_2$	4.2
		c) $[\text{CH}_3\text{HgSCH}_2\text{CO}_2\text{H}][\text{SCH}_2\text{CO}_2\text{H}]$	$k_{3c}'/K_1^*K_1'$? ^f
k_4	20.6	$[\text{CH}_3\text{HgSCH}_2\text{CO}_2\text{H}][\text{HSCH}_2\text{CO}_2\text{H}]$	$k_{4}'/K_1K_2K_1'$	3.2

a) See Section B.1 for method.

b) Assumes 100% contribution of this reaction to overall rate.

c) Primed rate constants relate to a single reaction.

d) True value, since contribution (see b) is necessarily 100%.

e) Carboxylate pK for sulfhydryl deprotonated MAA.

f) Value of K_1^* unknown.

contributions of these to the overall rate cannot be evaluated independently; however, *maximal* values of the rate constants k'_{2a} and k'_{2b} can be evaluated by considering each in turn as the only reaction occurring. $\log k'_{2a}$ is 3.4 or less (given the double negative charge on the transition state, probably much less). $\log k'_{2b}$ is 9.7 (which is in excess of the likely diffusion-controlled limit of 9-9.5 for such large ions), or less. Since only one reactant is charged, no charge repulsion effects are anticipated, and a fast, diffusion-controlled reaction seems likely. $\log k'_{2c}$ cannot be evaluated, since K_1^* , the acid-dissociation constant of the carboxylate group on the minority species $^-SCH_2CO_2H$, is unknown. A reasonably fast reaction with some retardation due to charge repulsion would be expected.

Three reactions can also be written for Process 3. $\log k'_{3a}$ and $\log k'_{3b}$ have maximal values of 4.5 and 4.2 respectively; as discussed above, the values are probably somewhat lower. Probably reaction c dominates the kinetics; again, there is no reason why this reaction should not be fast and diffusion-controlled. For instance, if a value of $pK_1^* = 5.0$ is assumed, $\log k'_{3c}$ is calculated to be 9.3 or less.

This appears to be the first time that the exchange kinetics of a sulfhydryl ligand at $\text{CH}_3\text{Hg(II)}$ have been characterized in such detail. The observation of anomalously slow kinetics for the high pH displacement reaction is especially significant. Similar behaviour would be anticipated for 2,3 dimercaptosuccinic acid, which is one of the most successful $\text{CH}_3\text{Hg(II)}$ poisoning antidotes to date; it may be that its efficacy is linked to this behaviour. This will be discussed further in Part 2, Chapter IX.

The rate constants k_1 and k_4 are compared with values determined for other thiols (either above or elsewhere) in Section 2 below.

2. Exchange involving other ligands.

Table 26 gives rate constants for displacement reactions involving other thiols; k_1 for MAA/MAA exchange is also included for comparison.

The results for displacement by PS^- , CS^- and GS^- are estimates based on the measured rate at pH 6 (see Section B.3 above). The assumption was made that the species dominating the kinetics at this pH in each case was the sulfhydryl deprotonated, amino protonated form of the ligand; the true constant could then be calculated by using the microscopic acid dissociation constants to estimate

Table 26. Rate constants for sulfhydryl ligand exchange at $\text{CH}_3\text{Hg(II)}$.

#	$\text{CH}_3\text{Hg(II)}$ -bound ligand (A)	Displacing ligand (B)	log (value)	$\log(K_{\text{fB}}/K_{\text{fA}})$
1	MAA (CO_2^-)	$^-\text{SCH}_2\text{CO}_2^-$	6.6	0 ^a
2	GSH	GS^-	8.8 ^b	0 ^a
3	MAA (CO_2^-)	$\text{PS}^- (\text{NH}_3^+)$	6.4 ^c	-2.1 ^d
4	MAA (CO_2^-)	$\text{CS}^- (\text{NH}_3^+)$	6.9 ^c	-1.5 ^d
5	MAA (CO_2^-)	$\text{GS}^- (\text{NH}_3^+)$	7.8 ^c	-1.0 ^d
6	PSH (NH_3^+)	$^-\text{SCH}_2\text{CO}_2^-$	8.5 ^e	2.1
7	CSH (NH_3^+)	$^-\text{SCH}_2\text{CO}_2^-$	8.4 ^e	1.5
8	GSH (NH_3^+)	$^-\text{SCH}_2\text{CO}_2^-$	8.8 ^e	1.0

a) By definition.

b) From reference 64.

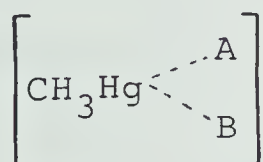
c) Estimates, based on conditional rate constant at pH 6.0; see text.

d) Based on measurements of formation constants in Chapter III.

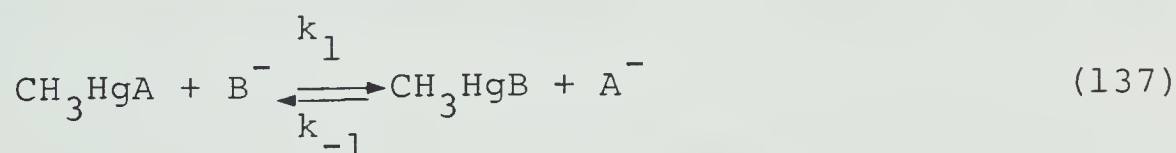
e) Calculated on the basis of c) and d) above.

the fraction of RSH in this form. Since the equilibrium formation constants of the $\text{CH}_3\text{Hg(II)}$ complexes of these acid-base species were calculated in Chapter III (see Figure 17), the reverse rate constants can also be estimated.

Geier and Erni have developed a theory to rationalise such displacement kinetics data for a variety of $\text{CH}_3\text{Hg(II)}$ -ligand systems (62). It is assumed that the reactants (CH_3HgA and B^-) diffuse together to form an associated transition state:



and that the probability of this dissociating to CH_3HgB rather than to CH_3HgA is proportional to the relative formation constants of CH_3HgB and CH_3HgA respectively. Mathematically, for the system



it is predicted that

$$k_1 = \frac{k_o \cdot K_{fB}}{K_{fB} + K_{fA}} \quad (138)$$

and that

$$k_{-1} = \frac{k_o \cdot K_{fA}}{K_{fB} + K_{fA}} \quad (139)$$

where K_{fA} and K_{fB} are (equilibrium) formation constants and k_o is the diffusion-controlled limit for the rate constant of a bimolecular reaction.

The dashed line in Figure 41 shows the magnitude predicted by Geier and Erni for $\log k_1$ on this basis, plotted as a function of $\log (K_{fB}/K_{fA})$. It should be emphasized that while the shape of such a curve results from theory, its *vertical position* depends on the value assumed for k_o . The curve shown assumes $k_o = 3 \times 10^9 \text{ M}^{-1} \text{ s}^{-1}$, a typical figure for the diffusion controlled limit when a small, mobile ion approaches an uncharged complex. For the present results, a lower value for k_o would be anticipated since

- a) both approaching ion and complex have some negative charge. The resulting repulsion is predicted (141) to lower k_o by a factor of 2 or 3.
- b) the ions involved (PS^- , CS^- , GS^-) are not small and spherical; thus, their diffusion rates through solution are likely to be slower.

The closed circles in Figure 41 represent the data of Table 26; the expected trend is observed. The points lie approximately on a curve of the form shown, having a

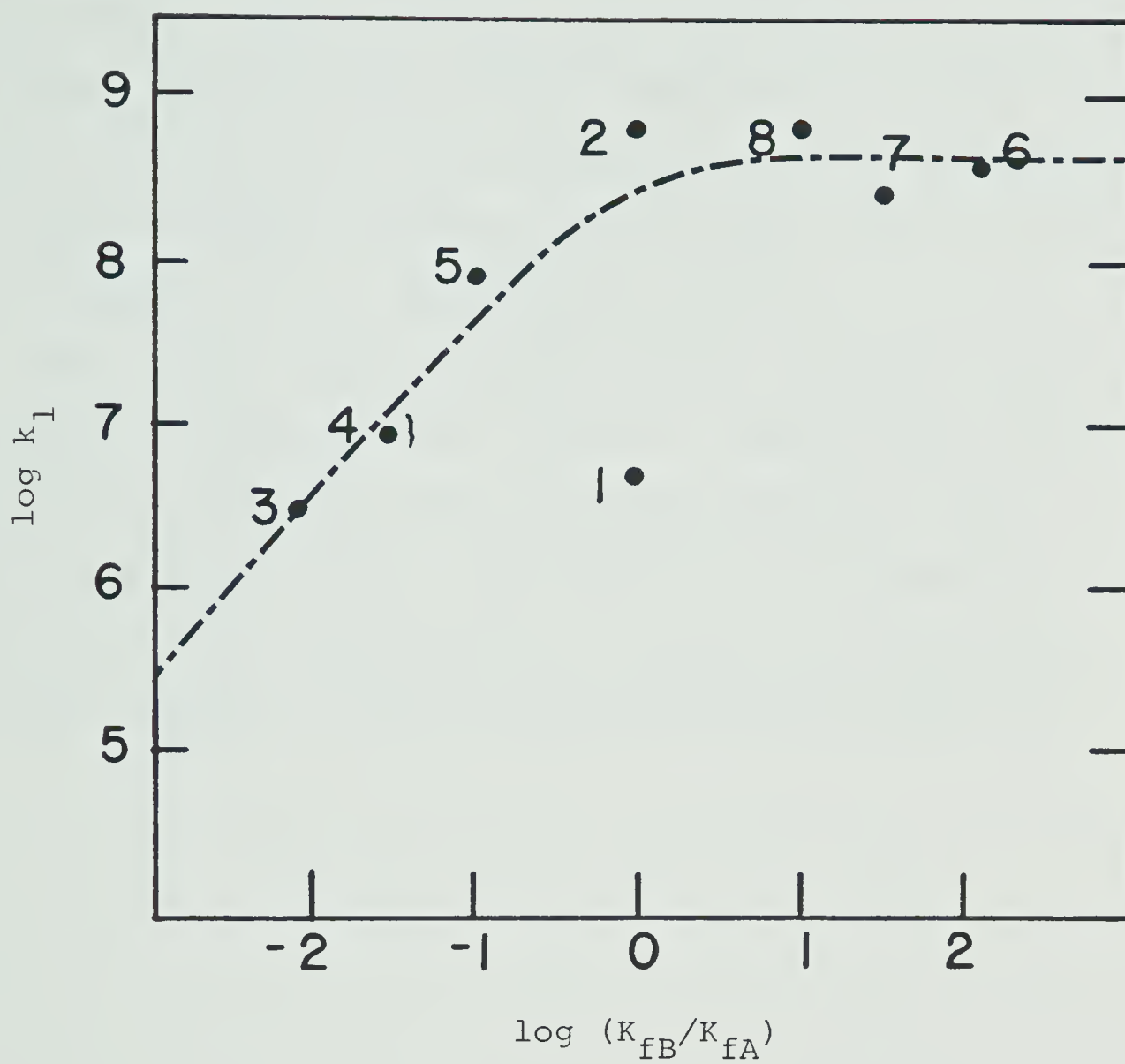


Figure 41. Displacement rate constants as a function of $\log (K_{fB}/K_{fA})$ for the systems of Table 26.

limiting value of $\log k_1$ ($\log k_o$) of about 8.6. In light of the factors discussed above, this seems entirely reasonable. The datum for GS^-/GS^- exchange (64), also shown, is in line with these conclusions. (By contrast, the high pH MAA/MAA exchange rate constant, point 1, lies well below the line. See Section 1 above).

Thus, these results provide further indication that transfers of $CH_3Hg(II)$ from ligand to ligand occur via an associative mechanism, and can be rationalised by the approach outlined above. This result has interesting implications for the mobility of $CH_3Hg(II)$ in biological systems, a matter to be further discussed in Chapter IX.

BIBLIOGRAPHY - PART 1

1. R.G. Pearson, ed., "Hard and Soft Acids and Bases", Dowden, Hutchison and Ross, Pennsylvania, U.S.A. (1973).
2. D.L. Rabenstein, Acc. Chem. Res. 11, 100 (1978).
3. K. Kohei and F. Masahiko, Toxicology 1, 43 (1973).
4. L. Dunlap, Chem. Eng. News 49(27), 22 (1971).
5. M.M. Jones and W.K. Vaughn, J. Inorg. Nucl. Chem. 40, 2081-8 (1978).
6. E. Nieboer and D.H.S. Richardson, Environ. Pollution (B) 1, 3 (1980).
7. J.M. Wood, F.S. Kennedy and C.G. Rosen, Nature 220, 173 (1968).
8. H.A.O. Hill, J.M. Pratt, S. Ridsdale, F.R. Williams and P.J. Williams, Chem. Commun. 341 (1970).
9. T.M. Lexmond, F.A.M. DeHaan and M.J. Frissel, Neth. J. Agric. Sci. 24, 79 (1976).
10. J.S. Thayer, A.C.S. Symp. Ser. 82, 188 (1978).
11. Y. Talmi and R.E. Mesmer, Water Res. 9, 547 (1975).
12. C.J. Cappon and J.C. Smith, Anal. Chem. 52, 1527 (1980).
13. J.V. Hatton, W.G. Schneider and W. Siebrand: J. Chem. Phys. 39, 1330 (1963).
14. D.N. Ford, P.R. Wells and P.C. Lauterbiar, Chem. Commun. 616 (1967).

15. G. Schwarzenbach and M. Schellenberg, *Helv. Chim. Acta* 48, 28 (1965).
16. D. Grdenic and F. Zado, *J. Chem. Soc.* 521 (1962).
17. S. Mansy, T.E. Wood, J.C. Sprowles and R.S. Tobias, *J.A.C.S.* 96, 1762 (1974).
18. J.H.S. Green, *Spectrochim. Acta.* 24A, 863 (1968).
19. J. Lorbeth and F. Weller, *J. Organometal. Chem.* 32, 145 (1971).
20. J.H. Clarke and L.A. Woodward, *Trans. Faraday Soc.* 64, 1041 (1971).
21. D.L. Rabenstein, C.A. Evans, M.C. Tourangeau and M.T. Fairhurst, *Anal. Chem.* 47, 338 (1975).
22. T.D. Waugh, H.T. Walton and J.A. Laswick, *J. Phys. Chem.* 59, 395 (1955).
23. R.B. Simpson, *J.A.C.S.* 83, 4711 (1961).
24. S. Libich and D.L. Rabenstein, *Anal. Chem.* 45, 118 (1973).
25. A.C. Dash and R.K. Nanda, *J. Indian Chem. Soc.* 51, 733 (1974).
26. R.J. Maguire, S. Anand, H. Chew and W.A. Adams, *J. Inorg. Nucl. Chem.* 38, 1659 (1976).
27. D.L. Rabenstein, R. Ozubko, S. Libich, C.A. Evans, M.T. Fairhurst and C. Suvanoprakorn, *J. Coord. Chem.* 3, 263 (1974).

28. J. Mulvihill, Science 176, 132 (1972).
29. D.W. Gruenwadel and N. Davidson, J. Mol. Biol. 21, 129 (1966).
30. R.B. Simpson, J.A.C.S. 86, 2059 (1964).
31. S. Mansy and R.S. Tobias, J.A.C.S. 96, 6874 (1974).
32. S. Mansy and R.S. Tobias, Biochem. 14, 2952 (1975).
33. A.J. Canty and R.S. Tobias, Inorg. Chem. 18, 413 (1979).
34. L. Prizant, M.J. Olivier, R. Rivest and A.L. Beauchamp, J.A.C.S. 101, 2765 (1979).
35. J. Hubert and A.L. Beauchamp, Can. J. Chem. 58, 1439 (1980).
36. J. Hubert and A.L. Beauchamp, Acta Crystallogr. B 36, 2613 (1980).
37. C.A. Evans, D.L. Rabenstein, G. Geier and I. Erni, J.A.C.S. 99, 8106 (1977).
38. M.T. Fairhurst and D.L. Rabenstein, Inorg. Chem. 14, 1413 (1975).
39. Y.S. Wong, A.J. Carty and P. Chieh, J.C.S. Dalton Trans. 1157 (1977).
40. F.A. Cotton and G. Wilkinson, "Advanced Inorganic Chemistry" 3rd edition. Wiley-Interscience, New York, N.Y., p. 505 (1972).
41. P.L. Goggin and L.A. Woodward, Trans. Faraday Soc. 62 1423 (1966).

42. P.L. Goggin, R.J. Goodfellow and N.W. Hurst, J.C.S. Dalton Trans. 561 (1978).
43. P.L. Goggin, G. Kemery and J. Mink, J.C.S. Faraday II, 1025 (1976).
44. J.C. Mills, H.S. Preston and C.H.L. Kennard, J. Organometal. Chem. 14, 33 (1968).
45. J. Relf, R.P. Cooney and H.F. Henneike, J. Organometal. Chem. 39, 75 (1972).
46. V.S. Petrosyan and O.A. Reutov, J. Organometal. Chem. 76, 123 (1974).
47. N.J. Taylor, Y.S. Wong, P.C. Chieh and A.J. Carty, J.C.S. Dalton Trans. 438 (1975).
48. G. Anderegg, Helv. Chim. Acta 57, 1340 (1974).
49. A.J. Canty, A. Marker and B.M. Gatehouse, J. Organometal. Chem. 88, C31 (1975).
50. A.J. Canty and B.M. Gatehouse, J.C.S. Dalton Trans. 2018 (1976).
51. A.J. Canty and A. Marker, Inorg. Chem. 15, 425 (1976).
52. A.J. Canty, G. Hayhurst, N. Chaichit and B.M. Gatehouse, J.C.S. Chem. Commun. 316 (1980).
53. A.J. Canty, N. Chaichit, B.M. Gatehouse and A. Marker, Acta Crystallogr. B, 34, 3229 (1978).
54. R.T.C. Brownlee, A.J. Canty and M.F. Mackay, Austral. J. Chem. 31, 1933 (1978).

55. G. Geier, I. Erni and R. Steiner, *Helv. Chim. Acta* 60, 9 (1977).
56. A.J. Brown, O.W. Howarth and P. Moore, *J.C.S. Dalton* 1589 (1976).
57. R.D. Bach and A.T. Weibel, *J.A.C.S.* 98, 6241 (1976).
58. N.W. Alcock, P.A. Lampe and P. Moore, *J.C.S. Dalton Trans.* 1324 (1978).
59. P.A. Lampe and P. Moore, *Inorg. Chim. Acta* 36, 27 (1978).
60. M. Eigen, G. Geier and W. Kruse, *Experientia, Suppl.* 9, 164 (1964).
61. G. Geier and I.W. Erni, *Chimia* 27, 635 (1973).
62. I. Erni and G. Geier, *Helv. Chim. Acta* 62, 1007 (1979).
63. R.B. Simpson, *J. Chem. Phys.* 46, 4775 (1967).
64. M.T. Fairhurst and D.L. Rabenstein, *J.A.C.S.* 97, 2086 (1975).
65. L.L. Murrell and T.L. Brown, *J. Organometal. Chem.* 13, 301 (1968).
66. R.D. Bach and A.T. Weibel, *J.A.C.S.* 97, 2575 (1975).
67. W.L. Hughes, *Cold Spring Harbor Symposia XIV*, 79 (1950).
68. Y. Hojo, Y. Sugiura and H. Tanaka, *J. Inorg. Nucl. Chem.* 38, 641 (1976).
69. D.L. Rabenstein, *J.A.C.S.* 95, 2797 (1973).
70. P.G. Simpson, T.E. Hopkins and R. Hague, *J. Phys. Chem.* 77, 2282 (1973).

71. I.K. Adzami, D.L. Nosco and E. Deutsch, J. Inorg. Nucl. Chem. 42, 1364 (1980).
72. T.S. Wong, P.C. Chieh and A.J. Carty, Can. J. Chem. 51, 2597 (1973).
73. Y.S. Wong, P.C. Chieh and A.J. Carty, Chem. Commun. 741 (1973).
74. L.T. Sytsma and R.J. Kline, J. Organometal. Chem. 54, 15 (1973).
75. R.T. Morrison and R.N. Boyd, "Organic Chemistry", 3rd edition, Allyn and Bacon, New York, N.Y., p. 290 (1973).
76. N.W. Alcock, P.A. Lampe and P. Moore, J.C.S. Dalton Trans 1471 (1980).
77. S.J. Lippard, Acc. Chem. Res. 6, 282 (1973).
78. I Amdur and G.G. Hammes, "Chemical Kinetics", McGraw-Hill, New York, N.Y., p. 62 (1966).
79. N.K. Wilson, R.D. Zehr and P.D. Ellis, J. Mag. Res. 21, 437 (1976).
80. M.A. Sens, N.K. Wilson, P.D. Ellis and J.D. Odom, J. Mag. Res. 19, 323 (1975).
81. M. Borzo and G.E. Maciel, J. Mag. Res. 19, 279 (1975).
82. J.L. Sudmeier, R.R. Birge and T.G. Perkins, J. Mag. Res. 30, 491 (1978).

83. J.D. Kennedy and W. McFarlane, J.C.S. Faraday II, 1653 (1976).
84. V. Lucchini and P.R. Wells, J. Organometal. Chem. 92, 283 (1975).
85. W. McFarlane, J.C.S. 528 (1967).
86. H.F. Henneike, J.A.C.S. 94, 5945 (1972).
87. L.A. Federov, E.I. Fedin, B.A. Kvasov and I.P. Beletskaya, J. Struct. Chem. 10, 231 (1969).
88. D.F. Evans, P.M. Ridout and I. Wharf, J.C.S. A, 2127 (1968).
89. R. Sheffold, Helv. Chim. Acta 52, 56 (1969).
90. M.T. Fairhurst, Ph.D. Thesis, University of Alberta, p. 107 (1975).
91. E. Grunwald, A. Loewenstein and S. Meiboom, J. Chem. Phys. 27, 64 (1957).
92. R.C. Weast, ed., "Handbook of Chemistry and Physics" 49th edition, CRC Press, Cleveland, Ohio, p. B244 (1968).
93. P.C. Jocelyn, "Biochemistry of the SH Group", Academic Press, New York, N.Y., p. 94 (1972).
94. R. Saetre, Ph.D. Thesis, University of Alberta, pp. 102, 113, 116 (1978).
95. R. Benesch and R.E. Benesch, Biochim. Biophys. Acta 23, 643 (1957).

96. H. Laitinen and W.E. Harris, "Chemical Analysis", 2nd edition, McGraw-Hill, New York, N.Y., p. 109 (1975).
97. Reference 94, p. 23.
98. S.J. Backs, M.Sc. Thesis, University of Alberta, p. 24 (1979).
99. J. Carlsson, M.P.J. Kierstan and K. Brocklehurst, Biochem. J. 139, 237 (1974).
100. R.G. Bates, "Determination of pH", 2nd edition, Wiley-Interscience, New York, N.Y., p. 73 (1973).
101. D.E. Hill and H.O. Spivey, Anal. Biochem. 57, 500 (1974).
102. Reference 90, p. 115.
103. J. Nolan and B. Kratochvil, unpublished.
104. Reference 98, pp. 81-83, 88-96, 103-107, 111-115.
105. J.L. Dye and V.A. Nicely, J. Chem. Educ. 48, 443 (1971).
106. W.E. Wentworth, J. Chem. Educ. 42, 96 (1965).
107. A. Albert and E.P. Serjeant, "The Determination of Ionization Constants", Chapman and Hall, London (1971).
108. E.D. Becker, "High Resolution NMR", Academic Press, New York, N.Y., p. 214 (1969).
109. H.S. Gutowsky and C.H. Holm, J. Chem. Phys. 25, 1228 (1956).

- 110. H.M. McConnell, J. Chem. Phys. 28, 430 (1958).
- 111. F. Bloch, Phys. Rev. 70, 460 (1946).
- 112. H.S. Gutowsky, D.W. McCall and C.P. Slichter, J. Chem. Phys. 21, 279 (1953).
- 113. Reference 90, p. 82.
- 114. Y. Theriault, personal communication.
- 115. W. Lund and E. Jacobsen, Acta Chem. Scand. 19, 1783 (1965).
- 116. E. Larsson, Z. Anorg. Chem. 172, 375 (1928).
- 117. D.L. Leussing, J.A.C.S. 80, 4180 (1958).
- 118. O.S. Musailov, B.A. Dunai and N.P. Komar, J. Anal. Chem. USSR 23, 123 (1968).
- 119. S.J. Backs and D.L. Rabenstein, Inorg. Chem. 20, 410 (1981).
- 120. D.A. Doornbos, Pharm. Weekbl. 102, 269 (1967).
- 121. Reference 108, p. 174.
- 122. E.W. Wilson and R.B. Martin, Arch. Biochim. Biophys. 142, 445 (1971).
- 123. J.T. Edsall and J. Wyman, "Biophysical Chemistry", Vol. 1, Academic Press, New York, N.Y., Chapter 9 (1958).
- 124. J.H. Ritsma and E. Jellinek, Receuil 91, 923 (1972).
- 125. E. Coates, C. Marsden and B. Rigg, Trans. Faraday Soc. 65, 863 (1969).

126. K. Wallenfels and C. Streffer, *Biochem. Z.* 346, 119 (1966).
127. L.J. Porter and D.D. Perrin, *Austral. J. Chem.* 22, 267 (1969).
128. D.L. Rabenstein and A.A. Isab, unpublished.
129. H. Sakurai and S. Takeshima, *Talanta* 24, 531 (1977).
130. B. Stanovnik and M. Tisler, *Anal. Biochem.* 9, 68 (1964).
131. N. Motohashi, I. Mori, Y. Sugiura and H. Tanaka, *Chem. Pharm. Bull* 24, 1737 (1976).
132. D.P. Hanlon, *J. Medicinal Chem.* 14, 1084 (1971).
133. J. Aaseth, *Acta Pharmacol. Toxicol.* 39, 289 (1976).
134. J. Aaseth and E.A.H. Friedheim, *Acta Pharmacol. Toxicol.* 42, 248 (1978).
135. J.S. Casas and M.M. Jones, *J. Inorg. Nucl. Chem.* 42, 99 (1980).
136. A.J. Canty, R.S. Tobias, N. Chaichit and B.M. Gatehouse, *J.C.S. Dalton Trans.* 1693 (1980).
137. Reference 100, p. 59.
138. J. Kieland, *J.A.C.S.* 59, 1675 (1937).
139. Robinson and Stokes, "Electrolyte Solutions", 2nd edn., Butterworths, London, p. 515 (1959).
140. A.T. Pilipenko, and O.P. Ryabwshko, *Ukr. Khim. Zh.* 32, 622 (1966); as in *Chem. Abs.* 65, 11412h (1966).

141. P. Debye, Trans. Electrochem. Soc. 82, 265 (1942).
142. L. Meites, "Handbook of Analytical Chemistry", McGraw-Hill, New York, N.Y., pp. 1-8 (1963).
143. E.J. King, "Acid-Base Equilibria", Vol. 4, in "Equilibrium Properties of Electrolyte Solutions", ed. R.A. Robinson, MacMillan, New York (1965).
144. C.W. Davies, J. Chem. Soc. 2093 (1938).

APPENDIX I

IONIC STRENGTH AND ACTIVITY CONSIDERATIONS

The effect of ionic strength on the activity of ions in solution, and hence on the measured values of equilibrium constants, has long been recognised. The relationship between ionic strength (μ) and activity coefficient (γ) was first formalised in the Debye-Huckel equation in its limiting form

$$-\log \gamma_{\pm} = A Z_A Z_B \sqrt{\mu}$$

where Z_A and Z_B are the charges on A and B ions respectively and A is a constant. A useful semi-empirical extension for use at high ionic strengths is the Davies equation. This exists in three variants in the literature

$$\text{a) } -\log \frac{\gamma_{\pm}}{n^2} = \frac{A\sqrt{\mu}}{1+1.5\sqrt{\mu}} - 0.2\mu \quad (\text{Meites (142)}) \quad (140)$$

$$\text{b) } -\log \frac{\gamma_{\pm}}{n^2} = \frac{A\sqrt{\mu}}{1+\sqrt{\mu}} - 0.2\mu \quad (\text{King (143)}) \quad (141)$$

$$\text{c) } -\log \frac{\gamma_{\pm}}{n^2} = \frac{A\sqrt{\mu}}{1+\sqrt{\mu}} - 0.1\mu \quad (\text{Davies (144)}) \quad (142)$$

Tabulated values of all three functions were compared with a variety of measured activity coefficients in an

attempt to select which function to use. However, due presumably to specific interaction effects, the variation between measured values for various activity coefficients taken from the literature, was of the same order as variations between the forms of the equation. The form due to Davies appeared to be the closest and was selected for use here; however, the arbitrary nature of the decision should be emphasised.

A constant ionic strength of 0.3 was used in this work. Ideally, μ should be as low as possible, since in the limit of infinite dilution all activity coefficients are conventionally unity. Thus, measured equilibrium constants would be thermodynamic quantities. This is not possible here, since the limit for detection of a sharp single-proton resonance on the A60-D spectrometer with acceptable signal-to-noise ratio is about 0.04 *M*. In the present case the two protons of the MAA methylene group give a stronger signal, but the linebroadening observed on many of these resonance nullifies this advantage.

Thus, in a solution acceptable for high pH ^1H NMR measurements, the contribution to μ of MAA alone approaches 0.2. A value of 0.3 was therefore selected to give a little "headroom". Ionic strength adjustment by addition of a swamping salt concentration is impossible here;

adjustments must be based on calculation of actual μ at each stage.

0.3 is a convenient choice for two other reasons:

- a) The extensive compilation and selection of pK's by Backs (104) was performed at $\mu = 0.3$;
- b) At $\mu = 0.3$ activity coefficients (as predicted by the Davies equation) are relatively insensitive to changes in ionic strength.

All constants used and determined in this work are "mixed", that is, terms for hydrogen ion are activities as estimated by glass electrode response; all other terms are concentrations. This is what is actually measured. Conditions are specified throughout so that others can estimate thermodynamic or concentration constants if desired, making their own assumptions.

In using literature value for pK's, it is necessary to correct values determined at other ionic strengths to $\mu = 0.3$; it may also be necessary to correct the type of constant, since both concentration and thermodynamic constants are encountered. This was performed as below:

Now
$$K = \frac{a_{H^+} \cdot [A^-]}{[HA]}$$
 for a neutral monobasic acid, by definition. The thermodynamic dissociation constant, K° , is defined as

$$K^{\circ} = \frac{a_{H^{+}} \cdot a_{A^{-}}}{a_{HA}} = K \cdot \gamma_{A^{-}} \quad (\text{assuming } \gamma_{HA} = 1) \quad (143)$$

This is true for all conditions. Thus, for the same constant measured under two sets of conditions

$$K' \gamma_1' = K'' \gamma_1'' \quad (144)$$

(Subscripts of γ 's refer to charge, all primes to a set of conditions.) Thus

$$K'' = K' \cdot \gamma_1' / \gamma_1'' \quad (145)$$

or

$$pK'' = pK' - \log \gamma_1' + \log \gamma_1'' \quad (146)$$

The first log term in this expression corrects back to the thermodynamic K° , and the second corrects back to the conditions defined by the double prime. Thus, the equation can be used in three situations:

- (1) By substituting values for γ_1' and γ_1'' from, say, the Davies equation, experimental K 's can be corrected to a different ionic strength.
- (2) By substituting 1.00 for γ_1' and an estimated value for γ_1'' thermodynamic values can be corrected to a finite ionic strength.

- (3) By substituting a value for γ_1' obtained from one estimating equation (e.g. Meites' form of the Davies equation) and a value of γ_1'' obtained from another (e.g. Davies' form) the K can be corrected to conform with the desired activity coefficient equation.

Similar correction equations to (146) can be developed for all charge types. A list is shown in Table 27.

Table 27. Equations for correction of acid dissociation constants.

Reaction	Equation
$\text{HA} \rightleftharpoons \text{A}^- + \text{H}^+$	$\text{pK}_a'' = \text{pK}_a' - \log \gamma_1' + \log \gamma_1''$
$\text{HA}^- \rightleftharpoons \text{A}^{2-} + \text{H}^+$	$\text{pK}_a'' = \text{pK}_a' - \log \frac{\gamma_2'}{\gamma_1'} + \log \frac{\gamma_2''}{\gamma_1''}$
$\text{HA}^{2-} \rightleftharpoons \text{A}^{3-} + \text{H}^+$	$\text{pK}_a'' = \text{pK}_a' - \log \frac{\gamma_3'}{\gamma_2'} + \log \frac{\gamma_3''}{\gamma_2''}$
$\text{HA}^+ \rightleftharpoons \text{A} + \text{H}^+$	$\text{pK}_a'' = \text{pK}_a' + \log \gamma_1' - \log \gamma_1''$
$\text{HA}^{2+} \rightleftharpoons \text{HA}^+ + \text{H}^+$	$\text{pK}_a'' = \text{pK}_a' + \log \frac{\gamma_2'}{\gamma_1'} - \log \frac{\gamma_2''}{\gamma_1''}$

Part 2

The Binding of Methylmercury(II) by Macromolecular Thiols
and by Erythrocytes

CHAPTER VI

INTRODUCTION

In Part 1 of this thesis, the ability of methylmercury(II) to form stable yet labile complexes with small sulfhydryl-containing molecules was examined. Using NMR, it was possible to quantify such interactions fairly precisely. In Part 2, the ability of recently developed pulsed Fourier Transform NMR methods to evaluate similarly detailed information for macromolecular systems is demonstrated. For the first time, it is possible to measure actual stability data for metal binding in systems as complex as the intact erythrocyte, and simultaneously to observe directly the molecular details of binding.

This Chapter describes the background (additional to that given already in Chapter I) to these studies. Section A below discusses previous studies involving $\text{CH}_3\text{Hg(II)}$ in biological systems, including its use as a protein sulfhydryl reagent, and identifies the various complex species which traditional methods of investigation have suggested to be of importance. Section B describes studies of antidote molecules used to counteract $\text{CH}_3\text{Hg(II)}$ poisoning, and the attempts made to rationalise the differing effectiveness of various antidotes. Section C describes

the more sophisticated NMR instrumentation and techniques required for direct observation of such systems.

A. Methylmercury(II) in Biological Systems

As was the case for small thiols, the preferential nature of $\text{CH}_3\text{Hg(II)}$ -sulfhydryl binding for protein thiols is well documented. In a monograph on sulfhydryl group assays, Ashworth (145) lists several hundred methods, many applicable to macromolecules and many involving mercury in some form as a titrant. (The uses of Hg(II) (146) p-chloro-mercuribenzoate (147) and $\text{CH}_3\text{Hg(II)}$ (67) are classic examples.) $\text{CH}_3\text{Hg(II)}$ as a titrant for protein sulfhydryls was proposed by Hughes (67), who reasoned that a small "mercurial" should be employed so that protein sulfhydryls buried in the protein structure, and therefore less accessible, would still be titrated. An amperometric titration procedure was developed by Leach (148), and refined to use smaller samples (using a determination of excess $\text{CH}_3\text{Hg(II)}$ after addition of a known amount) by Forbes and Hamlin (149). The use of such methods in a variety of protein systems has been reviewed (145). A recent potentiometric titration procedure was described by Berg and Miles (150), using $\text{CH}_3\text{Hg(II)}$ as titrant and employing a silver/silver-thiol electrode designed by

Toriba and Koval (151).

In a biological mixture, methylmercury(II) will be expected to distribute among the various sulfhydryls, both small and macromolecular, available to it. (The only exception to this may be in the stomach; Rabenstein has calculated that at the low pH and high chloride concentration present, about 2% of the methylmercury(II) may exist as CH_3HgCl (152).)

The sulfhydryl group is ubiquitous in biological systems; the field has been systematically reviewed by Jocelyn (93) and by Friedman (153). For this reason, the exact sites of the toxic action of $\text{CH}_3\text{Hg(II)}$ are a complex matter (154). Attention will be focussed here instead of upon the *transport* of $\text{CH}_3\text{Hg(II)}$ around the body.

Figure 42 is a simplified schematic of the routes by which $\text{CH}_3\text{Hg(II)}$ transports itself around the human body (152). Only principal routes and species are shown; minority species such as mercury biotransformed to Hg(II) (155) are neglected. $\text{CH}_3\text{Hg(II)}$ in food is absorbed into the bloodstream and distributed to the rest of the body. The liver extracts $\text{CH}_3\text{Hg(II)}$ from the blood and secretes it in the bile into the gastrointestinal tract (155). Here much of it is readsorbed into the bloodstream (enterohepatic recirculation) (156), accounting for the low excretion

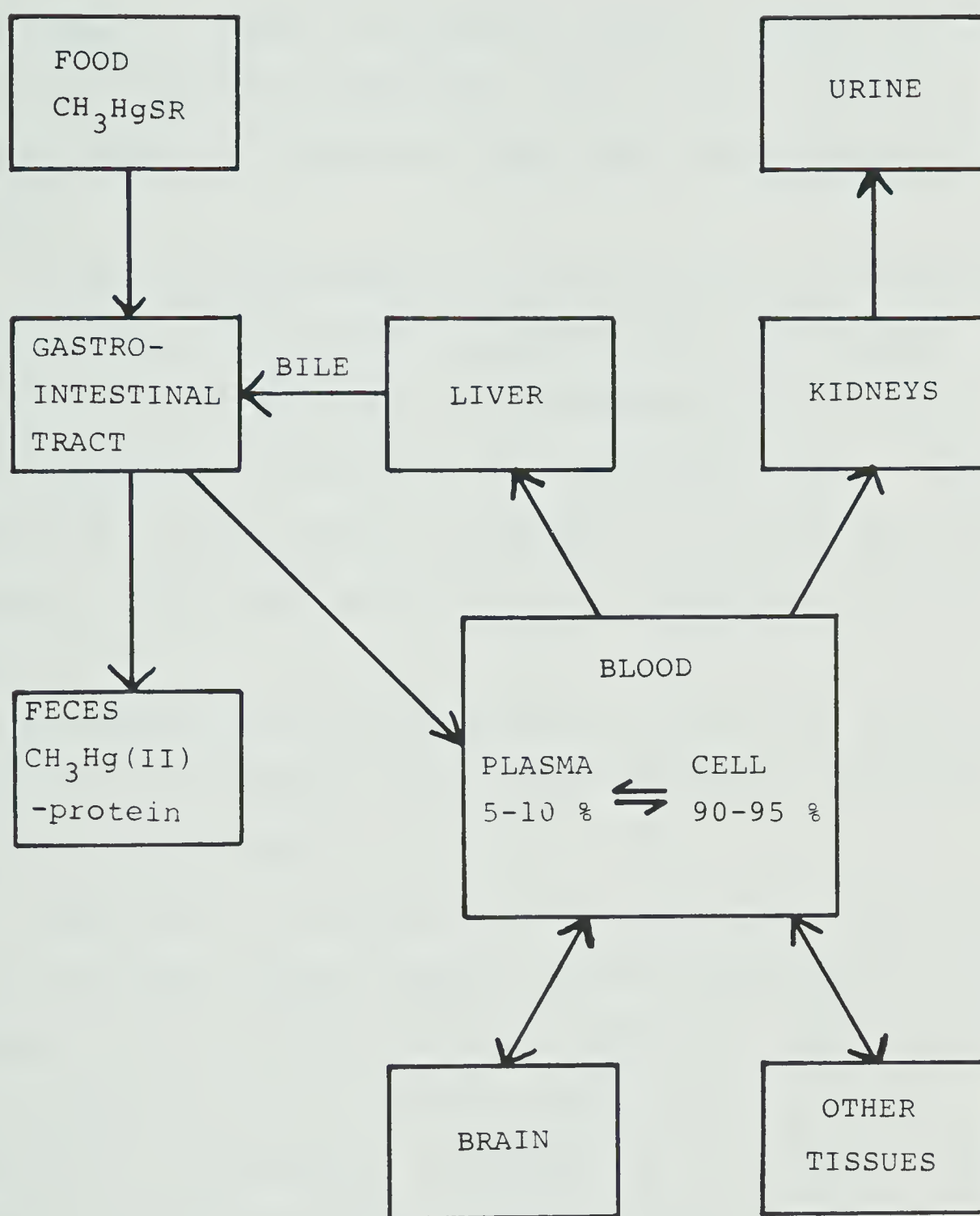


Figure 42. $\text{CH}_3\text{Hg}(\text{II})$ distribution in the body.

rate ($t_{1/2} \sim 70$ days) of $\text{CH}_3\text{Hg(II)}$ (157). Urinary excretion is normally unimportant (152), but is greatly enhanced under the action of some drugs (see Section B, below).

Figure 42 emphasises the central role of the blood in distribution of $\text{CH}_3\text{Hg(II)}$ around the body, and in particular of the *erythrocyte*. Approximately 90% of human blood $\text{CH}_3\text{Hg(II)}$ is found in the erythrocyte (154). (The remainder, in the plasma, is thought to be bound by serum albumin, which constitutes the major sulfhydryl fraction there (152).)

A schematic of the erythrocyte is given in Figure 43. There are two principal thiol species present, hemoglobin and glutathione (GSH).

Hemoglobin is present at about 5 mM. Its role as the main reversible oxygen carrier in blood has made it the subject of considerable research (158,159). Here, only those aspects of its structure relevant to the present study will be discussed. Hemoglobin is a tetrameric (four-subunit) protein of molecular weight about 16,700 per subunit (153). Normal adult hemoglobin has the structure $(\alpha_2\beta_2)$ where α and β are particular subunit types; this is shown schematically in Figure 44. The sulfhydryl group of Cys β -93 on each β chain is accessible to sulfhydryl

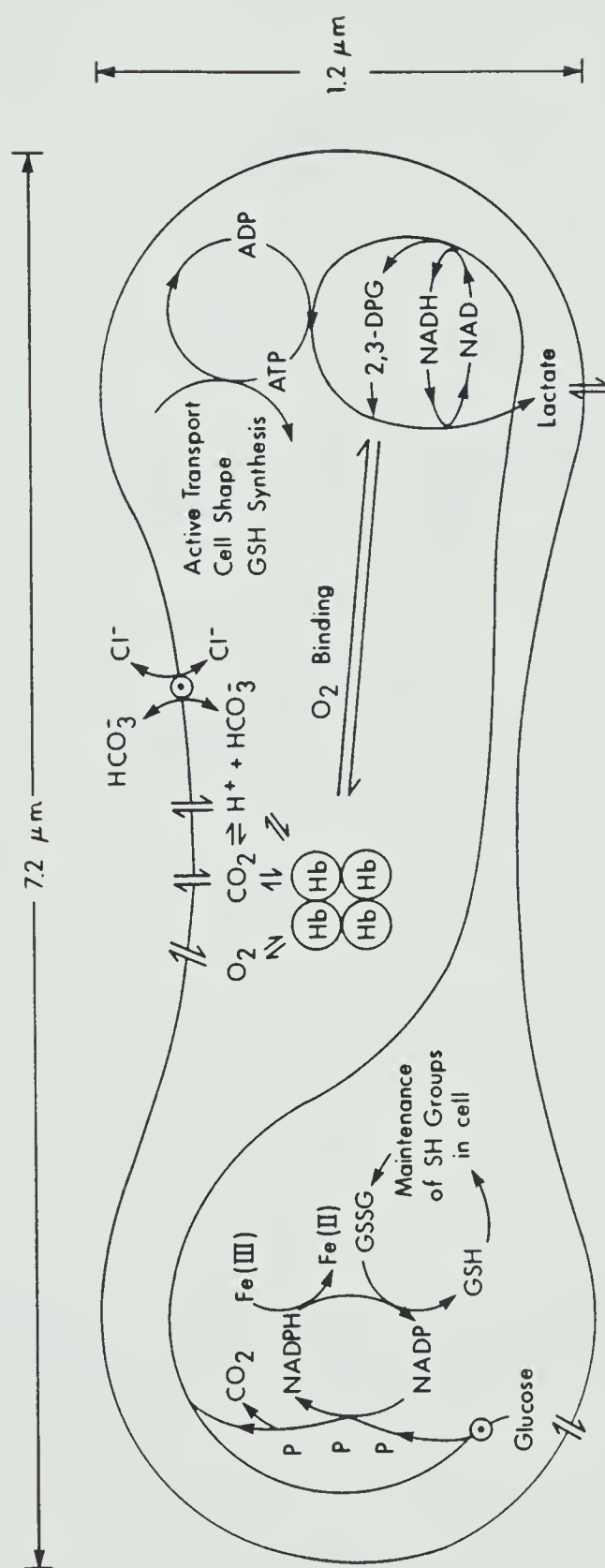


Figure 43. Schematic of the erythrocyte.

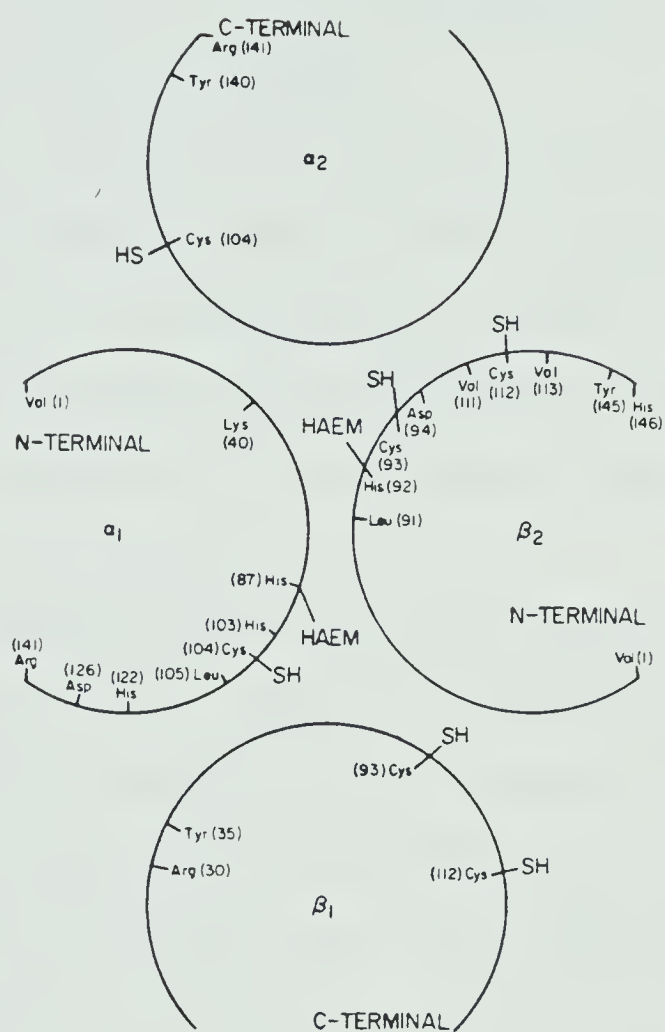


Figure 44. Schematic of the structure of hemoglobin.
Reproduced from Reference 93.

reagents (such as $\text{CH}_3\text{Hg(II)}$) in the native, folded, protein; those of Cy β -112 and α 104 are titratable only upon denaturation (93). Thus, the normal sulfhydryl titre of native hemoglobin is 2 per tetramer.

The other thiol present in erythrocytes at reasonable concentration is glutathione (GSH), whose $\text{CH}_3\text{Hg(II)}$ binding properties were characterized in detail in Part 1 (Chapter III) of this thesis, and elsewhere (64,69). GSH is present in the erythrocyte intracellular medium at about 2 mM (160,161).

GSH has an important role within the context of the *mobility* of $\text{CH}_3\text{Hg(II)}$ in the body. It was demonstrated in Part 1 of this thesis (Chapter V) and elsewhere (64) that exchange of $\text{CH}_3\text{Hg(II)}$ between sulfhydryls at physiological pH proceeds at a significant rate only by the associative displacement mechanism. Since steric factors make the close approach of two massive protein thiols unlikely, it seems probable that some small thiol entity is involved as a "shuttle" for $\text{CH}_3\text{Hg(II)}$ between hemoglobin (and other) macromolecules. Rabenstein and Evans have proposed that GSH is that entity (162). The rate of uptake of $\text{CH}_3\text{Hg(II)}$ by different organs in the rat has been found to be influenced by cellular GSH levels (163).

$\text{CH}_3\text{Hg(II)}$ complexes of glutathione (and glutathione-

related substances such as cysteinylglycine) have been detected in biliary excreted $\text{CH}_3\text{Hg(II)}$ (164-166). The GSH complex has also been identified in other organs (167, 168). However, due to the extensive workups and slow separations involved in these studies, and the lability of the complexes involved, there is a real possibility of such results being artifactual. The advantages of direct observation of intact systems by NMR will be discussed in Section C below.

B. Methylmercury(II) Antidotes

Poisoning by $\text{CH}_3\text{Hg(II)}$, and its treatment, have been the subject of a large number of clinical and pharmacological studies. The symptoms of poisoning, shown in Table 28, are characteristic of damage to the central nervous system (152).

In order to discuss approaches to increasing elimination of $\text{CH}_3\text{Hg(II)}$, some appreciation of its distribution around the body is necessary. A simplified schematic was presented in Section A (Fig. 42). This suggests some approaches to more efficient removal of $\text{CH}_3\text{Hg(II)}$ from the body:

- (1) Increase biliary excretion rate.
- (2) Increase fecal excretion rate, so that the competing

Table 28. Symptoms of $\text{CH}_3\text{Hg(II)}$ poisoning^a.

Symptom	Body burden (mg) ^b
Paresthesia	25
Ataxia	55
Dysarthria	90
Deafness	180
Death	200

a) Reference (152).

b) For a typical body weight of 51 kg.

enterohepatic recirculation will be less effective.

(3) Increase the rate of urinary excretion.

Magos, Clarkson and Allen found no correlation of biliary excretion rate of $\text{CH}_3\text{Hg(II)}$ with the efficiency of various antidote molecules (169). They stated that since free GSH levels in the bile are some three orders of magnitude higher than CH_3HgSG , any significant increase in biliary excretion would be unlikely. Thus, presumably successful antidotes operate on factors 2 and 3 above.

A series of papers by Aaseth and coworkers (133, 134, 170, 171) exemplify the approach taken in pharmacological studies, and are convenient for discussion since, unlike much of the literature, they were performed under the same conditions throughout. Aaseth et al. identified the mobilisation of brain $\text{CH}_3\text{Hg(II)}$ as the most critical factor in therapy, since the brain is where irreparable damage occurs (152). The molecules studied are given in Table 29.

The 1975 study (170) compared DL-homocysteine (HCSH), N-acetylhomocysteine (NAHCSH) and D-penicillamine (PSH). NAHCSH was less toxic than HCSH and gave increased $\text{CH}_3\text{Hg(II)}$ elimination, including some brain $\text{CH}_3\text{Hg(II)}$ mobilisation. PSH was similar in overall efficacy but gave less brain mobilisation, suggesting that the N-acetyl group was important for membrane permeability. Predictably,

Table 29. Complexing agents tested for $\text{CH}_3\text{Hg}(\text{II})$ poisoning.

$\begin{array}{c} \text{H}_2\text{NCH}_2\text{CO}_2\text{H} \\ \\ \text{CH}_2 \\ \\ \text{CH}_2 \\ \\ \text{SH} \end{array}$	$\begin{array}{c} \text{H} \\ \\ \text{CH}_3\text{CNCHCO}_2\text{H} \\ \quad \\ \text{O} \quad \text{CH}_2 \\ \quad \\ \text{CH}_2 \\ \\ \text{SH} \end{array}$	$\begin{array}{c} \text{H}_2\text{NCHCO}_2\text{H} \\ \\ \text{CH}_3-\text{C}-\text{CH}_3 \\ \\ \text{SH} \end{array}$	
Homocysteine	N-acetylhomocysteine	Penicillamine	
$\begin{array}{c} \text{H} \\ \\ \text{CH}_3\text{CN}-\text{CHCO}_2\text{H} \\ \quad \\ \text{O} \quad \text{CH}_2 \\ \quad \\ \text{CH}_3-\text{C}-\text{CH}_3 \\ \\ \text{SH} \end{array}$	$\begin{array}{c} \text{H}_2\text{NCHCO}_2\text{H} \\ \\ \text{CH}_2 \\ \\ \text{SH} \end{array}$	$\begin{array}{c} \text{H} \\ \\ \text{CH}_3\text{CN}-\text{CHCO}_2\text{H} \\ \quad \\ \text{O} \quad \text{CH}_2 \\ \quad \\ \text{CH}_2 \\ \\ \text{SH} \end{array}$	
N-acetylpenicillamine	Cysteine	N-acetylcysteine	
$\begin{array}{c} \text{H} \quad \text{O} \\ \quad \\ \text{HO}_2\text{CCHCH}_2\text{CH}_2\text{CN}-\text{CHCNCH}_2\text{CO}_2\text{H} \\ \quad \quad \\ \text{NH}_2 \quad \text{O} \quad \text{CH}_2 \\ \quad \\ \text{SH} \quad \text{SH} \end{array}$		$\begin{array}{c} \text{CH}_2\text{CH}-\text{CH}_2 \\ \quad \quad \\ \text{SH} \quad \text{SH} \quad \text{OH} \end{array}$	
Glutathione	2,3 dimercaptopropanol (B.A.L.)		
$\begin{array}{c} \text{CH}_2\text{CHCH}_2-\text{SO}_3^-\text{Na}^+ \\ \quad \\ \text{SH} \quad \text{SH} \end{array}$	$\begin{array}{c} \text{HO}_2\text{CCHCHCO}_2\text{H} \\ \quad \\ \text{SH} \quad \text{SH} \end{array}$		
2,3 dimercaptopropane-1-sulfonate	2,3 dimercaptosuccinic acid		

N-acetylpenicillamine (NAPSH) was found to be still more effective at both overall elimination enhancement and brain $\text{CH}_3\text{Hg(II)}$ mobilisation (133). L-cysteine, N-acetylcysteine and glutathione were ineffective, probably because of rapid body metabolism.

Interestingly, the best sulfhydryl antidote yet reported for brain $\text{CH}_3\text{Hg(II)}$ (134) appears to be 2,3-dimercaptosuccinic acid (DMSA). The reasons are not clear; the above studies suggest that membrane penetrability is an important factor, yet the doubly charged DMSA species would not be expected to have sufficient hydrophobic character. Possibly some specific transport mechanism is operative.

Two approaches other than conventional oral or intravenous drug administration have been suggested for $\text{CH}_3\text{Hg(II)}$ poisoning therapy. Kostyniak et al. have described the use of extracorporeal hemodialysis (172,173). Blood is removed from the body, mixed with a low molecular weight thiol, dialyzed to remove the $\text{CH}_3\text{Hg(II)}$ complex and returned to the body. Total $\text{CH}_3\text{Hg(II)}$ elimination is speeded up dramatically. The use with moderate success of a polythiolated resin has also been described (174). Both methods have the advantage that toxicity of absorbed drug is less of a problem; however, they rely on unassisted

redistribution of brain $\text{CH}_3\text{Hg(II)}$ to the methylmercury(II)-depleted blood as the only means of brain mobilisation.

This is a slow process (175). Norseth suggested that such procedures be used in conjunction with a good brain $\text{CH}_3\text{Hg(II)}$ mobilising agent, such as N-acetylpenicillamine (176). This has been attempted, with mixed success (177,178).

C. Observation of Small-Molecule NMR Signals in Biological Systems

Part 1 of this thesis demonstrated that NMR spectroscopy provided a convenient, highly precise method of following $\text{CH}_3\text{Hg(II)}$ -sulfhydryl group interactions in solution. In attempting to apply NMR in a similar manner in biological systems, two potential problems arise:

- (1) Lack of sensitivity.
- (2) Lack of spectral resolution due to overlapping resonances.

Means of overcoming these are discussed below. The subject has been recently reviewed (179,180).

1. Pulsed Fourier Transform NMR: the single-pulse experiment.

On the A60D spectrometer used in Part 1, 10 mM

represented the lower practical concentration limit for detection of a single proton resonance with adequate signal-to-noise ratio (SNR). Biological concentrations are usually much lower than this: for instance, GSH is present at 2-3 mM in erythrocytes (160). SNR can be enhanced by a factor of \sqrt{N} by summation of N spectra, since the noise is random in nature; however, collection of many conventional spectra is time-consuming (181).

The pulsed Fourier transform NMR method overcomes this problem (182). It is convenient to discuss the experiment using a rotating-frame magnetisation diagram, as in Figure 45 (179). The fixed spectrometer field H_0 is applied along the z axis. The x' and y' axes rotate (in the lab frame) around z at the spectrometer carrier frequency. At equilibrium the small excess of nuclear spins in the lower of the two energy states induced by the interaction with H_0 leads to a net macroscopic magnetisation M_0 , colinear with H_0 . Application of a pulse of radio-frequency power rotates the magnetisation through an angle α about the x' axis:

$$\alpha = \gamma H_1 t_w \quad (147)$$

where γ is the nuclear gyromagnetic ratio, H_1 the pulse intensity and t_w the pulse length (time). (Pulses are

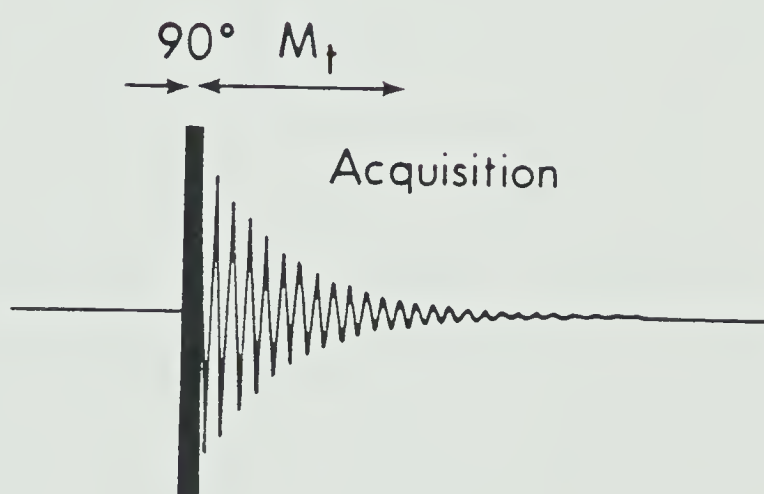
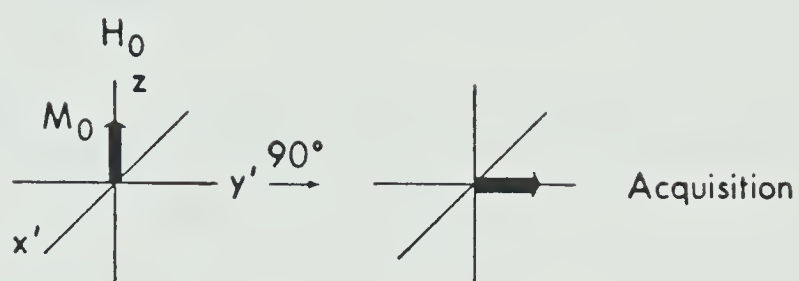


Figure 45. Rotating-frame magnetisation diagram and resultant receiver signal for the single-pulse FT NMR experiment. Reproduced with permission from Reference 179.

normally referred to in terms of α .) Here a 90° pulse is used, which puts the magnetisation along y' . Relaxation then occurs. In the $x'y'$ plane, magnetisation decays:

$$M_t^{x'y'} = M_0 e^{-t/T_2} \quad (148)$$

where t is the elapsed time and T_2 the spin-spin relaxation time, whereas along the z axis, it grows:

$$M_t^z = M_0 (1 - e^{-t/T_1}) \quad (149)$$

where T_1 is the spin-lattice relaxation time. The magnetisation detected by the spectrometer is that along the y' axis. The decay is modulated at the frequency difference between the carrier frequency and that of the nuclear precession. The free induction decay (FID) thus produced is additive for more than one type of nucleus. Each experiment lasts only a few seconds, including a delay to allow equilibrium to reestablish, so a large number of such FID's can be collected in a reasonable time, digitised and summed. Fourier transformation of the noise-reduced FID then yields a conventional frequency-domain spectrum. Such a technique vastly reduces detectable concentrations; with extended accumulation, proton concentrations as low as $\sim 5 \times 10^{-5} M$ have yielded acceptable spectra (183).

2. The spin-echo Fourier transform (SEFT) experiment.

Single-pulse FT NMR solves the SNR problem, but not that of spectral overlap. Figure 46a shows the spectrum at 400 MHz of human erythrocytes (179). The many overlapping hemoglobin resonances obscure those of small molecules such as GSH. However, as detailed below, discrimination between these two classes of resonances, to yield spectra of the type shown in Figure 46b is possible using the spin-echo Fourier transform (SEFT) experiment.

The SEFT pulse sequence is shown in Figure 47; the receiver signal is also shown. An initial 90° pulse is applied as before, then a delay period τ_2 . During the delay, the magnitude of the magnetisation for each type of nucleus decays according to its T_2^* (a resultant of the true T_2 and a term due to H_0 inhomogeneity--the latter term dominating). A 180° pulse is then applied. Detailed analysis (180) then shows that the dephasing due to H_0 inhomogeneity stops; in fact, the individual nuclear magnetisations now *rephase* at the same rate as they dephased during the first delay interval. The net signal grows again, and after a further delay τ_2 it is again at a maximum. At this point, the effects of H_0 inhomogeneity are cancelled completely. (The SEFT experiment was devised originally to remove such effects and permit accurate T_2

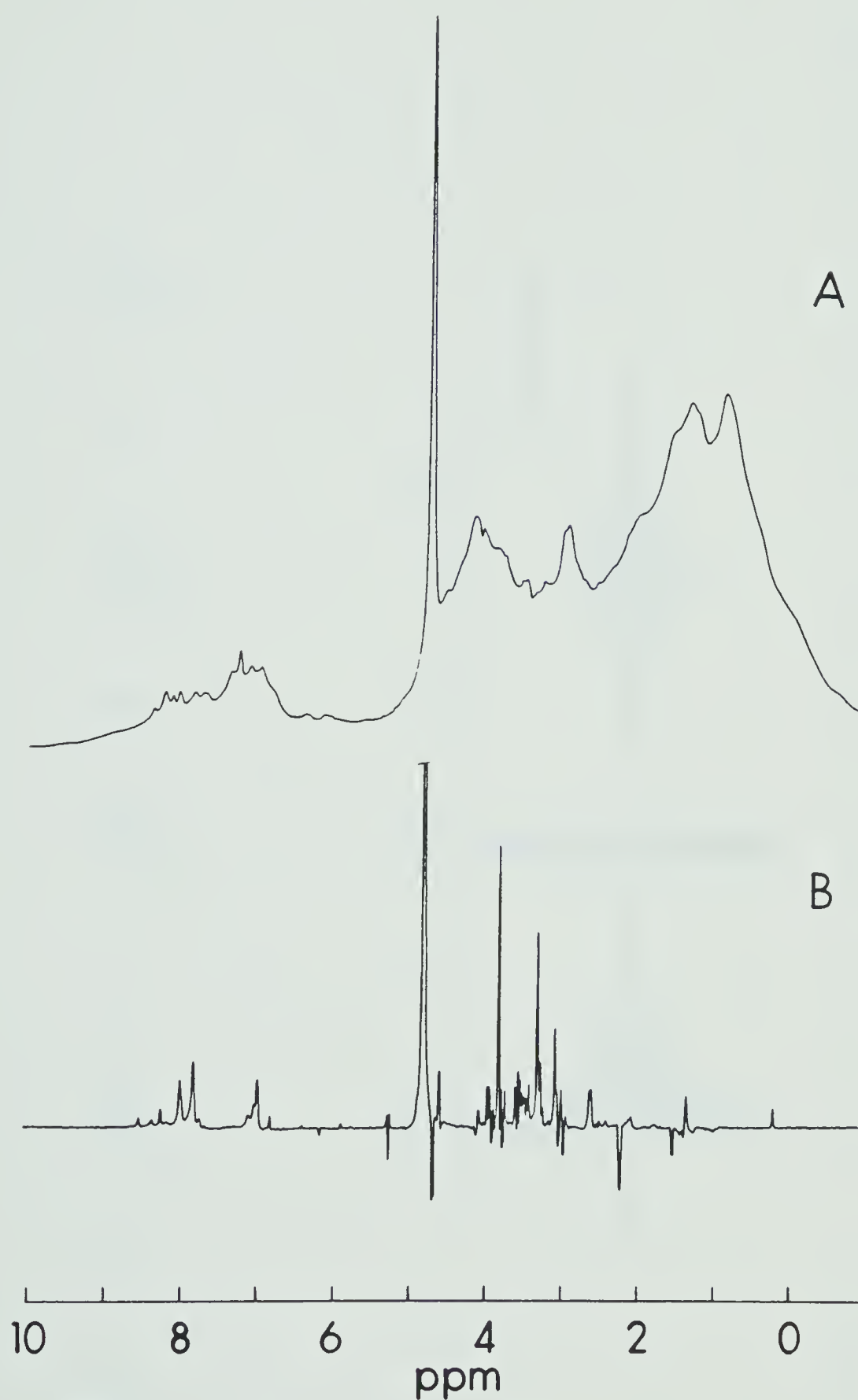


Figure 46. 400 MHz ^1H NMR spectra of erythrocytes A) Single-pulse, B) SEFT. Reproduced with permission from reference 179.

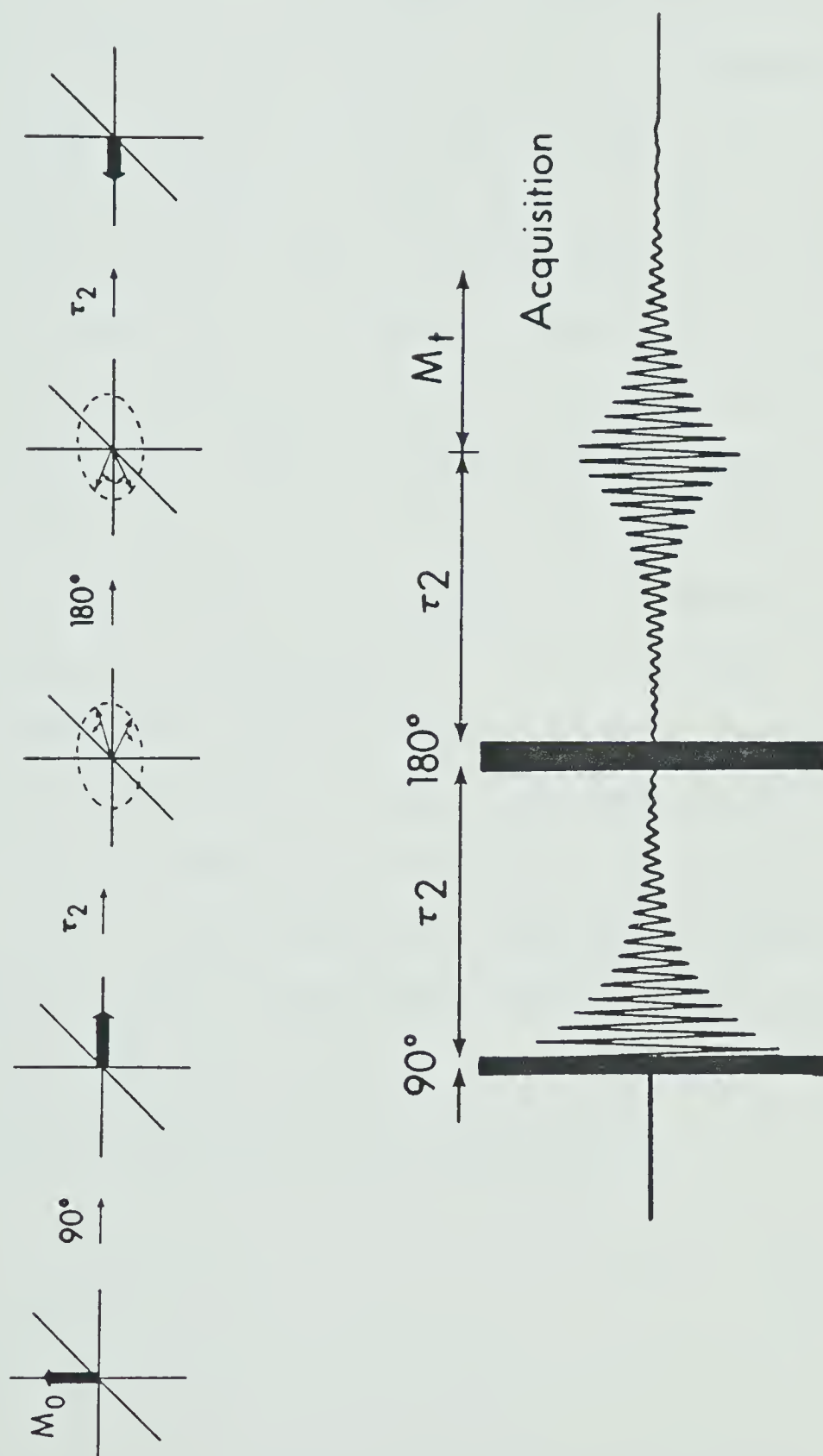


Figure 47. Rotating-frame magnetisation diagram and resultant receiver signal for the spin-echo FT NMR experiment. Reproduced with permission from reference 179.

measurements (184).)

A conventional FID is now collected. Since a time period $2\tau_2$ has passed, all signals are now smaller by a factor of $e^{-2\tau_2/T_2}$. For protein molecules, due to slow molecular tumbling T_2 is small, and the resonances virtually disappear after a few milliseconds. By contrast, T_2 for small molecules is much larger; thus at similar delays their signals remain substantially unchanged.

This technique is therefore capable of a high degree of discrimination against protein resonances and in favour of those of small, mobile molecules (179), enabling the *direct observation* of both chemical and biochemical processes in intact cellular systems. For instance, some of the processes of respiration in the erythrocyte, such as lactate production and the effects of cell starvation on glutathione metabolism have been observed *in situ* (185), as have the synthesis of glutathione (186) and the binding of metal ions to the various intracellular ligands (187). In contrast to more traditional methods, such as those involving radioactive tracers, no lengthy sample manipulations or separations are necessary.

3. The transfer of saturation by cross relaxation (TSCR) experiment.

The SEFT NMR experiment described in Section 2 above has certain disadvantages (188). In the present context, the most serious one is that slow chemical exchange kinetics associated with the small molecules being observed can contribute to the effective value of T_2 , lowering it, and thus lowering the degree of discrimination achievable. It was noted in Part 1 (Chapters III, V) that resonances were often exchange-broadened at 60 MHz; at 400 MHz the kinetics are still slower relative to the NMR time-scale. As shown in Chapter VIII, at the standard τ_2 value of 0.060 s used in the SEFT experiments, small molecule resonances often disappeared.

A different technique for selective hemoglobin "envelope" suppression in erythrocyte spectra was recently described (189). Spectra are shown in Figure 48. Spectrum A is the conventional (single-pulse) ^1H NMR spectrum. B shows the effect of a high-power presaturation pulse applied at the frequency of the HDO peak, prior to the 90° pulse. As expected, the HDO peak is nulled; however so (at least partially) are those of all resonances nearby, hemoglobin and small-molecule alike. This is therefore of limited utility.

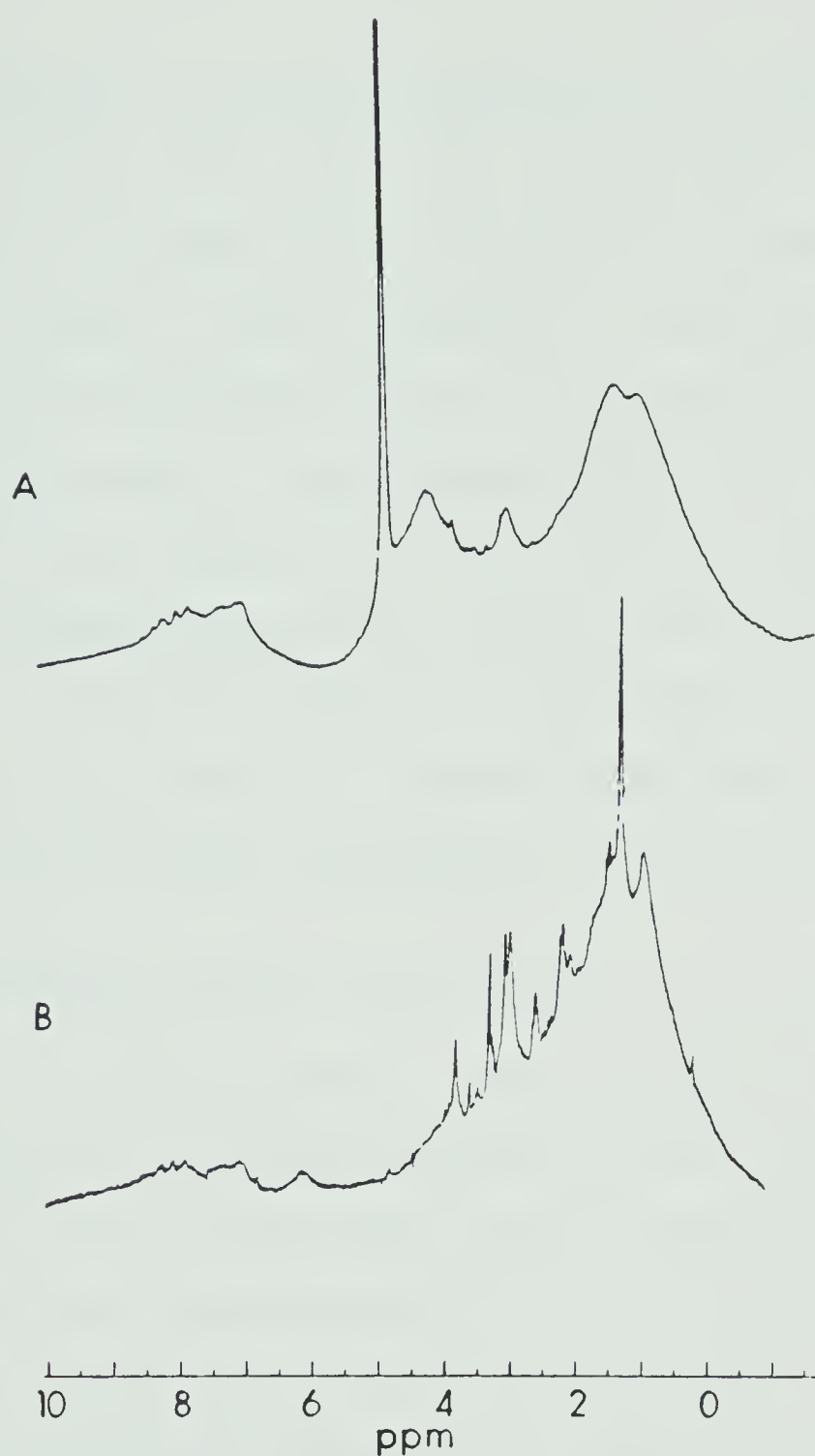


Figure 48. Spectra of hemolyzed erythrocytes. A) Single-pulse, B) with presaturation on HDO resonance. Reproduced with permission from reference 189.

However, if the presaturating R.F. pulse is applied instead in the region of 8.0 ppm, not only is that region suppressed as before, but the entire hemoglobin envelope is observed to be reduced. This is ascribed to transfer of saturation, due to spin diffusion by cross relaxation (190). There is a mutual exchange of spin magnetisation; thus the presaturation effect is transferred to other protein resonances, even if their resonant frequencies lie well away from the irradiated region. By way of contrast, resonances from small molecules such as glutathione are almost unaffected; slight effects due to protein-GSH interactions (191) are observed.

D. Approach to the Present Study

It was demonstrated in Part 1 that an NMR-based competition method for $\text{CH}_3\text{Hg(II)}$ -thiol complex formation constant measurement could provide precise data, enabling the detailed characterization of binding behaviour. However, these studies were made possible firstly, by the previous identification of the molecules (or sites) responsible for binding and secondly, by the simple and well-resolved nature of the NMR spectra.

The discussion of Sections A and B above has shown the desirability of extending such studies to $\text{CH}_3\text{Hg(II)}$

binding in protein and even intact cellular systems. However, in this case the binding sites are not well characterized, and conventional NMR spectra are poorly resolved. As discussed in Section C above, earlier studies have shown that high-field pulsed Fourier transform NMR spectrometers, used in conjunction with techniques such as the SEFT and TSCR experiments, may have considerable potential for overcoming these difficulties.

In Part 2 of this thesis, the application of these spectroscopic methods to $\text{CH}_3\text{Hg(II)}$ binding studies will be presented. In performing this work two objectives were borne in mind:

- (1) To provide a link between the chemical studies of Part 1 and the biological and pharmacological studies described in Sections A and B above, in order to better understand how binding constants (and other factors) contribute to $\text{CH}_3\text{Hg(II)}$ distribution and antidote action.
- (2) To demonstrate the usefulness of FT NMR spectroscopy as a subtle, non-invasive technique for the observation of metal binding in complex biological samples, yielding *simultaneously* qualitative (binding site) and quantitative (formation constant) data about the intact, unperturbed sample.

Chapter VIII reports the results of an NMR investigation of the complexes of $\text{CH}_3\text{Hg(II)}$ in human erythrocytes, including a competition study involving glutathione and hemoglobin from which K_{fc} for the hemoglobin complex at physiological pH was estimated. As far as could be ascertained, this is the first time that both unequivocal evidence for the sites of binding in a macromolecule-containing system, and quantitative binding information were obtained by this technique, without any separations or subsequent analysis outside the NMR tube being necessary.

Chapter IX describes experiments examining the effects of different antidote molecules on the distribution of $\text{CH}_3\text{Hg(II)}$ added to erythrocytes. The results are compared with the pharmacological studies described above (Sections A and B), and correlated with predicted results on the basis of the formation constant data measured in Chapters III, IV and VIII, illustrating again the power of FT NMR techniques to yield directly detailed information at the molecular level for complex biological systems.

CHAPTER VII

EXPERIMENTAL

Much of the apparatus, chemicals and techniques employed in Part 2 are exactly as in Part 1 (Chapter II), this will be assumed unless stated otherwise. The areas covered below are those which differ in some way from those in Part 1, or do not appear there.

A. Preparation of Erythrocytes for NMR Studies

Whole venous blood was collected in Vacutainers (Becton, Dickinson and Co.) containing EDTA solution to prevent clotting. Typically 2-10 Vacutainers (10-50 mls) of blood was used in the procedures detailed below; blood from several donors was normally pooled.

As explained below (Section C.2) in order to simplify the collecting of FT NMR spectra it was necessary to exchange the water (H_2O) in the cells for D_2O . This was accomplished as follows. The whole blood was centrifuged at 12,000 g for approximately ten minutes (Sorvall RC-5B Refrigerated Superspeed Centrifuge). The plasma and the thin layer of white cells was drawn off using a Pasteur pipet. The packed erythrocytes remaining were about half the original volume. These were resuspended in an equal

volume of isotonic (0.15 M) D₂O saline solution. (This solution has the same osmolarity as the interior of the erythrocytes, so there is no danger of swelling and rupturing due to internal osmotic pressure.) The suspension was recentrifuged and the supernatant removed as before. This washing procedure was repeated twice more, yielding packed erythrocytes with substantially all the intracellular H₂O replaced by D₂O.

For studies involving intact cells, glucose (5 mM) was added to the D₂O saline solution, to maintain the cells in a healthy metabolic state and more closely mimic the in vivo situation. (Starved erythrocytes display distinct metabolic properties (185).) For the same reason, packed cells were used within twenty four hours of preparation.

Packed erythrocytes alone are rather viscous; in order to facilitate transfer to the NMR tube, they were usually diluted with about one-fifth the volume of isotonic D₂O-saline.

Where desired, the cells were hemolyzed, by one of two methods. In some of the earlier studies, repeated freezing using a solid carbon dioxide-acetone bath, followed by thawing, was employed to rupture the cells. For the later studies, sonication was employed (Heat Systems-

Ultrasonics Model W-225R Sonicator). Ultrasonic vibration disrupts the cellular membrane; complete hemolysis was effected in about thirty seconds. The resulting clear, wine-coloured hemolysate was generally used as soon as possible, although it did not appear to deteriorate when stored frozen solid for some days.

B. Preparation and Assay of Hemoglobin Solutions

Literature methods (192,193) for the preparation of a solution of pure hemoglobin from hemolyzed erythrocytes usually involve a fairly lengthy procedure. Typically, cell debris is removed by high-speed centrifugation, and hemoglobin precipitated selectively from solution using carefully controlled concentrations of ammonium sulphate. This is then redissolved and dialyzed to remove the ammonium sulphate.

Initial attempts at such a preparation yielded acceptable amounts of hemoglobin; however, the quality of the product was not acceptable. It was found (by the assay described below) to contain 20-30% methemoglobin (MetHb), hemoglobin with the central porphyrin iron, normally in the Fe(II) oxidation state, irreversibly oxidised to Fe(III). This makes the sample unsuitable for two reasons. Firstly, since the normal level of MetHb

in vivo is 1-3% of the total (194), any studies performed on this product would have dubious relevance to the in vivo situation. Secondly, it is well known that paramagnetic ions (such as Fe(III)) cause more efficient relaxation of NMR signals (195), leading to linebroadening of resonances due to nearby nuclei. For instance, the hemoglobin histidine imidazole ring resonances, which appear at about 8 ppm, were very much less well resolved in such preparations than in hemolyzed erythrocyte preparations (196). Since it was desired to retain the capability of observing the hemoglobin resonances in these studies, such an effect is again undesirable. The poor quality of the product was due probably to the large number of manipulations involved, the extended time period (3-4 days) and (principally) to inexperience in handling such preparations.

To circumvent this problem, a simplified protocol was developed for preparation of hemoglobin solutions, based on the fact that a pure hemoglobin sample is not required. A temperature of 4°C was maintained throughout.

As has been noted throughout this thesis, a great deal of evidence shows that the degree of binding of $\text{CH}_3\text{Hg(II)}$ to other ligands is negligible when sulfhydryl groups are present. Thus, in studying the binding of

$\text{CH}_3\text{Hg(II)}$ to hemoglobin, the only potentially interfering substances will be other thiol molecules. In the intracellular environment (see Chapter VI, Section A) the only other thiol present at comparable concentration to Hb is glutathione, which is a small molecule and can be readily removed.

The procedure used involved, first, centrifugation of 10 ml hemolyzed erythrocytes at 20,000 g for 1 hour to remove cell debris. The resulting solution was placed in a dialysis bag (Spectrapor dialysis tubing, M. Wt. cutoff 6,000-8,000) with 0.2 g of CPG-lipoamide beads (see Section C.1 below), and dialyzed against 2×200 mls of D_2O phosphate buffer, $\text{pH}^* 7.0$, for twelve-hour periods (for the definition of pH^* , see Section C.2 below). Such a solution gave no indication of a significant ($>.2$ mM) concentration of any small molecule, as judged by the null SEFT NMR spectrum obtained under conditions where the hemoglobin resonances are suppressed.

The percentage metHb in the preparation was determined using a standard spectrophotometric assay (197). Sodium cyanide is added to convert the metHb to cyanometHb, which is then determined by its characteristic absorbance at 630 nm. Ferricyanide is then added to oxidise normal hemoglobin to the metHb form, and the determination

repeated. As determined by this technique, the above sample was about 2% metHb. The author is grateful to Mrs. C. Byers and to Ms. A. Sharma for assistance with the running of this assay.

The method developed for standardisation of the sulfhydryl content of the hemoglobin solution will be presented in Chapter VIII.

C. Miscellaneous Experimental Details

1. Lipoamide beads.

As discussed in Section B above, oxidation of the Fe(II) in hemoglobin is a major potential problem in its isolation. In the present studies it was also desirable that the β chain sulfhydryl groups be as nearly quantitatively reduced as possible. Both these conditions suggest the use of an antioxidant to maintain a reducing environment. In the past, dithioerythritol (DTE) has been used for this purpose. As shown in Figure 49a, it readily forms an intramolecular disulfide; thus any potential complications due to the formation of mixed disulfides with sulfhydryls of interest are minimised. However, the major problem in using DTE lies in its removal. Dialysis (or ultrafiltration) is necessary, and both during and after this lengthy procedure the solution is unprotected.

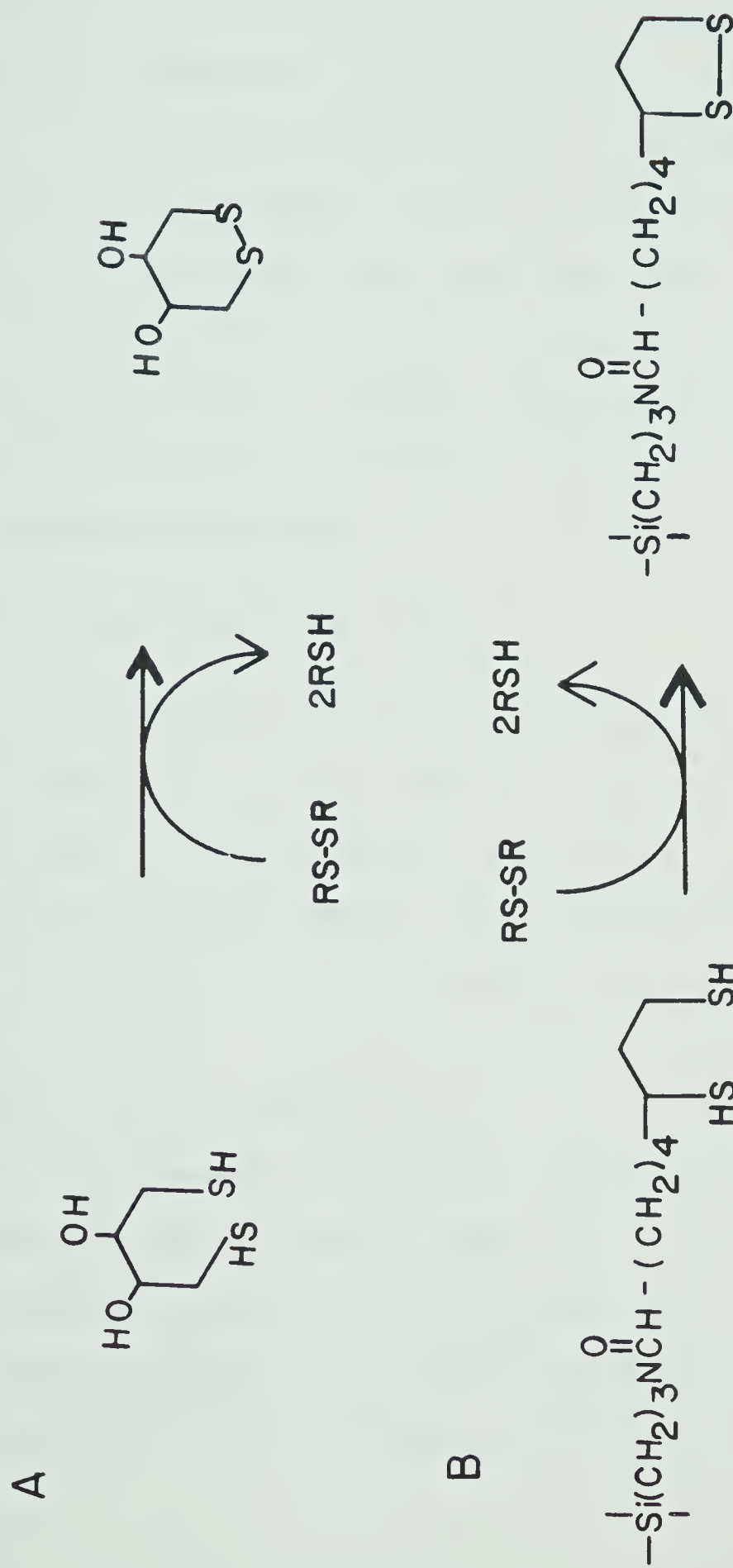


Figure 49. The use of a) dithioerythritol and b) CPG-lipoamide beads as antioxidants.

An ingenious alternative is the use of Controlled Pore Glass (CPG) supported lipoamide beads manufactured by Corning and marketed by the Pierce Chemical Co., Rockford, U.S.A. These consist of porous 150 μm diameter glass beads, with pore diameter $\sim 500 \text{ \AA}$, to which are covalently attached lipoamide moieties, see Figure 49b. These groups can function as an antioxidant, forming an intramolecular disulfide as for DTE. However, when desired, the beads can be easily removed by simple vacuum filtration, or even (with care) by decanting.

2. The use of deuterium oxide.

The power of FT NMR lies in the ability to extract an entire spectrum from the transient response (FID) to a single pulse of radiofrequency power (182). However, in the case of aqueous samples, this can also be a problem, since the inclusion of the resonance due to H_2O protons is almost inevitable. These are present at 1.10 M , whereas a typical analyte resonance is at $5 \times 10^{-3} M$; this dynamic range exceeds that of the spectrometer (with a 12-bit digitizer, a dynamic range of 4K is available). Thus the peak of interest is unlikely even to be seen.

Various options are available selectively to reduce the size of the H_2O resonance. Provided this lies well

away from analyte resonances, high-order roll-off frequency filtering can be used. This is not practicable here, since several peaks of interest lie within 1 ppm of the H_2O resonance. Various spectroscopic methods are available for water suppression (198). While these work, more or less satisfactorily depending upon other sample constituents, they do necessitate a compromising of the spectral conditions between the optimum for analytical data collection, and that for H_2O suppression.

The simplest method for removal of the H_2O resonance, where it is applicable, is substitution of deuterium oxide (D_2O) for H_2O . The deuteron having quite distinct nuclear properties, its NMR signals do not appear in the proton frequency range.

D_2O is of course technically a "non-aqueous" solvent, and strict correlation of solution properties (e.g. pH or pD) with those of H_2O solutions is only partially possible. The relationship

$$\text{pD} = \text{pH}^* + 0.4 \quad (150)$$

has been recognised for some time (199). Here pD is the value obtained on an operational scale for D_2O solutions exactly analogous to that for pH in aqueous solution, and pH^* is the value obtained using a glass electrode and aqueous

reference electrode, standardised using normal (H_2O) pH standard solutions (200). The exact value of the adjustment parameter in equation (150) was measured by Bates at 0.40 for a variety of solutions (200). In none of the studies described in Part 2 is pH (or pD) a critical parameter; generally, solutions were buffered near neutrality for the course of an experiment. pD measurements were made with the setup detailed in Chapter II, except when measurement in an NMR tube was necessary. In this case a glass capillary combination electrode having an outside diameter of ~ 2 mm was employed.

Deuterium oxide is expensive ($\sim \$400$ per litre for 99.7% D_2O). In view of this, some care was taken to recycle whenever possible. For instance, the D_2O used in the dialysis described in Section B above, which was still $\sim 98\%$ D_2O but contained an estimated 0.1 mM glutathione, was used to make D_2O saline for washing erythrocytes. All washings and other D_2O waste were collected and distilled from alkaline permanganate by Mr. D. Brown, to whom the author is indebted. The distillate was found to be $\sim 80\%$ D_2O , which is adequate for the initial wash given to erythrocytes.

D. NMR Measurements

1. Instrumentation and acquisition parameters.

Proton NMR spectra were measured at 400 MHz on a Bruker WH-400/DS spectrometer operating in the pulsed Fourier Transform mode. Samples were 0.4-0.5 ml of cells, hemolysate or solution in 5 mm O.D. NMR tubes, and were maintained at 25°C. The free induction decay was normally collected in 8K of data points; when greater frequency resolution was required, this was occasionally expanded to 16K or 32K. Quadrature detection was employed. The spectral width was from 500 Hz to 1640 Hz, again depending on the digital frequency resolution desired. Sufficient transients (between 16 and 400) were collected to give an acceptable signal-to-noise ratio.

Chemical shifts, δ , are reported relative to the methyl resonance of sodium 2,2-dimethyl-2-silapentane-5-sulfonate (DSS), and are based upon the glycine methylene proton chemical shift (erythrocyte studies, $\delta = 3.540$ ppm) or upon that of the methyl resonance of tetramethylammonium ion (hemoglobin studies, $\delta = 3.175$ ppm).

2. NMR pulse techniques.

The theory and literature behind these, together with

detailed pulse sequences and sample spectra, were given in Chapter VI.

In some studies, where only small molecules were present, a simple single-pulse experiment was performed. More often, samples contained macromolecular components. It was then necessary to suppress the resonance envelope from these to render visible the signals from small molecules. Two techniques were used for this.

For some spectra, the spin-echo Fourier Transform (SEFT) pulse sequence was used, with a relaxation delay of either .060 s or .015 s. A .060 s delay provides almost complete hemoglobin envelope suppression; a .015 s delay retains some of the Hb resonances, notably those of the histidine residues.

In some cases, phase modulation of multiplet resonances, induced by the SEFT pulse sequence (179), made precise chemical shift measurement difficult. In these cases the method of transfer of saturation by cross relaxation (TSCR), following a selective presaturation pulse, was employed instead. A high power decoupling signal was applied at 8.1 ppm for 1-2 seconds, then the 90° pulse applied and the FID collected as usual.

CHAPTER VIII

THE BINDING OF METHYLMERCURY(II) TO HUMAN ERYTHROCYTES
AND TO HEMOGLOBIN

In Chapters III and IV of this thesis, the $\text{CH}_3\text{Hg(II)}$ binding behaviour of several small thiols was characterized by using NMR spectroscopy to monitor the degree of competition with mercaptoacetic acid for the $\text{CH}_3\text{Hg(II)}$ added. The recent development of sophisticated multi-pulse NMR techniques which enable the observation of small-molecule resonances in the presence of large molecules (detailed in Chapter VI, Section C) led to the intriguing possibility of making similar measurements in hemoglobin-containing solutions, or even in erythrocytes. In addition, the multiple potentiality for identifying which molecules (and even which sites) were binding and for obtaining estimates of rates of cell penetration and of chemical exchange processes, all from a single technique, made this approach of considerable interest.

Section A below explores in detail the effects of $\text{CH}_3\text{Hg(II)}$ addition on the NMR spectrum of glutathione, both in the absence and in the presence of hemolyzed erythrocytes. Some preliminary conclusions are also offered regarding the relative $\text{CH}_3\text{Hg(II)}$ binding strengths

of GSH and hemoglobin sulfhydryls, and also about the rate phenomena mentioned above. This work was performed in collaboration with Dr. A.A. Isab.

Section B describes the development of an "NMRimetric" titration for hemoglobin sulfhydryl content. While examples of endpoint detection by NMR exist in the literature (201), it appears that this is the first time that a *macromolecule* has been titrated thus, serving to illustrate the analytical precision of which NMR is capable in such systems. Lastly, this titration is employed for standardization of hemoglobin as a thiol solution, and a competition study with glutathione performed to determine K_{fc} for the $\text{CH}_3\text{Hg(II)}$ -hemoglobin complex. Significantly, the result is in line with some previous indications in the literature but not others; thus the reservations previously entertained about applying separations-based technique to such labile systems seems justified.

A. NMR Study of the $\text{CH}_3\text{Hg(II)}:\text{GSH}$ System in Aqueous and Erythrocyte Solutions

A sample of intact human erythrocytes was prepared as detailed in Chapter VII (Section A), and the ^1H SEFT NMR spectrum obtained at 400 MHz ($\tau_2 = 0.060$ s). This is shown in Figure 50. Many of the peaks visible have

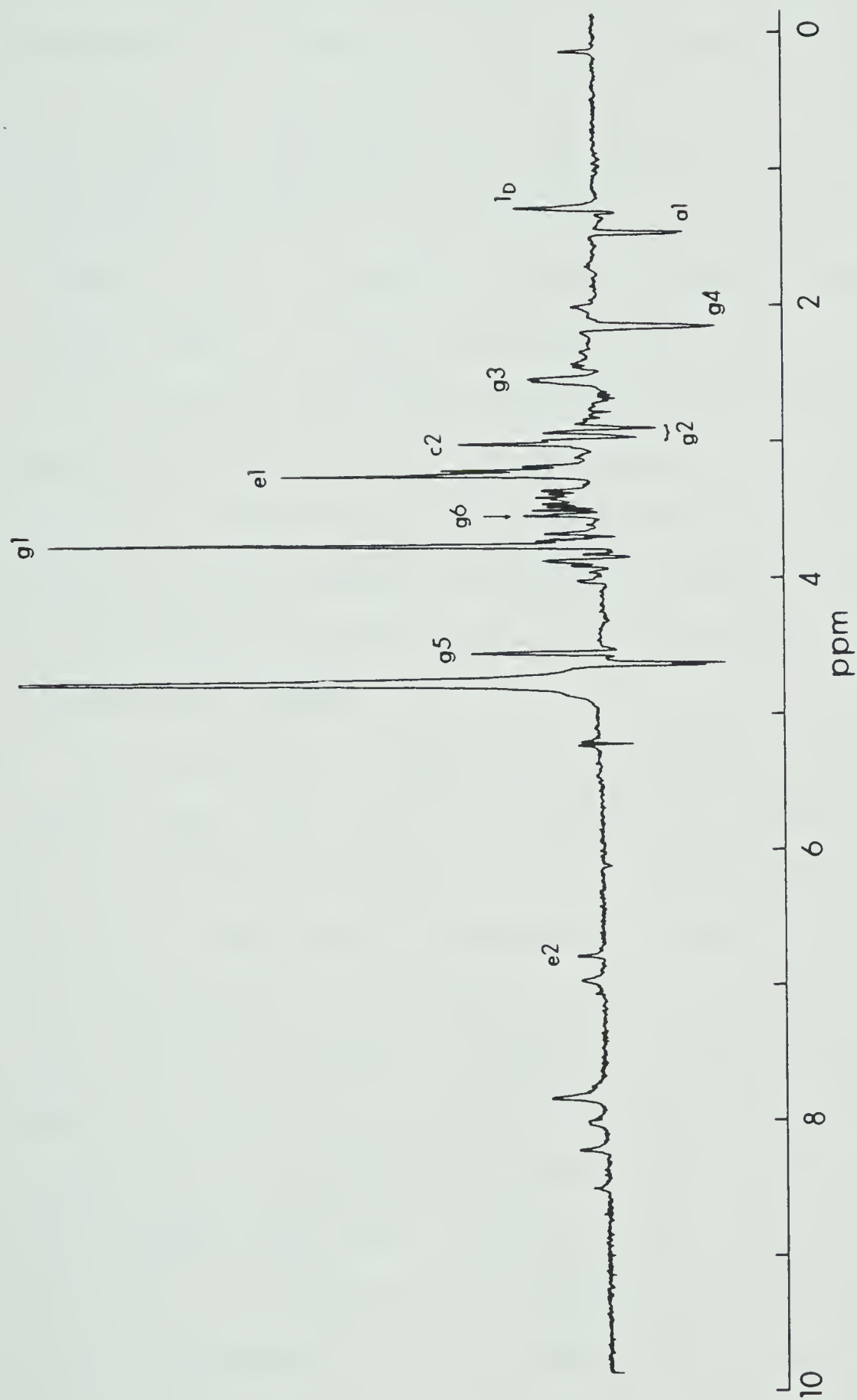


Figure 50. SEFT NMR spectrum of intact human erythrocytes at 400 MHz

($\tau_2 = 0.060$ s).

been assigned in previous work (185, 186). The intense resonance at 4.77 ppm is due to the residual HDO present in the cells, and those in the region 6.85-8.3 ppm to carbon-bonded protons on the imidazole groups of several hemoglobin histidine residues (185). The remaining resonances are due to small molecules present in the intracellular region of the erythrocyte (185,186). Resonances from molecules containing functional groups known to form complexes with $\text{CH}_3\text{Hg(II)}$ are identified and assigned in Table 30. It should be noted in particular that in Figure 50 well-resolved, reasonably intense resonances are observable for five out of six different GSH carbon-bonded proton types.

The majority of these resonances lie in the range 1.5-4.5 ppm; this region is expanded in Figure 51 (Spectrum A). Sufficient $\text{CH}_3\text{Hg(II)}$ to give a final concentration of 0.5 mM was then added (Spectrum B). Spectral acquisition was started about 1.5 minutes after this addition, and took about 2.5 minutes to complete. The pronounced change in the spectral pattern for the $\beta\text{-CH}_2$ methylene protons of the cysteinyl residue of glutathione (resonance g2) suggests that some interaction with $\text{CH}_3\text{Hg(II)}$ is occurring. Increasing the $\text{CH}_3\text{Hg(II)}$ concentration to ~ 1.0 mM (Spectrum C) causes resonance g2 to disappear

Table 30. Assignment of resonances in ^1H NMR spectra of erythrocytes^a.

Peak designation ^c vs DSS	Chemical Shift (ppm)	Assignment: Position in molecule to which ^1H is attached
a1	1.46	C(β) of alanine
c2	3.01	Methyl C of creatine
^1D	1.28	C(3) of lactate with C(2) deuterated
e1	3.25	C of methyls on quaternary N of ergothioneine
e2	6.77	C(4) of ergothioneine
g1	3.76	C(α) of Gly residue of GSH ^b
g2	2.92	C(β) of Cys residue of GSH
g3	2.55	C(γ) of Glu residue of GSH
g4	2.15	C(β) of Glu residue of GSH
g5	4.55	C(α) of Cys residue of GSH
g6	3.54	C(α) of glycine

(a) From references 105 and 186.

(b) Resonance for ^1H on C(α) of Glu residue of GSH is obscured by that for C(α) of Gly residue.

(c) As labelled in Figure 50.

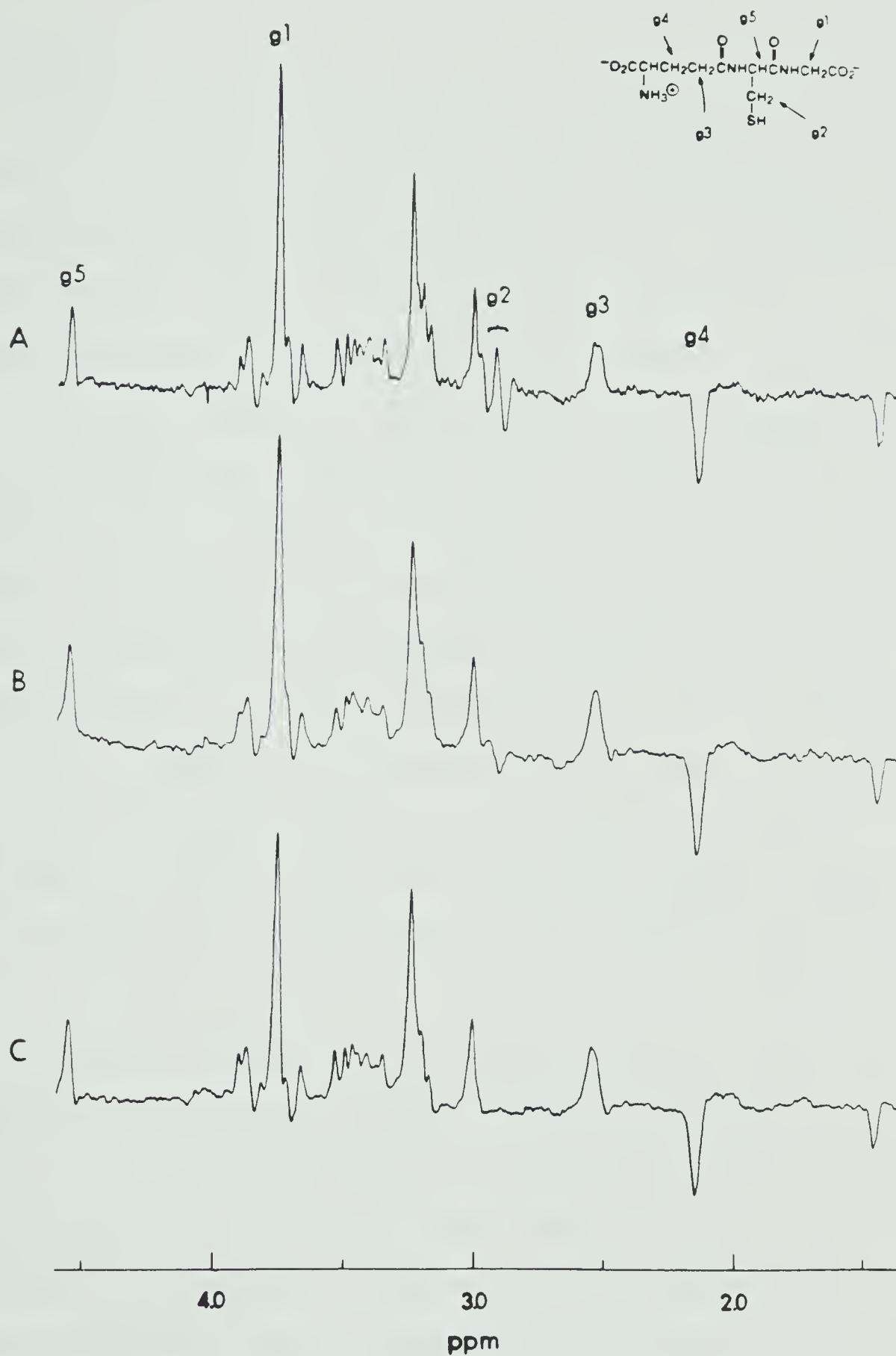


Figure 51. SEFT NMR spectra of intact human erythrocytes at 400 MHz a) alone, b) with 0.5 mM $\text{CH}_3\text{Hg(II)}$, c) with 1.0 mM $\text{CH}_3\text{Hg(II)}$.

completely.

Further evidence for GSH binding by $\text{CH}_3\text{Hg(II)}$ is provided by the decreased intensity of the resonance for the glycine residue methylene protons (g1). The cysteinyl residue methine proton resonance (g5) also shifts, although the shift is too small to be evident in Figure 51.

The exact origins of these effects are discussed below; qualitatively, they indicate some degree of GSH- $\text{CH}_3\text{Hg(II)}$ interaction. By contrast, there are no apparent changes in resonances for intracellular glycine, creatine, alanine, ergothioneine or lactate, indicating no significant degree of $\text{CH}_3\text{Hg(II)}$ complexation under these conditions. Binding is preferentially to GSH. (The lack of binding of ergothioneine in particular is of some importance to later studies and should be noted.) Transport of $\text{CH}_3\text{Hg(II)}$ into the cell is also seen to be fairly rapid.

To better understanding of the behaviour of the various GSH resonances in these spectra as $\text{CH}_3\text{Hg(II)}$ is added, spectra were collected for simple D_2O solutions of GSH and $\text{CH}_3\text{Hg(II)}$ in varying mole ratios. pD was maintained at ~ 7 throughout. Figure 52 shows conventional (single-pulse) and SEFT ^1H spectra for GSH alone (A and A' respectively) and for $\text{CH}_3\text{Hg(II)}:\text{GSH}$ ratios of 0.53 (B and

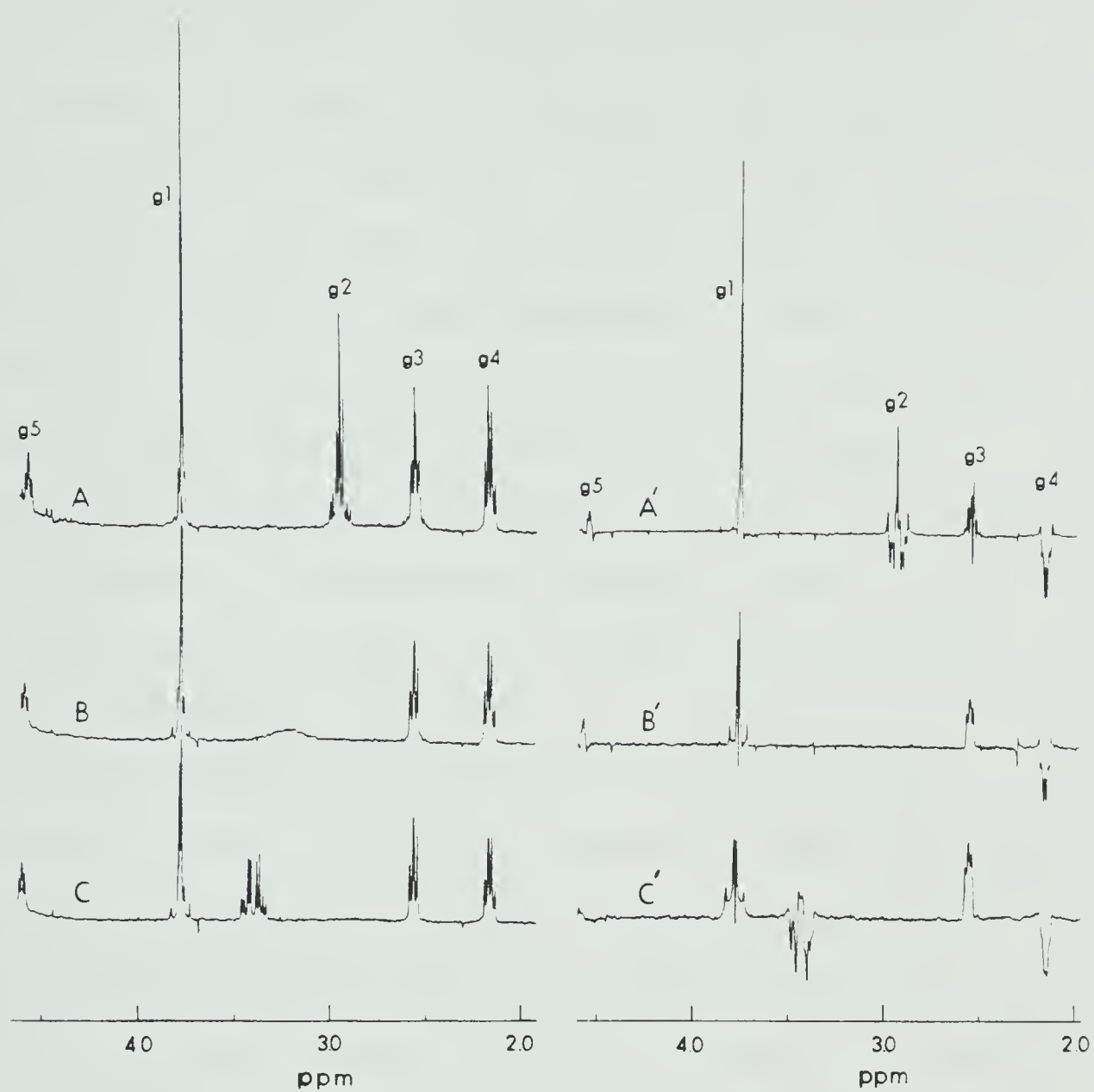


Figure 52. Single-pulse FT (A-C) and SEFT (A'-C') NMR spectra of A,A') GSH alone; B,B') $\text{CH}_3\text{Hg(II):GSH}$ 0.58:1; C,C') $\text{CH}_3\text{Hg(II):GSH}$ 1.09:1.

B') and 1.09 (C and C').

Resonances g2 and g5 together constitute an ABX spin system. For free GSH (Spectrum A) the spectral parameters are $\delta_A = 2.916$ ppm, $\delta_B = 2.995$ ppm, $\delta_X = 4.556$ ppm, $J_{AB} = 14.5$ Hz, $J_{AX} = 7.2$ Hz and $J_{PX} = 5.2$ Hz. Addition of $\text{CH}_3\text{Hg(II)}$ causes resonance g2 (which is the AB part of the above system) to broaden and shift (Spectrum B). When sufficient $\text{CH}_3\text{Hg(II)}$ has been added to complex the sulfhydryl group completely; g2 again becomes highly resolved. The spectral parameters are now $\delta_A = 3.354$ ppm, $\delta_B = 3.425$ ppm, $\delta_X = 4.596$, $J_{AB} = 13.8$ Hz, $J_{AX} = 6.0$ Hz and $J_{BX} = 5.1$ Hz.

The observation in Spectrum B of resonances at positions *intermediate* between those of A and C indicates that GSH is exchanging between the free and complexed forms. The broadening of g2 in B indicates that the exchange is fairly slow on the NMR timescale. The smaller shift of resonance g5 overall (0.04 ppm vs. ~ 0.48 ppm) is consistent with the greater distance of this proton from the site of complexation. Again, a single resonance is observed throughout the course of the experiment; however, in this case no linebroadening is observed. This is not unexpected. At 400 MHz, complexation shifts g2 by 192 Hz but g5 by only 16 Hz. Rearrangement of a

simplified lineshape equation for this exchange region (202) gives the expression

$$\text{linebroadening (Hz)} = 4\pi P_f^2 P_b \tau_b (v_f - v_b)^2 \quad (151)$$

where P_f and P_b are the free and bound populations, v_f and v_b their precession frequencies and τ_b the mean complex lifetime. Thus, since for two resonances on the same molecules, P_f , P_b and τ_b are necessarily the same, the linebroadening (Hz) observed for each varies as the square of the separation in frequency ($v_f - v_b$). The observed broadening for g2 in Spectrum B is difficult to estimate owing to the highly coupled nature of the AB subspectra; however, even if a value of 50 Hz is taken, the predicted broadening for g5 is then 0.3 Hz, less than the instrumental linewidth under typical shim conditions.

These effects are paralleled in the SEFT spectra (A'-C'). A' shows sharp signals for both g2 and g5 (note the phase-modulation of their multiplets), as does C'. In B', the slowly exchanging g2 signal disappears; the linebroadening described above has decreased the effective T_2 of these protons to a region where they are nulled by the .060 s SEFT sequence. By contrast, g5, which is narrow in Spectrum B, appears also in B'.

The effect of complexation on the intensity of res-

onance g1 is interesting, especially so since these protons are relatively distant from the site of complexation.

Spectra C and C' indicate that complexation causes the two methylene protons to no longer be equivalent, giving an AB pattern ($\delta_A = 3.76$ ppm, $\delta_B = 3.77$ ppm, $J_{AB} = 17.8$ Hz) instead of a singlet at $\delta = 3.75$ ppm. (In the spin-echo case, this is phase-modulated (180).) Presumably a conformational change occurs on complexation, rendering the protons non-equivalent. This is supported by the behaviour of the g2 resonance (above), and by the observation of similar behaviour on complexation of GSH by trimethyllead(IV) (203) or oxidized glutathione formation (204).

The observation of a sharp exchange-averaged resonance for g5 in samples containing a mixture of free and bound GSH permits estimation of the *maximum* lifetime of the complexed species. It was shown previously that bimolecular nucleophilic displacement of complexed GSH by GS^- is the major pathway for exchange in dilute aqueous solution at physiological pH (162). Using the rate constant determined there, and a typical GSH concentration of 2.2 mM (half complexed), the actual complex lifetime is predicted to be less than 10^{-3} s. The *upper* limit from Spectrum B (Figure 52) is 10^{-2} s.

As noted above, resonance g5 shifts only slightly as GSH is complexed by $\text{CH}_3\text{Hg(II)}$; nevertheless, the shift is unambiguous and amenable to measurement with reasonable precision, especially in the TSCR spectrum, where no phase-modulation occurs. Figure 53 shows the g5 resonance chemical shift, δ_{g5} , as a function of the $\text{CH}_3\text{Hg(II)}:\text{GSH}$ ratio (determined by prior standardisation). The change in δ_{g5} is linear up to a 1:1 ratio, and independent of the ratio thereafter, as expected; thus, the degree of complexation can be calculated from the observed chemical shift. Defining P_f , the fraction free, gives

$$P_f = \frac{\delta_o - \delta_b}{\delta_f - \delta_b} \quad \text{or} \quad P_b = 1 - P_f = \frac{\delta_o - \delta_f}{\delta_b - \delta_f} \quad (152)$$

where P_b is the fraction bound, δ_o the observed chemical shift and δ_f and δ_b the free and bound chemical shifts respectively.

Such an approach would also apply to resonance g2; in fact, since the range of chemical shifts is larger, this would in principle be preferable for precise determination of P_f . In practise (see above) exchange kinetics make g2 very broad and poorly defined for most conditions.

The chemical shift δ_{g5} can be measured to considerable precision on the WH 400 spectrometer. Figure 54 shows

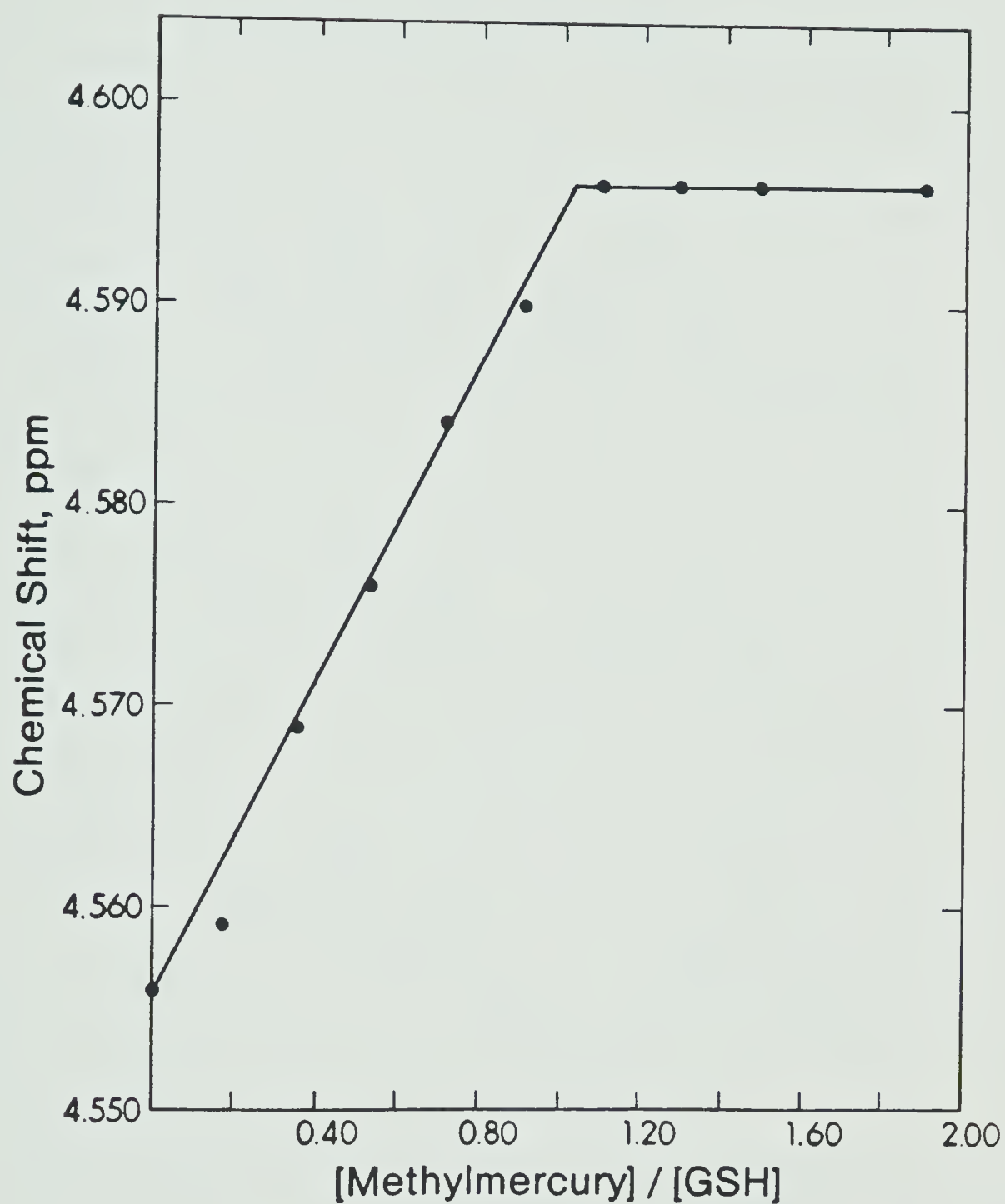


Figure 53. Glutathione g5 resonance chemical shift versus $\text{CH}_3\text{Hg(II)}/\text{GSH}$ ratio for $\text{CH}_3\text{Hg(II)}$ added to GSH (dilute aqueous solution).

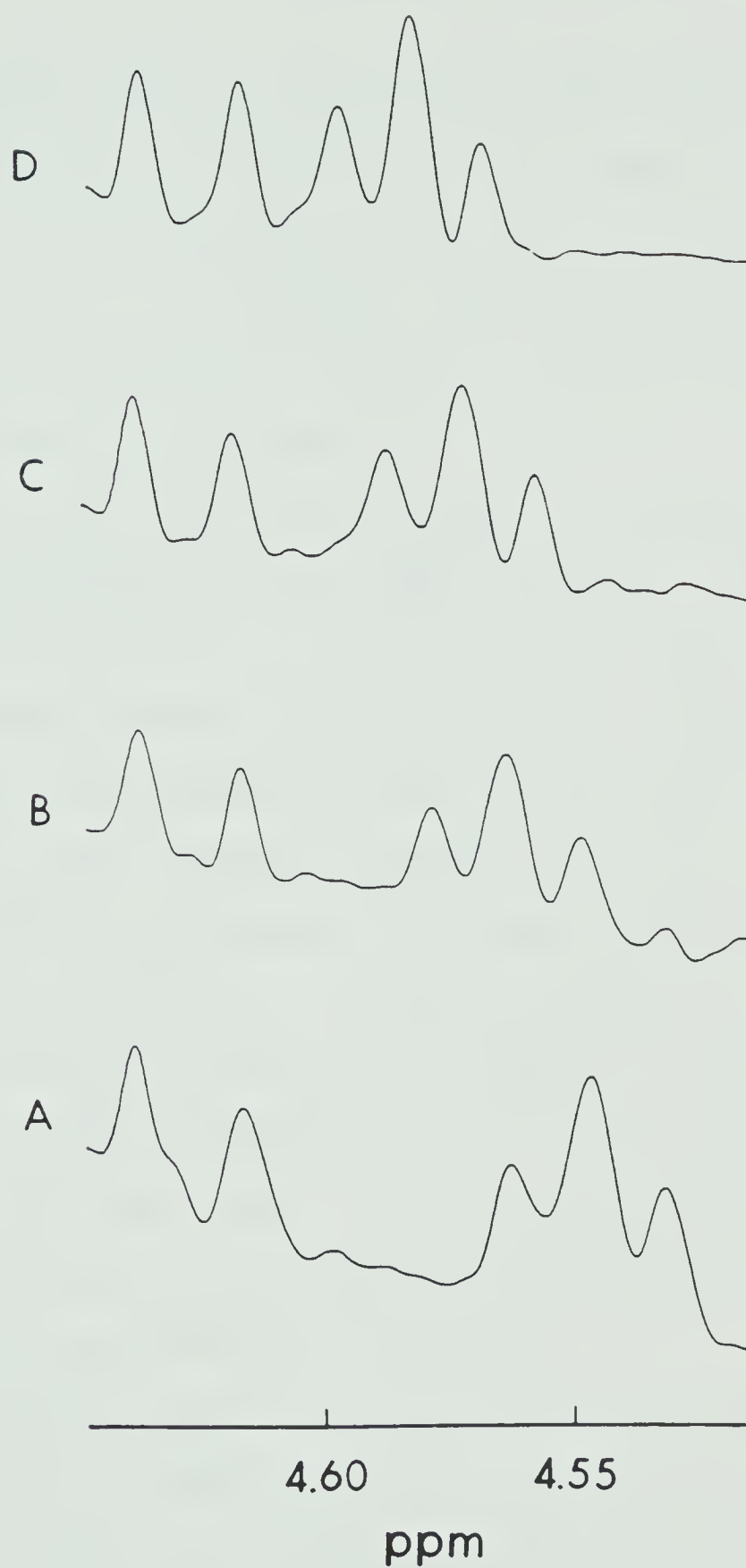


Figure 54. g_5 resonance region of TSCR spectra of hemolyzed erythrocytes, on addition (A-D) of increasing amounts of $\text{CH}_3\text{Hg(II)}$.

an expansion of this area, as observed in TSCR spectra of hemolyzed erythrocytes. The doublet on the left is due to the proton on C1 of β -D-glucose, and serves as a convenient secondary reference ($\delta = 4.63$ ppm). The upward shift of δ_{g5} on addition of increasing amounts of $\text{CH}_3\text{Hg(II)}$ (spectra A through D) is quite noticeable.

Using δ_{g5} , it was therefore possible to calculate the fraction of GSH complexed by the added $\text{CH}_3\text{Hg(II)}$, and from this to estimate the extent of competition for $\text{CH}_3\text{Hg(II)}$ between GSH and other thiols in erythrocytes. CH_3HgOD was added in increasing amounts to the erythrocytes, which were hemolyzed so that transport problems would not complicate matters; and δ_{g5} measured after each addition. No attempt was made to control pH. Hemolyzed erythrocytes have been found to be reasonably well buffered; in any case, at neutral pH any sulfhydryl groups will be protonated virtually quantitatively. Thus, the OD^- ion added with $\text{CH}_3\text{Hg(II)}$ showed almost exactly compensate for the D^+ ions displaced from the sulfhydryls by $\text{CH}_3\text{Hg(II)}$.

Figure 55 shows a plot of the fraction of GSH complexed, P_b , versus the total $\text{CH}_3\text{Hg(II)}$ concentration. The shape of the curve indicates (slightly) preferential binding of $\text{CH}_3\text{Hg(II)}$ to GSH. For comparison, the insert diagram shows the plots expected for GSH binding (relative to

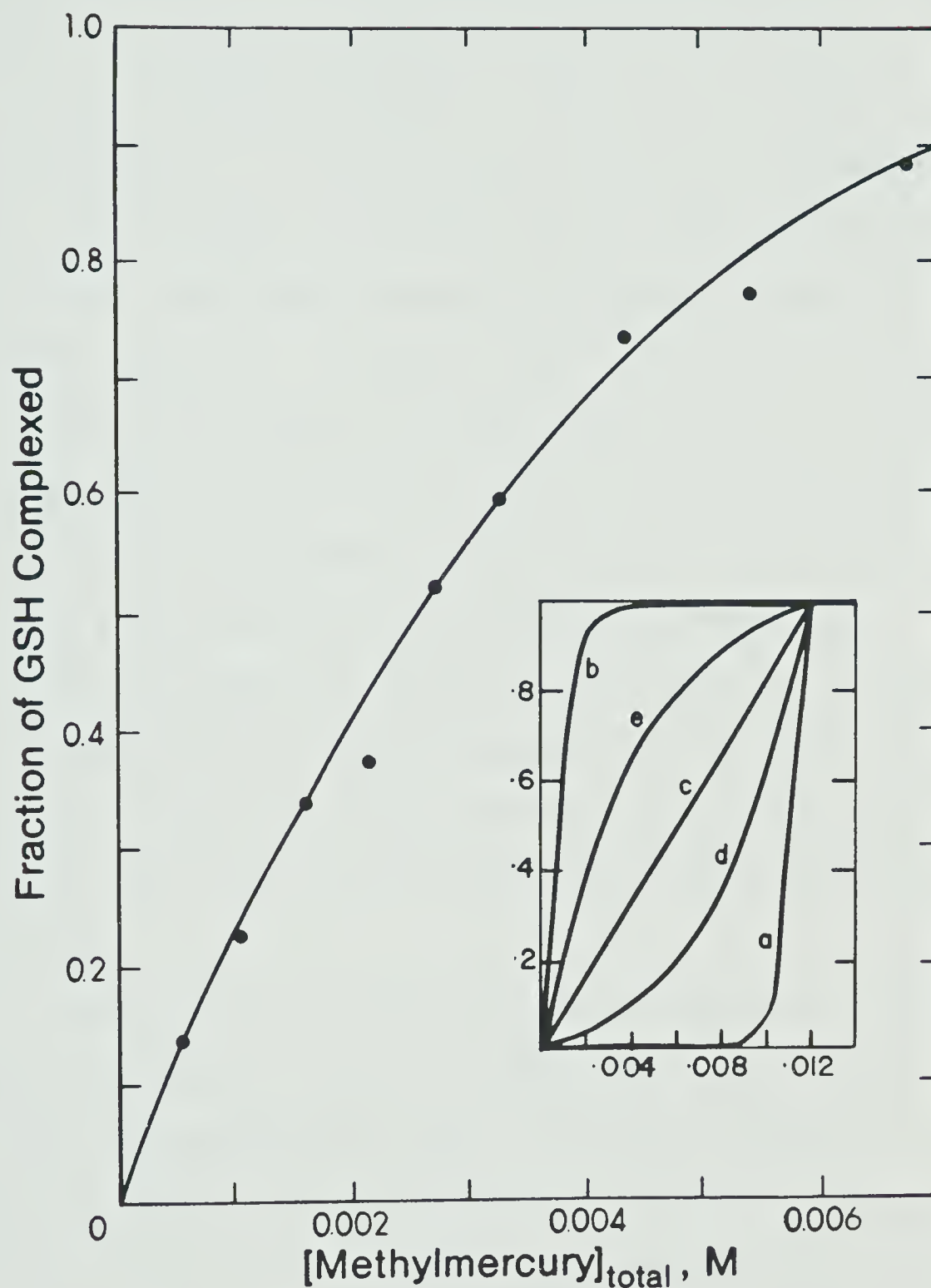
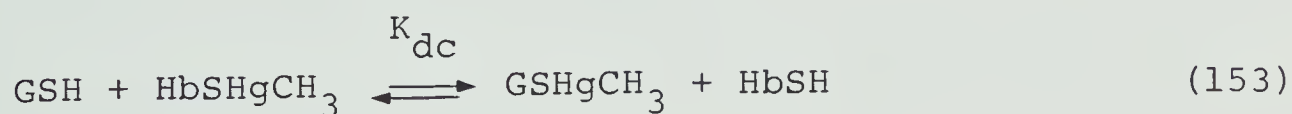


Figure 55. Fraction of GSH complexed by $\text{CH}_3\text{Hg}(\text{II})$, as a function of total $\text{CH}_3\text{Hg}(\text{II})$ added to a hemolyzed erythrocyte sample. Insert: expected curves for various situations; see text.

hemoglobin sulfhydryl binding) a) weaker by a factor of 10^3 ; b) stronger by a factor of 10^3 ; c) exactly as strong; d) weaker by a factor of 5 and e) stronger by a factor of 5. Concentrations of 2 mM (GSH) and 10 mM (Hb sulfhydryl) were used. If a value is assumed for the GSH concentration in the samples, the concentration of CH_3HgSG present at any stage can be computed. A typical level for intracellular GSH is 2.2 mM; substitution of this value and calculation of $[\text{CH}_3\text{HgSG}]$ shows that by no means is all the $\text{CH}_3\text{Hg(II)}/\text{GSH}$ complexed. This is confirmed by the work of Naganuma and Imura (205), who found by gel filtration of $\text{CH}_3\text{Hg(II)}$ -containing hemolysates that $\text{CH}_3\text{Hg(II)}$ was bound by a low molecular weight substance, and suggested that this was GSH. However, they also found that not all of the $\text{CH}_3\text{Hg(II)}$ was bound in this form, and concluded that some was bound to hemoglobin.

It is possible to use the curve of Figure 55 to obtain formation constant data, although the number obtained depends upon the assumptions made. Firstly, assuming that the competing ligand is hemoglobin, and that its concentration is a typical 5.2 mM (206), K_{dc} for the displacement reaction can be determined:



where

$$K_{dc} = \frac{[\text{GSHgCH}_3][\text{HbSH}]}{[\text{GSH}][\text{HbSHgCH}_3]} \quad (154)$$

Strictly, the free concentration terms should be of the form $([\text{RSH}] - [\text{RS}^-])$, but at pH ~ 7 deprotonated sulfhydryls are negligible.

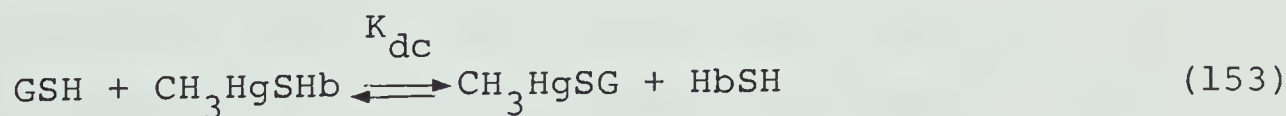
As discussed in Part 1, K_{dc} is the ratio of the two complex conditional formation constants. Calculation yields a value of 6 ± 2 , indicating that the formation constant of the GSH complex is six times higher. However, the values of K_{dc} calculated for successive points on Figure 55 were not randomly scattered, displaying a tendency to increase with $\text{CH}_3\text{Hg(II)}$ concentration. This is ascribed to the ligand concentrations being different from those assumed, or to the neglect of the effect of other ligands. For instance, membrane sulfhydryl groups are generally thought to amount to 2/3 of the GSH amount (152). Recalculation on this basis yields K_{dc} in the region 10-12, depending on the assumption made about the formation constant of the newly introduced complex. Scatter is lower than above (about 20%) and more random in nature, suggesting that this may be closer to the true situation. However, obviously there are too many unknowns for this experiment to be conclusive.

These experiments have illustrated the utility of Fourier transform NMR techniques (such as the SEFT or TSCR methods) for studying systems of biological complexity. As for well-defined, small-molecule samples, the detailed characterization of binding sites, the effect of binding on the NMR spectra, use of linebroadening to estimate rates of reaction and use of fast-exchange averaged chemical shift to estimate extent of competition, have now been demonstrated as obtainable even for a system as poorly defined and spectroscopically intractable as the hemolyzed erythrocyte. In Section B below, the analytical precision of which such methods are capable, by using careful measurement of chemical shifts, will be further demonstrated.

B. Measurement of $\log K_{fc}$ for the Hemoglobin- $\text{CH}_3\text{Hg(II)}$ Complex

1. NMR titration of hemoglobin sulfhydryls with $\text{CH}_3\text{Hg(II)}$.

The studies of section A showed that a competition study between hemoglobin and glutathione for $\text{CH}_3\text{Hg(II)}$, yielding a conditional displacement constant K_{dc} for the reaction



in a manner similar to that described in Part 1, was feas-

ible. The TSCR NMR technique was found to be especially suitable for monitoring the extent of competition; using this technique, the chemical shift of the glutathione cysteinyl methine proton resonance (δ 5) could be precisely measured, and used to estimate the extent to which the glutathione was bound to $\text{CH}_3\text{Hg(II)}$.

However, as shown above, the quantitative result for K_{dc} gained from the study of Section A depended upon the assumptions made as to the identity and concentrations of the competing species. In order to measure K_{dc} precisely, it is necessary firstly, to exclude all other species containing sulfhydryls and secondly, to know the concentrations of all species involved.

The preparation of a membrane-free, glutathione-free hemolysate sample was described in Chapter VII, Section B. Neither of the steps involved there (high-speed centrifugation to remove membrane debris or dialysis to remove small thiols such as glutathione) will of course remove other protein sulfhydryl groups. While Jocelyn (93) lists many of these, it does not appear that their concentration will be high enough to significantly affect the results, given the uncertainty (about $\pm 10\%$) in the final formation constant determination. It is therefore permissible (albeit loosely) to refer to the above sample as a "hemoglobin solution".

The preparation and standardisation of glutathione and $\text{CH}_3\text{Hg(II)}$ solutions was described in Chapter II (Sections B and C). These were identical in the present studies, except that they were carried out in D_2O instead of H_2O .

A sulfhydryl assay procedure for hemoglobin was developed, as discussed below. Many methods have been used for assaying protein sulfhydryl groups (see Chapter VI); however, a titration by $\text{CH}_3\text{Hg(II)}$ was felt to be desirable in the present case for several reasons. Firstly, the behaviour of $\text{CH}_3\text{Hg(II)}$ was already characterized in considerable detail and stock solutions were already available and standardised. Secondly, it is known that different "sulfhydryl reagents" can give different titres for the same protein sample, due to hindered accessibility of sulfhydryls buried within the protein structure (149). This was not anticipated to be a problem with hemoglobin (see Chapter VI, Section A), but could be with other proteins. Since the intention was to develop a general method for application to other macromolecular thiols, it was obviously desirable to use $\text{CH}_3\text{Hg(II)}$ for standardisation as well as competition; otherwise, a group not titrated during standardisation could nevertheless participate in $\text{CH}_3\text{Hg(II)}$ binding, giving erroneous results. Lastly, it

was hoped that by using $\text{CH}_3\text{Hg(II)}$ addition for the sulfhydryl assay, the titration could be fully integrated into the competition experiment itself.

The use of $\text{CH}_3\text{Hg(II)}$ as a sulfhydryl reagent was discussed in Chapter VI, Section A; typical endpoint detection was amperometric (146) or potentiometric (150). In principle, however, the titration could be self-indicating if followed by NMR. The $\text{CH}_3\text{Hg(II)}$ methyl group should display a constant chemical shift, characteristic of the hemoglobin complex, until all the Hb has been complexed. Thereafter, a shift due to the presence of excess CH_3HgOD will be observed.

In practise, however, this signal is not generally observed; the $\text{CH}_3\text{Hg(II)}$ is bound to the protein, so presumably transfer of saturation occurs also to the methyl group protons. A similar but much less pronounced effect was noted for glutathione in hemoglobin solutions (189), based upon a weak interaction (191); the interaction here is very much stronger and therefore the fatal disappearance of the signal is reasonable.

Endpoint detection in the titration was therefore accomplished using an "NMR indicator" molecule, ergo-thioneine (ergo). Its $\text{CH}_3\text{Hg(II)}$ complex conditional formation constant at pH 7.4 is approximately 10^8 , about three

orders of magnitude below that of glutathione, thus complexation of ergo is expected only after quantitative reaction with ordinary sulfhydryl groups. On the other hand, K_{fc} is much higher than for other potential $\text{CH}_3\text{Hg(II)}$ -coordinating sites, such as amino or carboxylate groups, so no interference by complexation to these was anticipated.

As shown in Figure 50, in the presence of glutathione two resonances from ergothioneine are easily visible, the nine protons of the methyl groups on the quaternary nitrogen and the C(4) proton, labelled as e1 and e2 respectively in Table 30. e1 is the more intense, but was found to shift by very little upon complexation.

e2, however, shifted quite adequately for use as an endpoint indicator. Figure 46 shows the chemical shift of a 10 mM D_2O solution of ergothioneine, buffered at pH 7.0 (pD 7.4), as a function of added $\text{CH}_3\text{Hg(II)}$ mole fraction. At mole ratios ($\text{CH}_3\text{Hg(II)}/\text{ergo}$) of up to ~ 1.0 , the trend is linear, indicating that the various free and $\text{CH}_3\text{Hg(II)}$ -bound forms of ergo are in fast exchange. Thereafter, the curve falls away; the chemical shift eventually stabilises at a ratio of about 10. This latter phase in the plot is probably due to further binding of $\text{CH}_3\text{Hg(II)}$ to the carboxylate group of ergo. The extremely drawn-out curvature of the plot indicates competition with the ergo carboxylate

by some other species, probably OD^- . (While the concentration of this is low ($\sim 10^{-7} \text{ M}$) compared to the ergo carboxylate, its log formation constant with $\text{CH}_3\text{Hg(II)}$ is about 9.4 (2); that for the ergo carboxylate, based upon the approximate pK of 1.3 (130) and the observed trend between pK's and $\log K_f$'s (24), is about 1.2. The exact extent of competition will also depend on the ability of the buffer to "supply" deuteroxyl ions to replace those complexed by $\text{CH}_3\text{Hg(II)}$.)

The second (curved) phase of the plot in Figure 56 is not useful for the present purposes; however the first (linear) is eminently suitable. If ergothioneine is added to a thiol solution which is titrated with $\text{CH}_3\text{Hg(II)}$, no shift will be observed for resonance e2 until all the thiol has been titrated; thereafter further additions will generate a linear shift change. Backward extrapolation of this line will give the amount of $\text{CH}_3\text{Hg(II)}$ added which titrated the thiol.

The actual titration was accomplished as follows. A 500 μl sample of $\sim 2 \text{ mM}$ hemoglobin solution in pH 7.0 phosphate buffer, with $\sim 2 \text{ mM}$ TMA to act as chemical shift reference and $\sim 2.5 \text{ mM}$ ergothioneine was carefully placed under argon in an NMR tube. The TSCR spectrum was collected (see Chapter VII, Section D2) and the e2 resonance

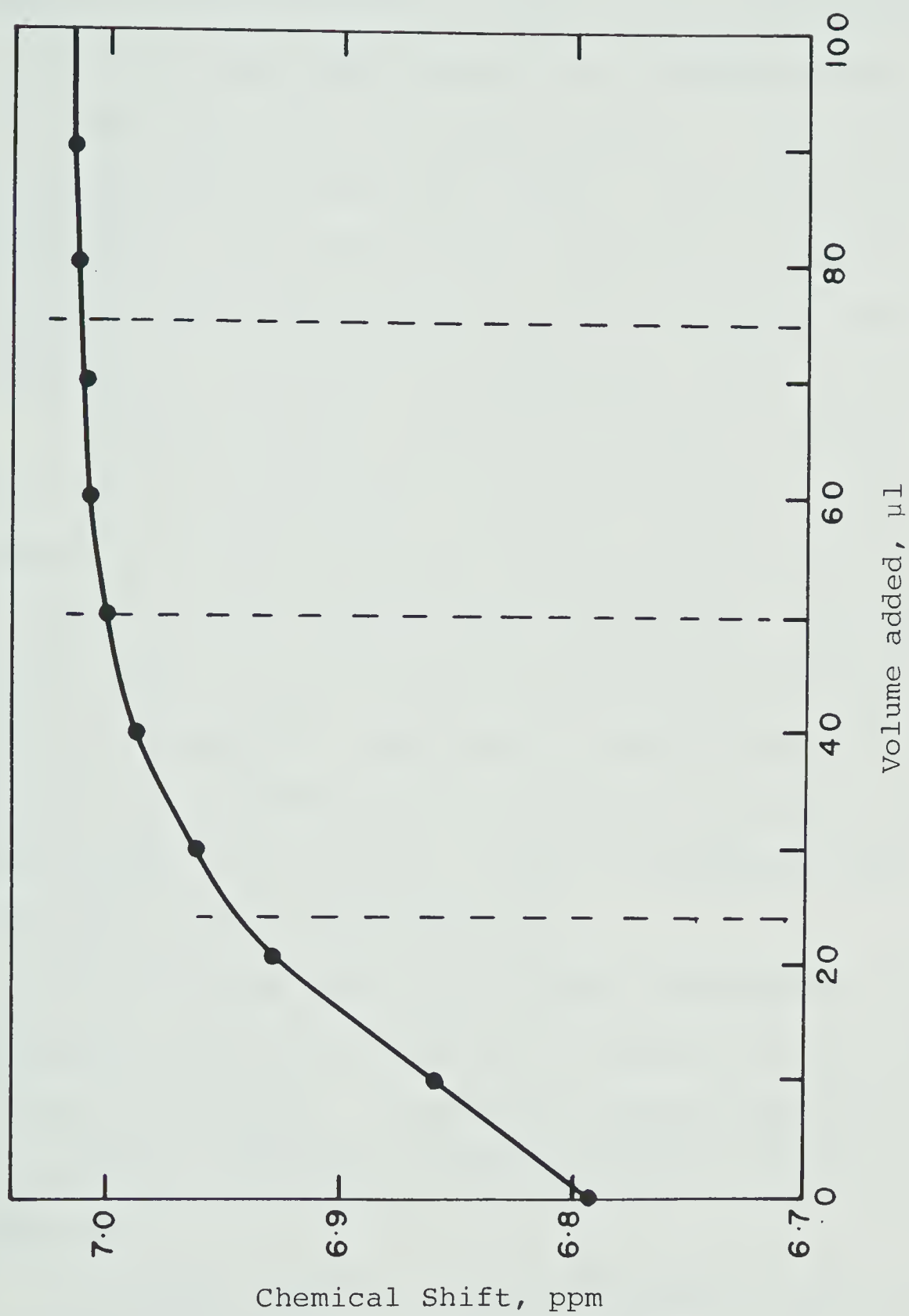


Figure 56. Ergothioneine e2 chemical shift versus volume $\text{CH}_3\text{Hg}(\text{II})$ (0.2 M) added for 50 μl of 0.01 M ergothioneine ($\text{pH}^* = 7$).

chemical shift determined. 10 μ l of 15.6 mM CH_3HgOD solution was then added using a 10 μ l microsyringe, and the sample replaced in the spectrometer. This was repeated until resonance e2 started to shift, and then until a satisfactory line was obtained (typically 3-5 additions). For second and subsequent titrations, a single addition was made to just below the equivalence point, to save time.

A typical set of titrations is shown in Figure 57. The linearity of the post-equivalence region and the sharpness of the equivalence break should be noted. Table 31 summarizes the data of these titrations. The agreement between them is $\pm 1.2\%$, which is adequate considering the method of addition. Comparison of these results with the standard spectrophotometric hemoglobin (molecule) assay (see Chapter VII, Section B) gave a sulfhydryl titre of 1.96 moles SH per mole hemoglobin.

The titration was also employed successfully with a sample of bovine serum albumin, a plasma protein containing a single sulfhydryl. It should be equally applicable to any material containing sulfhydryl groups accessible to $\text{CH}_3\text{Hg(II)}$.

An unusual feature of the NMR method of endpoint detection is that the precision available can be selected by the operator. Obviously, the steeper the slope of the

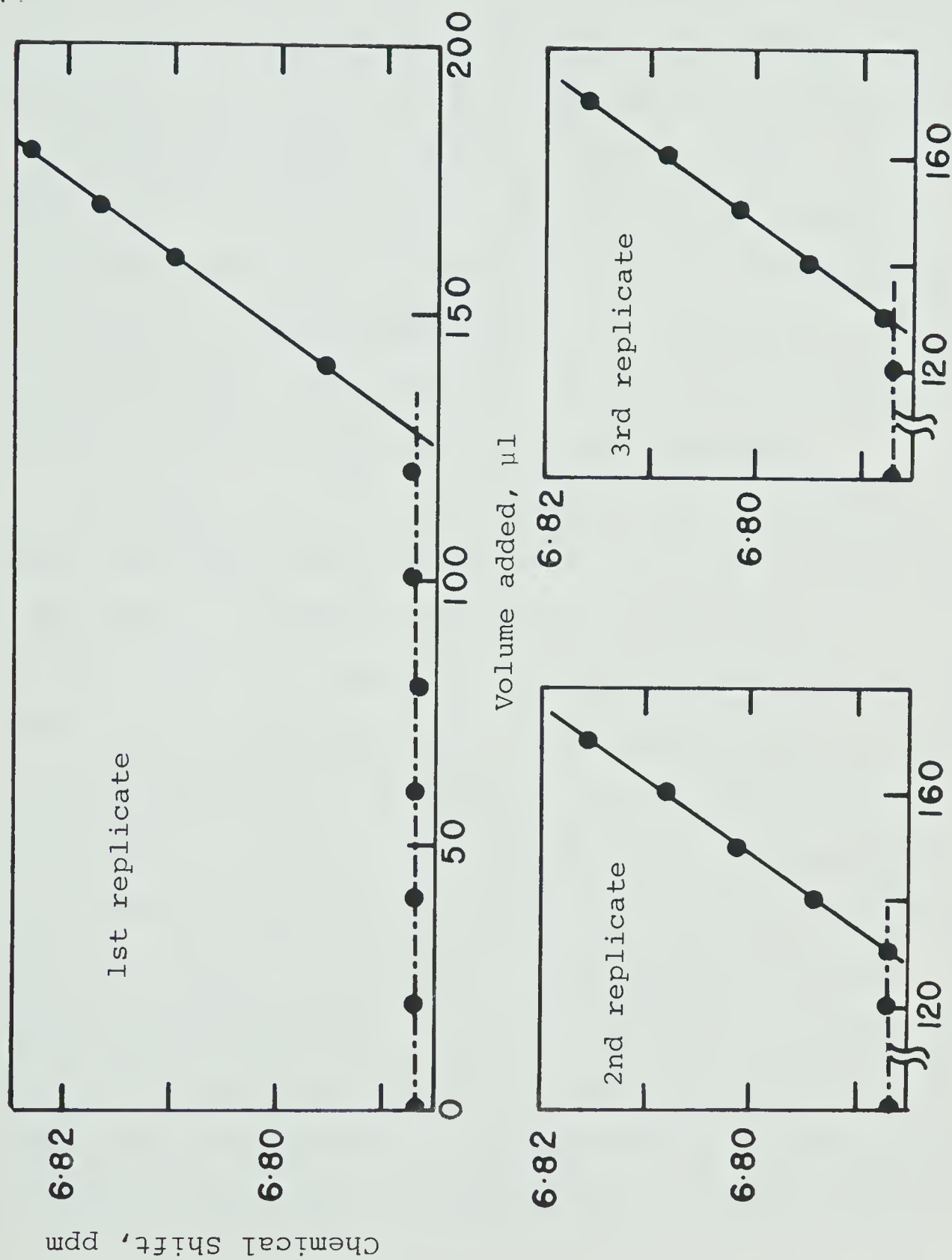
Table 31. Determination of hemoglobin sulfhydryl concentration by titration with $\text{CH}_3\text{Hg(II)}^{\text{C}}$ using ergothioneine as indicator.

Replicate	1	2	3
$\delta_{\text{e2}}^{\text{a}}$ at $\text{CH}_3\text{Hg(II)}$			
addition of: 0 μl	6.787	6.787	6.787
120 μl	6.787 ₅ ^b	6.787	6.787
130 μl	--	6.787	6.788
140 μl	6.796	6.794	6.795
150 μl	--	6.801 ₅	6.801 ₅
160 μl	6.810	6.808	6.808 ₅
170 μl	6.817	6.815 ₅	6.816
180 μl	6.823 ₅	--	--
correlation coefficient of line	0.9999	0.9996	0.9995
Intersection with baseline (μl)	127	130	129
Hemoglobin SH concentration, mM	3.9 ₆	4.0 ₆	4.0 ₂

(a) Chemical shift of the ergothioneine C(4) proton.

(b) 0.0005 ppm represents the frequency separation between data points in the digitized spectrum.

(c) Concentration = 15.6 mM.



e2 chemical shift plot, the more exactly the endpoint can be located. This can be achieved simply by lowering the ergo concentration, so that a smaller addition of $\text{CH}_3\text{Hg(II)}$ will give the same shift. Naturally, the number of spectral transients which have to be accumulated to observe e2 with an acceptable signal-to-noise ratio then rises. For the conditions of Figure 57, 16 transients were adequate. In principle, the ergo concentration can be lowered until other spectrometer noise sources limit its detection; in practise, the measurement precision will usually be dominated by the titrant delivery system, as was the case here.

As far as could be ascertained, this is the first time that a macromolecule functionality has been standardised using NMR as a method of endpoint determination in this manner. Given the sensitivity and precision demonstrated above, such techniques offer a good alternative to more conventional methods of endpoint detection, with some advantages. Firstly, as discussed above, the precision in the endpoint detection can easily be adjusted. Secondly in contrast to, for instance, ultraviolet/visible or fluorescent indicators, it is not necessary to design any particular chromophore into the indicator molecule, provided there is a proton on the molecule reasonably sensitive in shift to the state of complexation. Lastly, the con-

tinuous spectral monitoring of the situation means that unexpected binding to other ligands can be easily detected, as opposed to non-specific methods where interference would go unnoticed. For instance, conflicting reports (148,149) have appeared in the literature regarding the time required for reaction of $\text{CH}_3\text{Hg(II)}$ with sulfhydryls. In the present case, the matter is quickly and unequivocally settled, simply by leaving the last sample of the titration in the spectrometer and collecting the spectrum as a function of time. Any slow uptake (or dissociation) of $\text{CH}_3\text{Hg(II)}$ would result in a shift of the ergo e2 resonance, in fact, none is observed over a period of some hours.

2. The glutathione/hemoglobin competition study.

This was accomplished in a similar manner to the study described in Section A. The sulfhydryl content of a hemoglobin stock solution prepared by dialysis of hemolyzed erythrocytes was determined as described in Section 1 above. A sample was prepared containing 500 μl of this solution and exactly 1 mole equivalent of glutathione. The sample was buffered at pH* 7.0 (phosphate buffer, 0.05 M) and a small quantity of TMA added. Increasing amounts of $\text{CH}_3\text{Hg(II)}$ were then titrated in.

Figure 58 shows the glutathione cysteinyl methine proton resonance (g5) chemical shift, δ_{g5} , as a function of the amount of $\text{CH}_3\text{Hg(II)}$ added. Qualitatively, the same trend observed in Section A (Figure 55) is also seen here. The data was fitted by KINET to the following model: If C is defined as the total glutathione concentration (all forms), which is also the total Hb sulfhydryl concentration, x as the $\text{CH}_3\text{Hg(II)}$ concentration ($0 < x < 1$) and P_f as the fraction of GSH free, then

$$[\text{GSH}] = P_f \cdot C \quad (155)$$

and hence

$$[\text{GSHgCH}_3] = (1 - P_f) \cdot C \quad (156)$$

Thus, invoking mass balance in $\text{CH}_3\text{Hg(II)}$

$$[\text{HbSHgCH}_3] = (x - 1 + P_f) \cdot C = (x + P_f - 1) \cdot C \quad (157)$$

and invoking mass balance in hemoglobin sulfhydryls

$$[\text{HbSH}] = (1 - x - P_f + 1) \cdot C = (2 - P_f - x) \cdot C \quad (158)$$

Substitution of these terms back into equation (154) yields

$$K_{dc} = \frac{P_f (P_f + x - 1)}{(1 - P_f) (2 - P_f - x)} \quad (159)$$

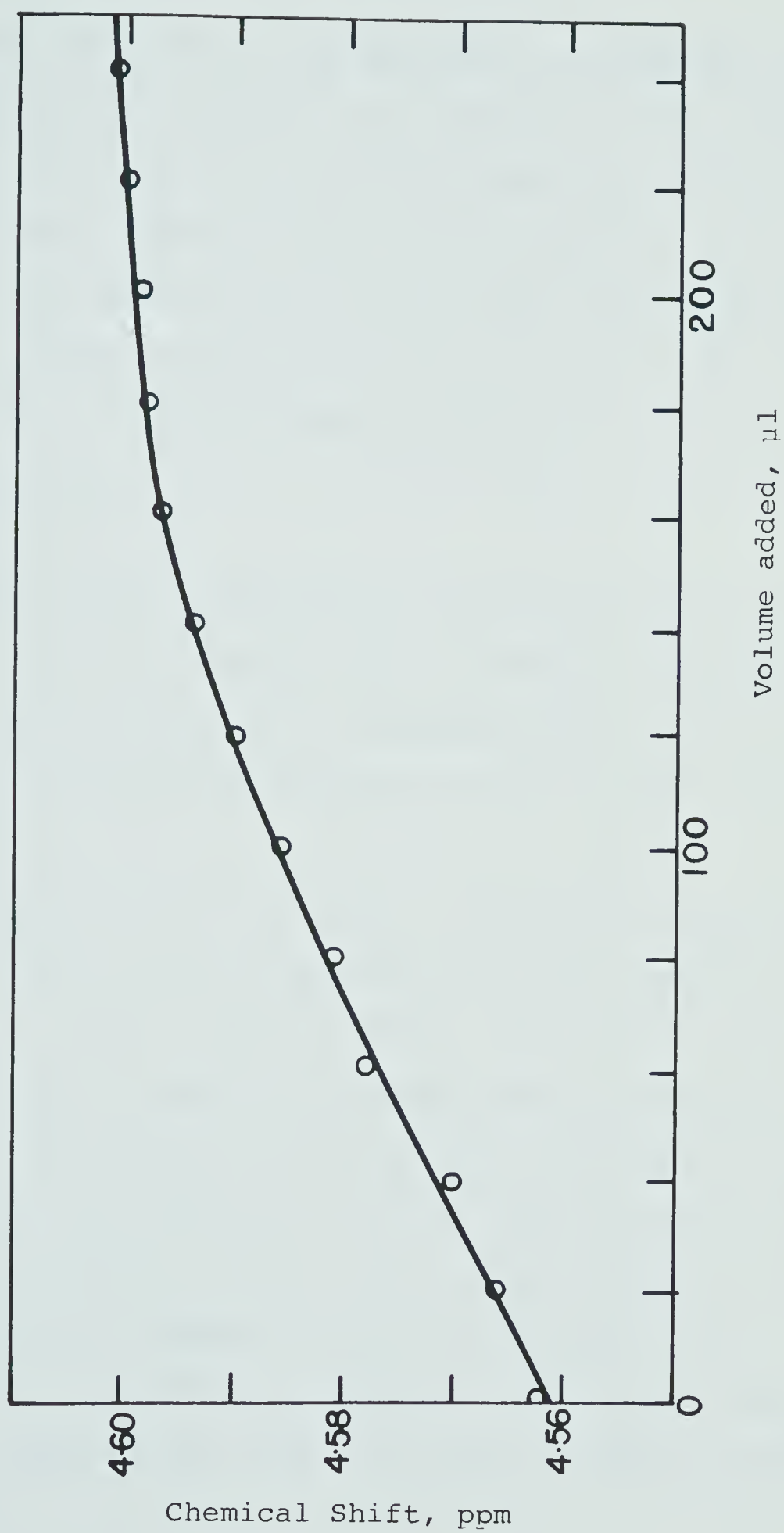


Figure 58. Glutathione g5 resonance chemical shift versus added $\text{CH}_3\text{Hg(II)}$ (15.6 mM) for sample containing Hb (4.0 mM sulphydryl) and GSH (4.0 mM).

The KINET fit of the data to this equation is shown as the solid line in Figure 58. The value of K_d returned by KINET was 0.11 ± 0.01 , indicating that K_{fc} for the glutathione complex at physiological pH is 9 (± 1) times higher than that for the complex with a hemoglobin sulfhydryl. Thus the value of $\log K_{fc}$ at pH 7.4 for the $\text{CH}_3\text{Hg(II)}$ complex of hemoglobin is 10.5.

C. Discussion

The results presented in this Chapter are of interest for two reasons; firstly, for the chemical information gained and secondly, for the demonstration of the feasibility of using such methods to gain detailed data of this type.

In general, the chemistry involved in hemoglobin-containing systems is qualitatively that previously observed in simple aqueous systems (see Chapters III, IV and V). $\text{CH}_3\text{Hg(II)}$ distributes itself among the various thiols present according to their relative affinities. The value of $\log K_{fc}$ measured at pH 7.4 for the hemoglobin sulfhydryl- $\text{CH}_3\text{Hg(II)}$ complex is 10.5 ± 0.1 , lower than but comparable to the figures observed in Part 1 for small thiols (11.1-11.7). No literature value could be found for comparison; however Naganuma and Imura, in a gel filtration study, con-

cluded that $\text{CH}_3\text{Hg(II)}$ in blood was predominately GSH-bound (205). Berg and Miles, in a method based on exclusion chromatography, analysed the constituents of a mixture of $\text{CH}_3\text{Hg(II)}$ (16.7 mM), bovine serum albumin (BSA, 5.9 mM) and cysteine (18.5 mM) (150). While this represents 68% complexation of the total thiol, only 46% of the BSA was complexed. Calculation using equation (159) gives $\log K_{\text{fc}} = 11.0 \pm 0.3$ for the BSA- $\text{CH}_3\text{Hg(II)}$ complex, comparable to the figure for Hb.

The viability of NMR as a probe for such systems, demonstrated in this chapter, is of some significance. For the first time, a gap in studies of toxic metals, between precise chemical measurements on simple, well-defined solutions of small molecules and biochemical or physiological studies of less defined macromolecular systems, has been at least partially bridged. In 1973, Rothstein wrote (154):

"Despite the prolific output of papers concerned with the nature of the sulfhydryl-mercury interaction, and with the role of sulfhydryl groups in protein function, such knowledge has not been particularly useful in advancing our understanding of mercury toxicity. The gap between the mercury-sulfhydryl reactions in a chemical sense, the consequent disturbance of protein function on the one hand, and manifestations in animals or man, on the other hand, has been too large."

It appears that the present techniques are capable of overcoming this problem to some extent. To further

illustrate this, Chapter IX reports the results of an investigation of the efficiency of various $\text{CH}_3\text{Hg(II)}$ poisoning antidote molecules using SEFT and TSCR FT NMR to identify the extents to which these can remove $\text{CH}_3\text{Hg(II)}$ from hemolyzed erythrocytes. These results are then directly compared to the formation constants of the various complexes determined in Chapters III, IV and VIII.

CHAPTER IX

THE EFFECTIVENESS OF SULFHYDRYL COMPOUNDS AS RELEASING AGENTS FOR $\text{CH}_3\text{Hg}(\text{II})$ IN HUMAN ERYTHROCYTES

A. Introduction

In preceding Chapters, NMR methods have been used to characterize in detail the complexation chemistry of a variety of thiols with $\text{CH}_3\text{Hg}(\text{II})$. The use of high-field NMR instrumentation with more sophisticated pulse techniques enabled the extension of these measurements to systems hitherto spectroscopically intractable such as the erythrocyte.

In this Chapter are reported the results of a brief study of the power of various sulfhydryl molecules to remove $\text{CH}_3\text{Hg}(\text{II})$ from the components of human erythrocytes. The studies provide further illustration of the potential of NMR for such studies. They are also of interest in that the data obtained can be compared, on the one hand; with that previously obtained for simple aqueous systems (see Chapters III, IV, V) and on the other hand, with pharmacological studies of the relative efficiencies of various thiols as $\text{CH}_3\text{Hg}(\text{II})$ poisoning antidotes in whole organisms (133,134,170,171) (see Chapter VI).

B. Results

In Chapter VIII it was shown that three major changes occurred in the SEFT and TSCR NMR spectra of hemolyzed erythrocytes when $\text{CH}_3\text{Hg(II)}$ was added:

- 1) Resonance g5 shifted slightly.
- 2) Resonance g1 reduced in relative intensity (relative to those of non-complexing molecules such as ergo-thioneine (ergo) or creatine (cre)).
- 3) Resonance g2 broadened (or disappeared) due to slow exchange kinetics.

The behaviour of δ_5 (the chemical shift of g5) was shown as a function of added $\text{CH}_3\text{Hg(II)}$ in Figure 54 (Chapter VIII). Figure 59 shows the intensity ratios g1/ergo, g1/cre and ergo/cre for the same samples. ergo/cre, as expected, has virtually zero slope although the scatter is considerable. The ratios g1/ergo and g1/cre are seen to provide an indication of the extent of complexation of GSH by $\text{CH}_3\text{Hg(II)}$.

These three indicators (δ_5 , g1/ergo and g1/cre) can therefore be monitored to indicate the extent to which added thiols *remove* $\text{CH}_3\text{Hg(II)}$ from erythrocytes. The setting up of experimental conditions is shown in Figure 60. Spectrum A is a portion of the SEFT NMR spectrum ($\tau_2 = 0.060$ s) of a sample of hemolyzed erythrocytes. As

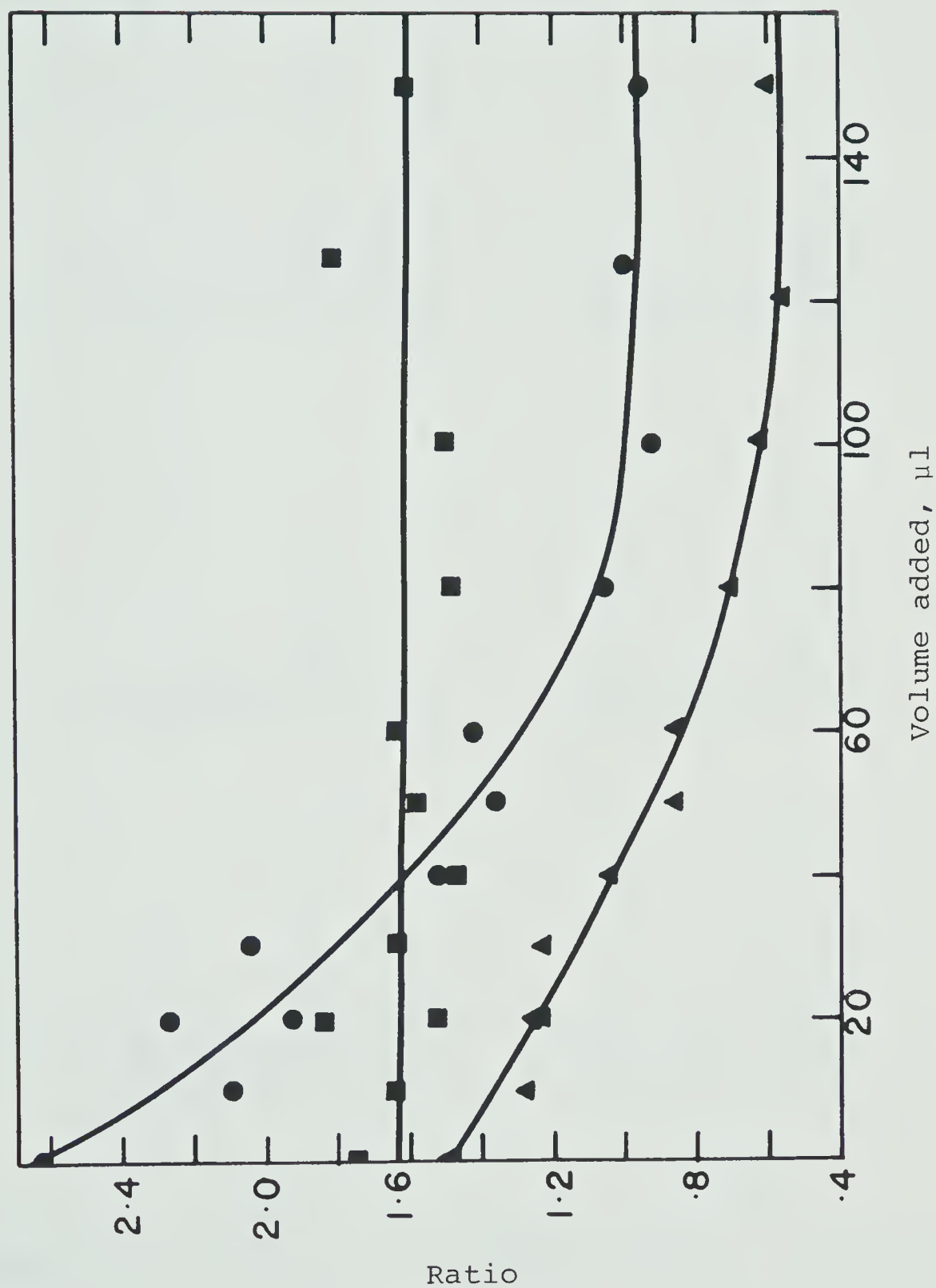


Figure 59. Intensity ratios for glutathione (gl), ergothioneine and creatine resonances in SEFT NMR spectra of hemolyzed erythrocytes, as a function of $\text{CH}_3\text{Hg(II)}$ (5.4 mM) added. gl/ergo; gl/cre; ergo/cre.

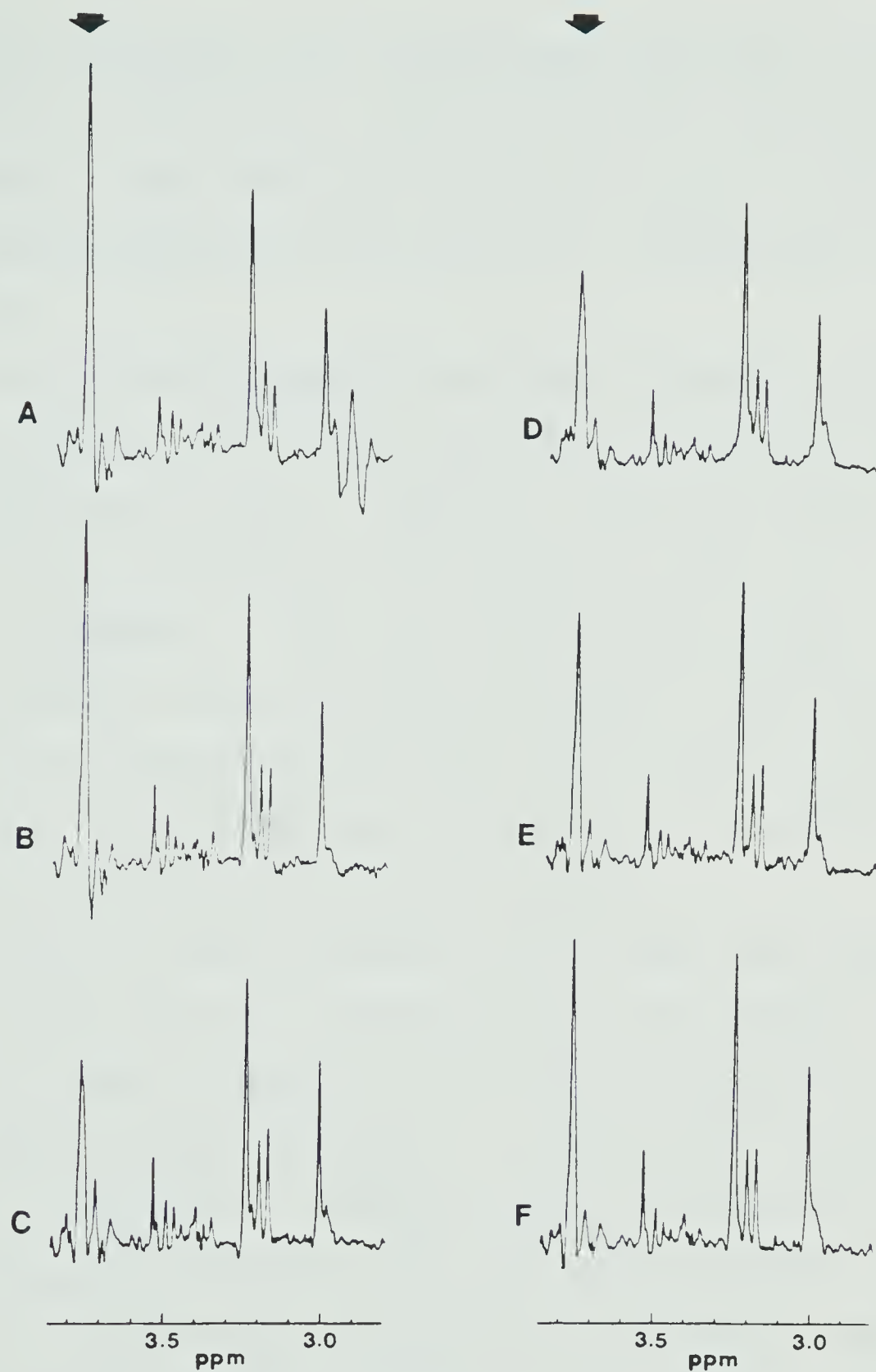


Figure 60. Portion of the SEFT NMR spectra of hemolyzed erythrocytes A) alone; B) + 2.1 mM $\text{CH}_3\text{Hg(II)}$; C) + 4.3 mM $\text{CH}_3\text{Hg(II)}$; D), E), F) as C) + 0, 1.3 and 2.0 mM BALSO_3H respectively.

$\text{CH}_3\text{Hg(II)}$ is added (B,C) the expected reduction in g2 is observed; in Spectrum C, approximately 75% of the GSH is complexed. These were the conditions adopted for the subsequent experiments; the $\text{CH}_3\text{Hg(II)}$ concentration is 4.3 mM.

2,3 dimercaptopropane-1-sulfonate (BALSO_3H) was then added (Spectra D,E,F) until approximately half the $\text{CH}_3\text{Hg(II)}$ had been removed again. Spectrum F shows the desired conditions; the BALSO_3H concentration is about 2 mM (4 mM sulfhydryl). Since (see Chapter IV) BALSO_3H is indifferent in terms of binding strength, it was expected that other compounds would remove more or less $\text{CH}_3\text{Hg(II)}$, but still give a measurable situation (i.e. $\text{CH}_3\text{Hg(II)}$ neither quantitatively removed or left).

Figure 61 shows resonance g5 for these same samples. As observed previously (Chapter VIII) the resonance moves to higher frequency on addition of $\text{CH}_3\text{Hg(II)}$ to the sample (Spectra A through C) and to lower frequency again as $\text{CH}_3\text{Hg(II)}$ is removed (Spectra D through F).

Comparitive studies using the other sulfhydryl molecules to remove $\text{CH}_3\text{Hg(II)}$ were then performed. Samples were hemolyzed erythrocytes containing 4.3 mM $\text{CH}_3\text{Hg(II)}$ and 4 mM thiol (2 mM for dithiols). Figure 62 shows observed spectra for some of the more widely used therapeutic thiols; Table 32 summarizes the data obtained. It is

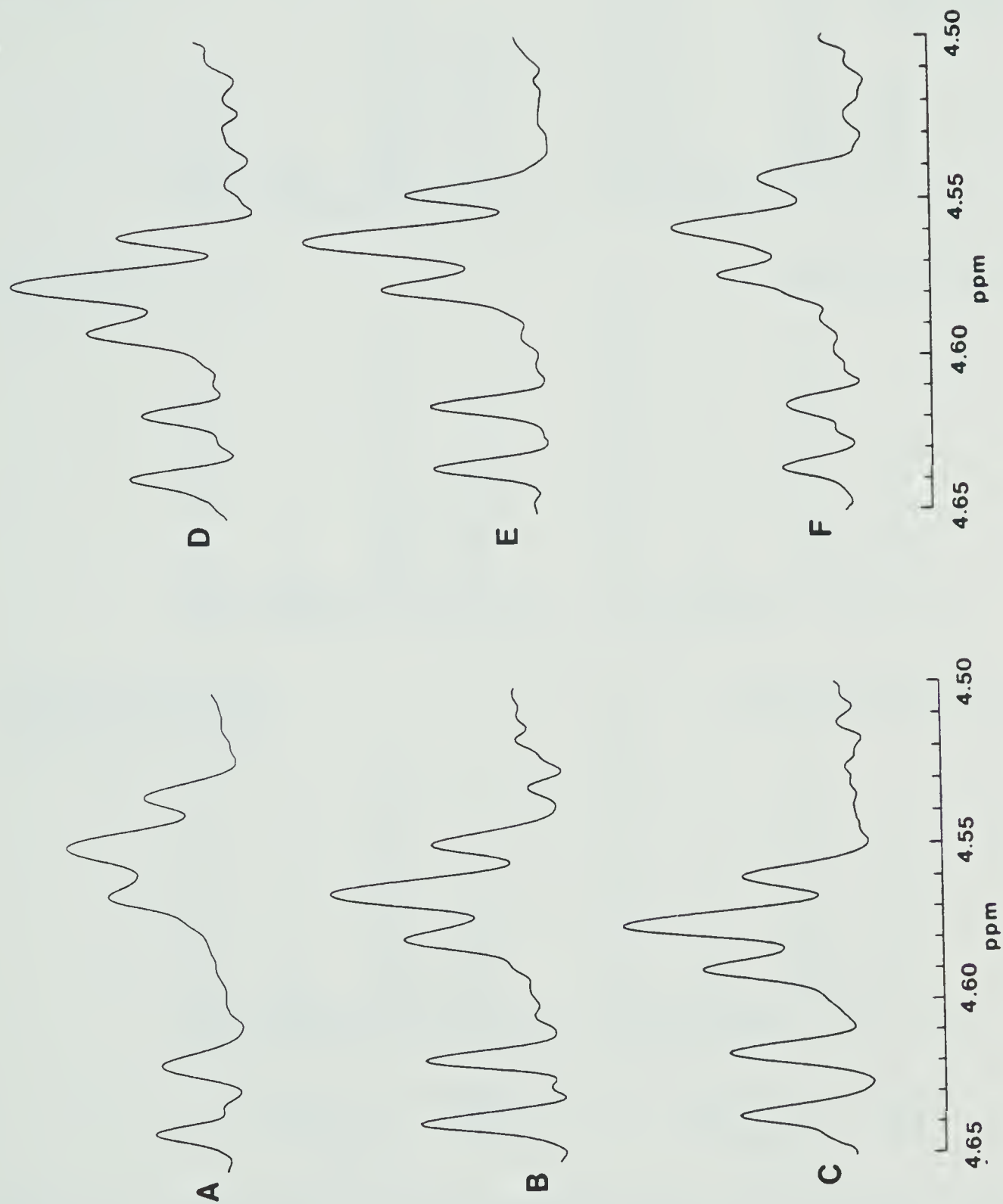


Figure 61. g5 resonance region of TSCR spectra of the samples of Figure 60.

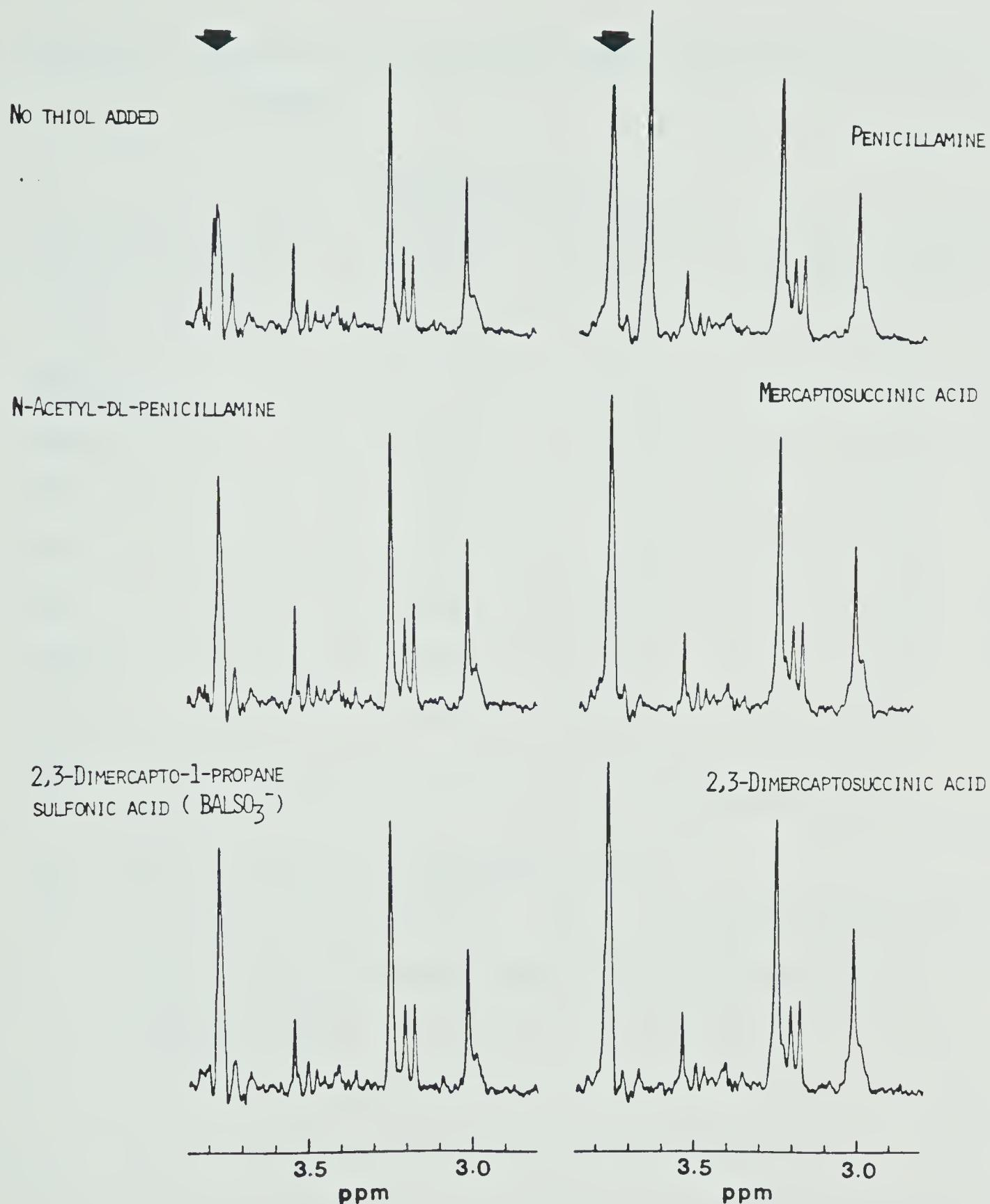


Figure 62. SEFT NMR spectra of hemolyzed erythrocytes with $\text{CH}_3\text{Hg(II)}$ (4.3 mM) and indicated thiols (4 mM sulfhydryl).

Table 32. Results of erythrocyte-bound $\text{CH}_3\text{Hg(II)}$ releasing studies.

Releasing thiol ^a	Intensity ratios:		δ_5 (ppm vs DSS)
	gl/ergo	gl/cre	
(None)	.44	.77	4.586
BALSO ₃	.87	1.69	4.568
DMSA	1.19	2.06	4.565
MAA	1.00	1.84	4.568
CSH	1.09	1.78	4.566
PSH	0.95	1.71	4.566
NAPSH	0.80	1.50	4.571
HCSH	0.78	1.33	4.571
ME ^b	--	--	--

(a) Abbreviations as previously given.

(b) Original study abortive. Rerun on another sample of erythrocytes indicates less efficient than either NAPSH or HCSH.

immediately obvious that the different thiols have widely differing releasing abilities for erythrocyte-bound $\text{CH}_3\text{Hg(II)}$. Detailed analysis is given below.

In some cases, a resonance was observed for the $\text{CH}_3\text{Hg(II)}$ methyl protons, in contrast to the studies of Chapter VIII. This is presumably $\text{CH}_3\text{Hg(II)}$ bound to the added thiol, which is in slow chemical exchange with the remainder of the $\text{CH}_3\text{Hg(II)}$. Chemical shift and approximate intensity data are given in Table 33 and some representative resonances in Figure 63. The chemical shifts display no apparent trend with binding strength; however, the range of values is very small.

C. Discussion

It was noted in Chapter III that values of $\log K_{\text{fc}}$ (conditional formation constant) at pH 7.4 did not exactly match the order of efficiency of various thiols as $\text{CH}_3\text{Hg(II)}$ poisoning antidotes found by pharmacological studies (133, 134, 170, 171). It is therefore of some interest to see how the present order of efficiency matches that of the $\log K_{\text{fc}}$ values. Figure 64 shows the gl/ergo and gl/cre intensity ratios, plotted as a function of $\log K_{\text{fc}}$ (see Table 16, Chapter IV). Within experimental error (estimated from the scatter in the ergo/cre ratio in Figure 64)

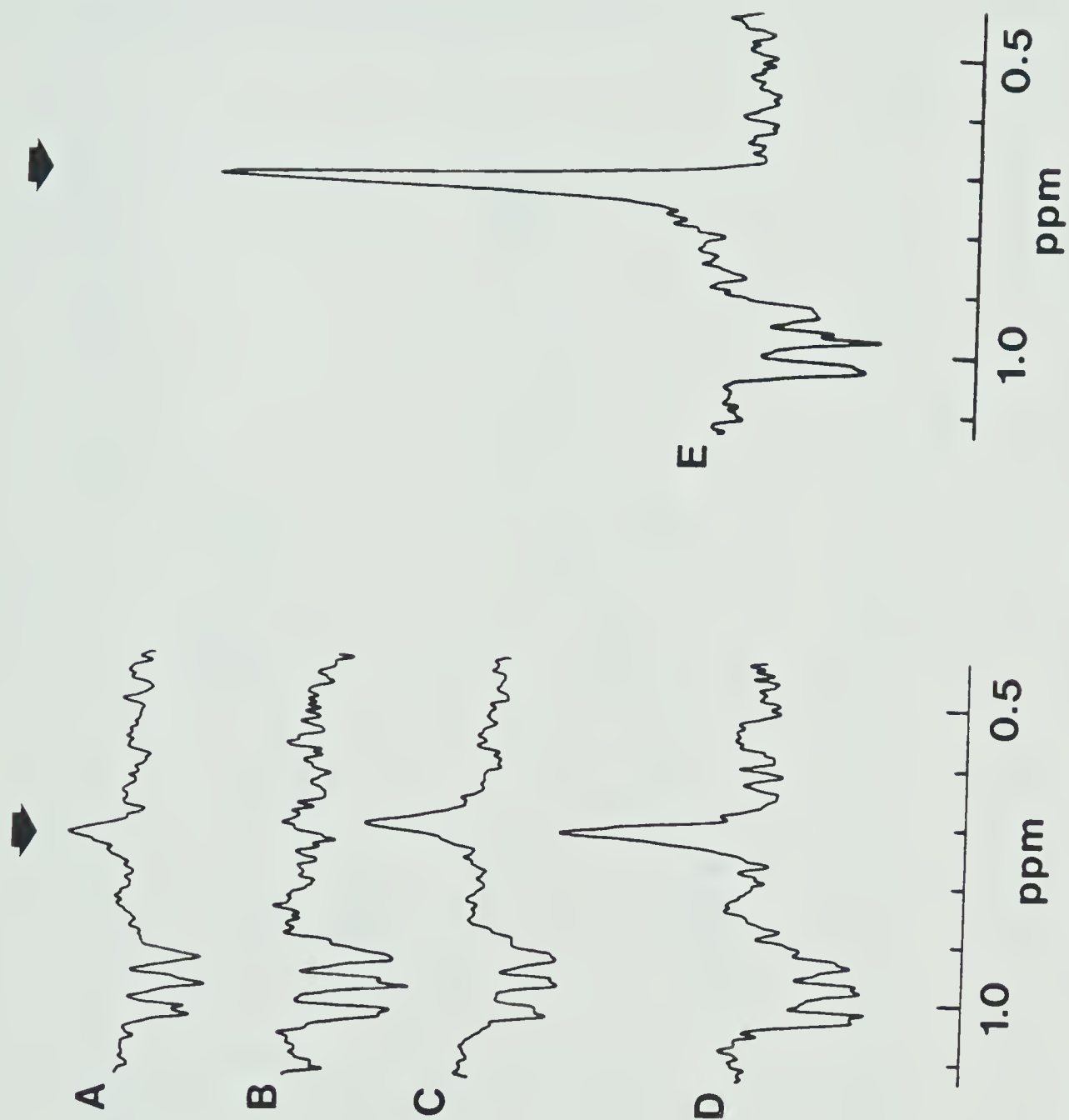


Figure 63. $\text{CH}_3\text{Hg(II)}$ methyl proton resonances observed during antidote studies involving A) PSH, B) BALSO_3H , C) DMSA, D) MAA, E) MSA.

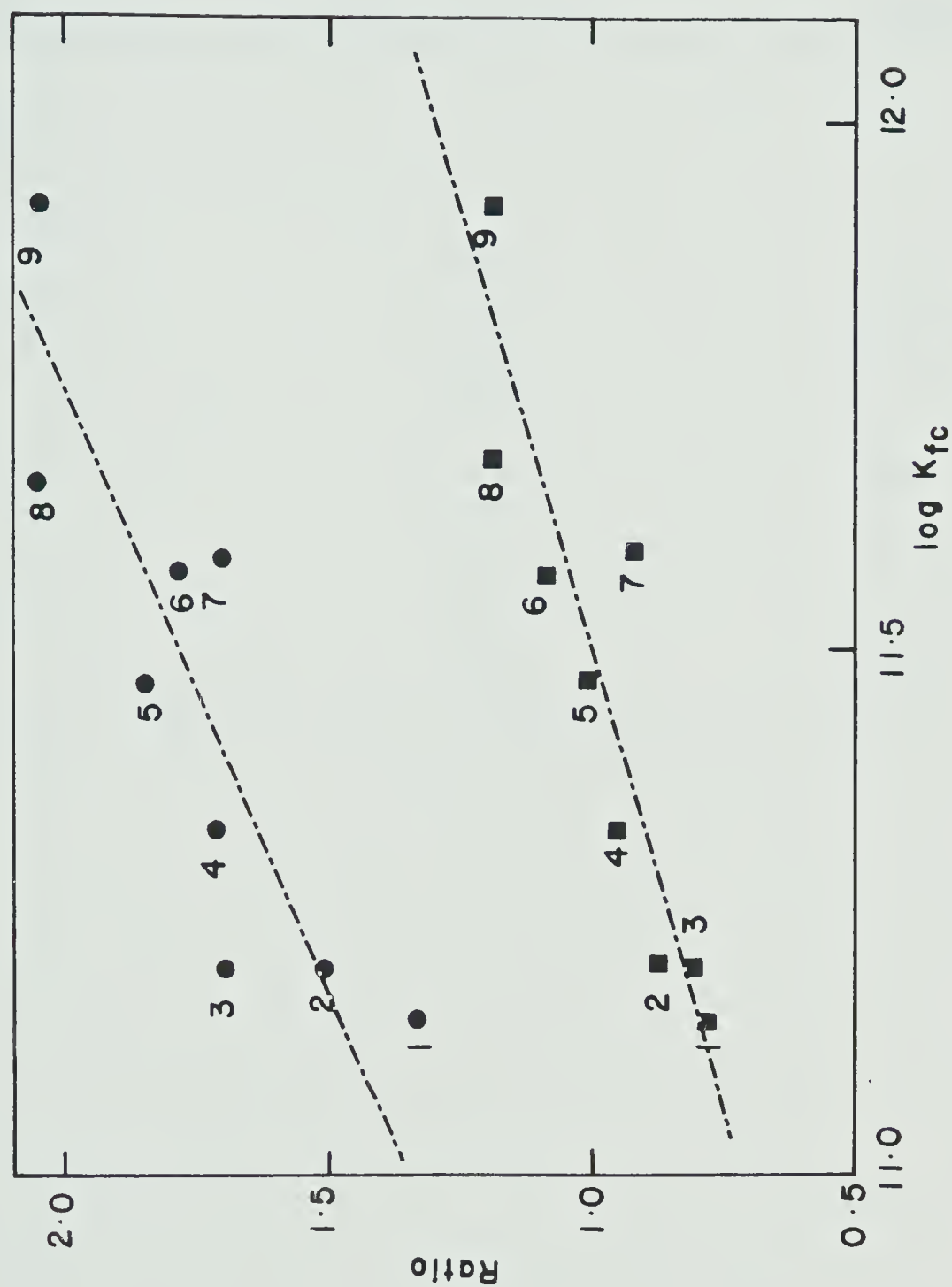


Figure 64. Intensity ratios gl/ergo (■) and gl/cre (●) for the antidote studies versus $\log K_{fc}$ of the antidote- $\text{CH}_3\text{Hg(II)}$ complexes. 1) HCSH, 2) BALSO_3H , 3) NAPSH, 4) PSH, 5) MAA, 6) CSH, 7) DTE, 8) MSA, 9) DMSA.

Table 33. Chemical shifts and intensities of $\text{CH}_3\text{Hg(II)}$ methyl resonances observed in antidote studies.

Thiol	δ (ppm vs. DSS)	Intensity
BALSO_3^-	-	-
DTE	-	-
DMSA	0.719	Medium weak
MAA	0.709	Medium
MSA	0.717	Strong
CSH	0.724	Weak
PSH	0.729	Very weak
NAPSH	0.715	Very weak
HSCH	0.723	Extremely weak

the increase is reasonably monotonic. Similar behaviour is observed for the plot of δ_5 versus $\log K_{fc}$ (Figure 65); thus, it appears that the distribution of $\text{CH}_3\text{Hg(II)}$ in the erythrocyte, and its removal, are governed by the relative affinities of the various ligands for $\text{CH}_3\text{Hg(II)}$.

The observation in some cases of $\text{CH}_3\text{Hg(II)}$ methyl proton resonances is interesting. The wide variations in intensity appear to be related to the amount of $\text{CH}_3\text{Hg(II)}$ bound to the "antidote" molecule. For instance, DMSA, which gives one of the most intense peaks, also has the highest $\log K_{fc}$ value. It may also be that kinetic effects play a part. It was concluded in Chapter V that sulfhydryl ligand exchange processes involving multiply charged sulfhydryl molecules (such as MAA, MSA and DMSA) would be slow compared to those involving less highly charged species (such as the thiol amino acids). In line with this, only weak (or no) $\text{CH}_3\text{Hg(II)}$ methyl proton resonances were observed for the thiol amino-acid experiments. The MSA resonance, the strongest observed, is also slightly narrower than the weaker resonances.

The factors determining distribution and removal of $\text{CH}_3\text{Hg(II)}$ from the intracellular thiol components of the erythrocyte are the same as those previously observed in the aqueous solution studies described in Part 1. Further evidence is also obtained for the slowness of kinetics of

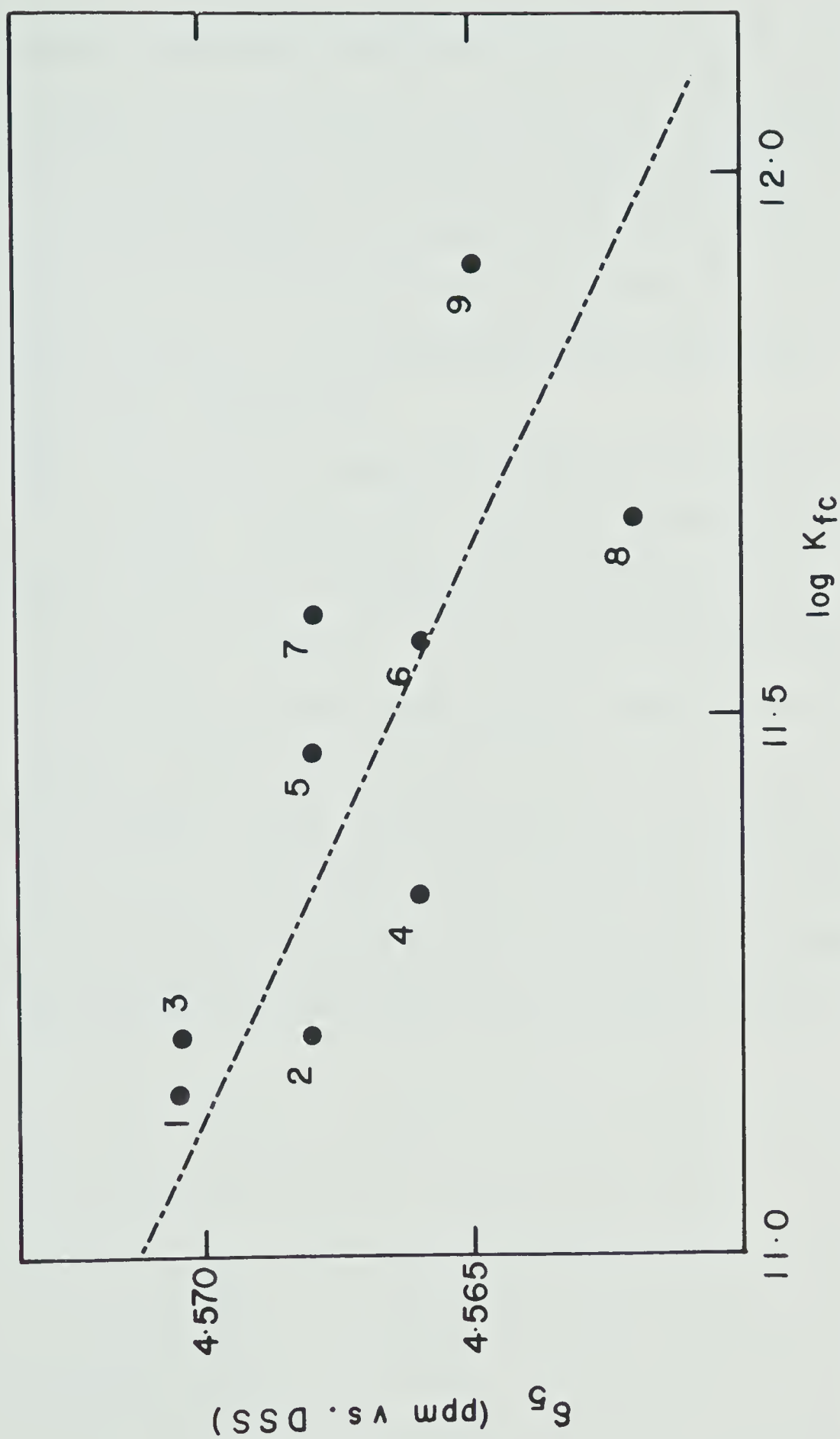


Figure 65. δ_5 for the antidote studies versus $\log K_{fc}$ of the antidote- $\text{CH}_3\text{Hg(II)}$ complexes. Identifications as for Figure 64.

displacement involving species such as MAA, MSA or DMSA.

It was suggested in Chapter V, on the basis of aqueous solution studies, that this slowness might partially account for the success of DMSA as a therapeutic agent (134). The observation of similar behaviour in systems more closely approximating the in vivo situation lends additional support to this hypothesis.

Again, it has been shown that NMR spectroscopy can be used as a precise, unambiguous, simple and rapid tool for investigating these delicately poised equilibria in a non-invasive manner. The use as a "screening" method for possible antidote molecules potentially applicable to many other systems is especially significant; it is anticipated that such methods should find wide use in the future, and contribute to our knowledge (both qualitative and quantitative) of the subtle interplay of interactions between metals and ligands which occur in biological systems.

BIBLIOGRAPHY - PART 2

145. M.R.F. Ashworth, "The Determination of Sulphur-Containing Groups, Vol. 2. Analytical Methods for thiol groups", Academic Press, New York, N.Y. (1976).
146. I.M. Kolthoff, W. Stricks and L. Morren, Anal. Chem. 26, 366 (1954).
147. P.D. Boyer, J.A.C.S. 76, 4331 (1954).
148. S.J. Leach, Austral. J. Chem. 13, 547 (1960).
149. W.F. Forbes and C.R. Hamlin, Can. J. Chem. 46, 3033 (1968).
150. G.C. Berg and E.F. Miles, Membr. Biochem. 2, 117 (1978).
151. T.Y. Toriba and L. Koval, Talanta 17, 1003 (1970).
152. D.L. Rabenstein, J. Chem. Ed. 55, 293 (1978).
153. M. Friedman, in "Amino-acids, peptides and proteins", Pergamon Press, New York, N.Y. (1973).
154. A. Rothstein, in "Mercury, Mercurials and Mercaptans", ed. M.W. Miller and T.W. Clarkson, Charles C. Thomas, Springfield, IU, USA. Chapter IV (1973).
155. T.W. Clarkson, Ann. Rev. Pharmacol. 12, 375 (1972).
156. T. Norseth and T.W. Clarkson, Arch. Environ. Hlth 22, 568 (1971).

157. J.K. Miettinen, reference 154, p. 233.
158. M.F. Perutz, *Scient. Amer.* 239, 92 (1978).
159. M.F. Perutz, *Brit. Med. Bull.* 32, 195 (1976).
160. D.L. Rabenstein and R. Saetre, *Clin. Chem.* 24, 1140 (1978).
161. K.G. Blume, N.V. Paniker and E. Beutler, in "Glutathione", ed. L. Flohe et al., Academic Press, New York, N.Y. p. 157 (1974).
162. D.L. Rabenstein and C.A. Evans, *Bioinorganic Chem.* 8, 107 (1978).
163. H.J. Segall and J.M. Wood, *Nature* 248, 456 (1974).
164. T. Refsvik and T. Norseth, *Acta Pharmacol. Toxicol.* 36, 6778 (1975).
165. T. Refsvik, *Ibid.* 42, 135 (1978).
166. E. Hirada, *Chudokuken Ho* 11, 22 (1978) (Japanese); as in *Chem. Abs.* 91, 103082m (1979).
167. S.O. Mata, K. Sakimura, T. Ishii and H. Sugano, *Biochem. Pharmacol.* 27, 1700 (1978).
168. D.J. Thomas and J.C. Smith, *Toxicol. Appl. Pharmacol.* 46, 547 (1979).
169. L. Magos, T.W. Clarkson and J. Allen, *Biochem. Pharmacol.* 27, 2203 (1978).
170. J. Aaseth, *Acta, Pharmacol. Toxicol.* 36, 193 (1975).
171. J. Aaseth, *Ibid. Suppl. II*, 41, 422 (1977).

172. P.J. Kostyniak, T.W. Clarkson, R.V. Cester, R.B. Freeman and A.H. Abbasi, J. Pharmacol. Exp. Ther. 192, 260 (1975).
173. P.J. Kostyniak, T.W. Clarkson and A.H. Abbasi, Ibid. 203, 253 (1977).
174. T.W. Clarkson, H. Small and T. Norseth, Arch. Environ. Hlth. 6, 610 (1963).
175. T. Norseth and T.W. Clarkson, Ibid. 21, 717 (1970).
176. T. Norseth, Acta Pharmacol. Toxicol. 32, 1 (1973).
177. L. Magos and T. Clarkson, Chem.-Biol. Interact. 14, 325 (1976).
178. J. Aaseth and T. Norseth, in "Clinical Chemistry and Chemical Toxicology of Metals", ed. S.S. Brown, Elsevier, New York, N.Y., p. 225 (1977).
179. D.L. Rabenstein, Anal. Chem. 50, 1265A (1978).
180. D.L. Rabenstein and T.T. Nakashima, Anal. Chem. 51, 1465A (1979).
181. R.R. Ernst, Rev. Sci. Instr. 36, 1689 (1965).
182. T.C. Farrar and E.D. Becker, "Pulsed and Fourier Transform NMR", Academic Press, New York, N.Y., (1971).
183. D.L. Rabenstein and R.S. Reid, unpublished.
184. E.L. Hahn, Phys. Rev. 80, 580 (1950).
185. F.F. Brown, I.D. Campbell, P.W. Kuchel and D.L. Rabenstein, FEBS Lett. 82, 12 (1977).

186. A.A. Isab and D.L. Rabenstein, *Ibid.* 106, 325 (1979).
187. D.L. Rabenstein and A.A. Isab, *Ibid.* 121, 61 (1980).
188. R. Freeman and H.D.W. Hill, in "Dynamic NMR", ed. L.M. Jackson and F.A. Cotton, Academic Press, New York, N.Y., Chapter V (1975).
189. D.L. Rabenstein, A.A. Isab and D.W. Brown, *J. Mag. Res.* 41, 361 (1980).
190. K. Asaka, M. Konrad and R.S. Goody, *FEBS Lett.* 96, 287 (1978).
191. N.S. Kosower and E.M. Kosower, in "Glutathione: Metabolism and Function", ed. I.M. Arias and W.B. Jacoby, Raven Press, New York, N.Y., p. 159 (1976).
192. D.L. Drabkin, *J. Biol. Chem.* 164, 703 (1946).
193. M.F. Perutz, *J. Crystal Growth* 2, 54 (1968).
194. A. Makaren, in "Clinical Chemistry", 2nd edition, ed. R.J. Henry et al., Harper and Row, New York, N.Y., Chapter 23 (1974).
195. Reference 108, p. 207.
196. R.S. Reid, D.L. Rabenstein and A.A. Isab, unpublished.
197. Reference 194, p. 1149.
198. D.L. Rabenstein and A.A. Isab, *J. Mag. Res.* 36, 281 (1979), and references cited therein.
199. P.K. Glascoe and F.A. Long, *J. Phys. Chem.* 64, 188 (1960).

200. Reference 100, p. 373.
201. Reference 90, p. 22.
202. Reference 90, p. 35.
203. D.L. Rabenstein, S.J. Backs and A.A. Isab, J.A.C.S.,
in press.
204. D.L. Rabenstein and Y. Theriault, unpublished.
205. A. Naganuma and N. Imura, Toxicol. Appl. Pharmacol.
47, 613 (1979).
206. S. Natelson and E.A. Natelson, "Principles of Applied
Clinical Chemistry", Vol. 2, Plenum Press, New York,
N.Y., p. 32 (1978).

B30328